Borehole Image Measurements

Electrical Azimuthal Acoustic

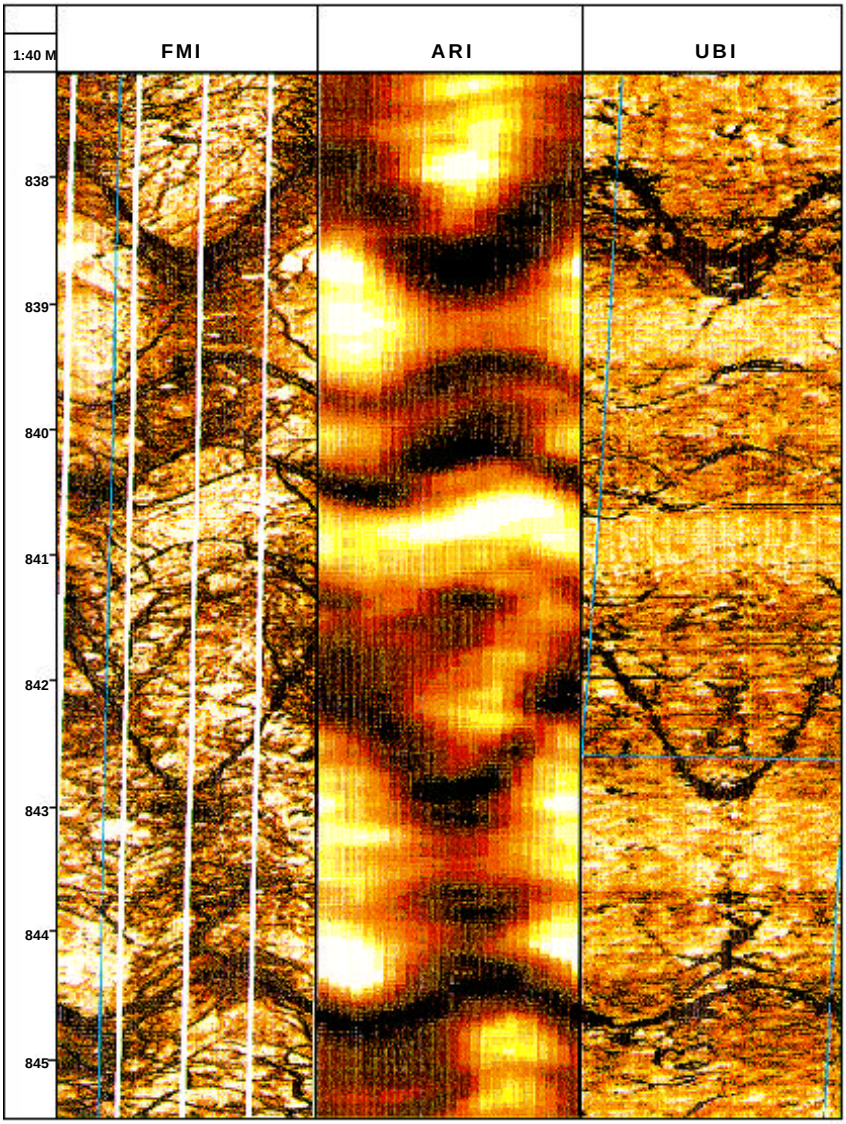

Version 9.2

Types of Dipmeter Tools

Dipmeter measurements have evolved through two major stages. The first tools were mechanical systems. The tool orientation was determined from a pendulum and magnetic compass. Both of these were subject to limitations due to inherent friction. The three-arm, three-button ***CDM*** (**C**ontinuous **D**ipmeter) yielded one three-point solution to a bedding plane. The four-arm, four-button ***HDT*** (**H**igh-**R**esolution **D**ipmeter **T**ool) permitted four three-point solutions to each bedding plane.

The advent of solid state systems eliminated the friction problem and also allowed a much larger sampling rate. The four-arm, eight-button ***SHDT*** (**S**tratigraphic **H**igh-Resolution **D**ipmeter **T**ool) can be computed by several different methods in which as many as 28 different dip solutions can be generated for each bedding plane.

The ***FMS*** (**F**ormation **M**icro**S**canner) contains the same four-arm, eight-button dipmeter capability as the SHDT but also provides an electrical image of the borehole. The first generation FMS tools have 27 image buttons mounted on two of the pads. The second generation FMS tools have 16 image buttons mounted on all four pads.

The ***FMI*** (**F**ormation **M**icro **I**mager) has four arms but with eight pads arranged as primary with flapper. This allows a much larger borehole coverage with 24 image buttons on each pad for a total of 192 image buttons.

Objectives of Formation Imaging and Dipmeter

Recognition and interpretation of geological events is the primary goal of both electrical images and dipmeter computations. The objective of this manual is to show the relation between the subsurface measurements and geologic fractures.

The major subdivision includes fracture recognition, structural interpretation, and stratigraphic interpretation. Fracture recognition includes the characterization and analysis of fractures, vugs, and other carbonate features.

Structural interpretation includes the determination of structural dip, evaluation of unconformities, and the analysis of faults.

Stratigraphic interpretation is the identification and orientation of sedimentary structures in various environments. The depositional environments studied are: eolian, fluvial, deltaic, deepwater, longshore bars, tidal, and reefs.

DIP Measurement Systems

Mechanical Systems

CDM 1956
Continuous Dipmeter

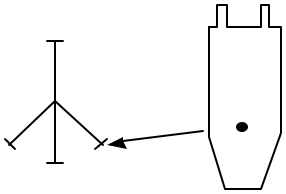

HDT 1968
High Resolution Dipmeter

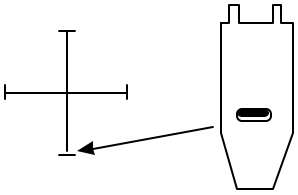

Solid State Systems

SHDT 1982
Stratigraphic Dipmeter

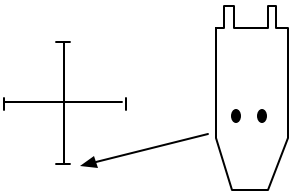

FMS (2 Pad) 1986
Formation Micro Scanner

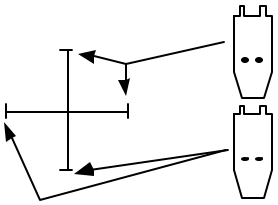

FMS (4 Pad) 1988
Formation Micro Scanner

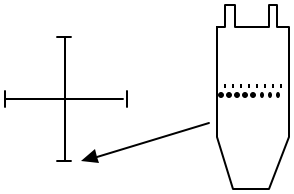

FMI (8 Pad) 1991
Formation Micro Imager

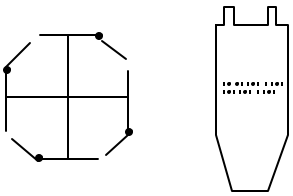

Introduction

The Formation MicroScanner* tool (FMS) and the Formation Micro Imager (FMI) allow continuous observation of detailed vertical and lateral variations in formation properties. The processing of the electrical currents recorded by the microelectrodes provides like images with the following features:

- high vertical resolution (about 0.2 in. [5 mm])
- very large dynamic range - from less than 0.2 ohm-m to more than 10,000 ohm-m
- high sensitivity, allowing detection of very thin events (fractures) that have an aperture on the order of a few microns or tens of microns, or with low contrasts in resistivity
- high sampling rate – one sample each 0.1 in. [2.5 mm] vertical displacement
- low sensitivity to heavy mud, borehole ovalization, and rugosity.

Two versions of the FMS tool are available in the field; one is a hybrid of the ***Dual Dipmeter**** tool (also known as a Stratigraphic High-Resolution Dipmeter Tool [SHDT]) with two imaging pads, and the other is four-pad version. The first version has 27 button electrodes on two pads arranged in four rows and the four-pad version has 16 buttons per pad in two rows. The four-pad tool has superseded the two-pad variety in most locations.

The FMI has a four-arm eight-pad array. The pads contain 24 buttons each for 192 buttons total. The tools include a general purpose inclinometry cartridge, which provides accelerometer and magnetometer data. The triaxial accelerometer gives speed determination and allows recomputation of the exact position of the tool. The magnetometers determine tool orientation.

During logging, each microelectrode emits a focused current into the formation. The button currently intensity measurements, which reflects microresistivity variations, are converted to variable-intensity gray or color images. The observation and analysis of the images provide information related to changes in rock composition and texture, structure, or fluid content.

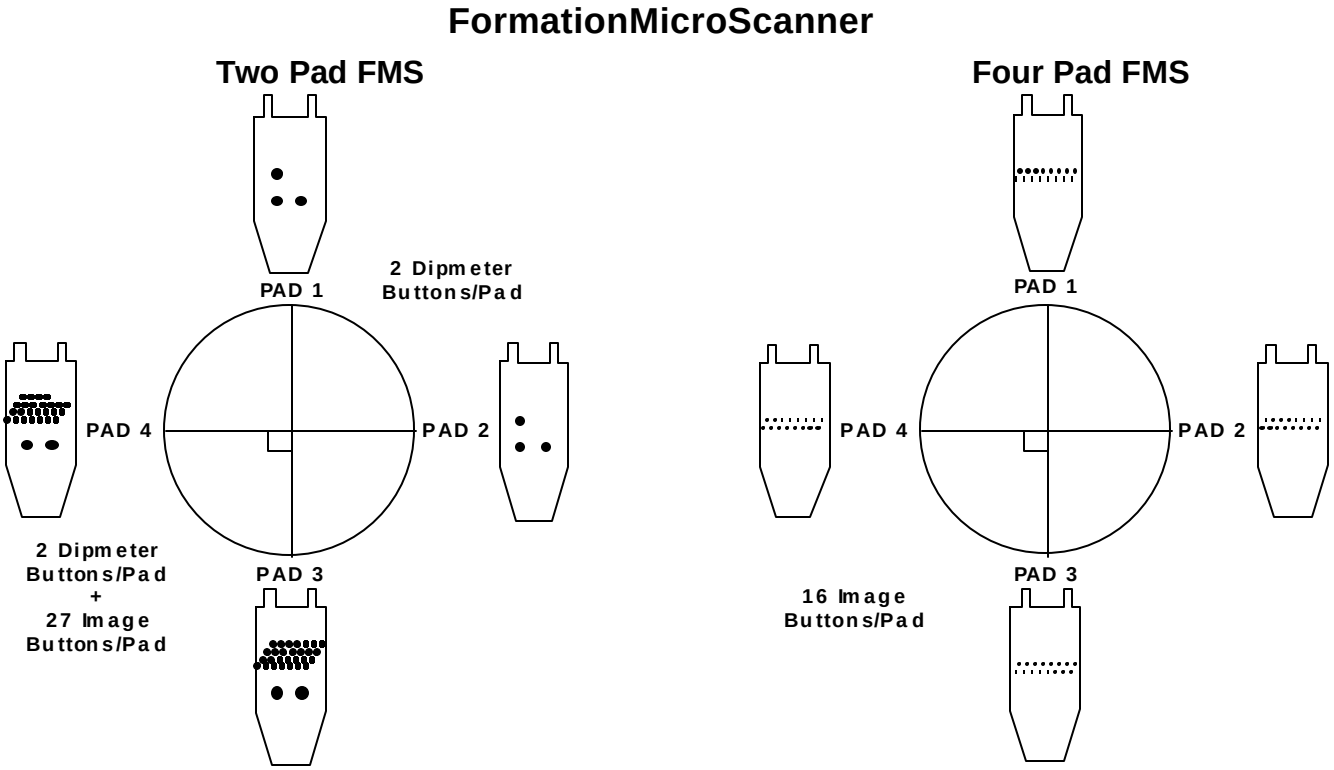

FMS Specifications

The specifications for the FMS are:

- operates in borehole environments up to 20,000 psi and 350°F;
- log sin 6.5-in. to 21-in. boreholes;
- logs in wells up to 72° deviation;
- first reading in 2.5 ft. above TD;
- logging speed is:
  - 900 ft/hr with MTU or CCC in system,
  - 1,600 ft/hr with HMT and TCC in system, or
  - 3,200 ft/hr in dipmeter only mode; and
- must have electrically conductive mud.

Length	31 ft	[9.45 m]
Weight	537 lb	[243 kg]
Minimum closing diameter	5.0 in.	[127 mm]
Minimum recommended hole size	6.25 in.	[160 mm]
Maximum opening diameter	21 in.	[533 mm]
Pressure rating	20,000 psi	[1400 bars]
Temperature rating	350°F	[175°C]
Logging speed		
Dip and Images	1600 ft/hr	[500 m/hr]
Dip only	3200 ft/hr	[1000 m/hr]

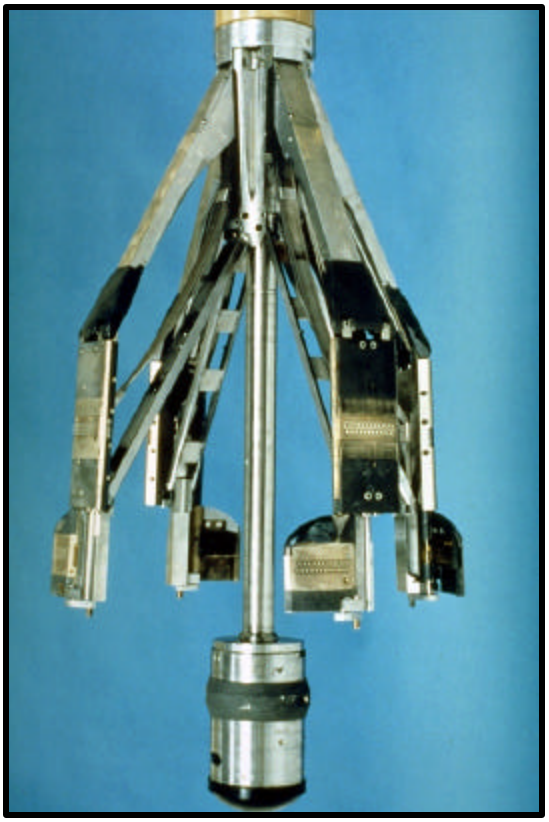

Formation MicroScanner Tool and General Specifications

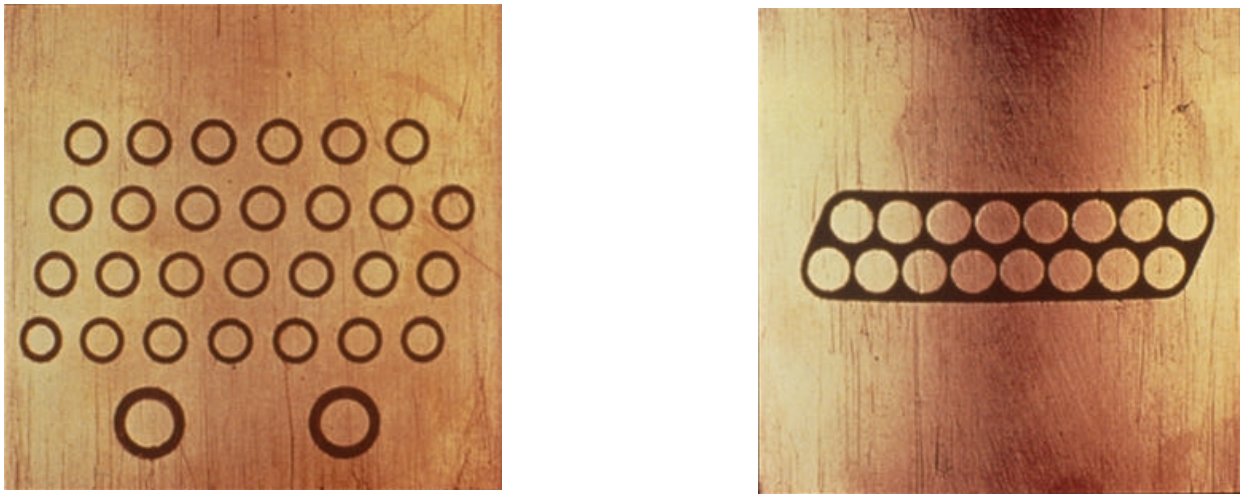

The 27-electrode arrangement for the two-pad tool (left) and the 16 electrode arrangement for the four-pad tool (right). Both pads measure about 3.25 in.^{2} [8 cm^2].

Formation Micro Imager

The Formation Micro Imager or FMI tool is a new generation tool with twice the borehole coverage of the FMS tool. The extra coverage is obtained by the addition of a flapper pad below and offset from each of the regular pads. Smaller buttons are employed to increase the image resolution by approximately 20%. The total number of buttons is increased from 64 to 192 which results in a tripling of the number of samples taken. An additional advantage of the FMI is that it is combinable with other logging tools so that often fewer trips in the hole are needed to run all logging services.

The FMI can be run in a "Pads Only" mode to reduce logging time for those cases where time is more critical than the increased hole coverage. Similarly, a "Dipmeter Only" mode is available to quickly acquire traditional dipmeter-type data over intervals where borehole images are not required.

FMI Pad Configuration

8 Pad

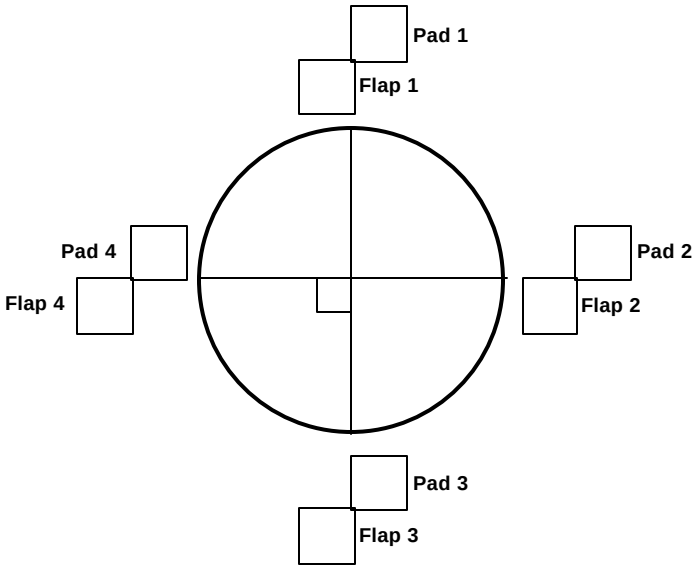

FBST PAD Configuration

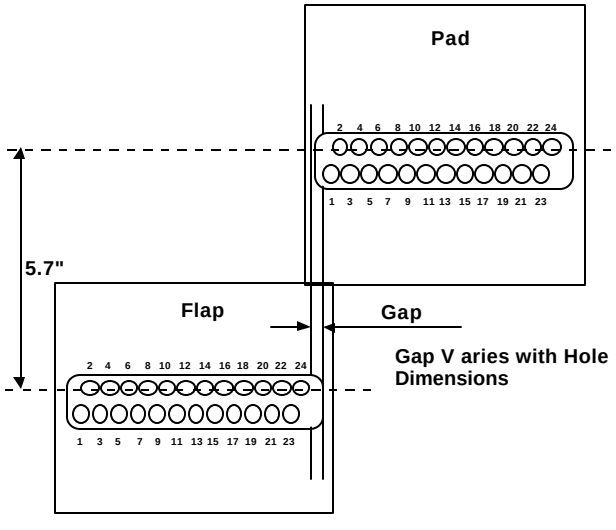

Effective Button Diameters

The effective button diameter of FMS devices has varied slightly with different tool designs. Effective button size results in the ability to image greater detail. With the 5 mm buttons in the FMI tool, it is possible to resolve features which are 0.2 in. thick.

Borehole Coverage (One Logging Pass)

The lower display details the borehole coverage which can be achieved with a single logging pass of the different tool types as well as the hole size limitations of each tool. For instance, the FMI tool may be run in boreholes from 6.25 in. to 21 in. diameter. In an 8 in. borehole, the FMI covers approximately 80% of the total borehole.

Effective Button Diameter

FMS

- **2 Pad** ..... **6 mm**
- **4 Pad** ..... **6.7 mm**
- **4 Pad (Slimhole)** ..... **5 mm**

FMI

- **8 Pad** ..... **5 mm**

One Pass Coverage

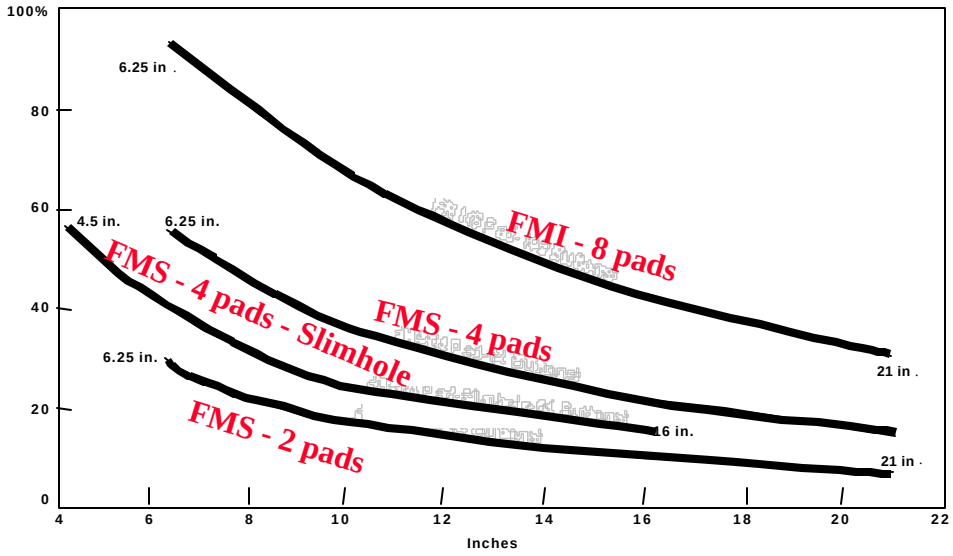

Coverage

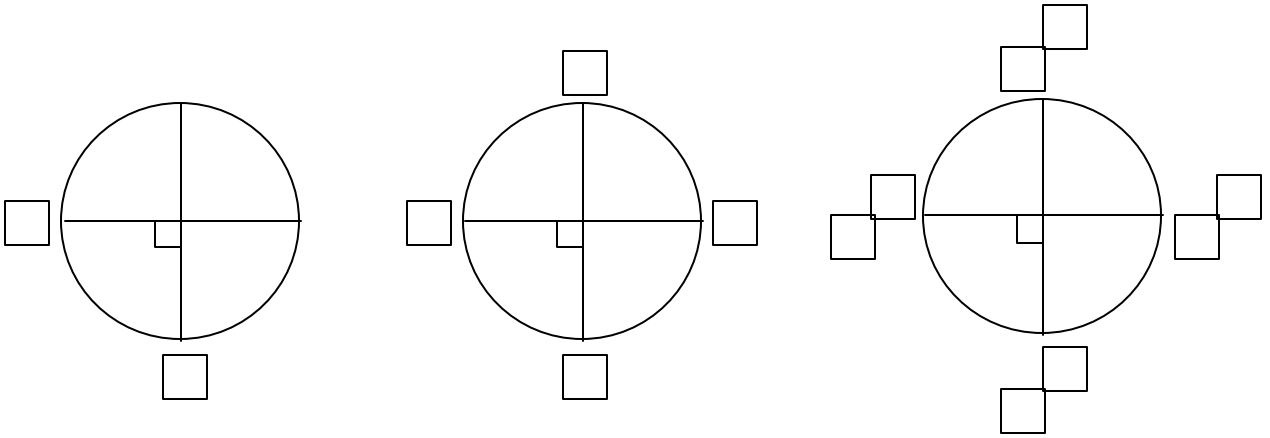

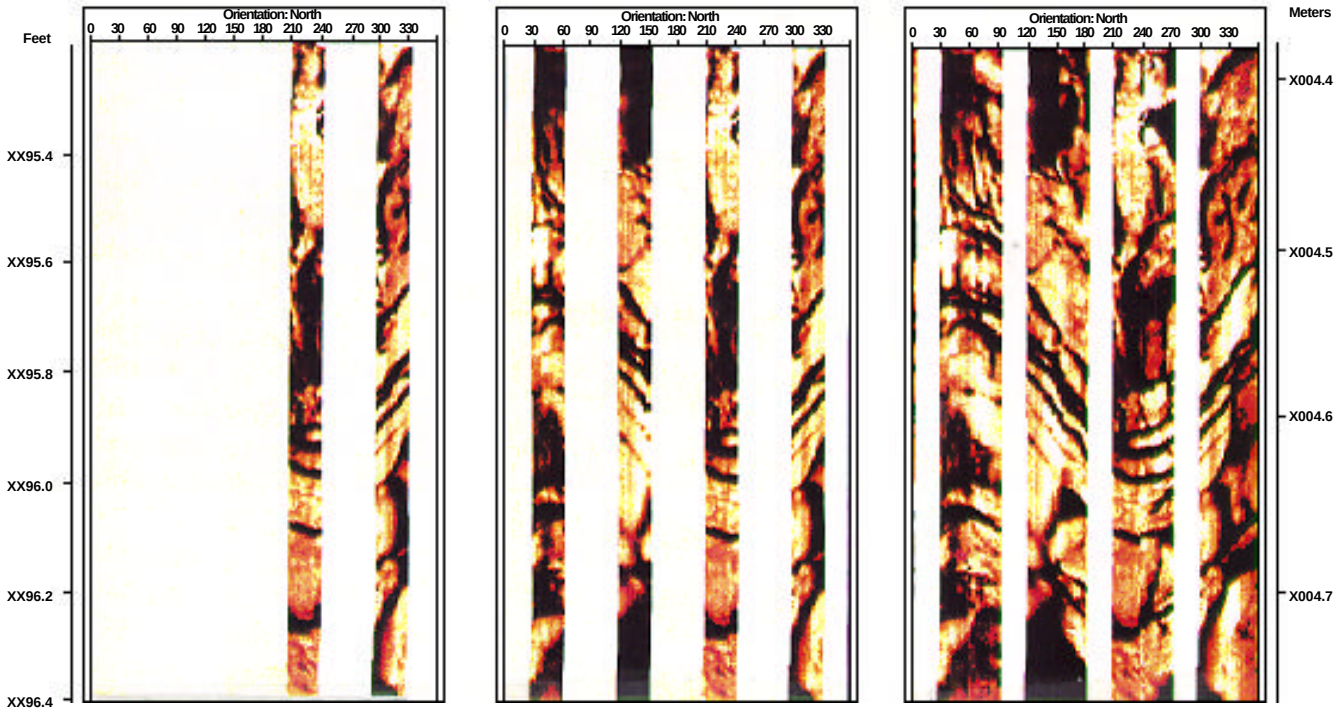

2 PAD **4 PAD** **8 PAD**

Data Acquisition

The data acquired by the FMS are enormous. Three hundred feet of logged interval require 10 Megabytes for acquisition alone. This is 20,000 blocks on a Vax. Data are acquired at these rates:

every 1.5 in.:

All Tools

- the two caliper measurements
- the three components of tool acceleration,
- the three components of the Earth's magnetic field, and
- the Emex current intensity.

every 0.1 in.:

All Tools

- current intensities from 10 SHDT buttons (this includes the speed buttons),
- tool acceleration components (Z-axis only after CSU edit),
- a time word, and
- the Emex voltage;

2 Pad Tool

- current intensities from 54 image buttons (two arrays of 27 image buttons each),

4 Pad Tool

- current intensities from 64 image buttons (4 arrays of 16 image buttons each)

8 Pad Tool

- current intensities from 192 image buttons (8 pads of 24 image buttons each)

Data Acquisition Guidelines

Mud Program

Because the tool emits current into the formation, it theoretically works only in water-base mud. Mud resistivity should not exceed 50 ohm-m; however, the mud must not be too conductive. For good image quality, the ratio of formation resistivity to the mud resistivity should be below 1,000. When the mud is to conductive relative to the formation, the current tends to flow into the borehole, reducing the sharpness of the images. An FMS measurement may be recorded in oil-base muds if the water content is at least 30 to 40%. The quality of the data obtained under such conditions is not very predictable, some data sets are usable while others are marginal.

Borehole Coverage

One pass of the two-pad tool covers 20% of the borehole wall in an 8.5-in. hole. This is often insufficient to either precisely define the geometry of the features, or to detect them. Making repeat runs with the tool rotating between each run will increase borehole coverage and lateral continuity. The four-pad tool increases coverage to 40% in one run, in four perpendicular directions, and may be preferred over the two-pad tool. Although a single pass is usually sufficient, additional coverage may be useful to detect or follow features such as fractures. In this case, repeat passes are recommended in anticipation that tool rotation will provide improved coverage. If the hole is ovalized to any great extent, the tool will tend to lock into a consistent alignment and no new data is gained. The larger diameter of the four-pad electrodes causes a slight but barely detectable loss of resolution, which as not been found to adversely affect interpretation.

Repeatability

To control the validity and the geological reality and representativeness of the features, a repeat section must always be recorded. Normally repeat sections of the same sector of the borehole wall will be indistinguishable even when the data are acquired by different pads. In some rare instances changes in logging conditions, such as oil flow into the wellbore or borehole breakouts, can be observed between logging passes.

Borehole Deviation

With borehole deviation <10°, centralized the tool minimizes poor pad contact caused by oblique positioning of the tool relative to the borehole axis. Imperfect pad contact caused by drilling-related ovalization of the borehole may result in a blurred image, particularly in the direction of elongation. The tool can be run in horizontal wells with the use of the **T**ough **L**ogging **C**ondition (**TLC***) system.

Logging Speed and Sampling

The maximum recording speed is 1,600 ft/hr (500m/hr) for image acquisition. The button current intensity is sampled every 0.1-in. [2.5 mm]. The two caliper measurements, the three components of tool acceleration and the three components of the Earth's magnetic field are sampled every 1.5-in. [3.8 cm]. A gamma ray tool can be run in combination with a wide array of other logging tools.

Mud Program

- Mud resistivity cannot exceed 50 ohm-m.
- Formation resistivity/mud resistivity < 1,000 for optimum contrast.
- Electrical Images cannot be acquired in oil-base muds.

Logging Speed

- 1,600 ft/hr (500m/hr) for image acquisition.
- 3,200 ft/hr (1,000m/hr) for dipmeter acquisition.

ARI - Azimuthal Resistivity Imager

The ARI tool takes 12 deep, directional resistivity measurements around the borehole. With a vertical resolution down to 8 in., this tool provides high quality, calibrated resistivity data for both petrophysical and geological use. Directional heterogeneity's within a formation can be evaluated, dip computations on this data provide structural dip information and image analysis provides information concerning fracture aperture and orientation. From an image analysis standpoint, the primary limitation of this tool is its reduced resolution when compared to FMS images. The detail needed for stratigraphic studies is not normally available in ARI images. Also, without the benefit of FMS images, it is often difficult to recognize some features such as fractures or thin beds. The two sets of images, FMS and ARI, complement one another. The FMS images provide great resolution for doing detailed analysis while the ARI images provide a means of quickly locating the larger scale events such as the more dominant fractures and for helping to confirm whether a fracture is natural or mechanically induced.

Each array of 12 electrodes, arranged 30 degrees apart, sends a focused current into the surrounding formation (A). The current is focused into the immediately adjacent formation so that deep resistivity is measured azimuthally. Each electrode also emits a reference current (B) along a shorter path through the mud to evaluate the borehole effect on the deep measurements.

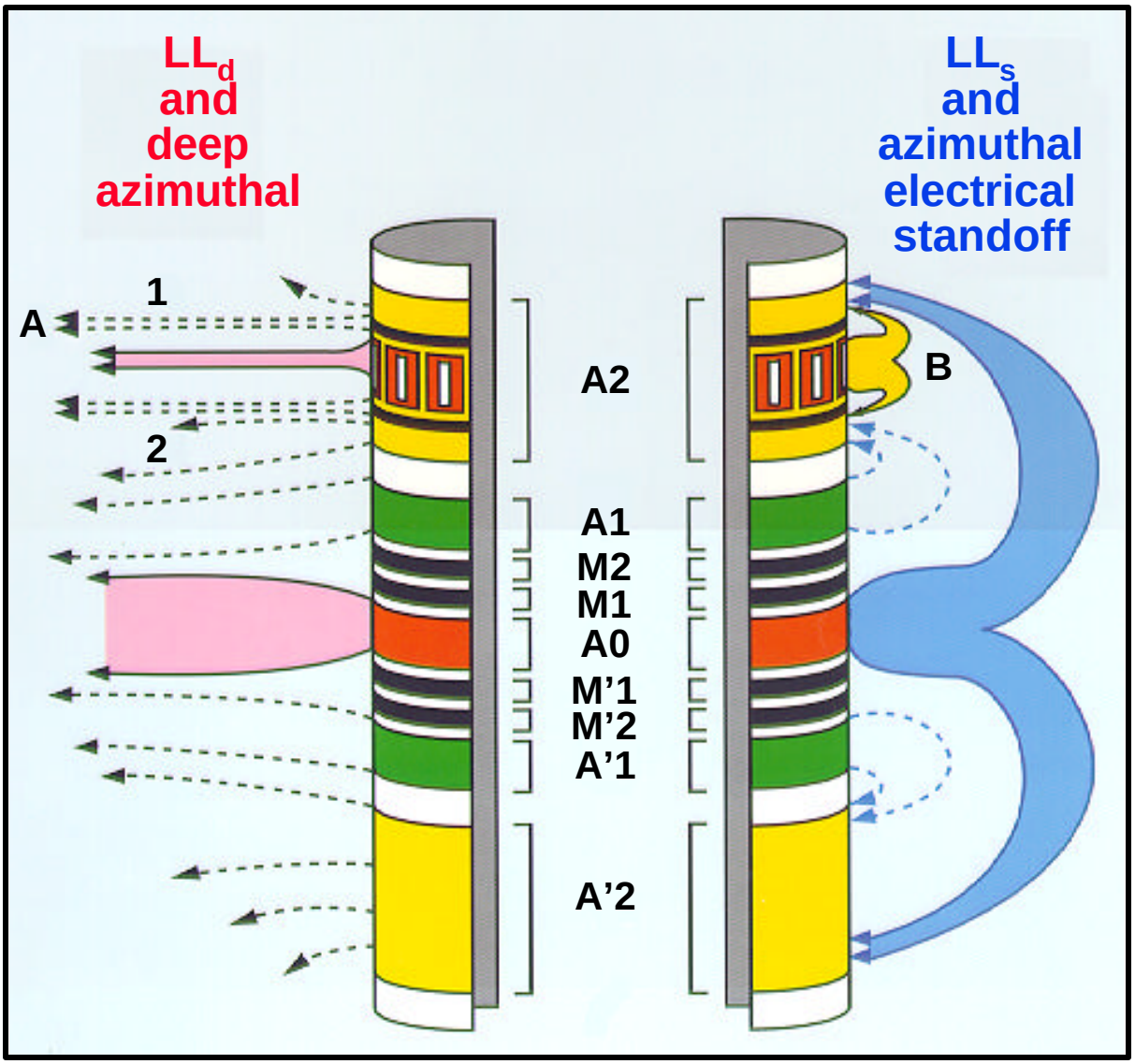

Specifications

Tool length	33.2 ft.
Tool diameter	3 5/8 in.
Weight	279 lbm
Logging speed	3600 ft/hr (1100 m/hr) for 1-in. sampling
	1800 ft/hr (550 m/hr) for dip
Maximum temperature rating	350°F (175°C)
Maximum pressure rating	20,000 psi
Minimum borehole diameter	4 1/2 in. without standoff
	5 1/2 in. with standoff
Combinability	Combinable above and below with all logging tools except Formation MicroScanner* and Stratigraphic High-Resolution Dipmeter (SHDT) tools
Resistivity range	0.2 to 100,000 ohm-m

ARI Images

The accompanying display shows a comparison of ARI images with FMI images over the same section of borehole. Although the ARI images do not have the definition seen on the FMI images, the dominant fractures are clearly identified. Note that often multiple events such as small, closely spaced fractures or thin beds are seen by the ARI as a single feature. Also, discrete events sometimes tend to appear as continuous features.

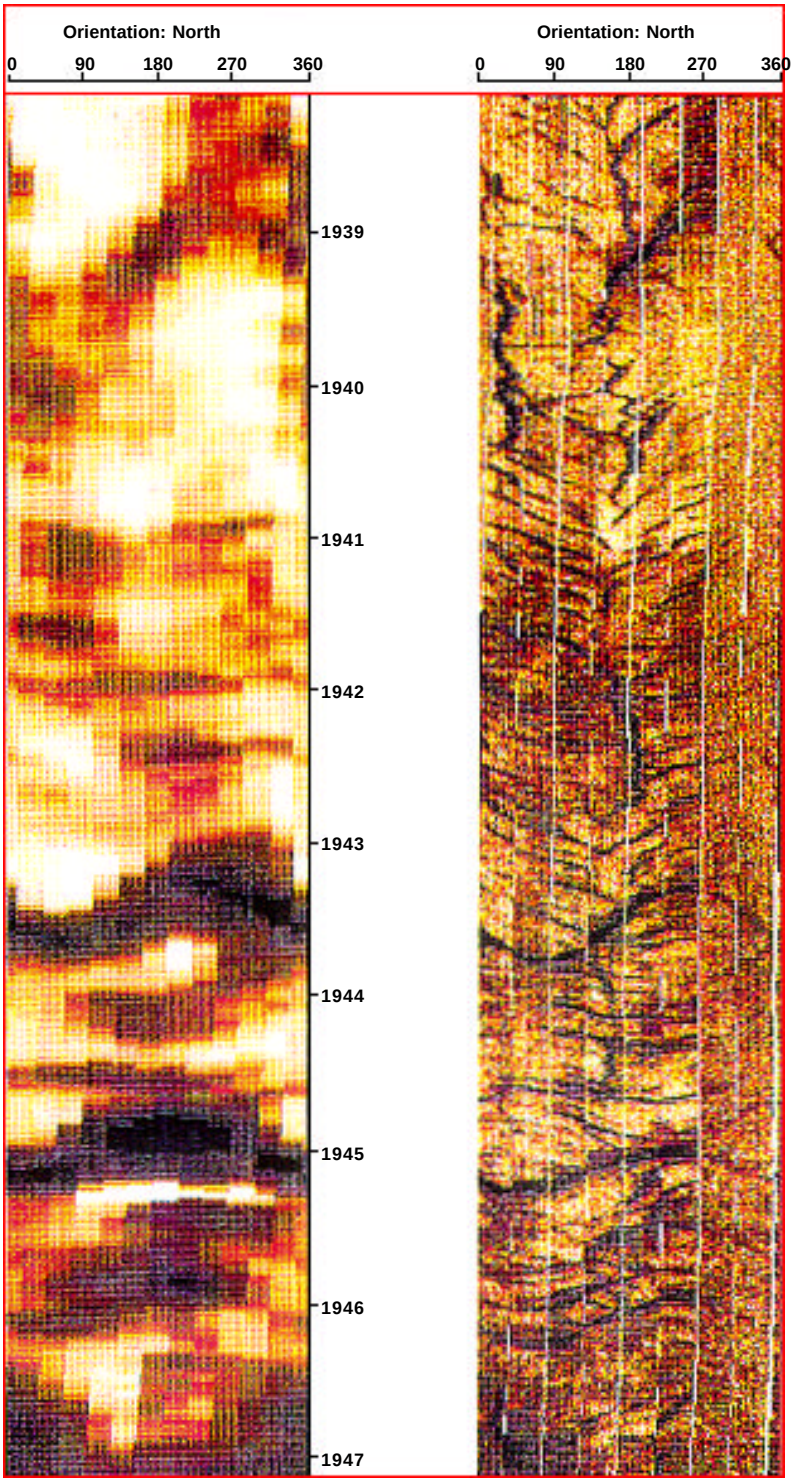

UBI - Ultrasonic Borehole Imager

The Ultrasonic Borehole Imager provides high resolution acoustic images of the borehole wall. Due to the fact that electrical imaging tools do not normally work well in oil based muds, acoustic tools provide the best images in this type of environment. Amplitude and travel time measurements are displayed as images which can be analyzed in a manner similar to electrical images. Transit time provides a high resolution azimuthal view of the borehole geometry. Such things as borehole breakouts, caused by drill pipe cutting a groove into the low side of the borehole can easily be found. Also, when fluid pressure changes allow part of a formation to slide along a fracture or bedding plane, the displacement or shear sliding can be observed and analyzed. Although many of these mechanical aspects of the borehole geometry are of limited geological interest, they are often critical to the efficient drilling and completing of the well. Under the proper conditions, acoustic images will see most of the larger fractures and many of the bedding surfaces. However, small scale or low contrast bedding and facies changes often are not seen in the acoustic data. Another serious drawback is it is almost impossible to obtain reliable fracture aperture information from acoustic images.

The figure to the right demonstrates the ability of the UBI to acquire good quality data even in a difficult environment. Although this section of the borehole contains many thin caves, the image quality remains good.

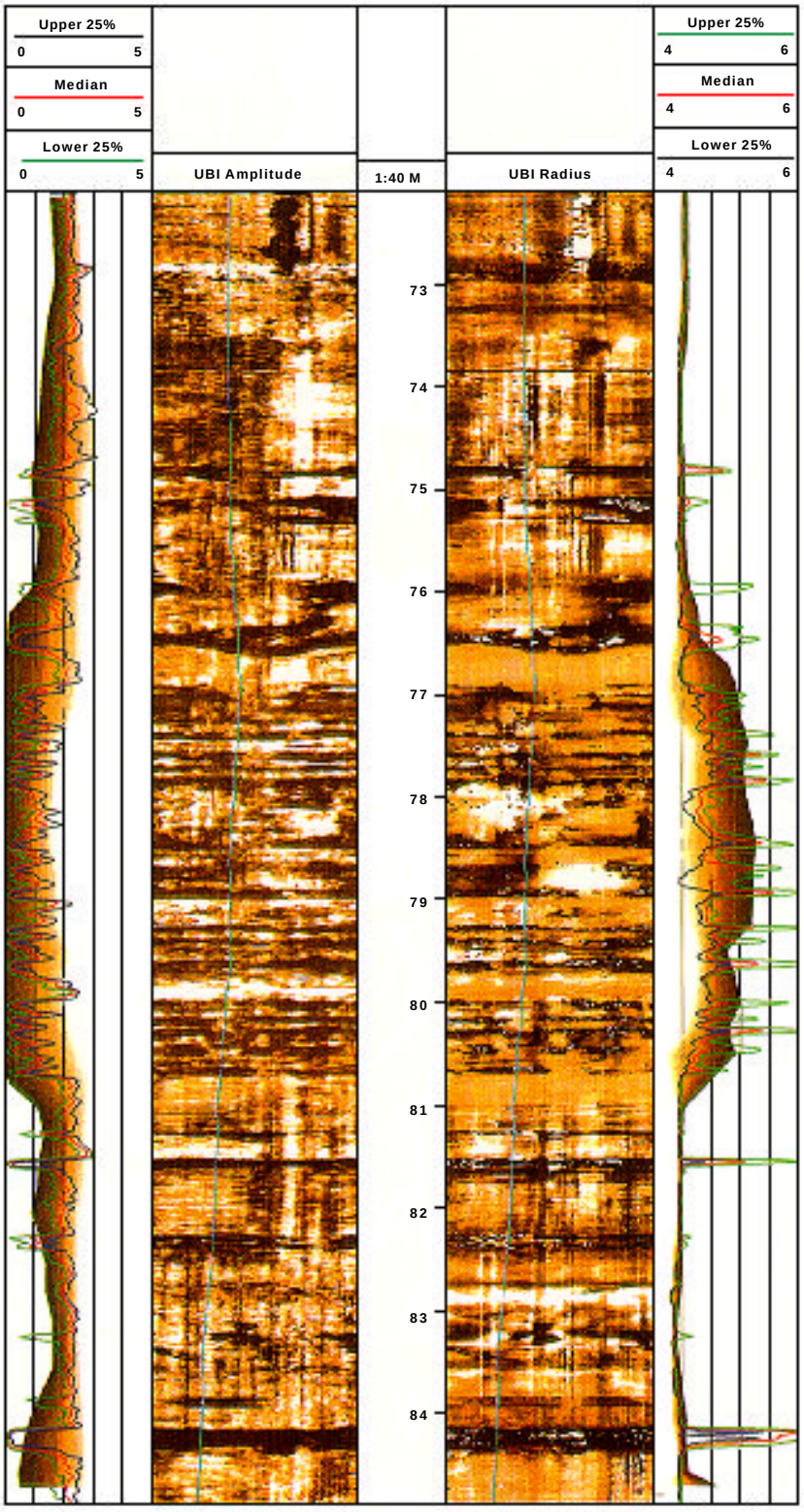

Pseudo Images

It is often desirable to make an image type analysis when true image data is not available. In such cases the limited data from such tools as the HDT, OBDT or SHDT can be transformed into pseudo-images which can be analyzed with imaging software. There are several cases where this procedure is very useful. In very rugose hole conditions, it is often difficult for automated dip computations to provide good, reliable results. The analyst can usually find enough correlation's visually to make a valid interpretation. Also, when apparent dips (relative to the borehole) are high, automated dip computations generally do not work well. There are many instances in which there is little or no distortion at a fault making it impossible to locate by dip patterns. These fault planes often are easily located and analyzed from the pseudo-images.

Some caution is needed in the use of pseudo-images. Because of the scarcity of real data, complex features such as highly fractured intervals will be difficult to interpret. The most effective use of this technique is where features such as beds, fractures or faults are planar and consistent around the borehole.

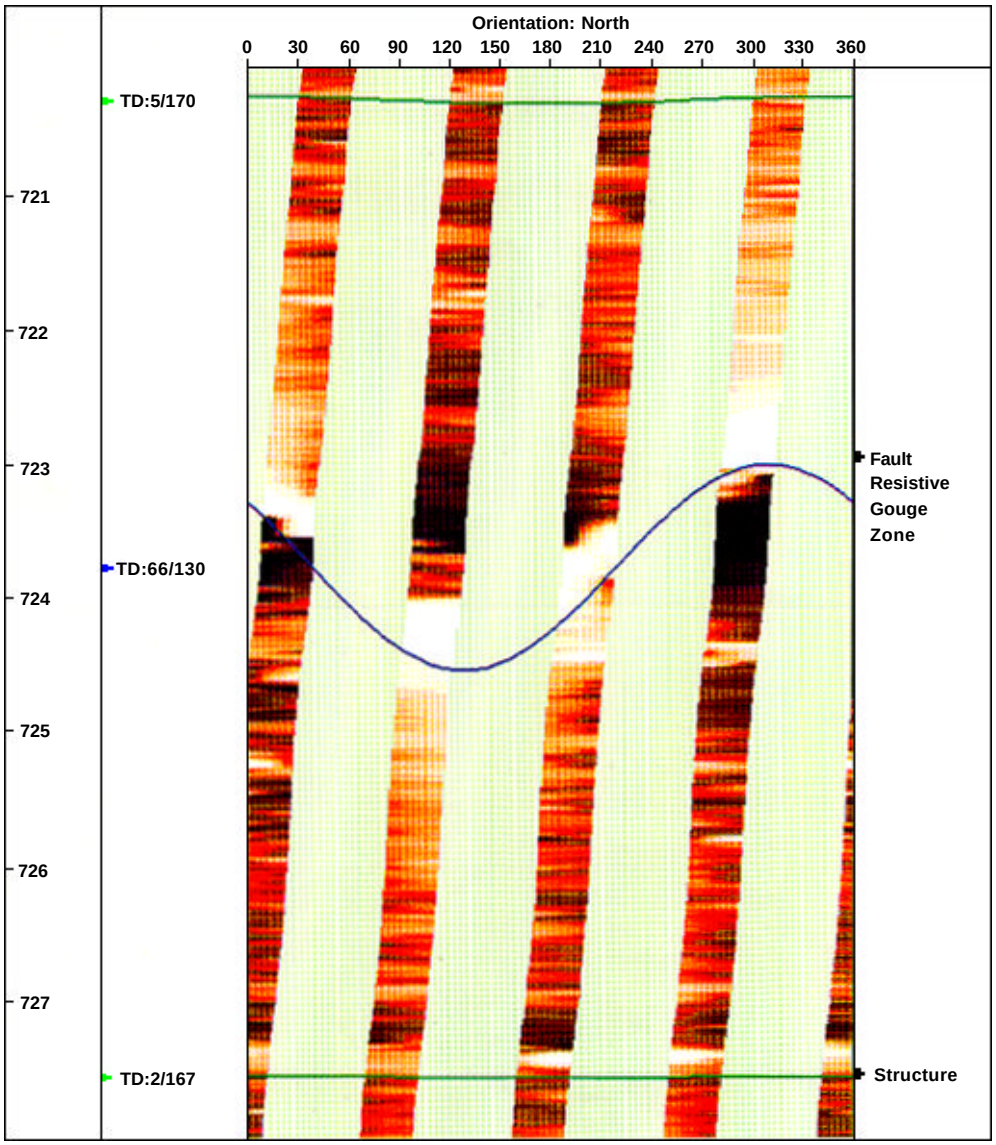

RAB Resistivity-at-the-Bit

The RAB Resistivity-at-the-Bit tool combines a focused high-resolution, high-resistivity Rt measurement with a correlation resistivity that uses the drill bit as the measure electrode. An accurate resistivity can be obtained when the mud is salty or the formation resistivity is high. It has a high vertical resolution (a few inches) with four depths of investigation to determine early-time invasion. The azimuthal resistivity images of the borehole can be used for structural dip computation and other geological interpretations. Important information such as location and orientation of faults, folds and structural changes can be determined so that decisions can be made with more confidence at the earliest possible time.

This example shows a comparison of FMI images versus unfiltered and filtered RAB images from an offshore California well. The filtering of the RAB images produces a clearer, more interpretable image. The clear imaging of overturned and normal bedding features demonstrates the type of detail that can be obtained with the RAB tool. Also important is the ability to locate zones of interest which would require a more detailed evaluation with FMI data.

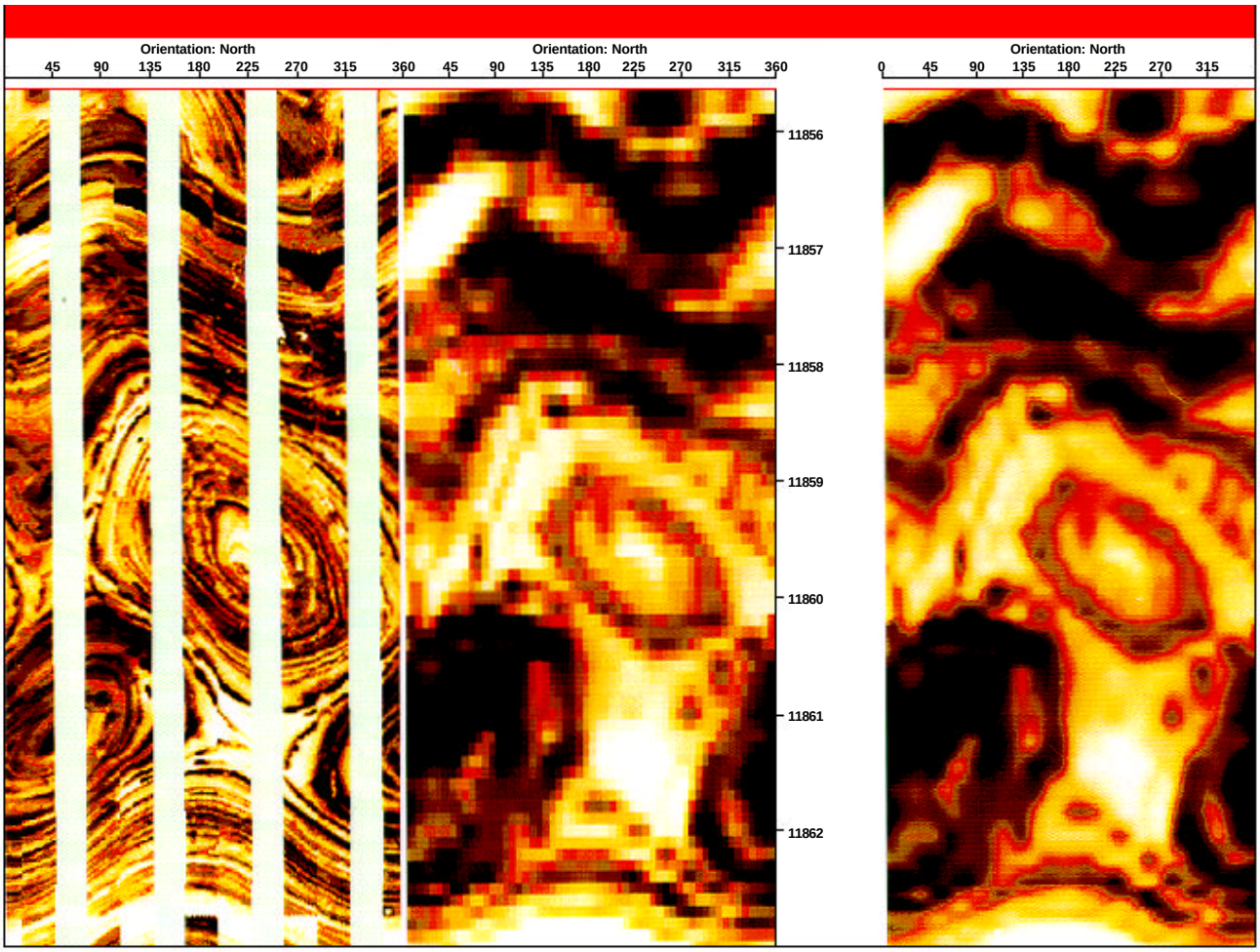

Processing and Presentation

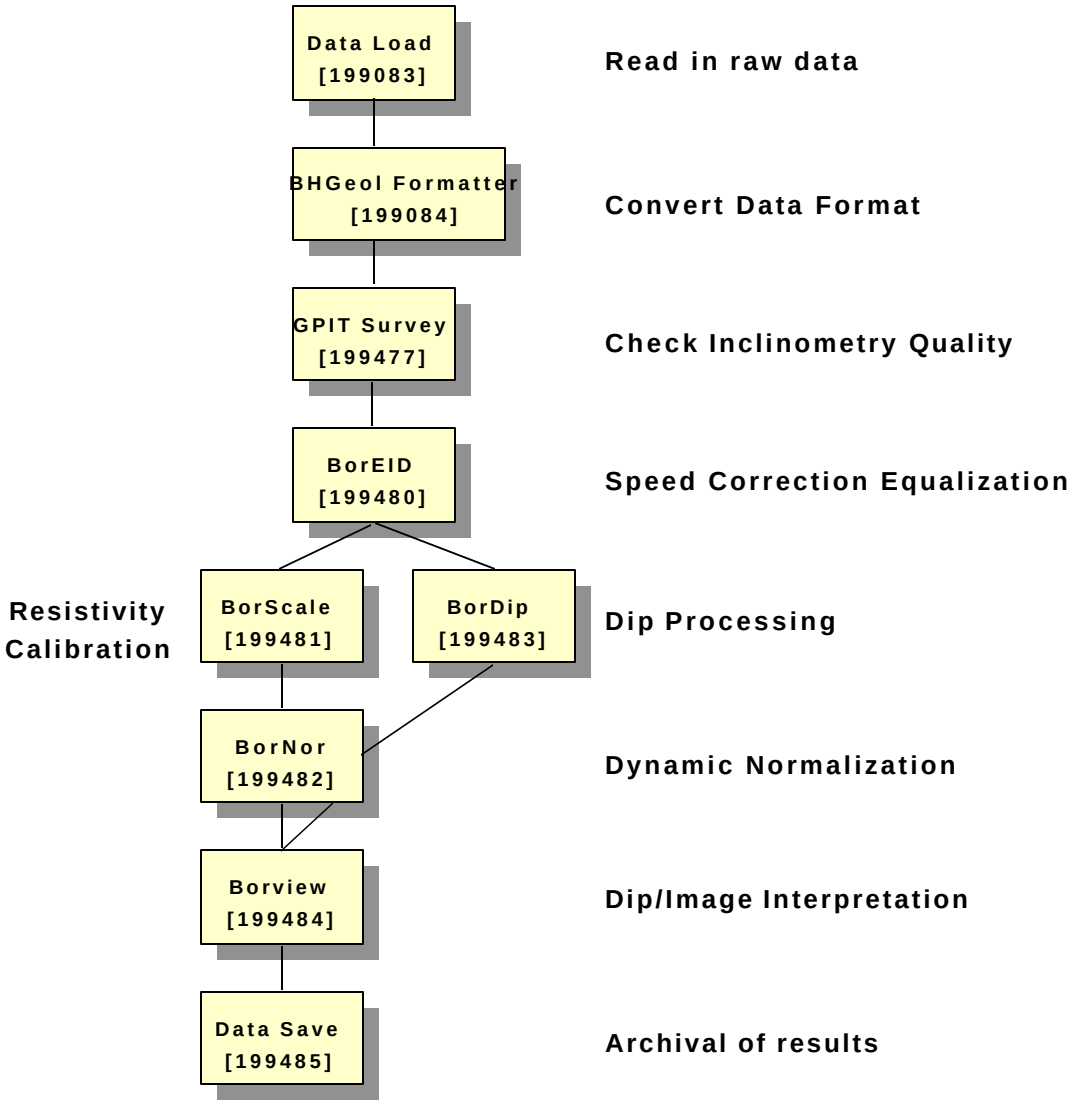

Flowchart of FMI Processing Chain

Version 9.2

FMS Processing Chain

The primary purpose of computer processing of raw FMS/FMI data is to convert the raw acquisition data into the best visual representation. Field data files are first read onto the computer using a module called ***Data Load***. The Convert modules merely change the acquisition data format into a form more convenient for further processing.

It is sometimes possible to repair bad inclinometry data. Such data restoration is performed in the module, ***GPIT Survey***. In practice, this module is normally used to validate the quality of the data acquired during field recording.

Next, equalization of the buttons is next performed by ***BOREID***. Each button is making an independent uncalibrated measurement. To provide a uniform response, the data in each button channel are modified so that their mean and standard deviation are the same as the mean and standard deviation of all the data from the whole pad over the entire processed interval. This boosts the signal from weak buttons and reduces the output of very sensitive ones. The overall effect is to make the responses of individual buttons consistent with each other. Additionally, a correction is made for the effects of changing EMEX voltage to make the output more comparable to a calibrated resistivity tool. Speed corrections are then performed within the module ***BOREID***. Corrections for magnetic declination are also performed at this time. Two methods of speed correction are available; one employs accelerometer information, the other is an image based process. Normally both methods are used; the accelerometer information provides the initial correction which is then "fine-tuned" by the image based technique. ***BOREID*** also attempts to locate and repair isolated bad buttons based on a comparison of the overall response of the buttons). Dead button channels, i.e., those showing little or no activity are replaced with the average of the adjacent buttons. The analyst can optionally repair any individual bad button data channels that were not corrected automatically.

BorDip computes dip magnitude and direction. BorNor is used to dynamically normalize the images in order to enhance the image contrast. Interactive interpretation of the images is done in BorView. All results of processing and interpretation can be archived using Data Save.

Optionally, a program called ***BorScale*** may be run to calibrate the image data response to that of a shallow log, such as an SFL* (Spherically Focused Log) or a MicroSFL* (MicroSpherically Focused Log).

Any of the processed data can be converted to a slightly different format for display an interactive analysis on the Image Examiner Workstation.

Speed Correction

The so-called speed correction process is a major part of FMS data processing. Here the goal is to position each button measurement at the proper depth in the hole. Each tool pad has horizontal rows of button sensors; the two-pad tool has four rows with a total of 27 buttons per pad, the four-pad tool has two rows with a total of 16 buttons per pad and the eight-pad device has 24 buttons per pad. At any given time, the data from each row of buttons are coming from different depths.

As can be seen in the adjacent figure, a boundary is seen at different times as each row of buttons crosses it. If the tool were moving uphole at a constant speed, a simple shift of each row would bring all the data into alignment. Although cable speed may be constant, the tool is usually sticking and bouncing to some extent as it comes uphole. To apply a constant shift under such changing conditions would result in either an over-correction or an under-correction. Both of these cases would leave the images with a "saw-tooth" appearance.

The initial increment to shift each row is derived from downhole accelerometer measurements. The local acceleration is first integrated to determine tool speed, which is then integrated to calculate the actual depth shift to apply. Another method of speed correction is based on the image data itself. Since there are two rows of buttons on each FMS pad, it is possible to examine the similarity of boundaries crossed by each row of buttons. If the same interface is found to be displaced between rows, a correction can be calculated to adjust the data back to its correct depth. The accelerometer and image based methods are normally used together to generate the best results.

Also, a geometrical correction is applied using the caliper data to account for the shift in pad position as they follow the changing borehole shape.

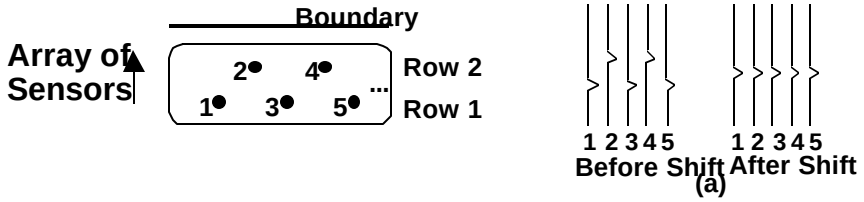

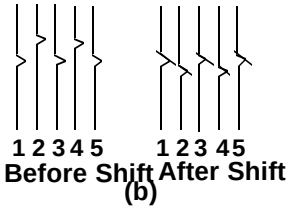

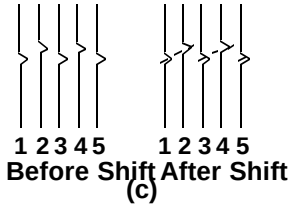

Effect of Nominal Depth Shift When:

a) **tool speed equal cable speed, correct depth shift is performed**
b) **tool speed is greater than the nominal speed, depth shift over-corrects for true position of boundary**
c) **tool speed is than the nominal speed, depth shift under-corrects for true position of boundary**

The importance of complete speed correction can be seen on these sets of images. The images on the left have been processed with only the nominal row shift applied. This is the case where tool motion is assumed to be a constant speed. There is a great amount of "saw-toothing" and smearing of the images. The images to the right are the same except that accelerometer and image-based speed corrections have also been applied.

Comparing the two results shows the partially corrected images to be alternately stretched or compressed. The full speed correction places the data at its true position in the well. The small-scale, stratigraphic features are much more easily seen and interpreted. Under cases of extremely jerky tool motion, some "saw-toothing" can be seen in the images but with normal hole conditions these should be rare occurrences.

Oriented Enhanced Images

With SPEED CORRECTION NO SPEED CORRECTION

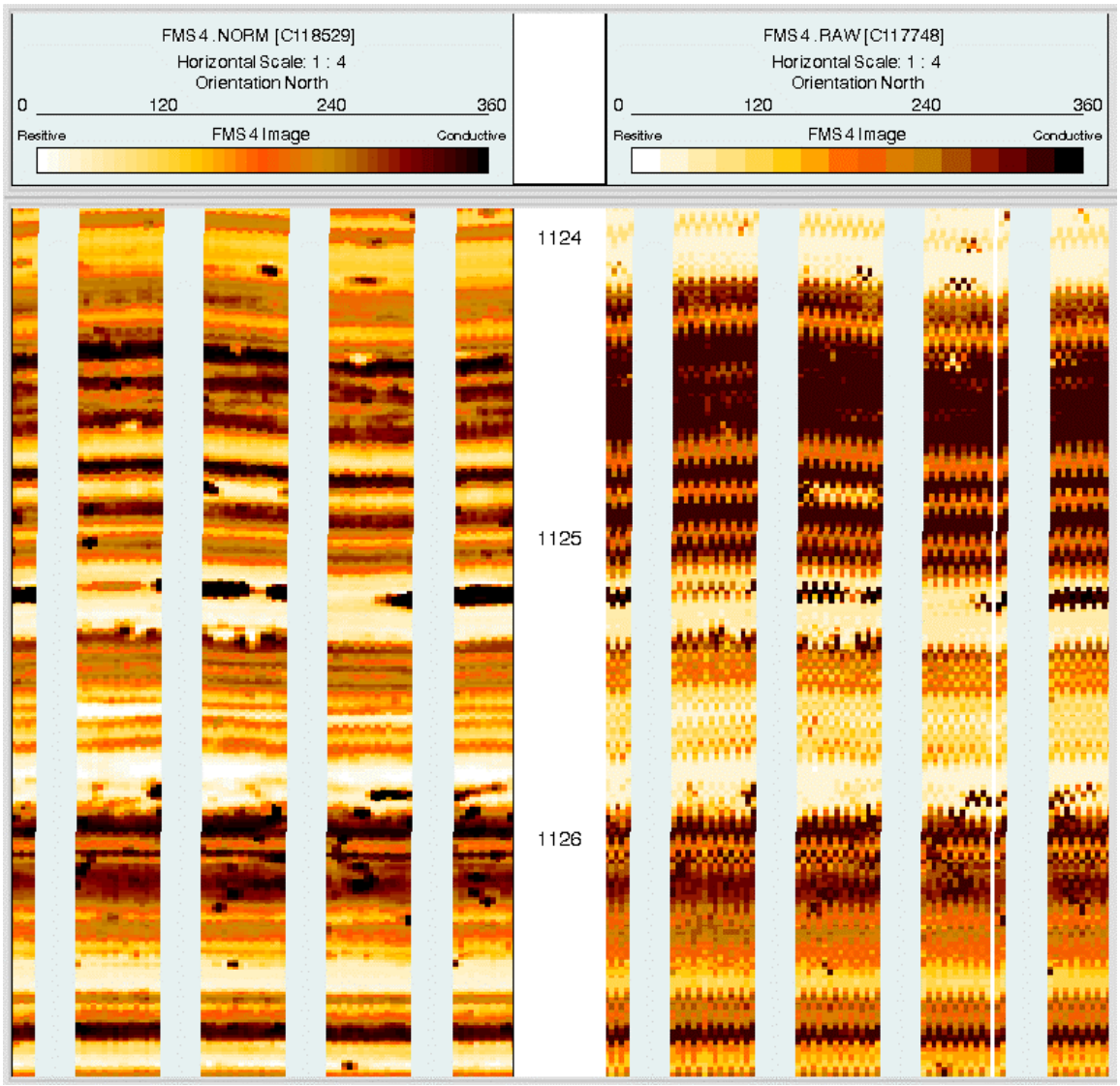

Correction of Bad Button Data

The detection and correction of bad buttons is normally handled automatically in the BOREID module. However, should the analyst wish, it is possible to perform some additional corrections or to perform all corrections manually. Some actions to be performed on the data are rather obvious, others are more subjective. A dead button on one of the pads has to be repaired, otherwise some of the downstream processing will not be effective. The repair is made by removing the bad button channel and then replacing that data with the average of the two adjacent buttons. When adjacent buttons have to be repaired, a multiple pass scheme is employed to spread the nearest good data across the bad buttons. Intermittent buttons usually have to be corrected manually.

Before Correction

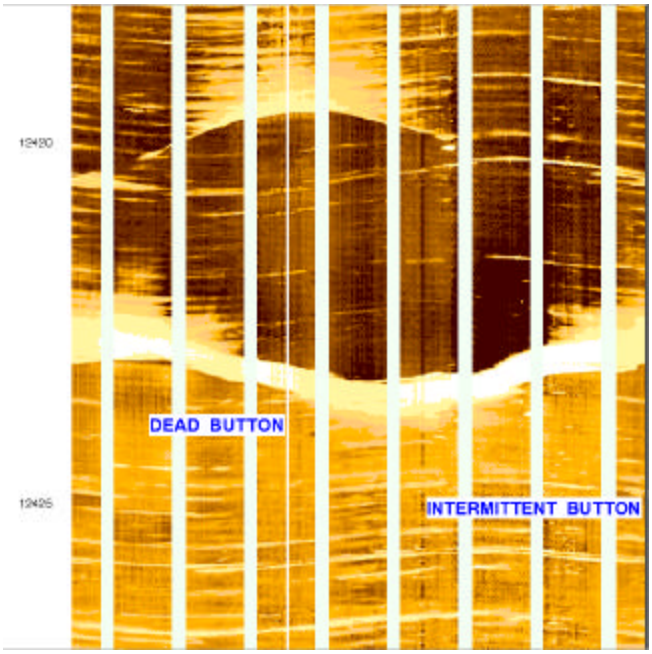

After Correction

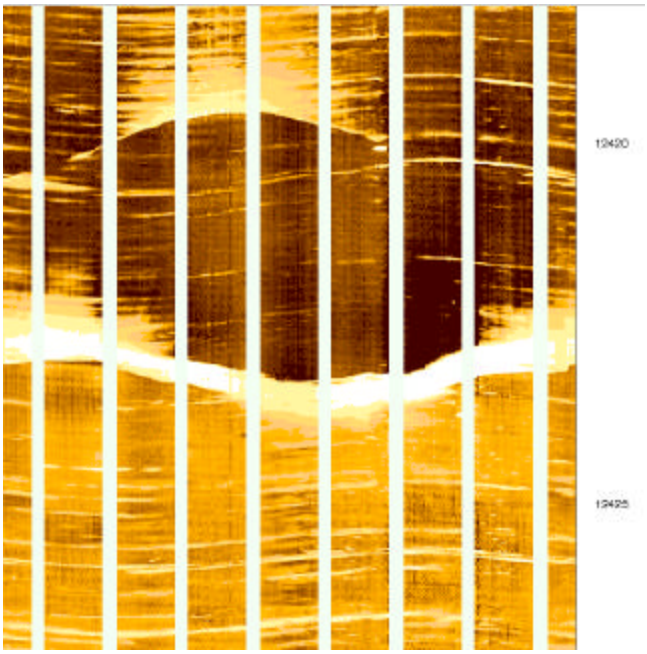

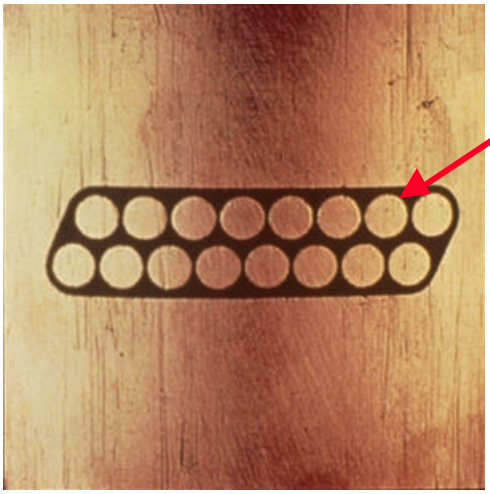

If one dead or intermittent button, then the two overlapping buttons on the other row “cover” the gap.

Equalization

The primary purpose of equalization is to statistically modify the data from each individual button in such a manner that each button will have essentially the same resistivity response as all the others. Raw button values from the tool will often exhibit varying responses to a given resistivity. One button may operate with a slight offset, while other buttons produce values with different magnitudes. Tool design limitations do not allow for the independent calibration of each button; to compensate for this variation in tool response, button-to-button equalization processing is performed on the data.

The equalization done in BOREID uses a moving window type of processing. At any particular instant, all button data within an analyst-defined vertical window is considered. After completing the equalization over this section of data, BOREID moves up by an analyst-defined step length and then equalizes this section of log. This process is repeated until the program has stepped through all the data. By using reasonable window lengths and by setting the step interval to retain a large overlap with the previous window position, it is possible to maintain consistent results over the entire length of log. To further aid the equalization process, only trimmed statistics from the data window are used. In practice, this means that data from the extreme ends of the data histogram are not allowed to influence the equalization. This is beneficial in that it excludes unusual data, i.e. from washouts and noise in low signal-to-noise regions. The primary intent is to have only data from the rock matrix drive the equalization processing. This type of processing often improves the contrast between pads when one or two pads are not making good contact with the borehole. A window of 15 ft. is normally chosen to keep the effects of small scale variations from affecting the large scale equalization corrections.

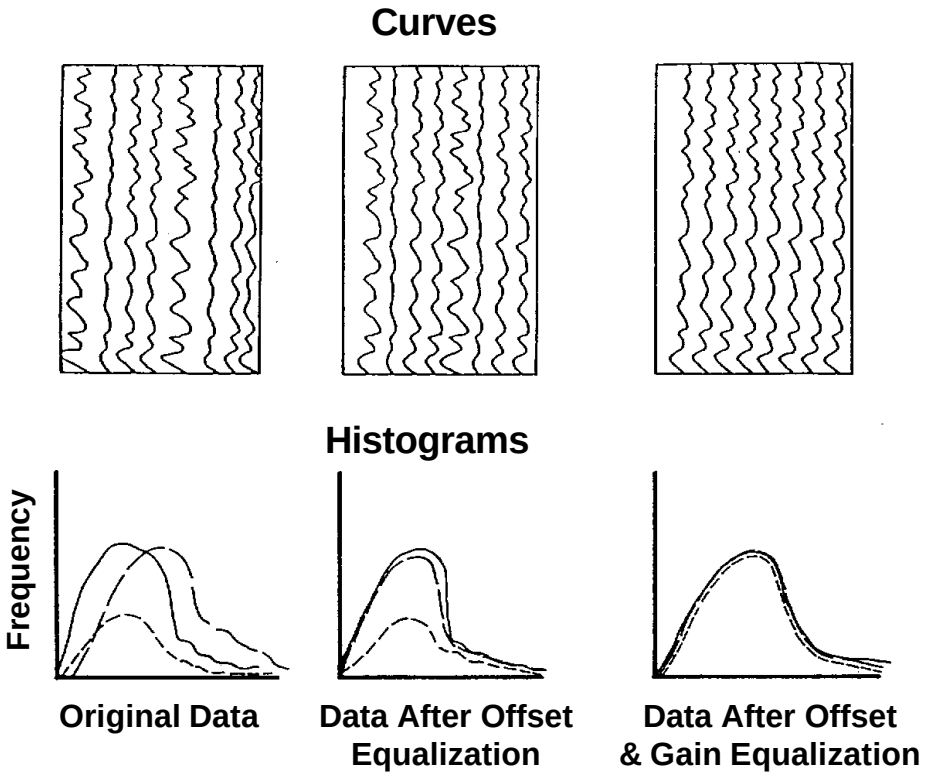

EMEX Correction

While logging, the FMS tool will continuously adjust the level of current it is putting into the formation to maintain an adequate signal response regardless of the formation resistivity. To retain the proportionality between FMS data and formation conductivity, a correction must be made to account for the variations in focusing current. One of the recorded measurements of the tool is EMEX voltage, which preserves the degree of compensation being applied to the tool at any time. Although EMEX correction does not normally result in dramatic changes in the images, it is needed to maintain the link between FMS data and traditional resistivity logs.

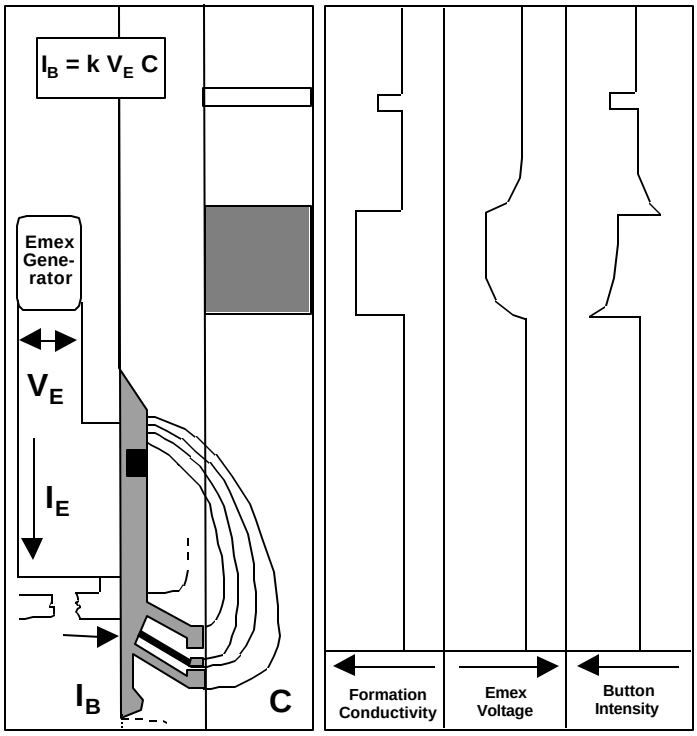

Image Enhancement

BORNOR is a program for performing a dynamic normalization of the data which results in an enhancement of the local contrast of the images. Often we are most interested in the shape or spatial geometry of features, for instance, when trying to fit a plane through an interface to determine dip. A technique similar to that shown in the adjacent figure is used to repartition all the data within a shore vertical window, normally 1.0 ft. If the data originally had a narrow range, i.e., little variation in color, the process of splitting it up into several classes brings out any small variations in formation resistivity that the tool measured. The dynamic range of the FMS tool is quite broad and methods such as BORNOR are needed to exploit that sensitivity when trying to enhance a particular feature or to display the data onto hardcopy devices that have only a limited number of gray levels or colors available. Image enhancement is a frequent process when interactively working with FMS images on the Image Examiner Workstation. Here the user has control of the enhancement by selecting only a portion of the image to be used on the basis for redistributing the color spectrum. In some cases it is desirable to enhance only a selected feature such as a fracture or vuggy porosity. An extreme form of enhancement called binarization is often used. Generally done on the workstation, the analyst will set a resistivity value and all values less than this threshold will be black and all values greater will appear as white. This way a fracture will stand out as a black image on a white background.

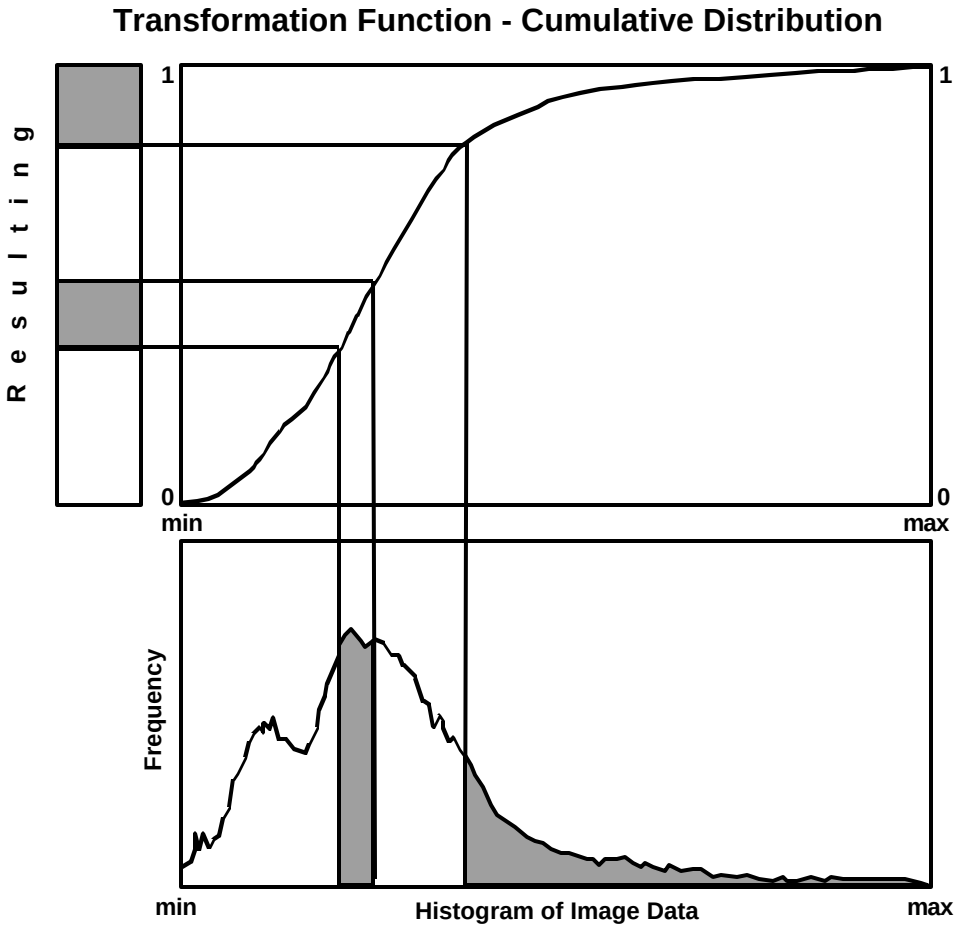

Static vs. Dynamic (Equalized vs. Enhanced) Images

The adjacent figure presents the same data processed by two different means. The image on the left has been processed through EMEX correction and equalization which is a static processing. The right-hand image has additionally been through BORNOR to produce an enhanced image which is a dynamic processing. On this display, the images are plotted azimuthally, i.e., it is as if we are inside the borehole looking at the images, then cut this cylinder at North and rolled it flat.

It should be apparent that the DYNAMIC image shows more detail than the other image. If we were looking to pick dips from particular bedding interfaces, count thin beds in a sequence, or look for any subtle variations, the ENHANCED version would be easiest to use. However, if we want to examine resistivity differences between zones, distinguish open fractures from healed or minor fractures, or even correlate to other logs, it is more convenient to use the STATIC images.. The two processes complement each other and should be used together.

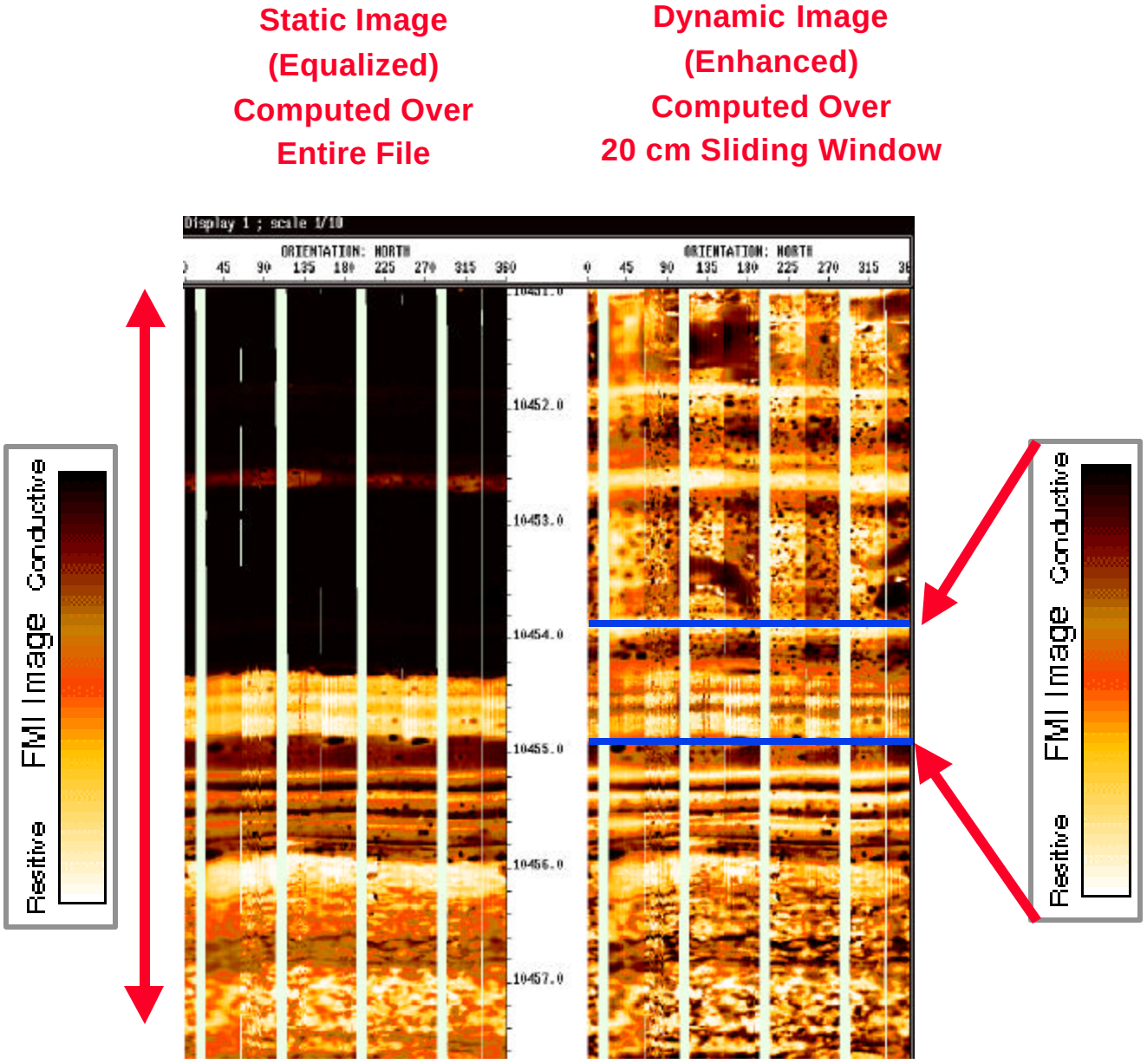

BORSCA - FMS Matched to Resistivity

The need for a "calibrated" FMS resistivity has often been stated. The original system of uncalibrated button levels and random gray scales for the images limits the application of the tool. It is difficult to compare FMS logs run on offset wells, and often between passes on the same well. Also, efforts to quantify sand counts and determine open versus healed fractures are hampered by the standard statistical scaling of the buttons.

The BORSCA processing option, the direct descendant of the original FMSRES Program provides a technique to match the conductivities of the FMS buttons to the conductivity of a SFL (Spherically Focused Log) or Laterolog Shallow (LLS) run over the same interval as the FMS. Techniques of resolution matching and least- squares fitting are employed. The resulting resistivity-normalized buttons will then allow the use of consistent scales between passes and multiple wells, which will allow meaningful comparisons and production predictions to be made. Also, reservoir delineation and sand counts should be much more consistent.

Considerable effort has gone into making this module reliable and flexible. The analyst can exclude sections of log from the calibration process which prevents random events such as washouts from biasing the results.

Processing Theory and Technique

The processing begins by generating a single curve from the four-pads of the FMS that has vertical and lateral attributes similar to an SFL measurement. This is accomplished by vertically filtering and laterally averaging the FMS image files. The single FMS curve is then matched to the SFL curve over the logged interval, using a least-squares fitting technique. The coefficients obtained from this fit are then applied to the unfiltered FMS image files. These files can then be displayed with LGG or FLIP using meaningful gray scales. High resolution resistivities can also be output at appropriate sample rates for further processing in Laminated Sand Analysis (LSA) or other high resolution applications.

Over a given section of hole, the appearance of a calibrated image may be similar to the uncalibrated version, or it could look drastically different depending on the range and values of resistivity encountered. If the original data spanned a broad range of resistivities and are mapped across the available spectrum, then calibration will probably shift the color classes only slightly. One the other hand, if the data came from a single formation or short interval that has only a narrow range of resistivities, statistical processing may cause the uncalibrated images to appear to span the entire spectrum, whereas the calibrated values will remain in a narrow range of colors. By tying the images to an absolute scale, we are able to compare separate intervals within a single well and to analyze zones from different wells, all within a consistent, independent framework.

Static versus Resistivity Matched

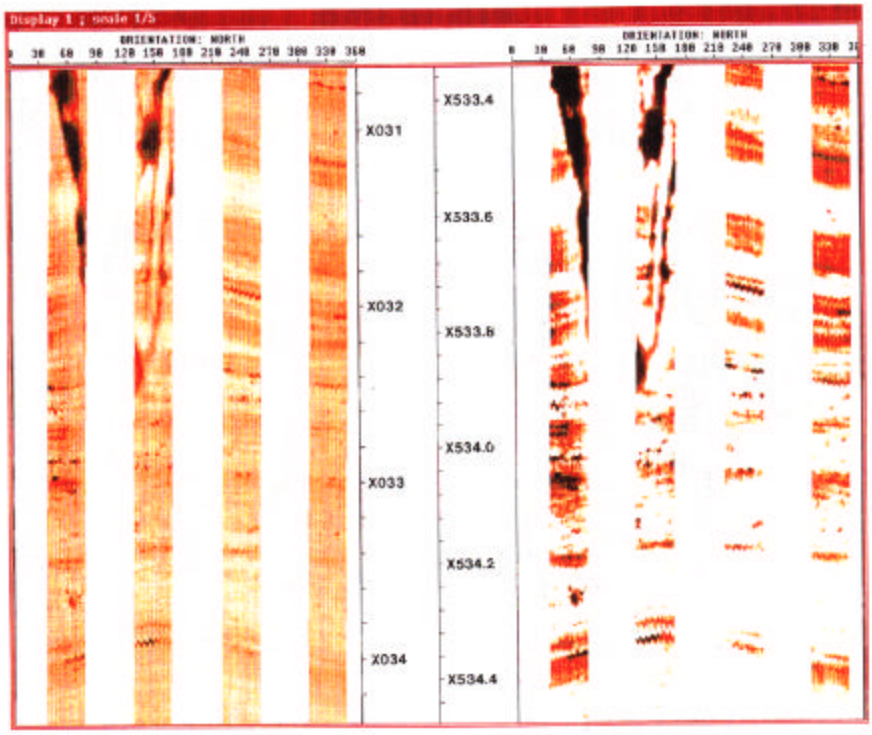

Static **Resistivity Matched**

Threshold Process

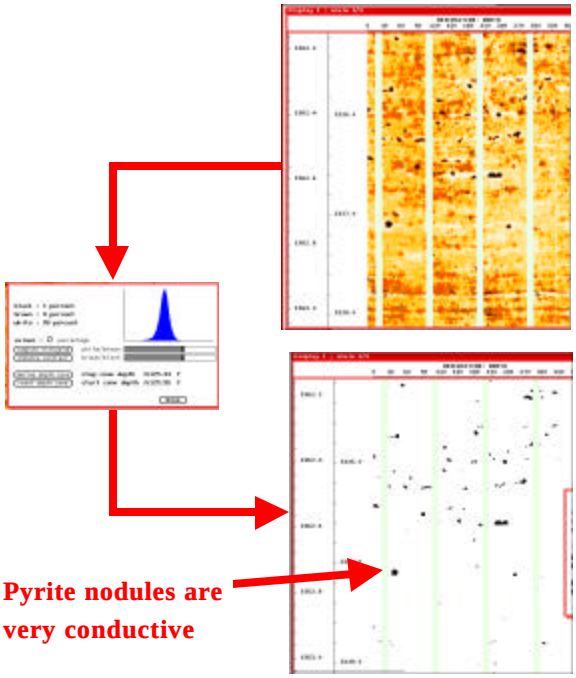

Original Static Image

Threshold Image

Pyrite nodules are very conductive

Resistivity Measurement

Electrical images are resistivity measurements. The color presentation represents changes in the resistivity of the formation in front of the pad. This may be influenced by the lithology, the shale content, and the fluid contained within the porosity. The images shown below illustrate these resistivity changes. The dark colors at the top of the sand and at the base represent the conductive shale which encases the sand. The bottom of the sand contains saltwater in the porosity which results in a low resistivity response. There is a dramatic change at the oil/water contact. Resistive oil has replaced the conductive salt water above this point which changes the image color to white. There is also a textural change in the sand. The dark bedding shown above the oil/water contact is caused by shale in a fining upward sequence.

Channel Sand

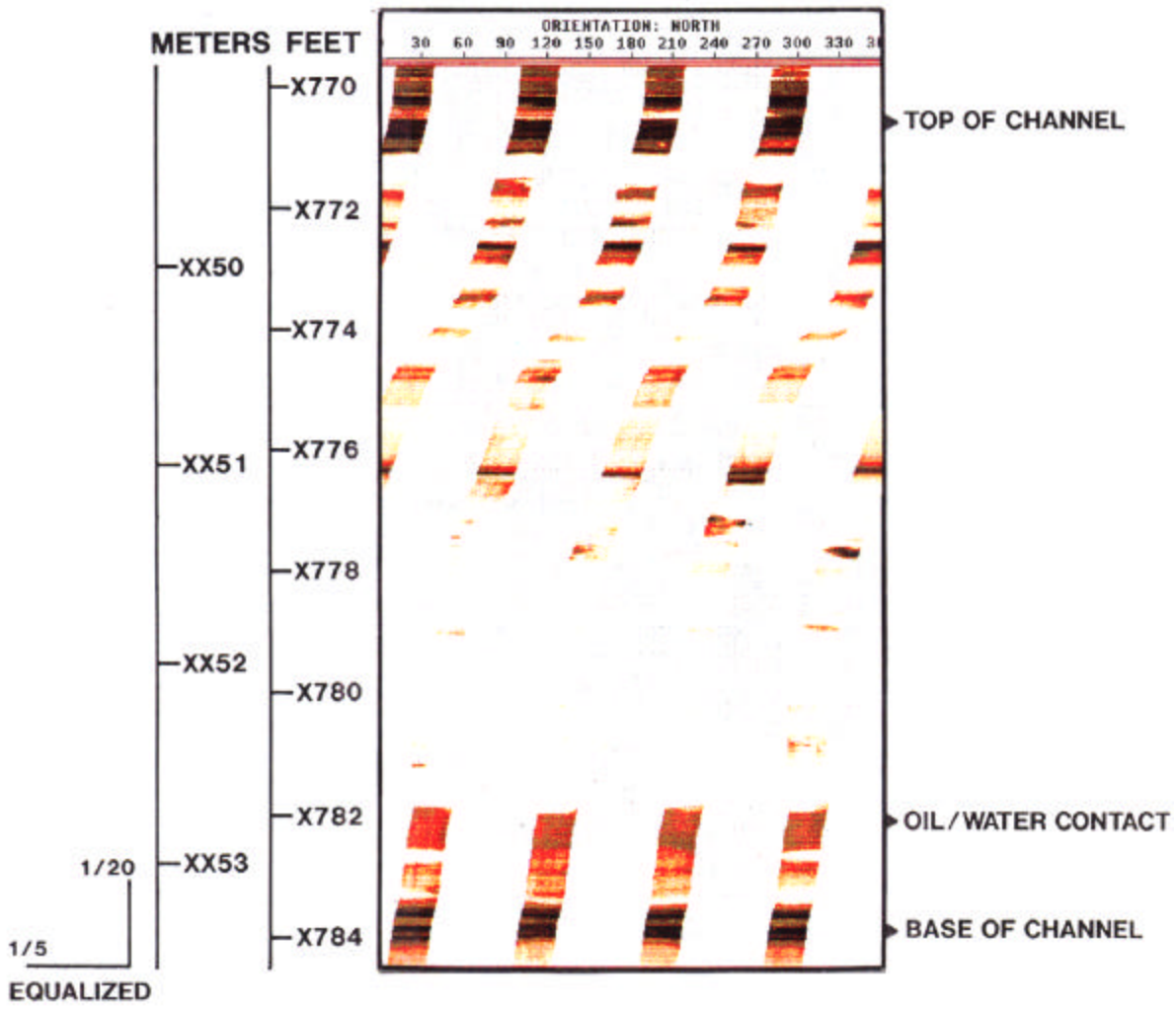

Color Options

Images can be presented using a variety of color scales. The yellow option is by far the most popular. Under this system the most resistive zones are white, but then progressing through yellow, red, brown, and black as the resistivity decreases. Color hardcopy plots will normally use this yellow color scheme, although it is possible to generate plots based on several color palettes.

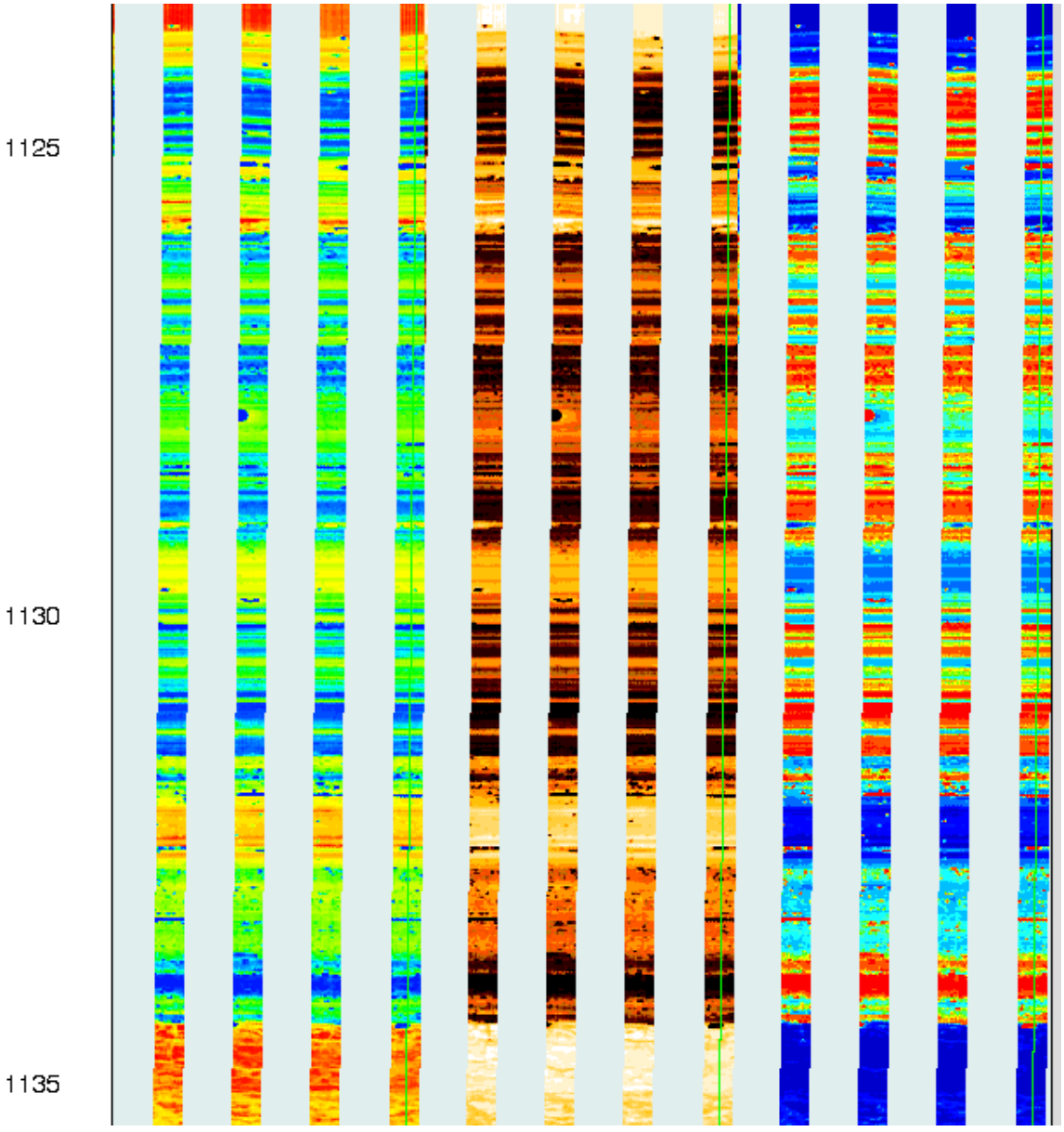

Straight vs. Azimuthal Plots

More and more we have come to view the azimuthal display as our "standard" plot. It provides an effective means of visualizing the orientation of beds and other features, such as fractures, and it is a convenient means of displaying data from multiple passes. An obsolete form of presentation is the "straight" plot option that was used to display images from the original 2 pad FMS tool. The images presented in the figure below are from right to left:

pad #4 Wiggle Trace

pad #4 Equalized Image

pad #4 Enhanced Image

pad #3 Enhanced Image

pad #3 Equalized Image

pad #3 Wiggle Trace

with each being plotted vertically, i.e., no orientation is included although it can be determined from the short-tail on the borehole drift tadpole, which gives the direction of pad #1. Although the straight plot allows several views of the data, it became too restrictive when trying to display data from a four or eight pad tools or from multiple logging passes.

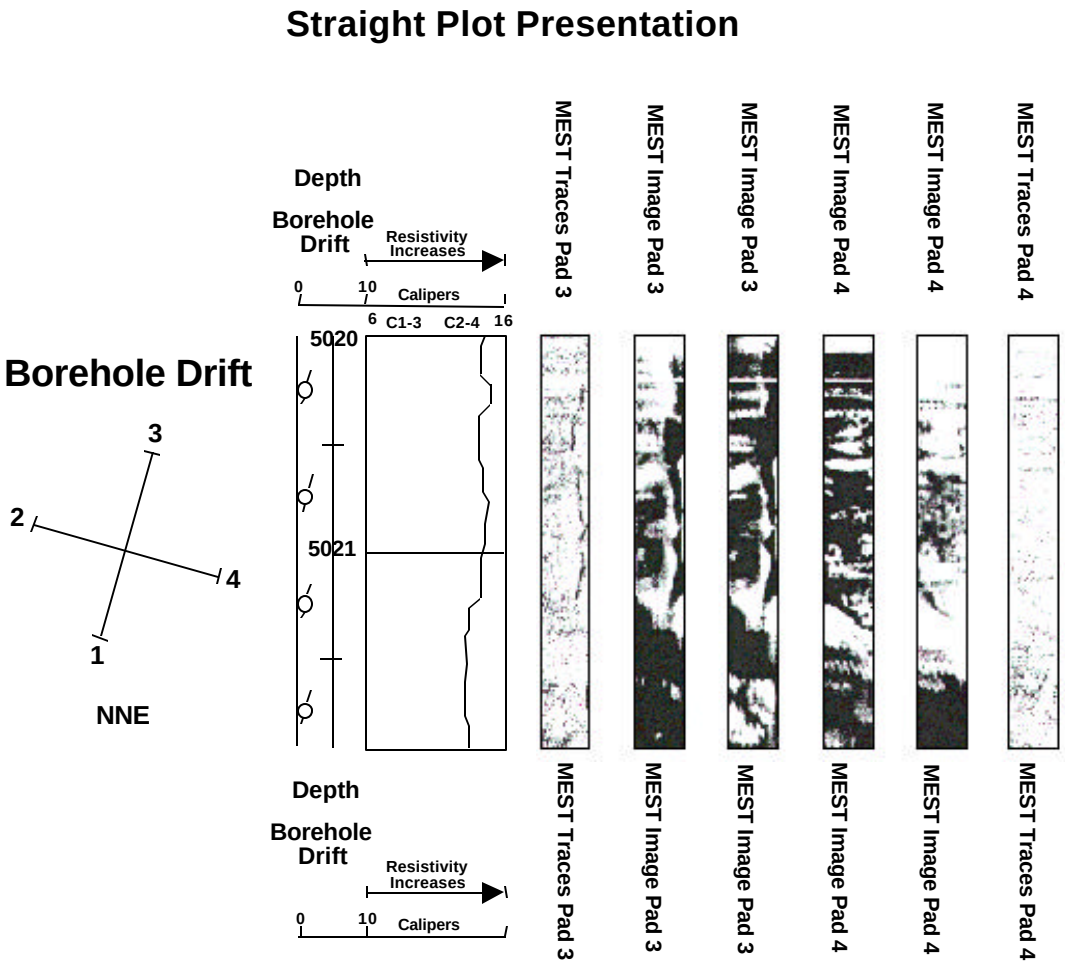

Standard Plots

For a quick review, the types of plots we see most often are:

- Straight plots (below): Most useful for examining different aspects of the same data, particularly with the two-pad tool.
- Azimuthal Plot (top p. 24): Best for correlation and general use, especially if it has been calibrated to a SFL or MicroSFL.
- Azimuthal Plot (bottom p. 24): Enhancement bring out the most detail from images, but distorts comparisons between fractures and between different zones.

Straight Plot

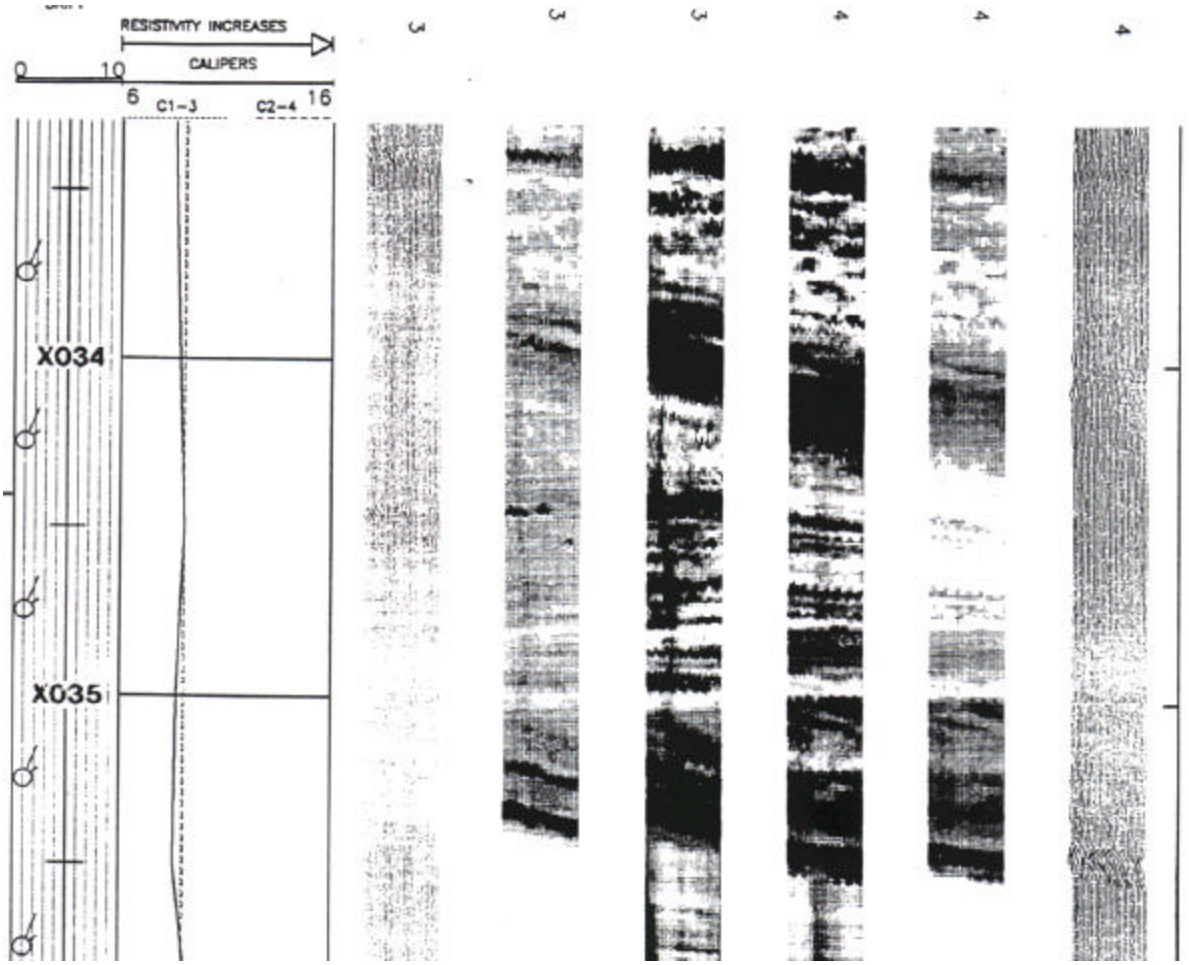

Scales

Normally, the vertical and horizontal scales are chosen to be the same. This yields an image presentation with a true aspect ratio and does not distort the apparent dip magnitudes. Occasionally, it is advantageous to present the data in an expanded or condensed scale to allow an easier interpretation. The presentation below shows the effect of scale changes. The image on the left is presented on a 1/40 vertical scale and a 1/5 horizontal scale. This flattens the apparent dip but allows an overview of the formation. The middle display is presented on a 1/5 vertical and a 1/5 horizontal scale. The dips are shown in their true apparent position. The display on the right is presented on a 1/5 vertical and a 1/10 horizontal scale.

Electrical Images

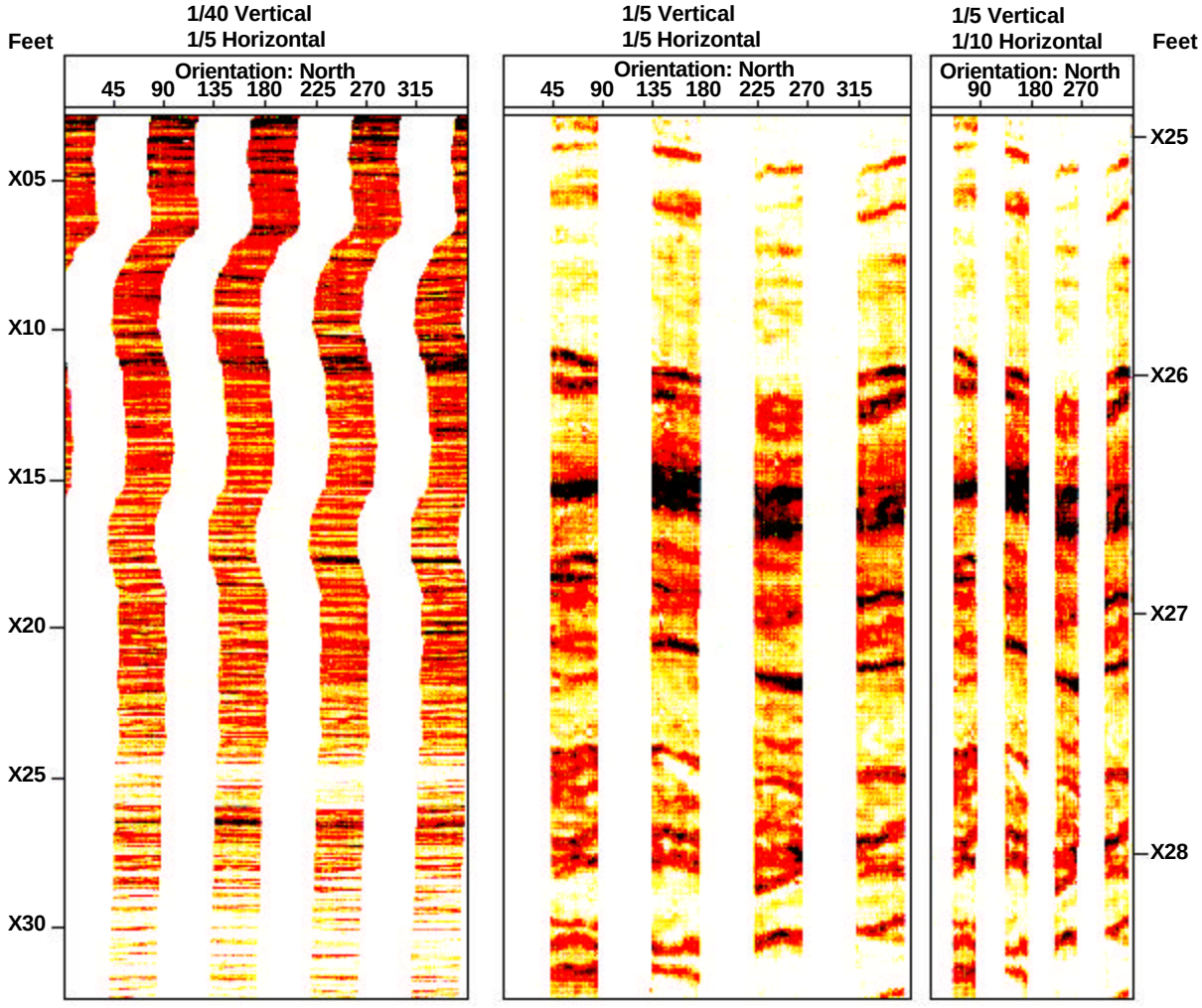

Dip Computation Methods

Objective of this Chapter is to show the various methods of dip computations. Dips may be computed from dipmeter processing or from manual picks.

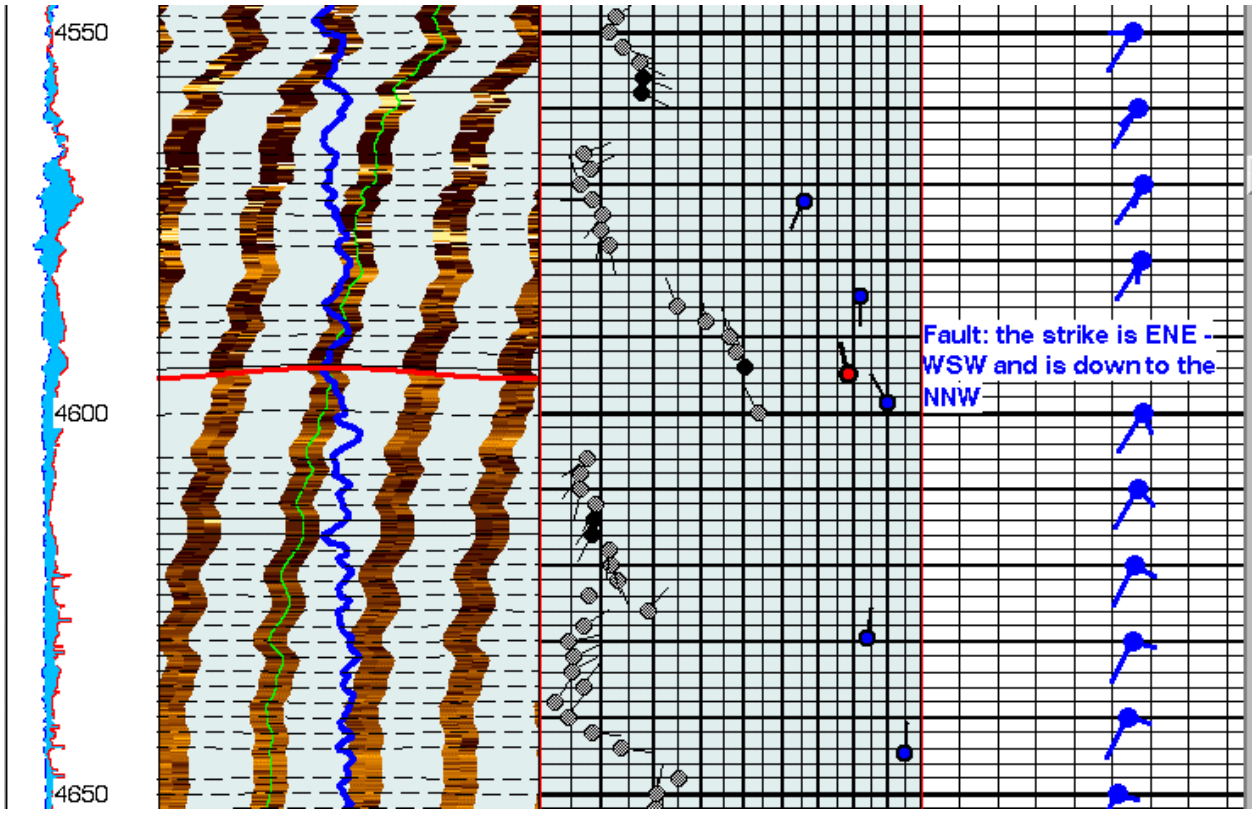

The Tadpole

The basic method of presentation of computed dip answers is the arrow or tadpole plot. Each tadpole consists of a dot with an attached headless arrow or tail. The computed dipmeter result is composed of many, often thousands, of tadpoles. From the tadpoles it is possible to recognize changes in dip and direction up and down the well.

The Dipmeter Tool

The dipmeter makes measurements enabling us to compute the dip of bedding planes. Computing these dips requires the following information:

1. The relative position of 3 points on the plane.
2. Orientation of the tool.
3. Angle and Direction of deviation of the tool.

Defining the Plane:

Points on the same bedding plane are located by correlating high-resolution conductivity curves from pads at known positions on the borehole wall. The figure below demonstrates a borehole intersected by a thin, steeply dipping bedding plane. The plane is resistive, relative to the formations above and below. The four pads continuously record a conductivity or dip curve as the tool is pulled up the borehole. As each pad passes the intersection of the resistive bed with the borehole wall, the corresponding dip curve shows a change in the conductivity. The dip or slope of the bedding plane causes the pads to encounter and record the change in resistivity at different depths on the log. The difference in depth, or shift, of corresponding peaks on the curves allow the dip of the bedding plane to be calculated trigonometrically.

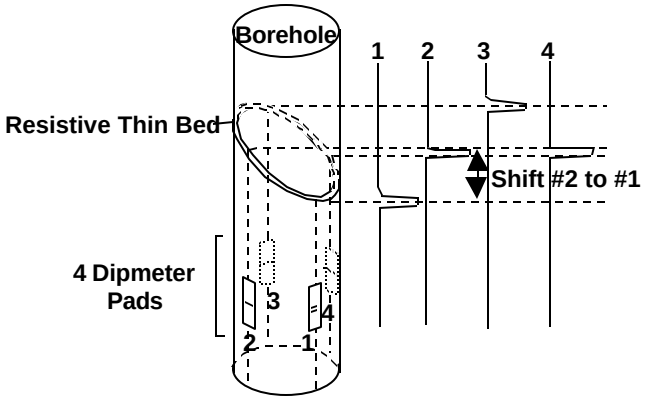

The Calipers:

To accurately place the curves relative to each other in space, we must know the distance between opposing pads in a pair. These data are supplied by the two caliper measurements. Boreholes are frequently out-of-round, and the corresponding caliper configuration will resemble the figure below.

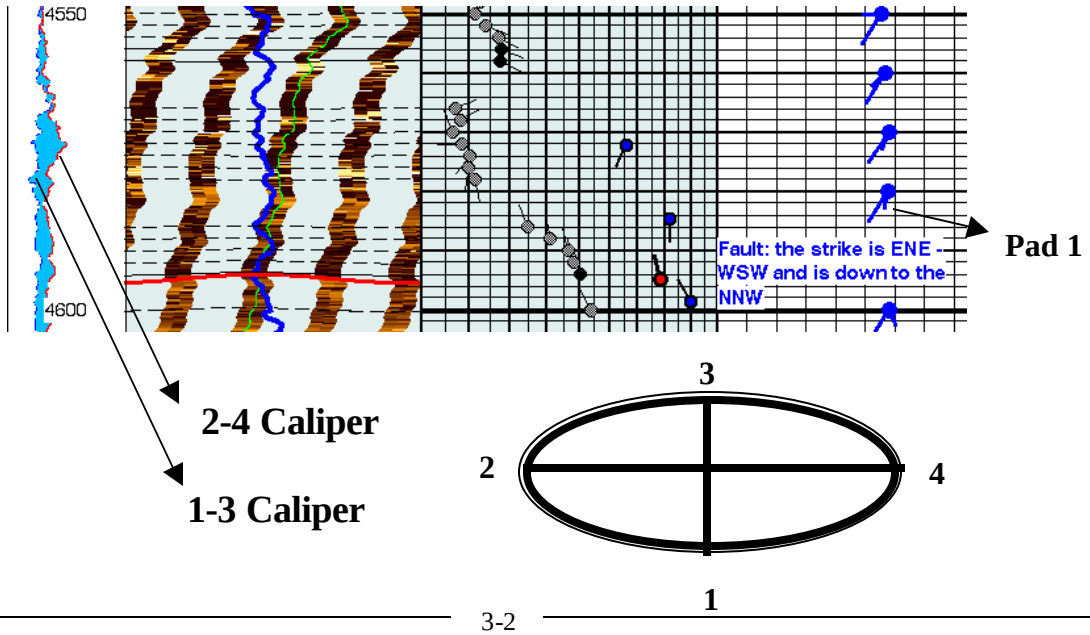

By measuring the displacement of the event between each of the curves and knowing the precise depth scale, the actual displacement may be read in inches or fractions of inches of borehole. The dip angle relative to the plane of the electrodes can be calculated trigonometrically. Hole deviation and direction, orientation of the number one pad, the true dip angle and direction relative to a horizontal plane can also be calculated.

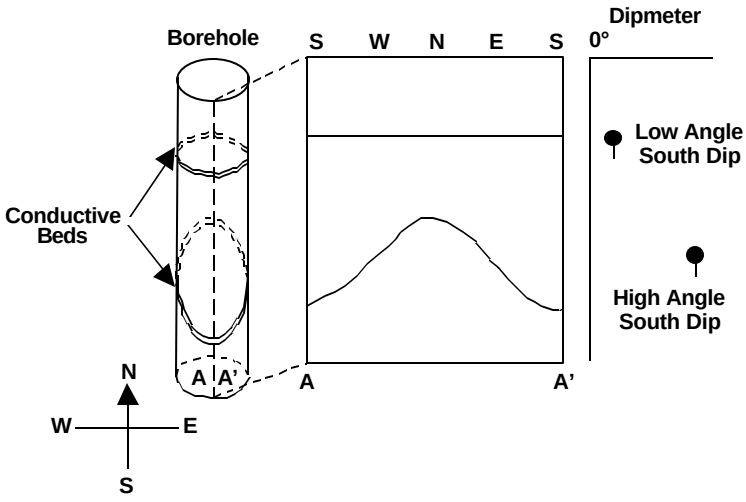

Speed Correction

The rate at which the cable supporting the tool is wound on the logging unit is always measured, and for most logs it is sufficient to assume that the logging tool is moving at the same rate as the cable at the surface, except where the hole is unusually sticky. As a result, the velocity of the tool is not uniform and will alternatingly accelerate and decelerate with changes in friction. A system using the downhole accelerometer data is used to provide a speed correction for tool velocity changes. Even small changes in tool velocity, if left uncorrected, could produce large errors in the accuracy and detail of the conductivity curves. This is demonstrated in the figure below.

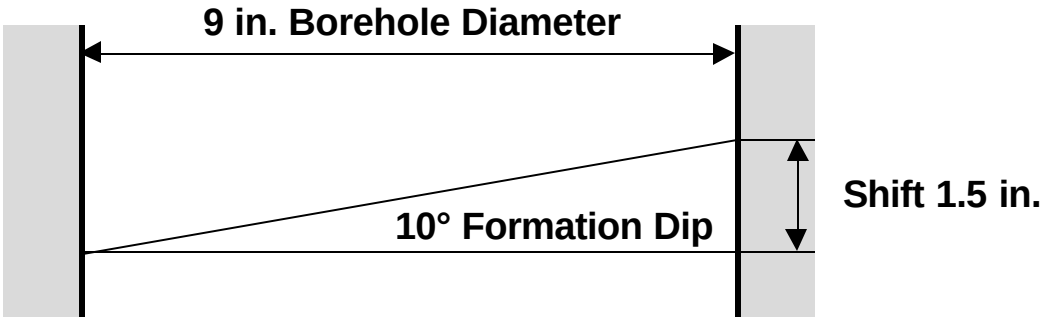

If the tool moves at 80% of the cable speed, the computed dip is 12.4 ° rather than 10 °.

If the tool moves 1.5 times the cable speed, the computed dip is 6.7 ° rather than 10 °.

Shifts in Dip Curves

The four curves at the bottom of the page are quite similar. The shifts between curves are measured in inches or fractions of inches. These shifts result from bedding planes intersecting the 8-inch-diameter borehole at an angle of approximately 30°. This angle is the apparent dip, as shown on the figure. Apparent dip is a function of formation dip and deviation.

High Resolution Measurements

Because even 1° of structural dip may be significant in determining the location of oil or gas traps, it is essential to record dip curves of very high detail. For example, apparent dip of 1° will cause a shift of 0.14 inches across an 8-in. hole. Focused dip curves sampled every 0.l-inch make it possible to measure shifts of this order.

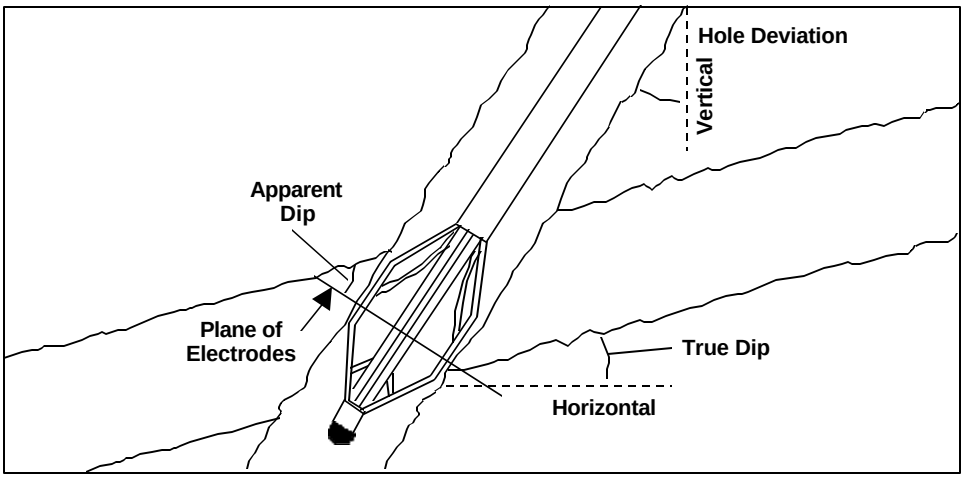

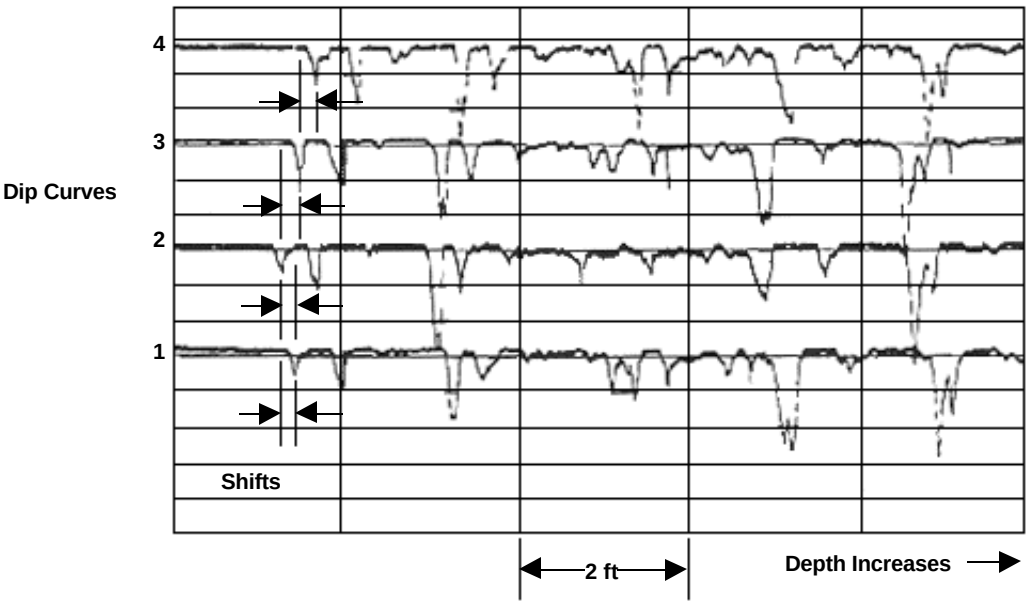

Orientation of Tool

The second type of information needed to compute dips is the orientation of the tool. To orient the computed dip geographically, the orientation of the tool with respect to north must be known. The azimuth of pad number one is measured for this purpose. A magnetometer is used to measure the angle between the number one pad and magnetic north. In some areas of the far north magnetic systems cannot work, and special gyroscopic dipmeter tools are used.

Azimuth

The terms **Azimuth #1, Pad 1Az**, or **P1AZ** noted on log headings are synonymous: and are defined as = Azimuth of #1 pad with respect to north.

Magnetic Declination

True north is the reference for the orientation of the tool. True north and magnetic north are frequently different; this difference is called magnetic declination. Maps showing current values of magnetic declination are available for all parts of the globe. The figure below is a map showing magnetic declination for the complete globe. At point A on the map magnetic north will be 20° east of due north; 20° must be added to the magnetic north bearing to obtain the orientation of the tool with respect to true north. East Declination refers to conditions where magnetic north is east of true north. East declination requires the declination value be added to the magnetic north azimuth measurement. West Declination refers to conditions where magnetic north is west of true north. West declination requires the declination value be subtracted from the magnetic north azimuth measurement.

Magnetic Declination

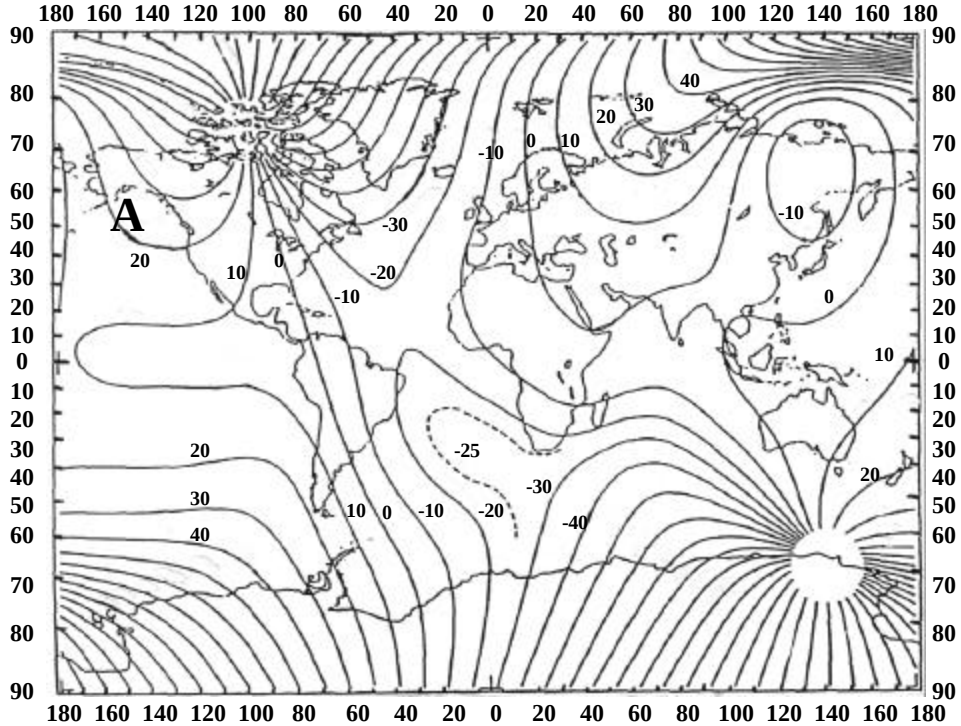

Dip Sensor Correlations

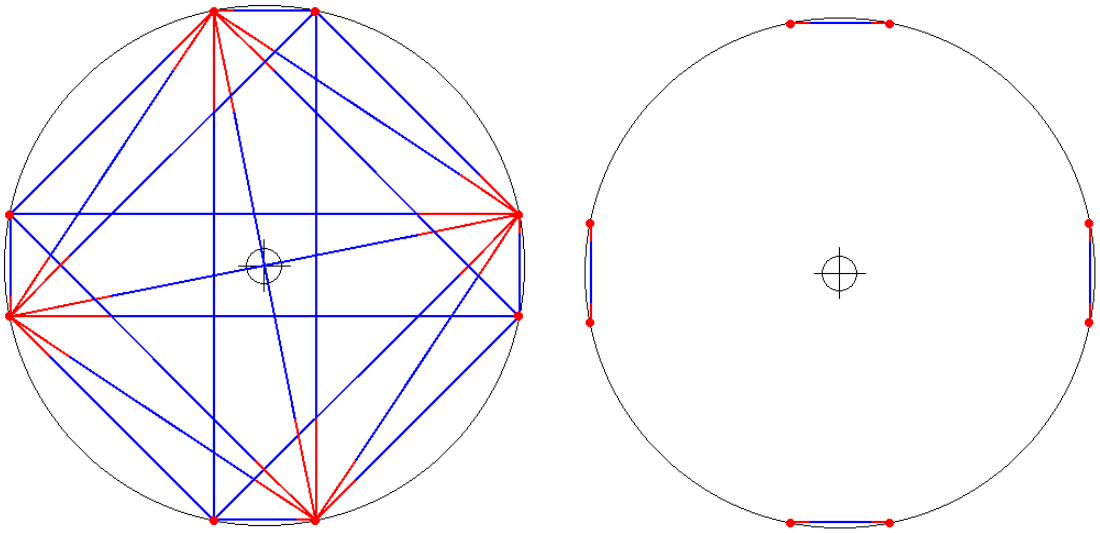

MSD **CSB**

MSD (Mean Square Dip) Correlates all eight curves in all combinations. This yields 28 displacements. The system likes high contrast planar events.

CSB (Continuous Side-by-Side) Correlates only the two curves of each pad and does not correlate between pads

This yields four dip vectors, one at each pad position. CSB dip is the three-dimensional vector result of individual pad dip vectors.

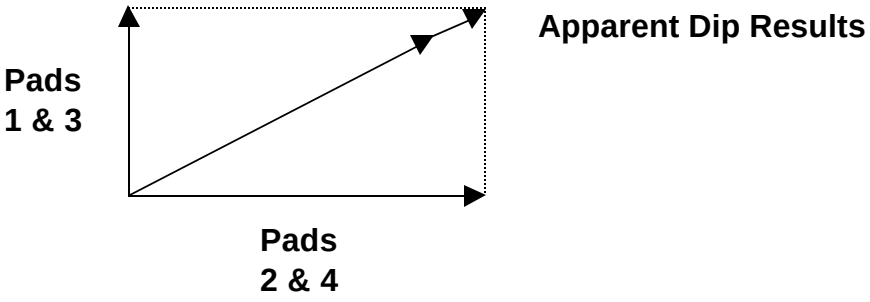

The system is better than MSD in very high dip, as well as in environments with very low contrast, such as cross-bedded sandstones.

Interval Correlation

One method used to obtain dip information from the raw data involves correlating intervals of the dip curves. To a mathematician, correlation coefficient is a measure of agreement between any two curves. Numerically, coefficients may run from zero, representing two completely dissimilar curves, to one, representing two identical curves. The following parameters must be selected:

Correlation Length

The computer calculates the similarity between a section of one curve and an equal section of another curve. The length of the interval on the first curve is the correlation length or interval. The computer then moves one of the curves by some small, preset increment and recomputes the coefficient This process is repeated many times. The correlogram is computed from the correlation coefficient at each step. The maximum coefficient is taken as the best fit of the curves, and the curve shift is taken at that point. The process is repeated for all curve pair combinations at that depth; the result is the relative position of correlated points around the borehole and a dip answer.

Step Length

The first curve is then shifted the step length, usually 25 to 50% of the correlation interval, and the process is repeated at the next level, resulting in another dip answer.

Search Angle

The range on the depth scale searched for correlations before the computer proceeds to another pair of curves at that interval.

After the computer has selected a set of correlations, the calculation of true dip angles is straightforward. Modern developments in data acquisition and machine correlation have improved the density and reliability of dip results far beyond earlier systems. The newer tools with eight or more correlation curves yield a high rate of redundancy for greater accuracy, confidence, and resolution. Much of this data is now available at the wellsite in a short time for timely decision making.

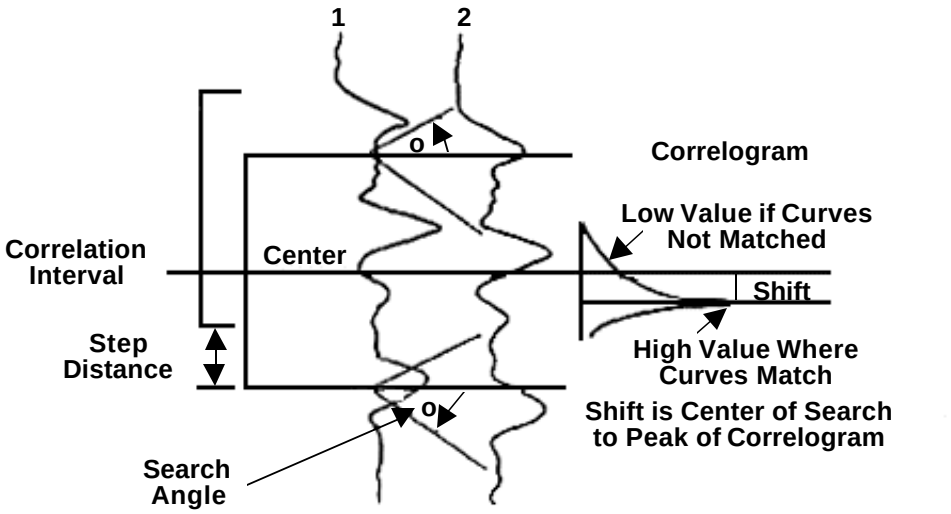

Dip Computations

The information recorded with the FMS tool contains not only the image button data, but also all of the inclinometry, caliper, and resistivity data that are available with the Stratigraphic High Resolution Dipmeter Tool (SHDT). It is then possible to run all of the standard dip computation programs that are used in analyzing SHDT data, as well as some other types of processing that are unique to the FMS. There are two primary types of traditional dip computations: mean square dip (MSD) and continuous side-by-side (CSB) computations.

Mean Square Dip

At any one depth level there are 28 possible cross correlations. The correlation method requires defining an interval length, a step, and a search angle. The MSD method considers the same depth interval on each curve and uses only the data within that interval to make correlations. In the case of low apparent dip it can be seen that nearly all the data points within the interval are considered when the correlation is made. As the apparent dip increases less and less points enter into the correlation. In areas where high dips, or high apparent dips because of deviated hole conditions, are expected, an initial displacement can be entered by the use of a "focusing" plane. This focusing plane can be chosen as either a fixed plane with orientation defined by the analyst or a plane defined from a previous dip calculation. The MSD program is primarily used to determine structural dip by finding strong planar events crossing the borehole. The button-button displacements are computed and the best-fit plane through them is found.

Continuous Side-by-Side

The CSB computation makes use of the correlations between the two dip buttons on each pad. There will be a great similarity between the two microresistivity curves recorded by each pad because the two measure buttons are separated by a small horizontal spacing. Each pair of microresistivity curves is cross-correlated using short correlation intervals, 12 in. or less, to produce a vector parallel to the dip plane. A similar vector from an adjacent pad combines to define a dip plane. The CSB program is responsive to the fine bedding structure of the formation, making it particularly effective for defining stratigraphic features. The close proximity of the buttons makes possible the measurement of very high dips, which are nor detected using pad-to-pad correlation. Such dips can then be used as input to the focusing option of the MSD program.

Computation Systems

There are three basic types of interpretation problems that users of dipmeter data may wish to solve. These three types of problems are:

Structural interpretation
Large-scale stratigraphic features
Maximum detail, very fine stratigraphic features

Often, it is desirable to interpret a combination of the above from a single dipmeter log. As a result, a variety of systems have evolved to handle widely different requirements. The most commonly used and generally applicable approach is the correlation interval system described in the earlier section. For the analysis of structure and large-scale sedimentary features, a 4-foot correlation interval and a 1-foot or 2-foot step is usually the first approach to analysis. For special applications or difficult logging conditions, other values of these parameters may be more useful.

Effects of Parameter Selection

For each step, a single dip answer is produced, and all the data within that correlation interval is used to obtain that single dip. A 4-foot interval may contain from 0 to 100 or more correlations due to bedding contrasts, but only a single dip is calculated, based on the best fit of the correlation curves.

Large correlation intervals tend to smooth the dip results.
Short correlation intervals allow the system to find more detailed results.

Comparing Correlation Intervals

The figure to the right contains a 75-foot section of dipmeter computed using several correlation intervals. Note that although the dip direction trend is similar in each, the implied cross-sectional view of the formation is significantly different.

Plot A (6”X3” CSB)
Plot A clearly shows detailed internal sedimentary structures with a much better suggestion of environment than do the other computations.
Plot B (2’X1’ MSD)
Plot B retains much of the character of Plot A but with some apparent averaging and smoothing at dip magnitude boundaries.
Plot C (4’X2’ MSD)
Plot C suggests more large-scale features. This plot fails to indicate the more complex internal sedimentary structures evident on plot A.
Plot D (8’X4’ MSD)
Plot D shows only large-scale features.

Conclusion

The choice of the computation parameters should be influenced by the type of information required to support exploration and production programs.

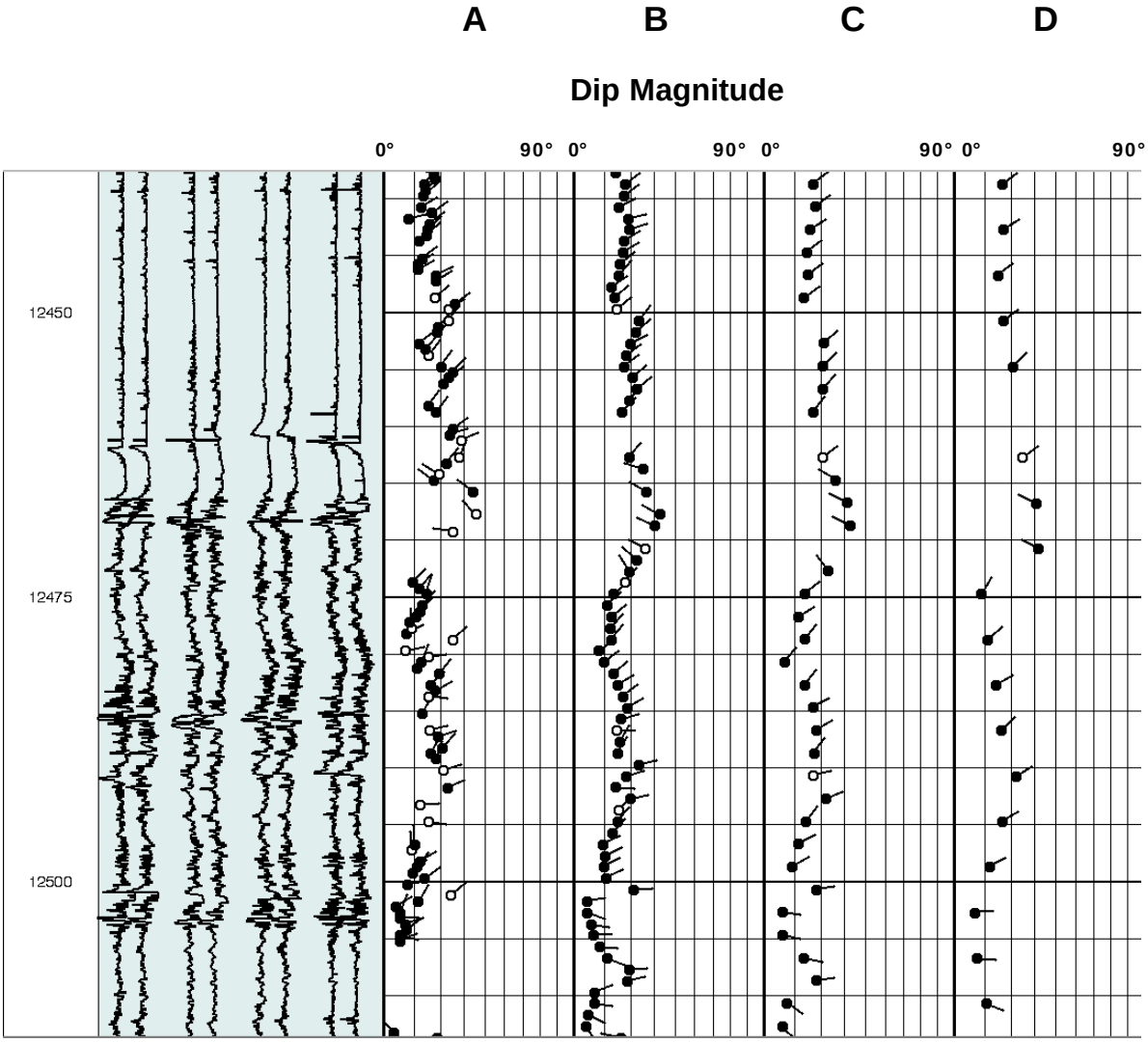

	A	B	C	D
Correlation Length	**6 in.**	**24 in.**	**48 in.**	**96 in.**
Step Length	**2 in.**	**12 in.**	**24 in.**	**48 in.**

Below is an example of a 4'X2' MSD computation over a short section with the dip sinusoids superimposed on the dip curves. It is important to note that although the computed dips follow the general character of the dip curves they do not relate directly to any particular event. The dip computed by an interval correlation method represents the best correlation of the dip curves as seen within the correlation window. Therefore the dip computed is a statistical measure of the dips of all the surfaces within the correlation window. To determine the dip of a specific surface, i.e. a fault plane or scour surface, it is necessary to pick the dip manually.

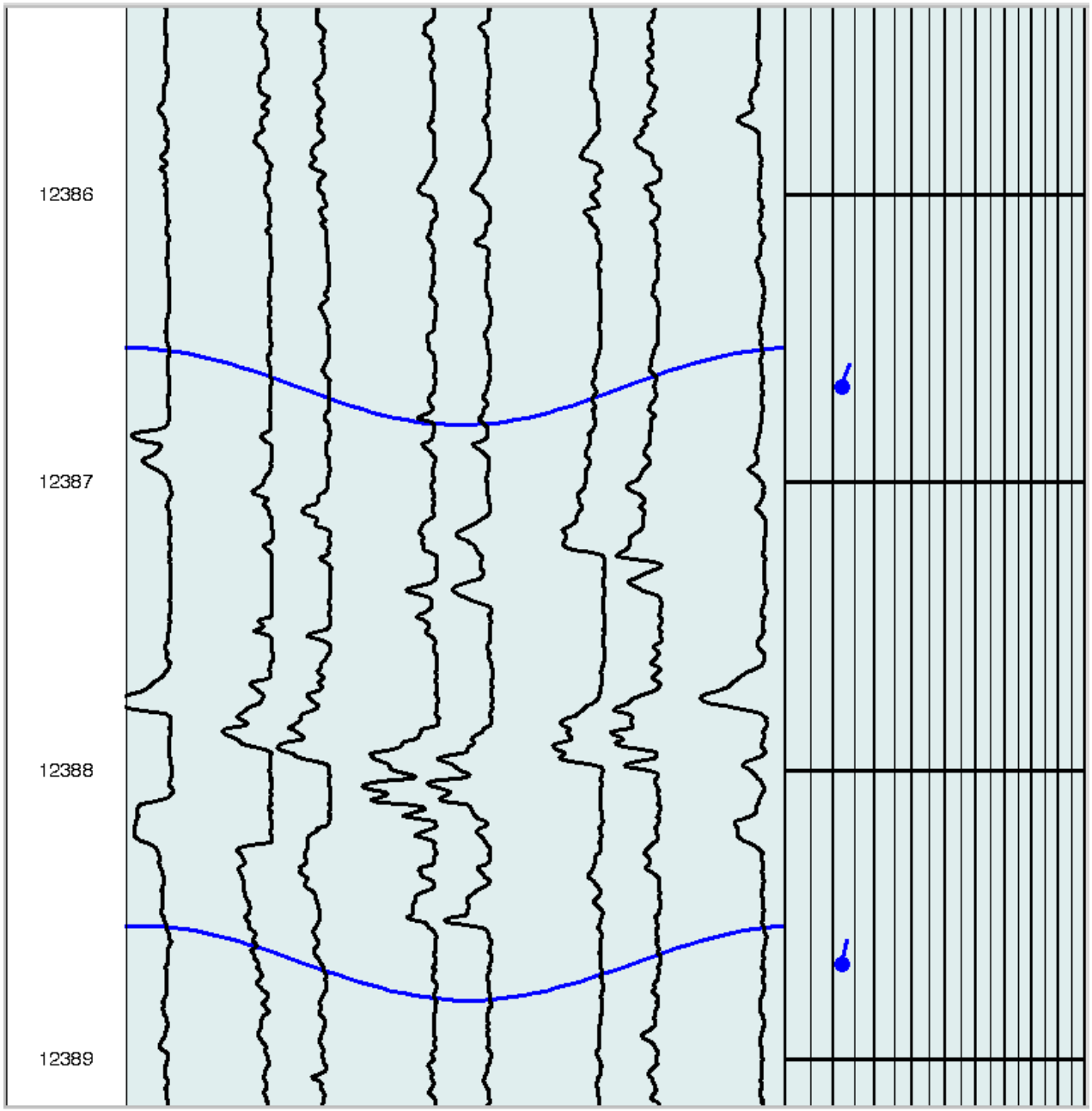

In the plot below, the images from the FMI have been added in the background. Automated dip computations using only the dipmeter curves can give a good statistical representation of the features seen by the tool. However there is a wealth of additional information contained in the images which can only be exploited fully by manually picking dips interactively.

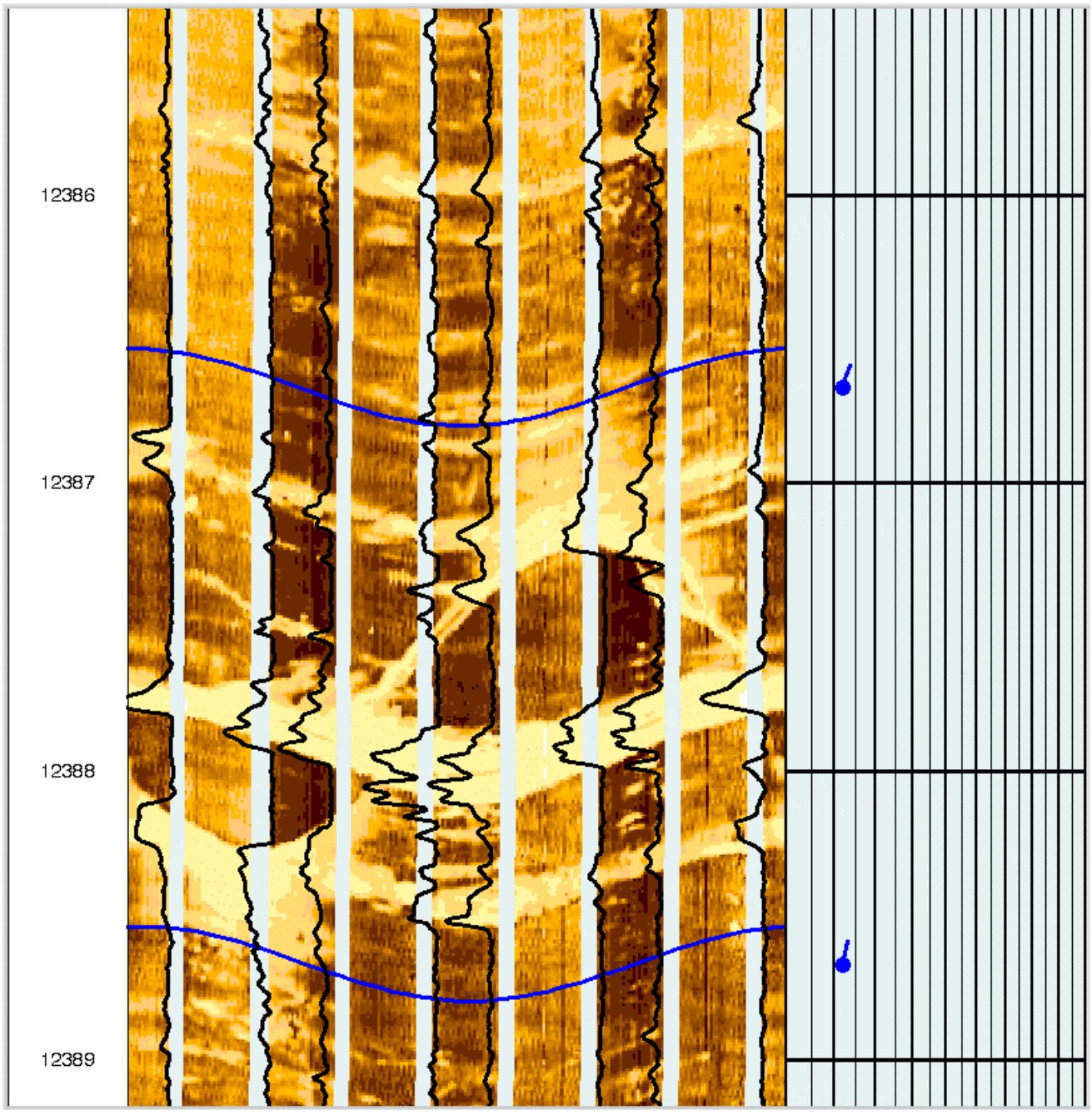

The red tadpoles added into the plot below are from a 12”X6” MSD computation. Note the increased detail produced by the shorter correlation interval. Also note that the dips computed at any particular depth are not identical because different portions of the curves were used in the computation. The blue tadpoles were generated by correlating 4’ sections of the data while only 1’ of data was used to compute the red tadpoles.

On the following page, some additional dips, shown in green, have been picked manually. Unusual events such as the high amplitude fracture are often difficult to compute by automated means.

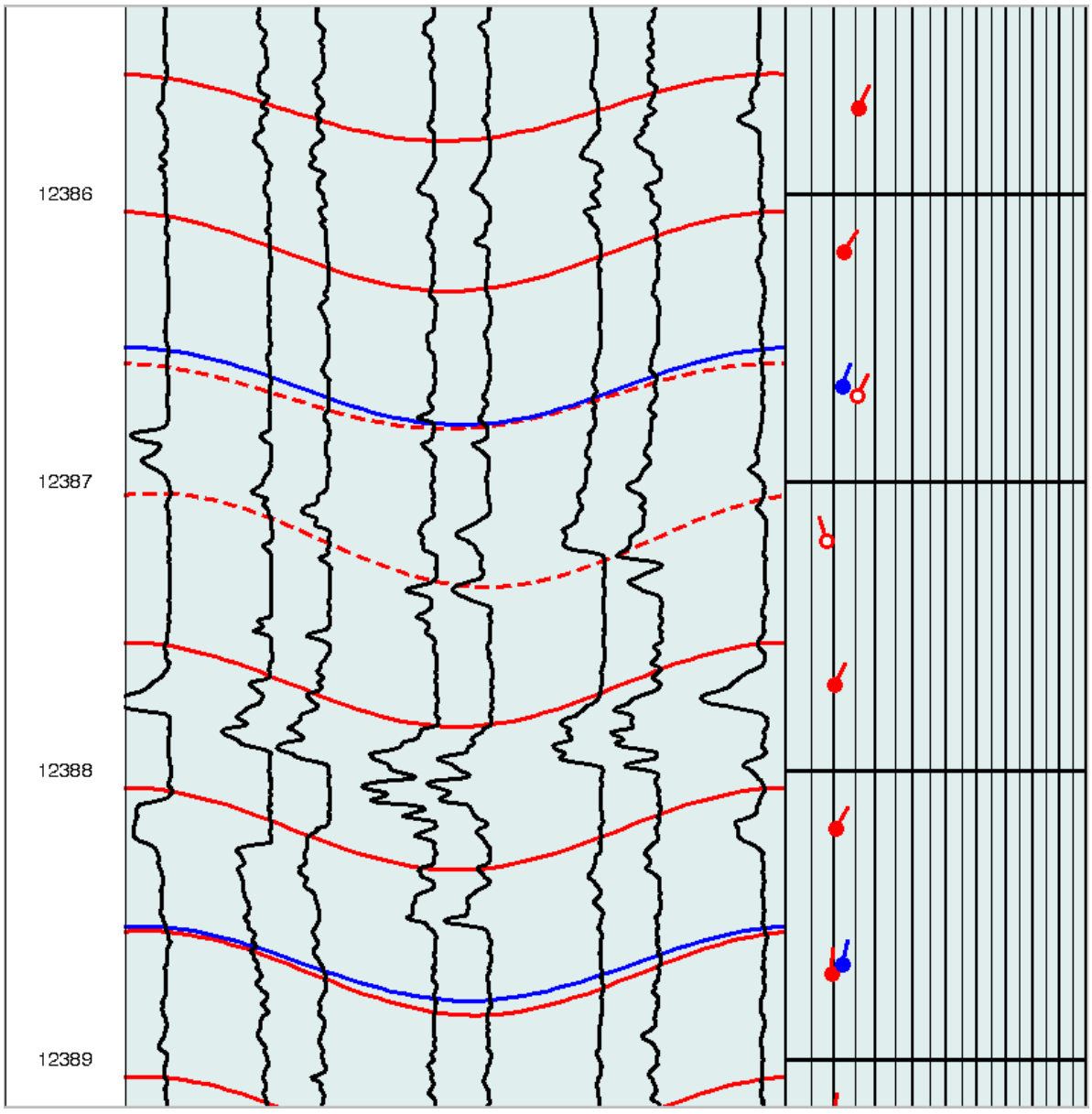

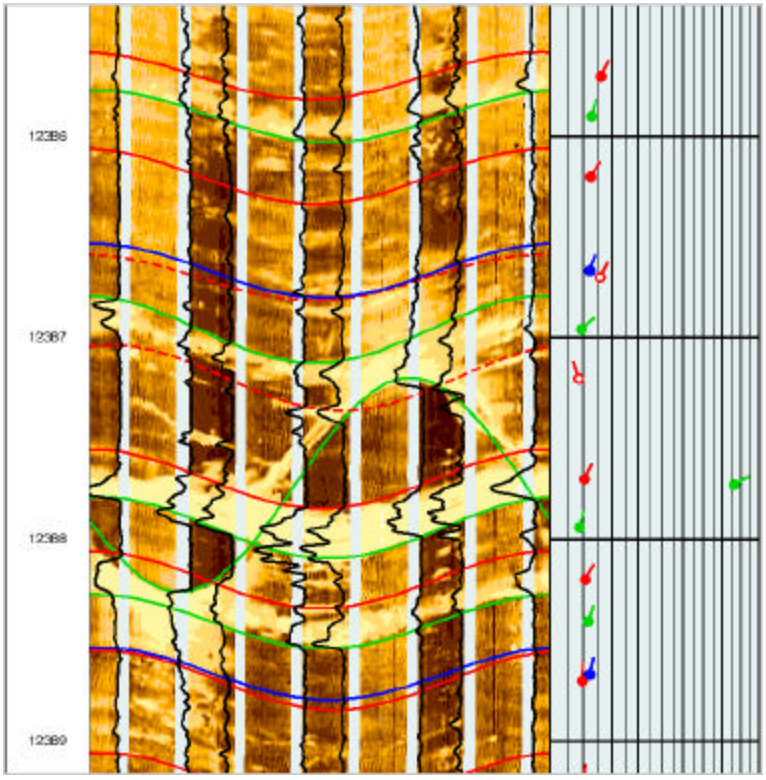
12386
12387
12388
12389

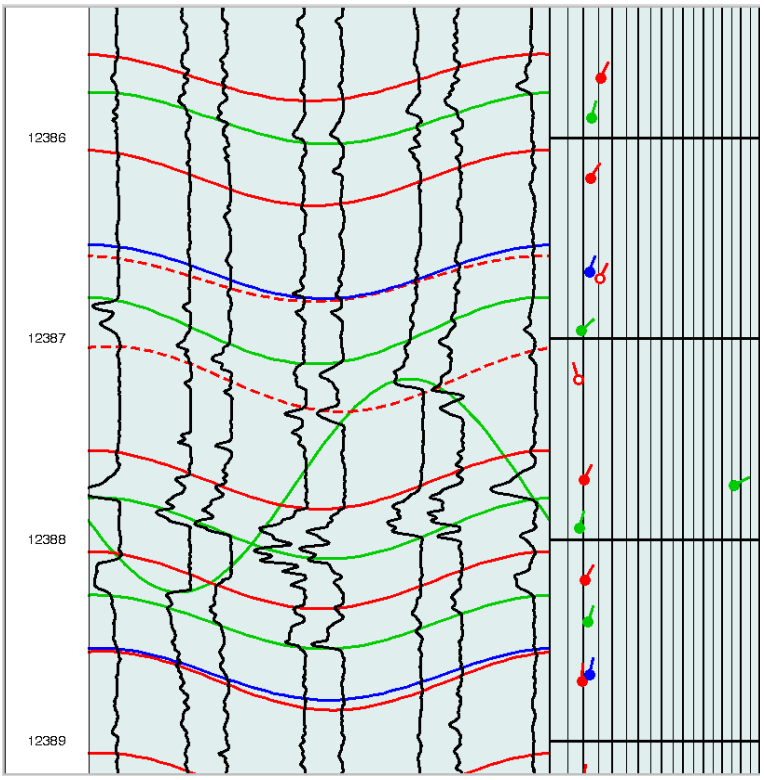
12386
12387
12388
12389

Dip Computation

In essence, the computation of dip values is simply the description of the orientation of a plan that best fits the interface in which we are interested. To describe this orientation, we traditionally use two angles. ***Dip magnitude*** is the angle between a horizontal plane and the lower side of the dip plane. This represents the magnitude of the downward tilt of the plane. The other angle used in called the ***dip azimuth*** , which is the compass direction toward the lowest point of intersection of the dip plane and the borehole cylinder. Dip azimuth is then the direction of maximum downward dip.

Computers can use any number of methods to internally represent dip orientation. However, a human being usually needs a graphical representation of the data to fully visualize the geometry of a problem. When manually calculating dips from images, either on the workstation or from azimuthal hardcopy plots, we are not looking at a cylinder with a plane cutting through it. As seen in the figure to the right, we cut the borehole cylinder along one direction, usually at North, and unroll it. **The dip plane that cuts through the cylinder now appears as a sine wave.** The magnitude of the sine wave is proportional to the dip magnitude of the plane. The direction at the lowest point on the sine wave is the direction of the dip azimuth.

When manually picking dips on he workstation, at least three points have to be selected on the interface. The computer software will then compute the magnitude and azimuth of the plane or sine wave fitting through those points. If more than three points are selected, a least-squares fits is calculated, taking all points into consideration.

An important issue to cover at this time is what reference are we using for our dip values. When we calculate dips directly from images, we are looking at **apparent dip** or the dip in relation to the borehole. If the well were perfectly vertical, the apparent dip would be the same as **true dip**, which is referenced to North, East, and vertical. However, if the borehole is deviated, apparent dips have to be rotated to remove that deviation to get a true dip value. For this reason, dip values will usually be expressed with either an **AD**, for apparent dip, or **TD**, for true dip.

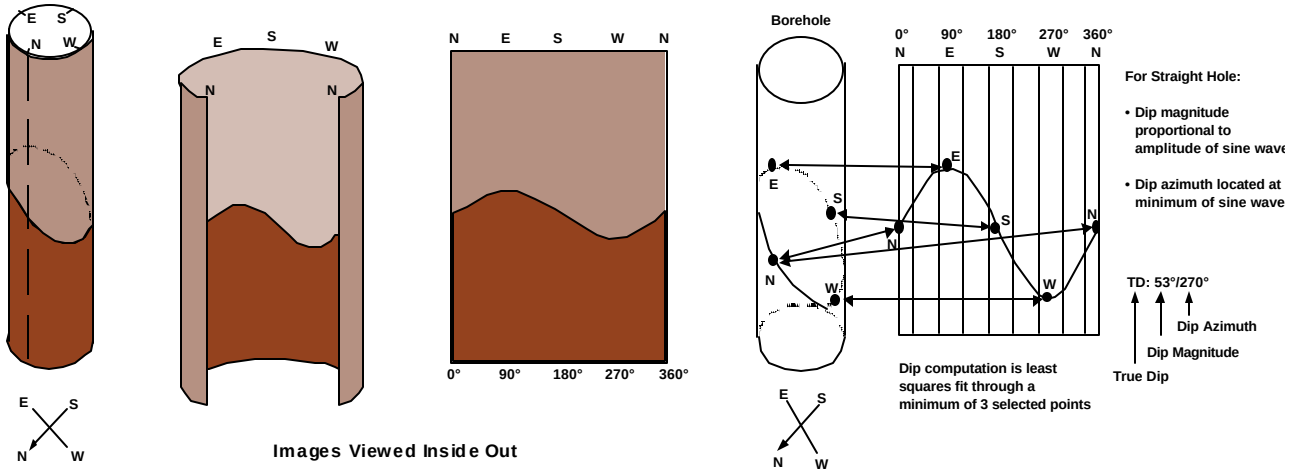

Dip Computation from Images

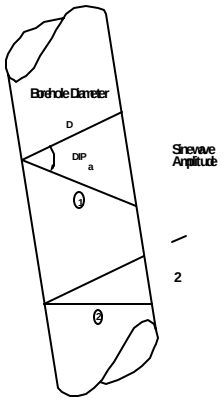

Apparent Dip = $\tan^{-1}$ (A1/D)

1. High angle dip viewed on strike.
2. Flat or 0° dip will have an apparent dip equal to the borehole deviation.

If borehole is inclined, a correction is required to compute **True Dip**.

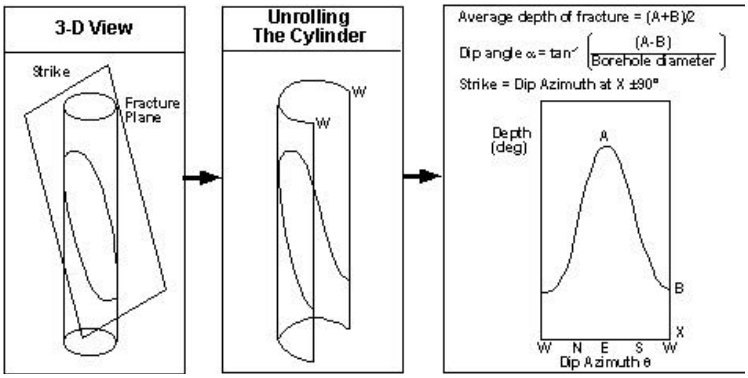

Any plane not perpendicular to the borehole axis intersects the cylinder (or borehole surface) along an ellipse, which, when cut an unrolled, is represented by a sinewave. The azimuth of the lowest point of the sine wave (the trough) indicates the apparent azimuth of the dipping plane. Its apparent dip angle is the maximum dip read at the inflection point. Its tangent is equal to the difference between the bottom (B) and the top (A) of the sine wave divided by the borehole diameter.

Example: A = 5210.3 ft
B = 5211.0 ft
borehole diameter = 8.5 in.

$$\alpha = \tan^{-1}\left[\frac{5211.0 - 5210.3}{\frac{8.5}{12 \text{ in.}}}\right]$$

$$\alpha = \tan^{-1}\left[\frac{0.7}{0.7083}\right]$$

$$\alpha = 44.66 \text{ degrees}$$

Image Examine Workstation

Image interpretation can be enhanced by means of a computer workstation equipped with Image Examiner Software. This allows such interactive processing advantages as:

- scale changes of both the vertical and horizontal to enhance the interpretation
- display of other logs for correlation on the same scales
- graphic enhancement of specific features such as bedding, texture, vugs, and fractures
- dip computation of bedding surfaces, fault planes, and fractures
- correlation of images to whole core extends the interpretation to non-cored sections
- cores may be oriented from features present in both the core and wellbore
- quantification of images, such as sand count and calibration to core porosity, increases interpretation accuracy.

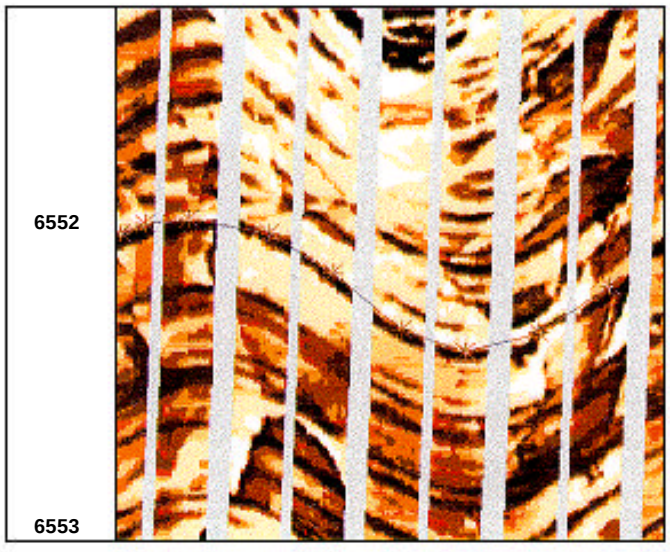

Manual picking of points for dip computation

Manual Dip Picking

Manual dip picking is one of the primary uses of the workstation. To begin the process, an azimuthal image display is created and the user is asked to move a set of crosshairs with the mouse to a bedding interface. By clicking or depressing the middle button on the mouse, an x is marked at that location. Although only three points are necessary to define a plane, it is a good practice to pick at least one point on each pad, as in the figure to the left. After the point are chosen, the software then calculates the best fit plane through the points, saves the dip result and displays the sinewave which represents the dip plane (right figure).

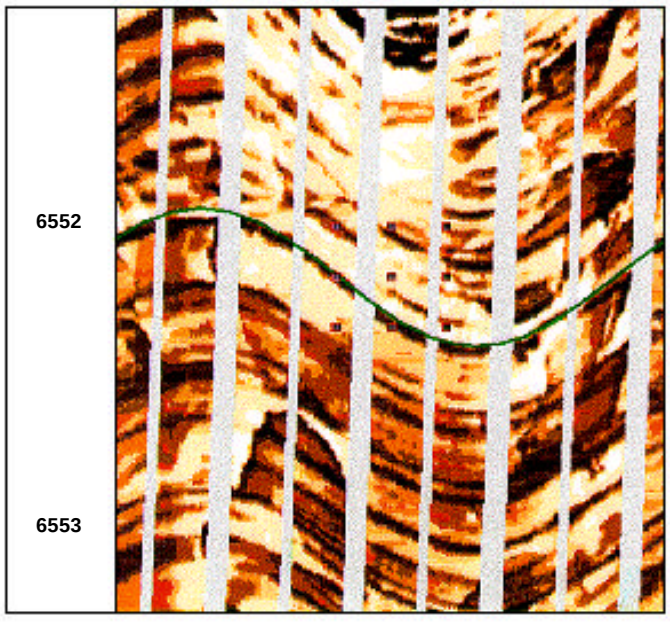

Calculated dip plane

Manual Dip Computation

An additional method of selecting surfaces from images is through the use of the “steerable” sinewave. In this method, a sinewave is superimposed over the images, as at 6553 ft on the upper figure below. By using the mouse to manipulate the depth, amplitude and phase of this sinewave one can bring it into alignment with any surface seen on the images. This method is particularly useful when bedding is nearly parallel. The user can quickly compute a large number of dips.

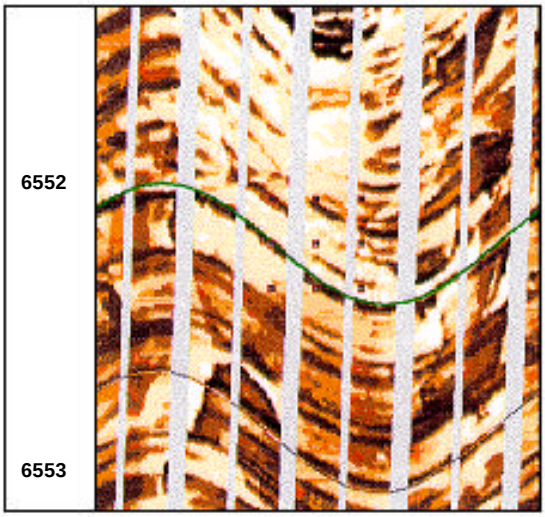

Manual dip computation using the steerable sinewave

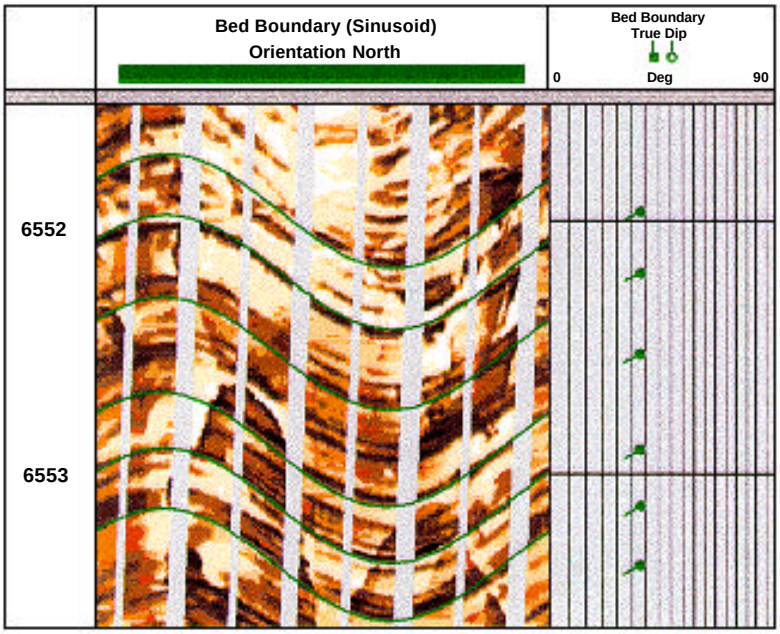

Results of multiple dip computations

Dip Presentations

There are three common modes of presenting dip information: apparent dip (AD), true dip (TD), and structural dip deletion (SD). Apparent dip refers to dip values that are referenced only to the borehole. They are not compensated for the deviation of the borehole from vertical. True dip values have been compensated for borehole drift. They are referenced to the fixed Earth coordinate system of North, East, and vertical. Structural dip delete values have been compensated for borehole drift and structural dip. The primary usage of this mode of dip presentation is to rotate out the effects of post depositional deformation in order to look at the geometry of the original deposition. Apparent dip and true dip displays are essentially "automatic" presentations: the former is non-compensated for borehole drift and the latter is compensated continuously by independent measurements of borehole drift. Structural dip deletion is an interpreted mode of display. An analyst must determine what values of structural dip values are then mathematically rotated out of the true dip to generate structural dip deletion displays.

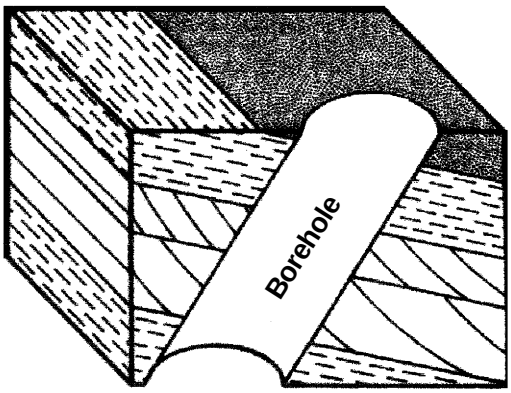

AD: Apparent Dip Non-compensated

TD: True Dip Compensated For Borehole Drift

SD: Structural Dip Deletion Compensated For Borehole Drift and Structural Dip

Dip Modes

The three dip modes are shown in the figure below. Again, true dip and apparent dip can each have only a single value. The value of structural dip deletion or relative dip will be determined by the value of structural dip input by the analyst. In this example, a value of 28° magnitude at an azimuth of 242° was used to generate the "relative" dip result.

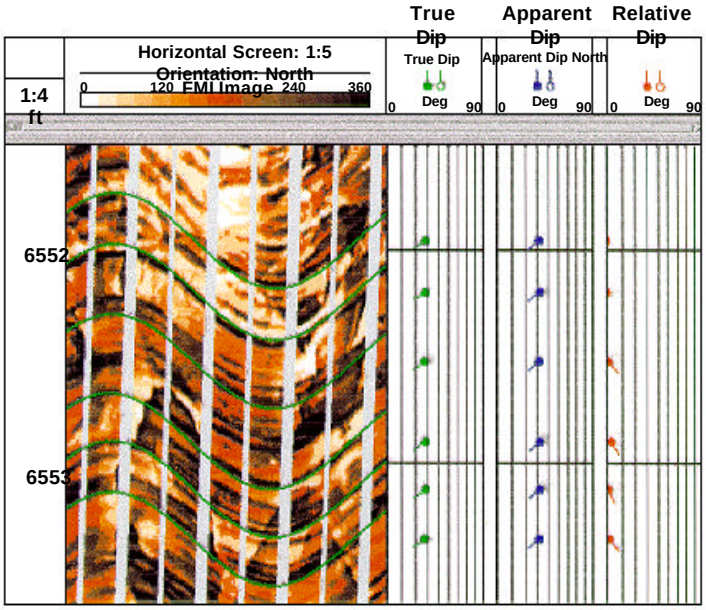

Although we usually speak in terms of dip planes, the actual interface may not have a smooth or "planar" appearance. When dips are generated by computer, a quality value is output that gives a measure of the quality of the fit of the data points to a plane. In this way, the analyst can determine which individual dips are more reliable. It is usually not a good idea to reject all lower quality dips out of hand. Many of these dips accurately reflect the best approximation of a plane through a given interface and, as such, have geological meaning.

When using the workstation or manual techniques, no quality indicator is available. It is then the responsibility of the analyst to associate some degree of reliability with each dip.

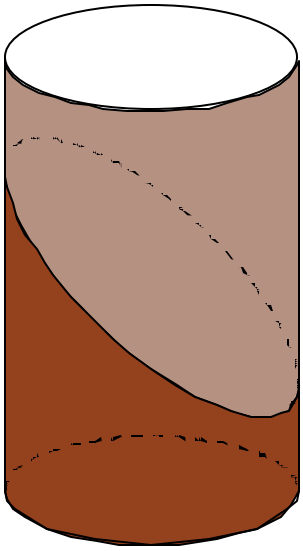

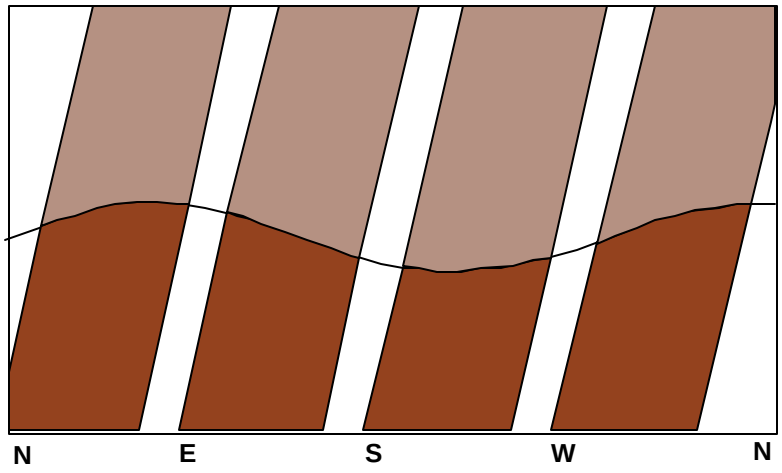

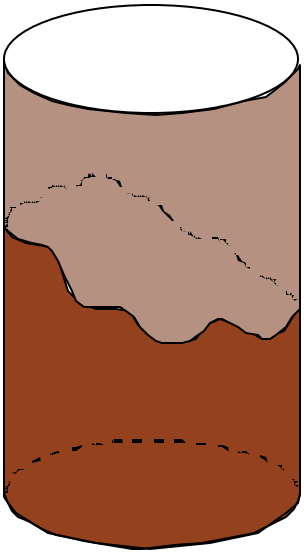

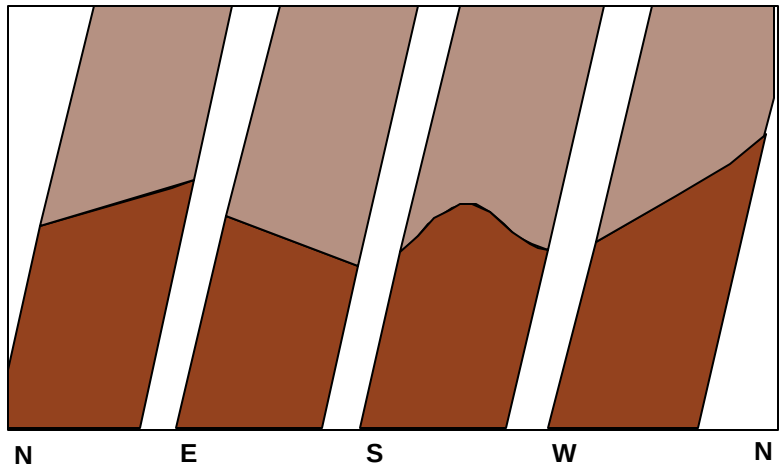

Fractures

Objectives of this Chapter:

- **The characterization of fractures from electrical images. This includes the classification of fractures into *open, mineral-filled, or vuggy* and whether the fractures are:**
  - **natural;**
  - **polygonal; or**
  - **mechanically includes.**
- **And the fracture strike/dip orientation.**

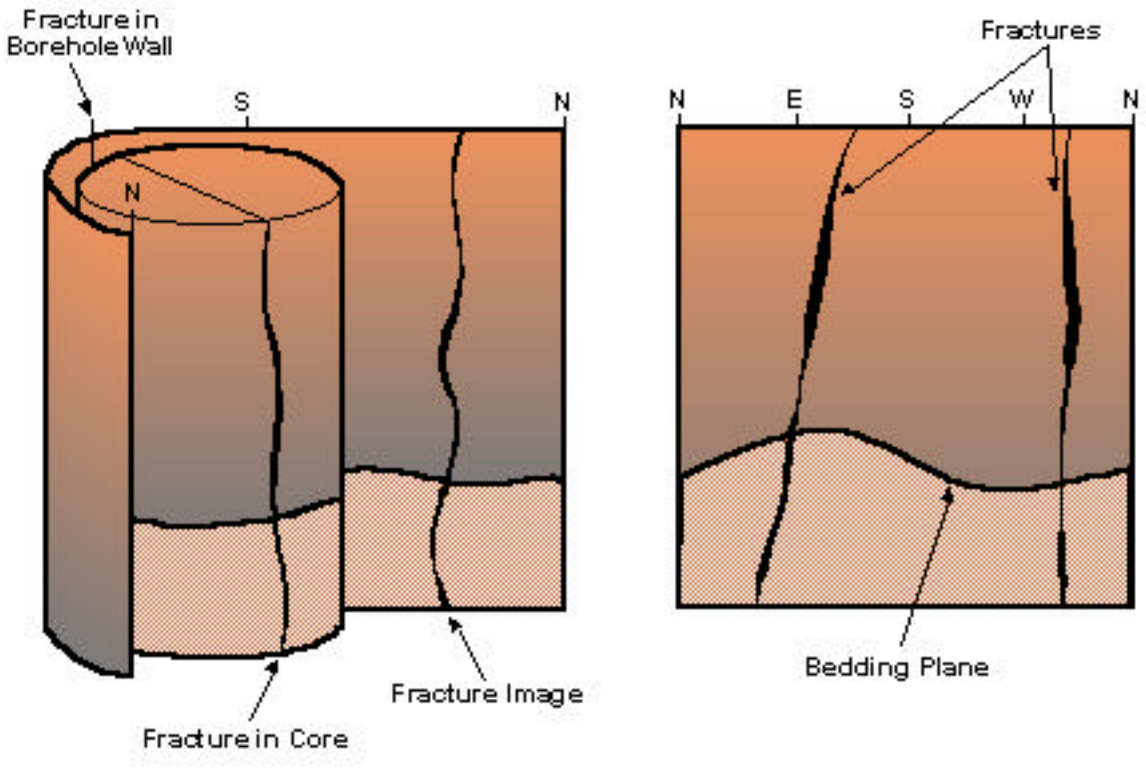

Unwrapped Image of Borehole Wall

Fractures

Naturally occurring open fractures are very important to producibility in many carbonate and sandstone reservoirs. There are two methods of interpretation: fracture characterization (visual inspection of the electrical images) and fracture analysis (computer assisted evaluation). There are three factors which affect the electrical images and must be considered before an accurate interpretation is possible:

- ***Rm,*** resistivity of the mud at formation temperature;
- ***Rxo,*** resistivity of the flushed zone;
- ***Fracture geometry.***

Characterization of fracture systems from electrical images includes: the identification of the fracture type as to vertical, polygonal, or mechanically induced; the definition of the fracture morphology as to open, mineral-filled, or vuggy; and the dip/strike orientation.

Fracture Identification

Vertical fractures in a vertical borehole can be identified as a high amplitude feature which crosses other bedding planes. The feature is conductive if open and resistive if mineral-filled. Vertical fractures may be oriented by normal dip computation methods. Producibility and recovery efficiency in some reservoirs is influenced by the fracture angle. The angle most often used as criteria is 75°. Fractures with dip angles of more than 75° are vertical fractures while those less than 75° are high angle fractures.

Polygonal (syneresis) fractures are caused by the chemical or mechanical dewatering of a carbonate or by tectonic forces. The type of fractures often appears at changes in the lithology. Polygonal fractures have a braided appearance and are often referred to as “chicken-wire” fractures. These cannot be oriented.

Mechanically induced fractures are created by the drilling process or by a hydraulic frac. These fractures are always open and may be oriented by conventional dip methods. The strike orientation of mechanically induced fractures reflects the present day least principle stress direction.

Fracture Morphology

Fractures may be open, mineral-filled, or vuggy. Open fractures are more conductive than the surrounding matrix. The degree of conductivity depends on the resistivities of the mud and the flushed-zone, and the fracture geometry. Visual inspection of the images may be used only as a guide to interpretation. A salt mud system will enhance the appearance of fracture while a fresh mud system will reduce the appearance. Mineral-filled fractures will appear less conductive than open fractures. Vuggy fractures exhibit irregular enlargements along the fracture plane.

Fracture Identification

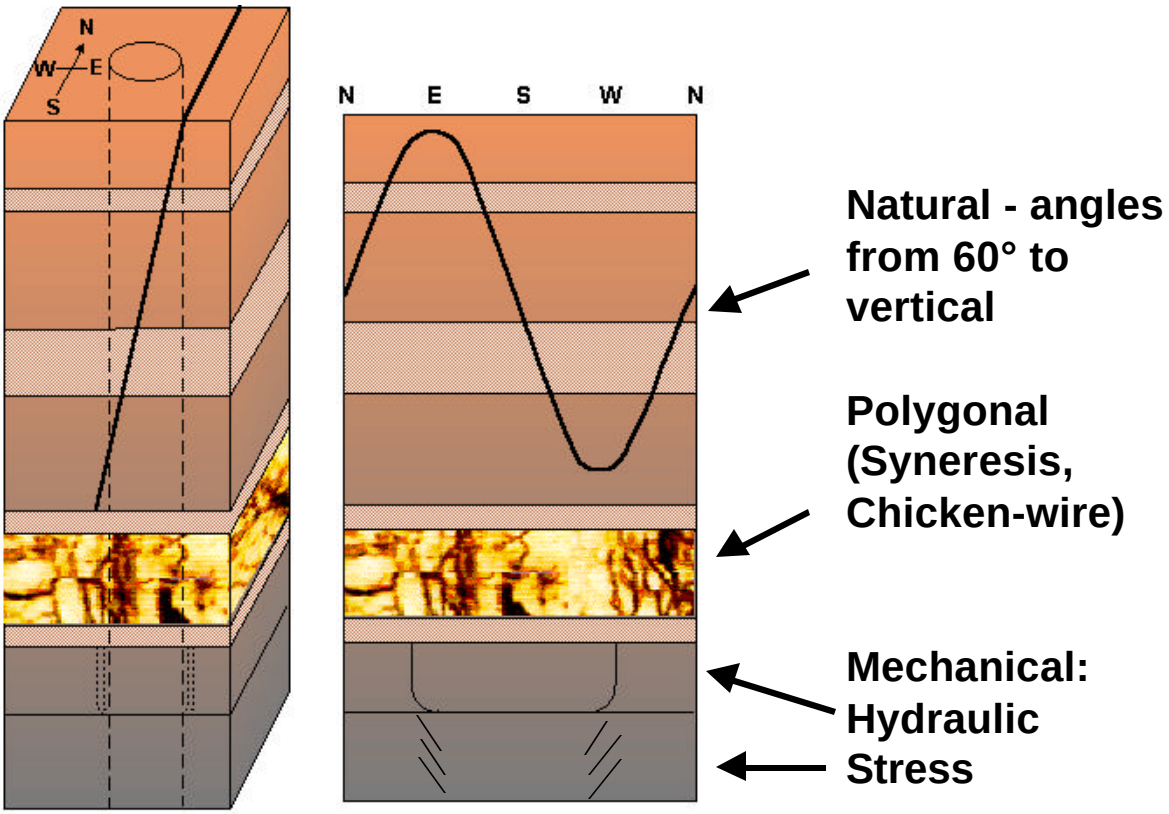

Fracture Morphology (Open, Mineral-Filled, Vuggy)

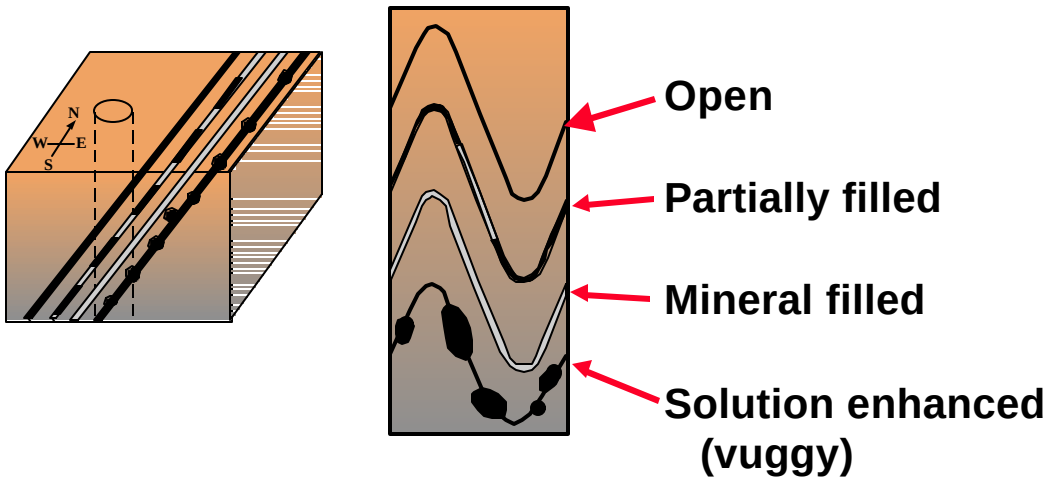

Neutron/ Density Log

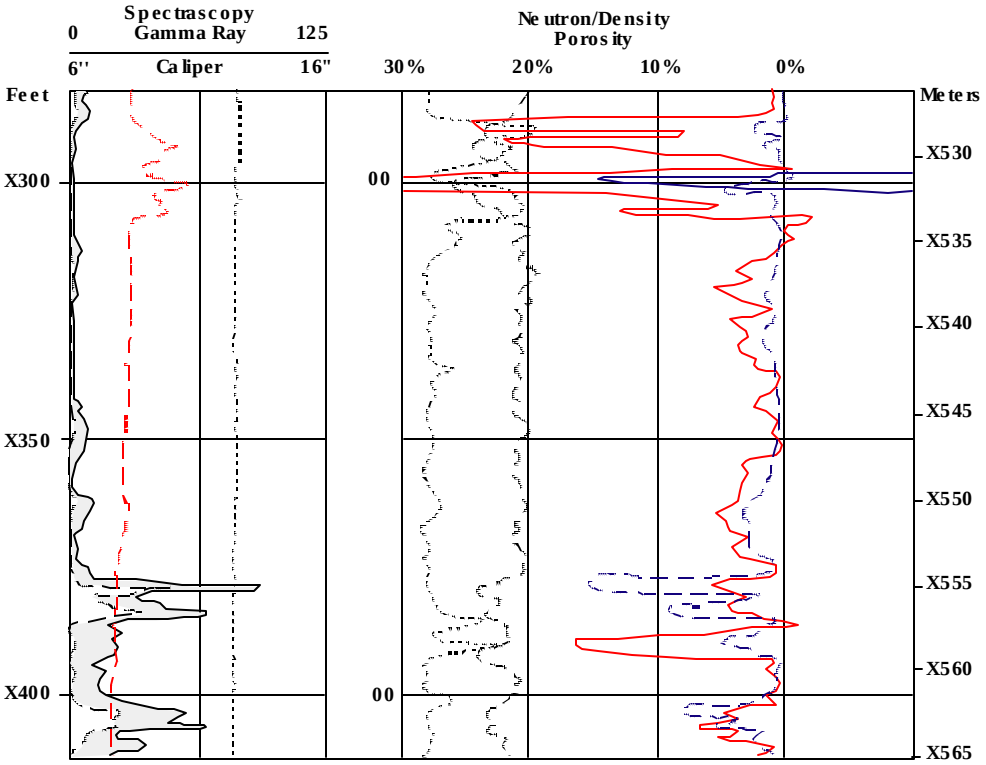

Carbonate Vertical Fractures

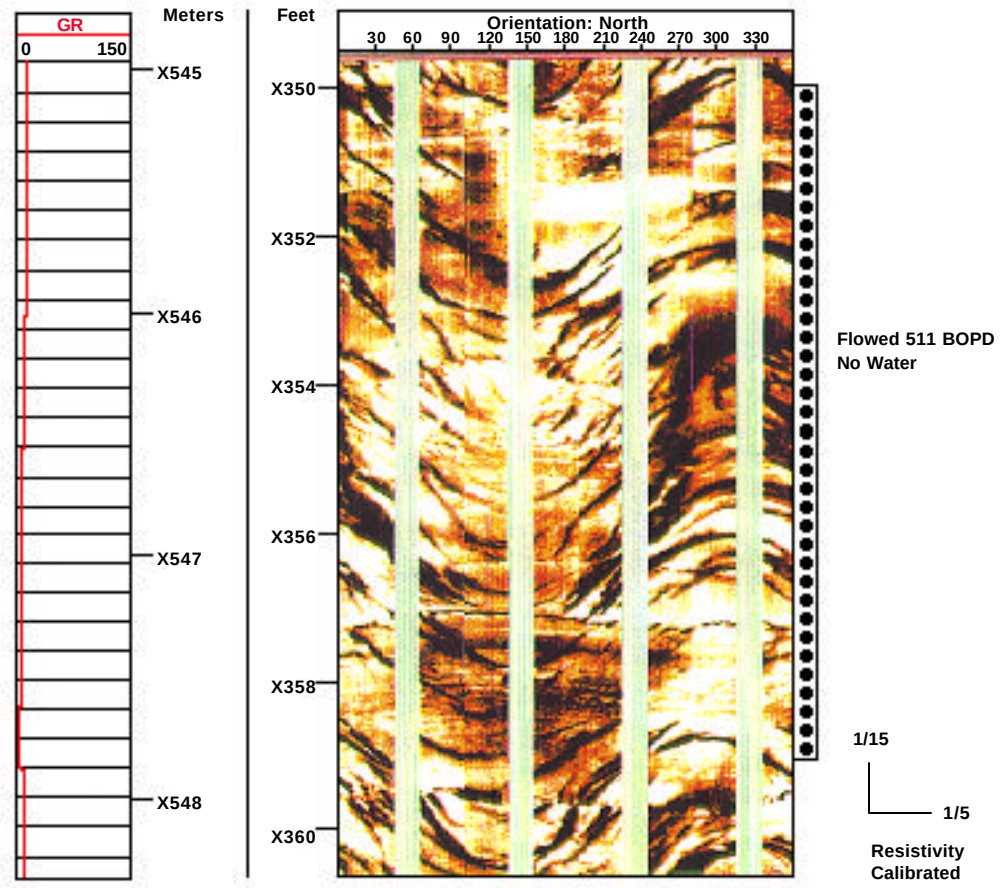

Fracture Orientation

Accurate orientation of fractures is required to properly locate offset development or injection wells. Often the orientation of mechanically induced fractures is used to decide the practicality of hydraulic fracs. A sine wave is fit through the fracture, in a BORMAP presentation, to compute the dip. If this is done manually, then the dip is apparent and not borehole compensated. Strike of the fracture is measured perpendicular to the fracture azimuth. The angle of the fracture from horizontal is used to classify the fracture as either vertical (greater than 75°) or high angle (less than 75°). The dip computation may be from overlays, geologic workstation, FMS Dip, or Fracview. Computer assisted interpretation programs allows statistical plots of the data.

Straight line image plots from the two pad tools are more challenging to interpret. The fracture must be present on both pads or data from multiple passes must be used to determine the fracture orientation. The Pad No. 1 azimuth is determined from the borehole drift plot. The small arrow is the azimuth of Pad No. 1. Pads 3 and 4 are oriented clockwise from the Pad No. 1 azimuth. If the fracture is present on both pads, then the strike of the fracture can be plotted on an azimuth diagram and measured. Multiple passes may be handled in a similar manner.

Fracture Orientation (From BORMAP)

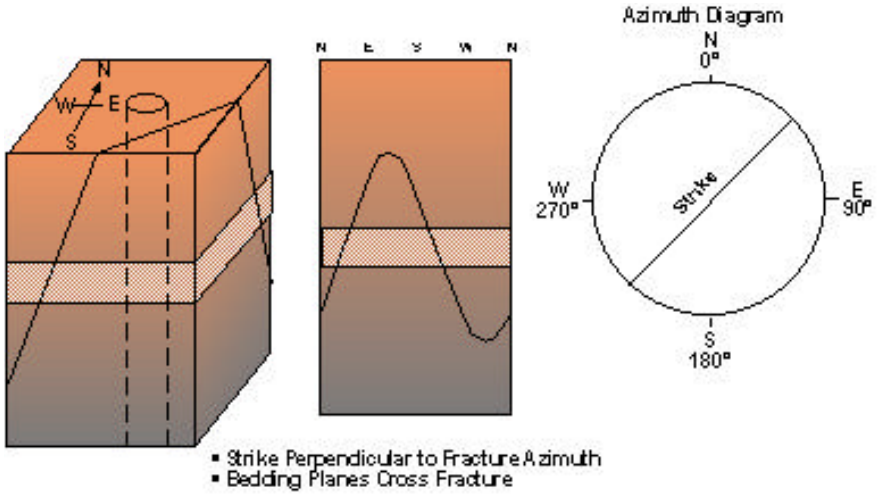

Fracture Orientation (From Straight Line Images)

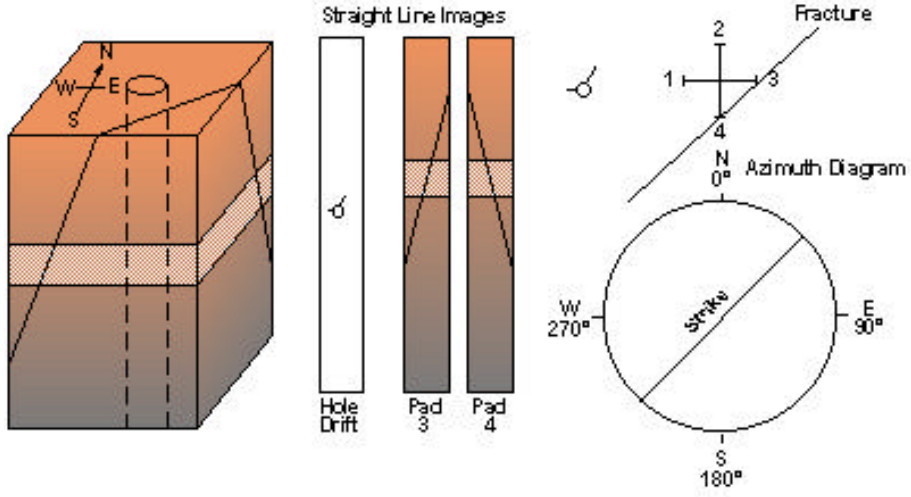

Fracture Example 1

Objective of this example: Fracture Characterization.

Geological Background: Jurassic Carbonate.

Available Data: Equalized and Enhanced Images, Litho-Density and Neutron Logs, Perforation as marked.

Evaluation:

Identification: ☑ Natural Vertical ❑ Polygonal (Syneresis) ❑ Mechanical Induced

Morphology: ☑ Open ❑ Mineral-Filled ❑ Vuggy

Orientation: Fracture Angle: **85°/113°**

Fracture Strike: **23° - 203°**

Azimuth Diagram:

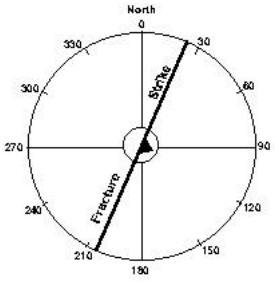

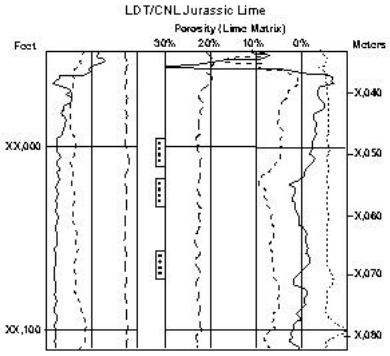

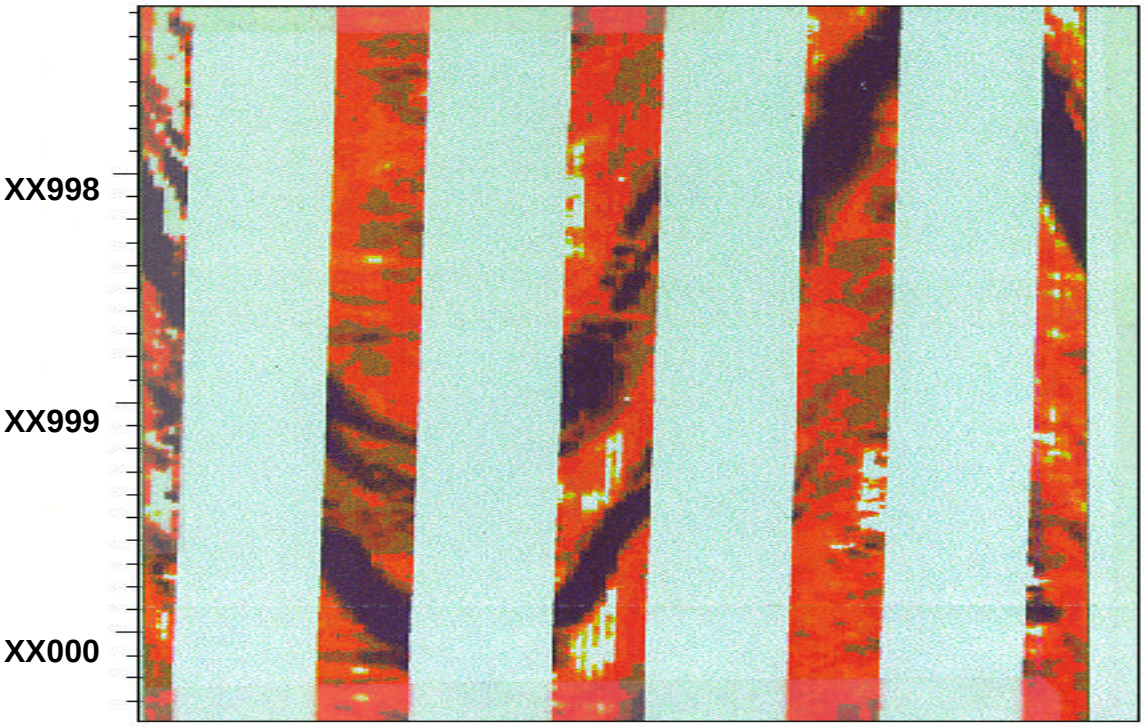

Fracture Example 2

Objective of this example: Characterization of a vertical fracture.

Geological Background: Carbonate.

Available Data: Resistivity Calibrated Images, NGT, Natural Gamma Ray.

Evaluation:

Identification: ☑ Natural Vertical ❑ Polygonal (Syneresis) ❑ Mechanical Induced

Morphology: ☑ Open ☑ Partially Mineral-Filled ☑ Mineral-Filled ❑ Vuggy

Orientation: Fracture Angle: Vertical

Fracture Strike: **38° - 218°**

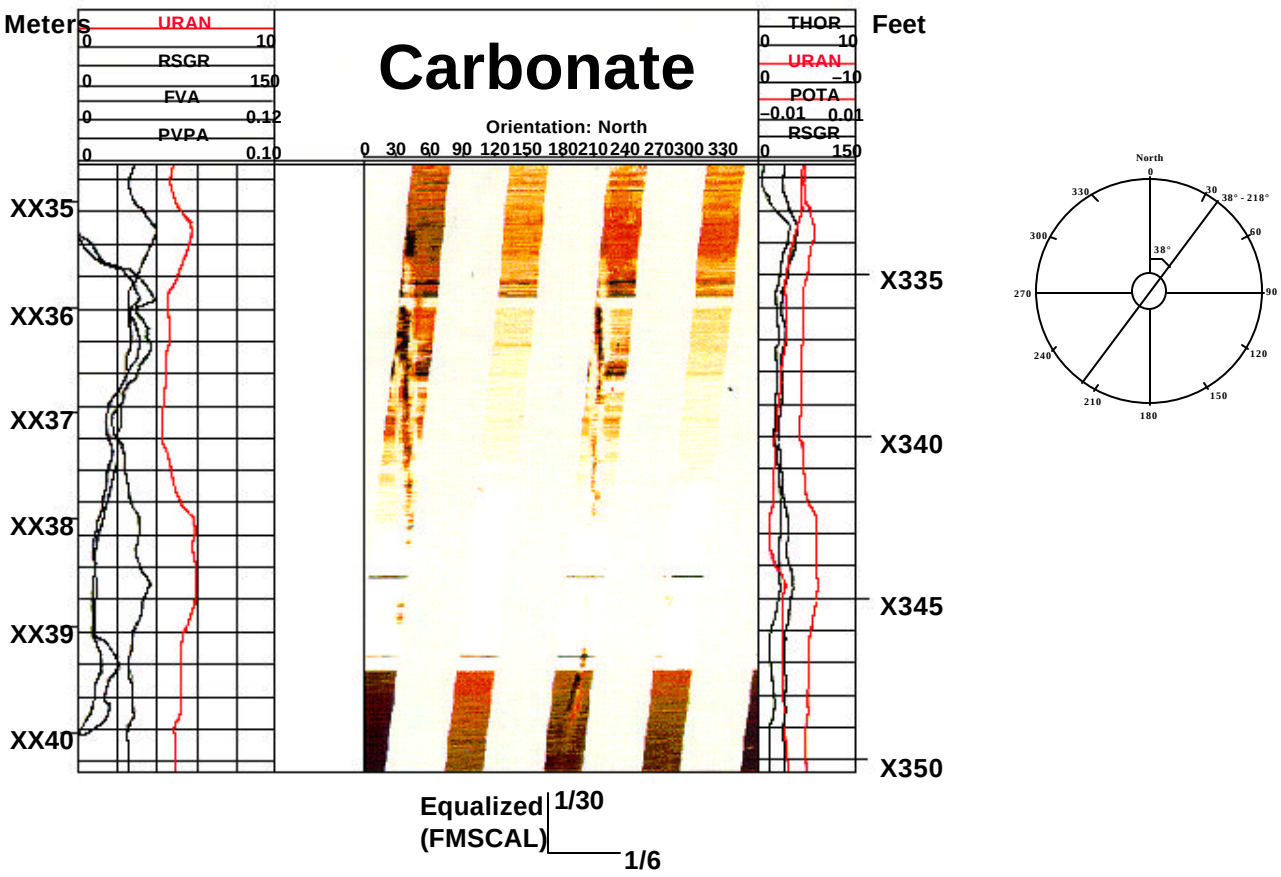

THOR - Thorium
URAN - Uranium
POTA - Potasium

RSGR - Total Gamma Ray
FVA - Mean Fracture Aperture
PVPA - Total Fracture Porosity

Fracture Exercise 1

Objective of this example: Characterization of a vertical fracture.

Geological Background: Cretaceous Reef.

Available Data: Equalized Images.

Evaluation:

Identification: ❑ Natural Vertical ❑ Polygonal (Syneresis) ❑ Mechanical Induced

Morphology: ❑ Open ❑ Partially Mineral-Filled ❑ Mineral-Filled ❑ Vuggy

Orientation: Fracture Angle:_____

Fracture Strike:_____

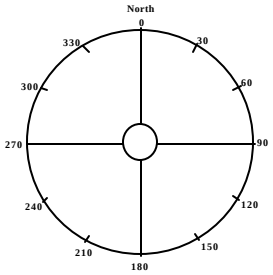

Static Images Cretaceous Reef

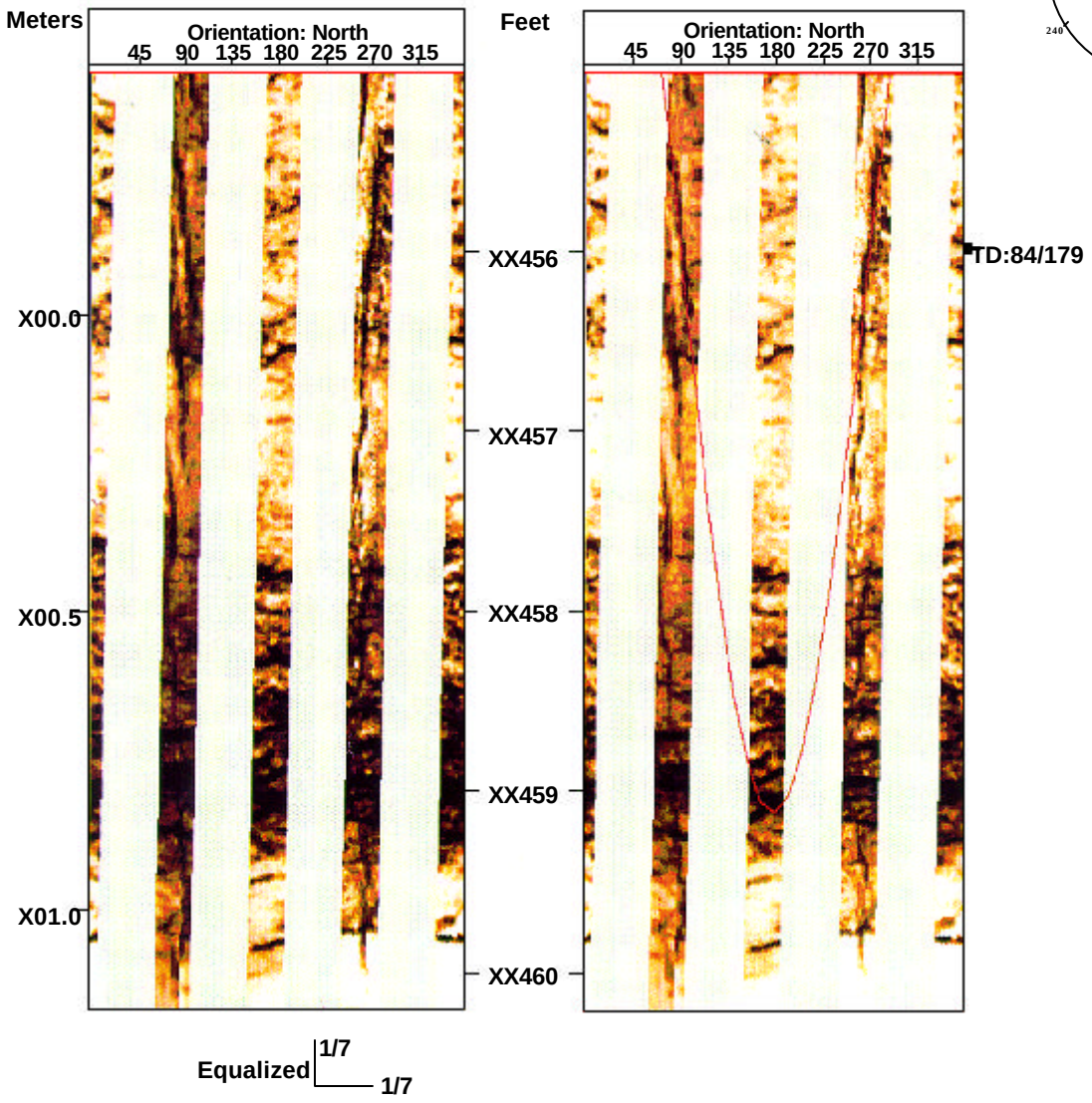

Fracture Exercise 2

Objective of this example: Characterization of a vertical fracture.
Geological Background: Pennsylvanian Sand.
Available Data: Equalized Images.
Evaluation:
Identification: ❑ Natural Vertical ❑ Polygonal (Syneresis) ❑ Mechanical Induced
Morphology: ❑ Open ❑ Partially Mineral-Filled ❑ Mineral-Filled ❑ Vuggy
Orientation: Fracture Angle: _____
Fracture Strike: _____

Azimuth Diagram:

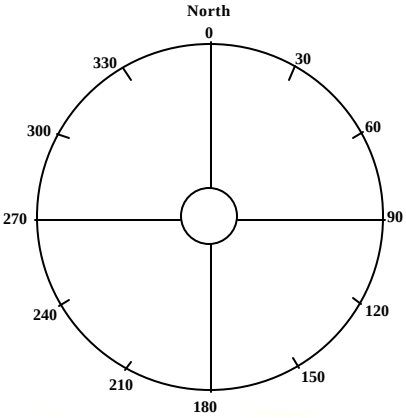

Fractures, Pennsylvanian Sand

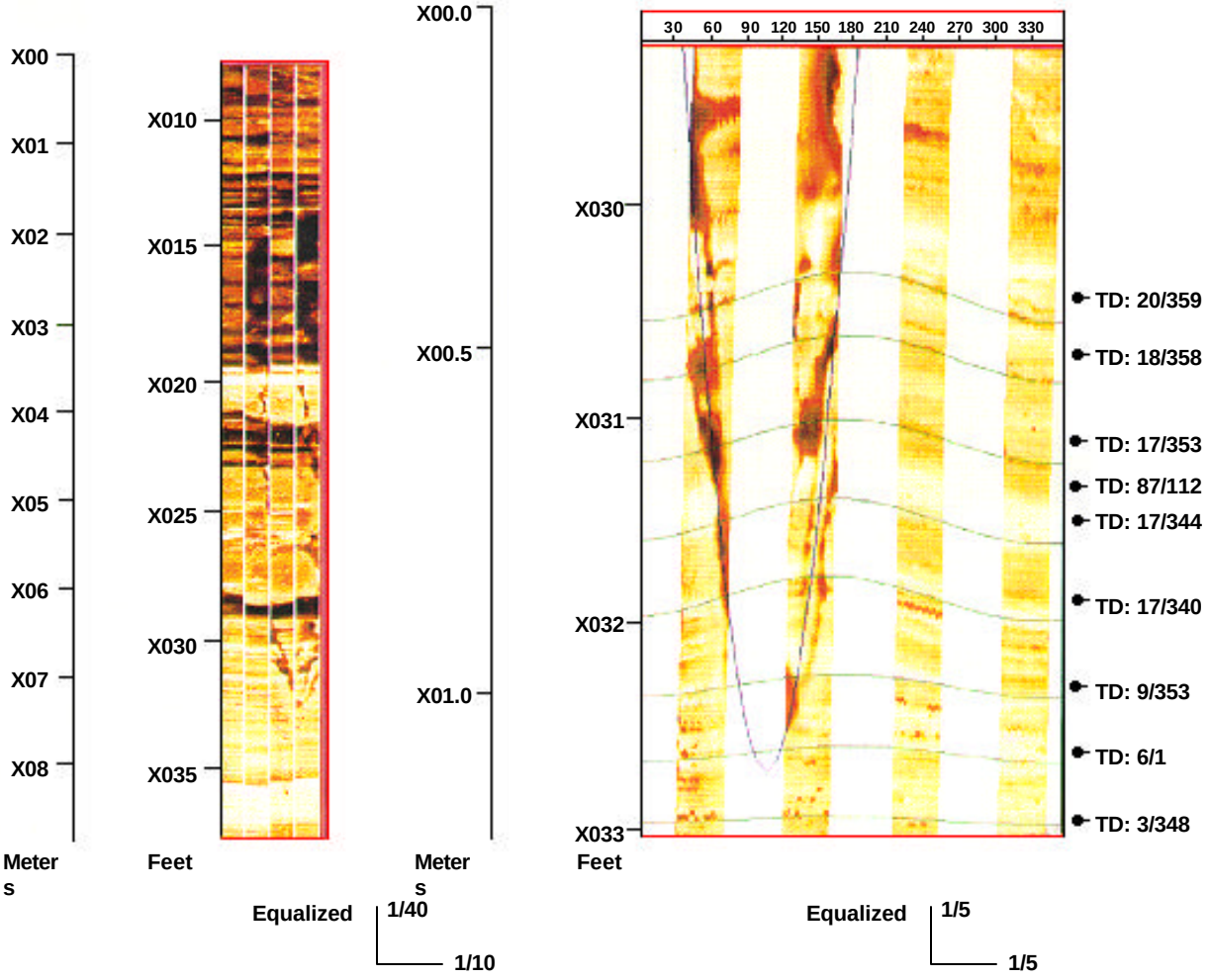

Fracture Exercise 3

Objective of this example: Characterization of a vertical fracture.
Geological Background: Carbonate.
Available Data: Resistivity Calibrated Images.
Evaluation:
Identification: ❑ Natural Vertical ❑ Polygonal (Syneresis) ❑ Mechanical Induced
Morphology: ❑ Open ❑ Partially Mineral-Filled ❑ Mineral-Filled ❑ Vuggy
Orientation: Fracture Angle: _____
Fracture Strike: _____

Azimuth Diagram:

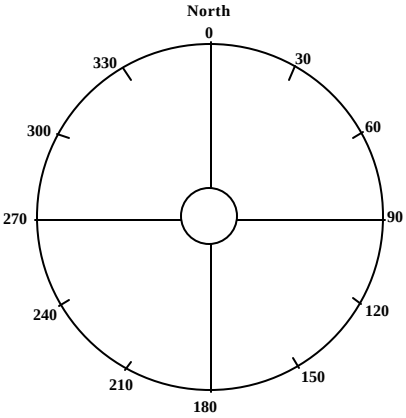

Carbonate

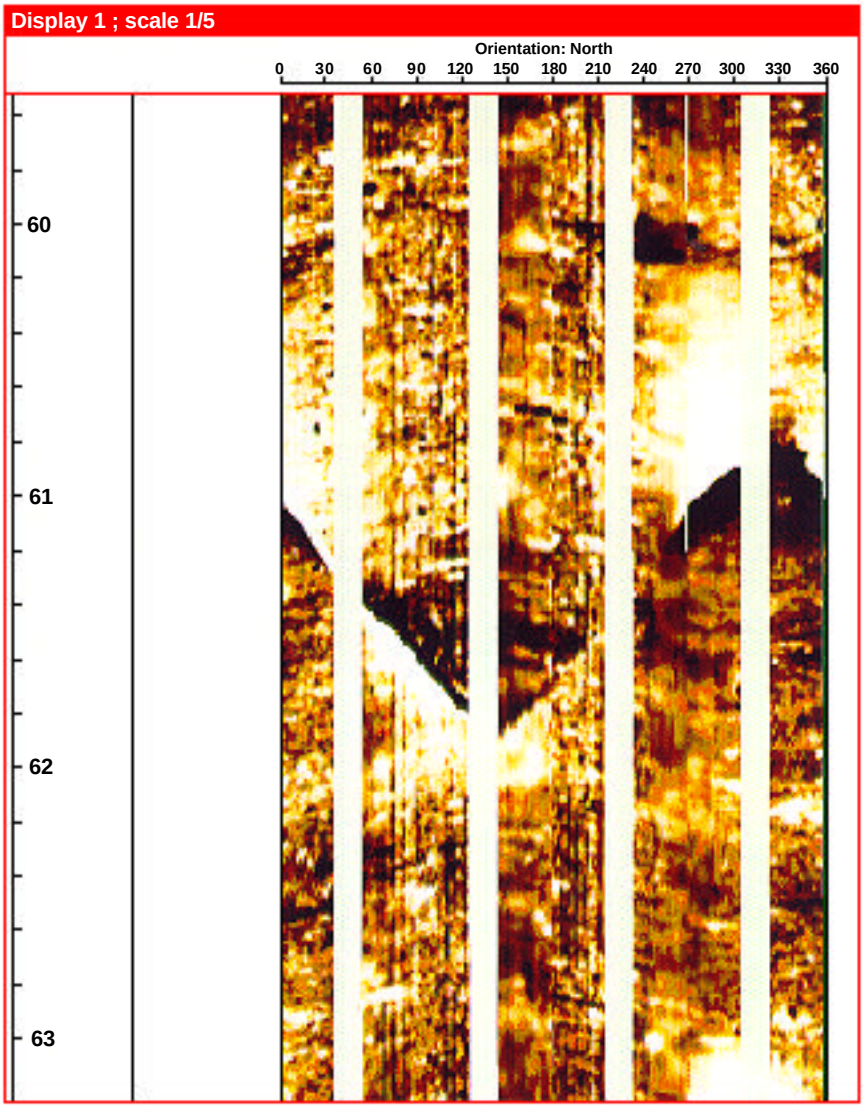

Feet **Resistivity Calibrated 1/5::1/5**

Fracture Exercise 4

Objective of this example: Fracture Characterization.
Geological Background: Carbonate.
Available Data: Resistivity Calibrated Images.
Evaluation:
Identification: ❑ Natural Vertical ❑ Polygonal (Syneresis) ❑ Mechanical Induced
Morphology: ❑ Open ❑ Partially Mineral-Filled ❑ Mineral-Filled ❑ Vuggy
Orientation: Fracture Angle: _____
Fracture Strike: _____

Carbonate

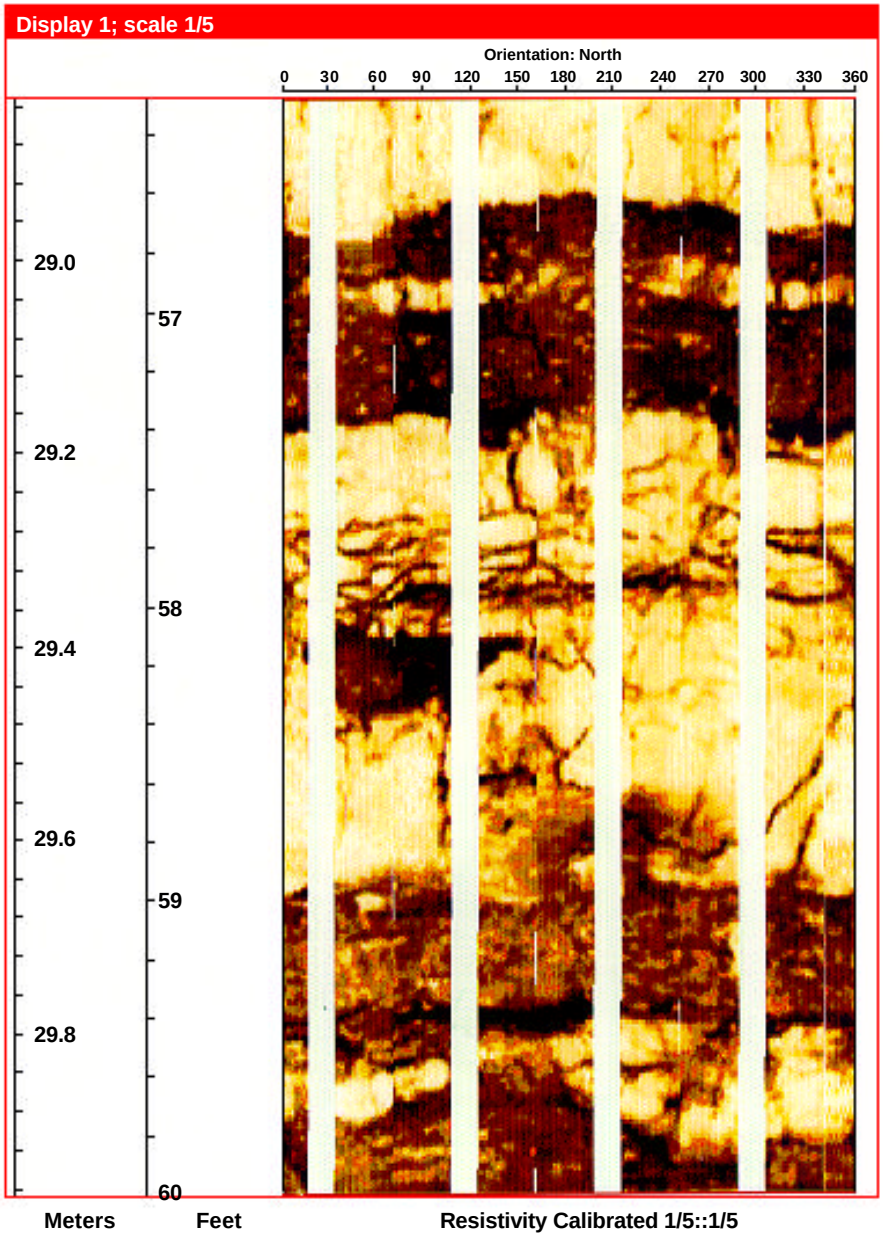

Mechanically Induced Fractures

Fractures are also caused by the drilling process. These are often interpreted from other logs as open fractures. These can be recognized on electrical images by:

- Never crosses the borehole, i.e., does not make a sine-wave.
- Often has curvature at termination;
- Always open - no vugs or mineral-filled;
- Cannot be micro-faulted;
- Oriented parallel to maximum and intermediate principle stresses; usually vertical; and
- Oriented along the least principle stress direction.

A primary use of drilling induced fractures is to orient the direction of hydraulic fracs. A frac will propagate along the strike of the drilling induced fractures.

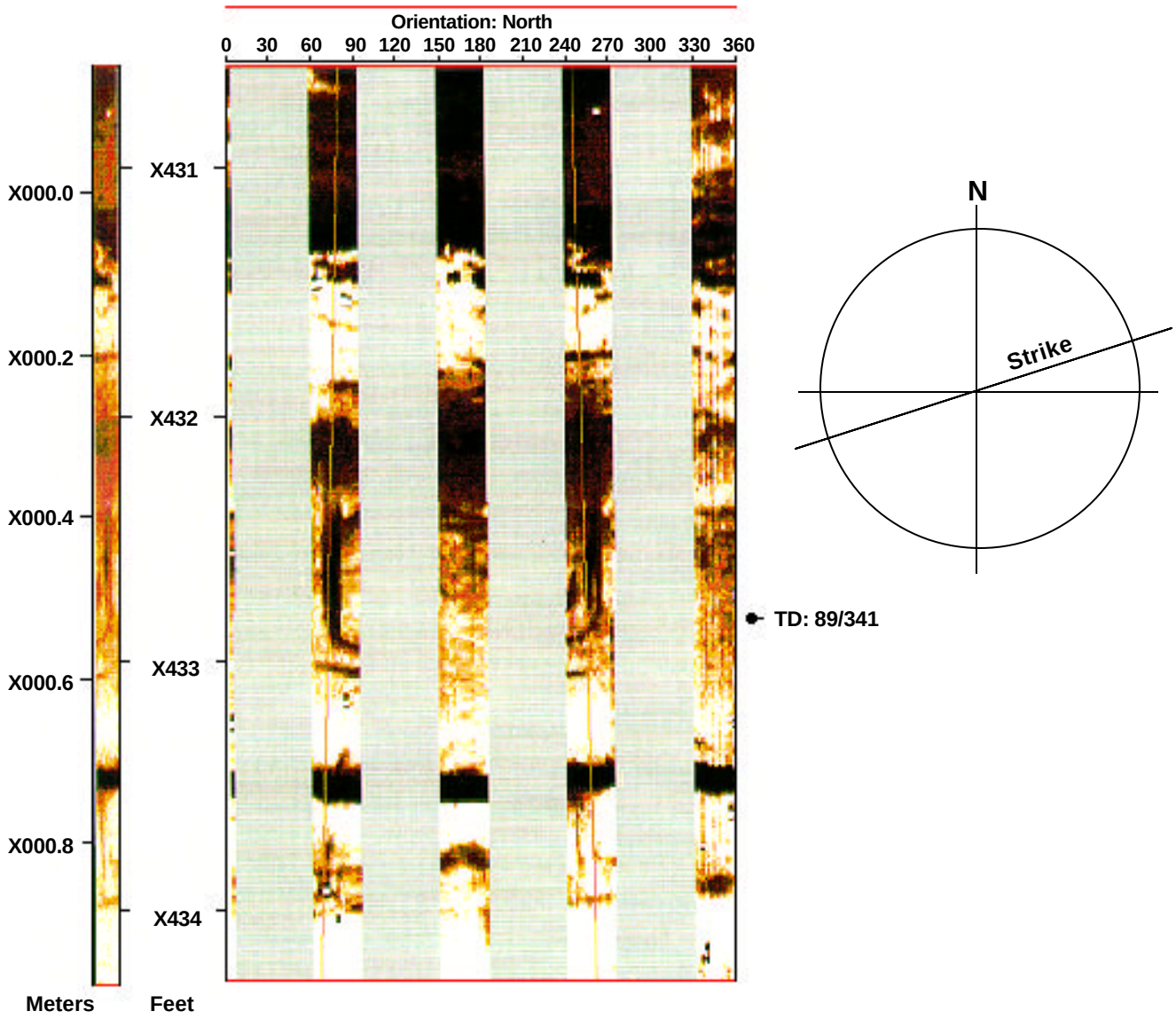

Mechanically Induced Fractures, Open Hole Hydraulic Frac

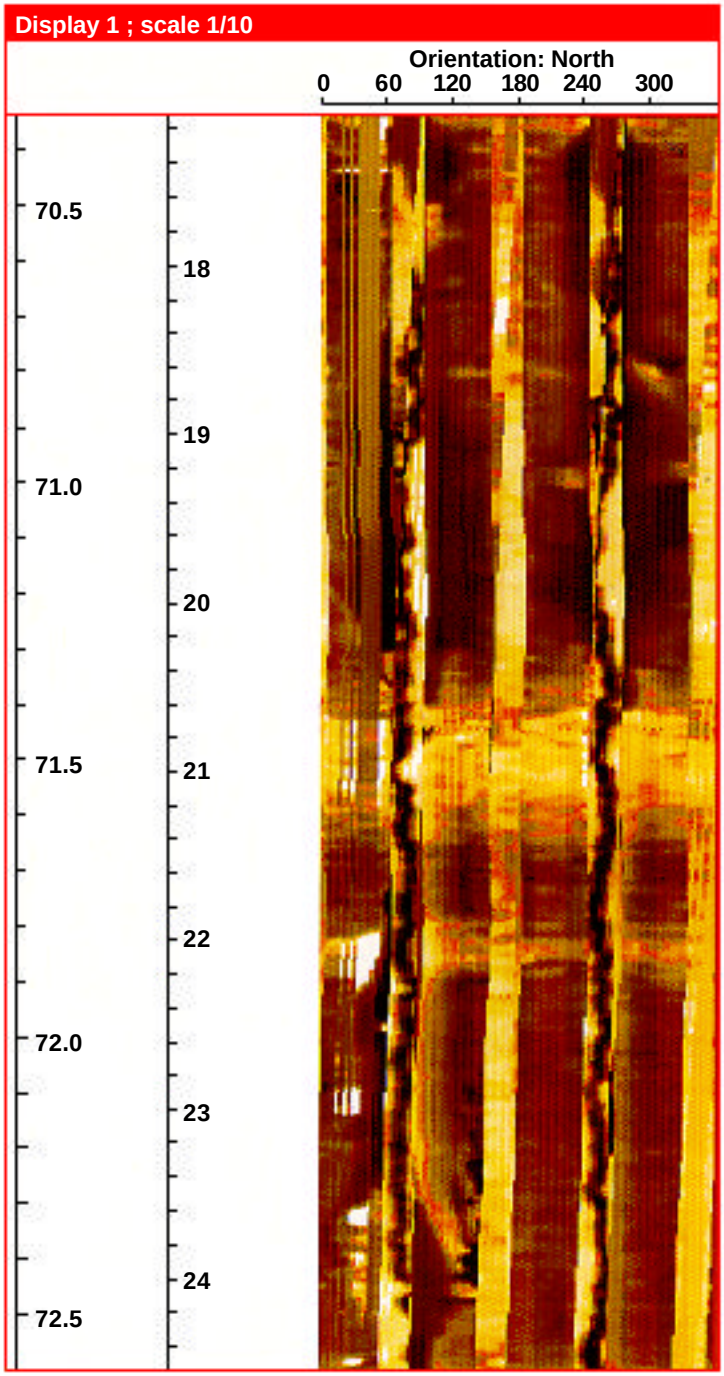

Fracture Exercise 5

Objective of this example: Fracture Characterization.
Geological Background: Carbonate.
Available Data: Resistivity Calibrated Images.
Evaluation:
Identification: ❑ Natural Vertical ❑ Polygonal (Syneresis) ❑ Mechanical Induced
Morphology: ❑ Open ❑ Partially Mineral-Filled ❑ Mineral-Filled ❑ Vuggy
Orientation: Fracture Angle: _____
Fracture Strike: _____

Carbonate

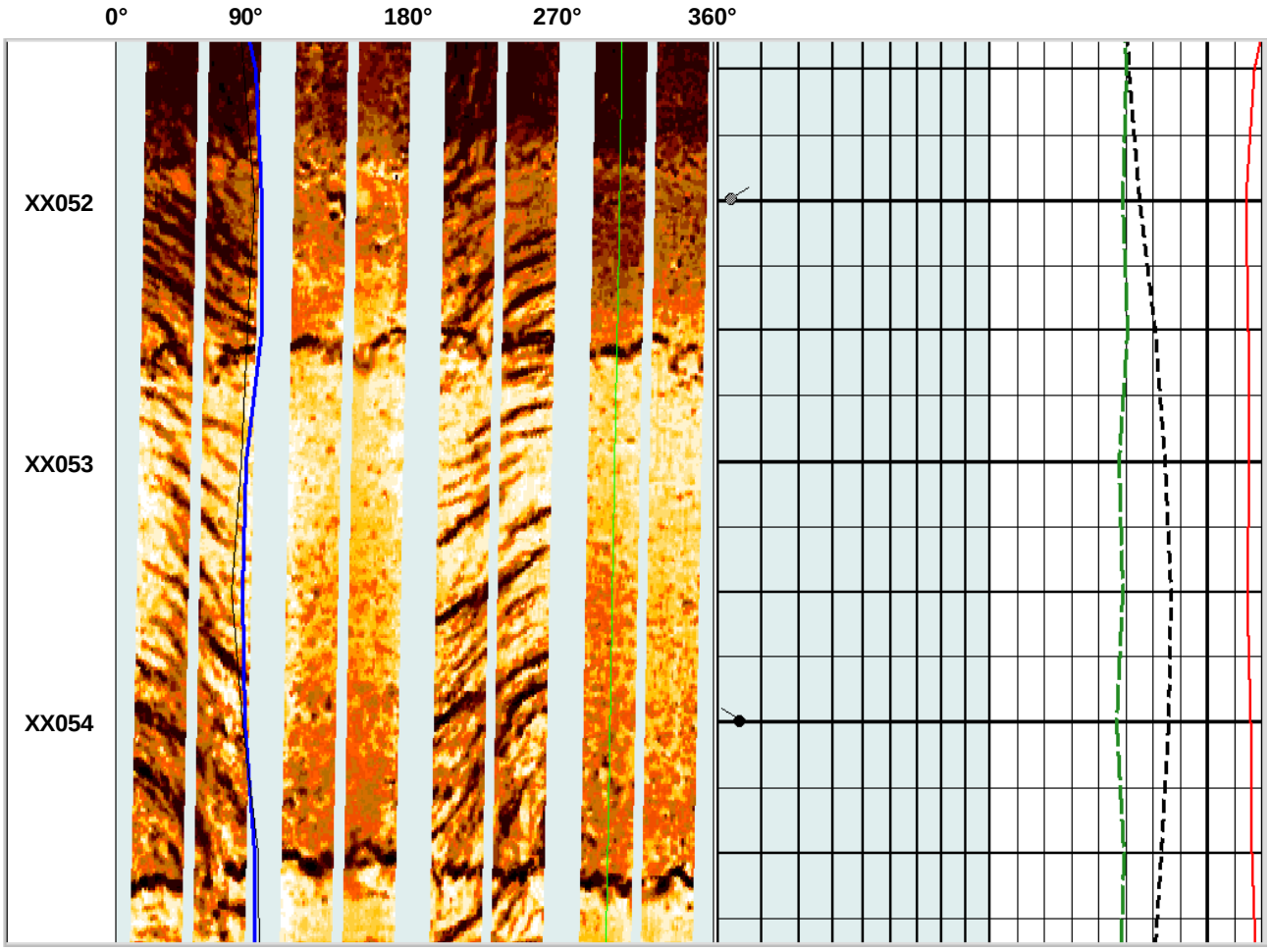

Fracture Example

Objective of this example: Evaluation of unconformities.
Geological Background:
Available Data: Electrical Images.

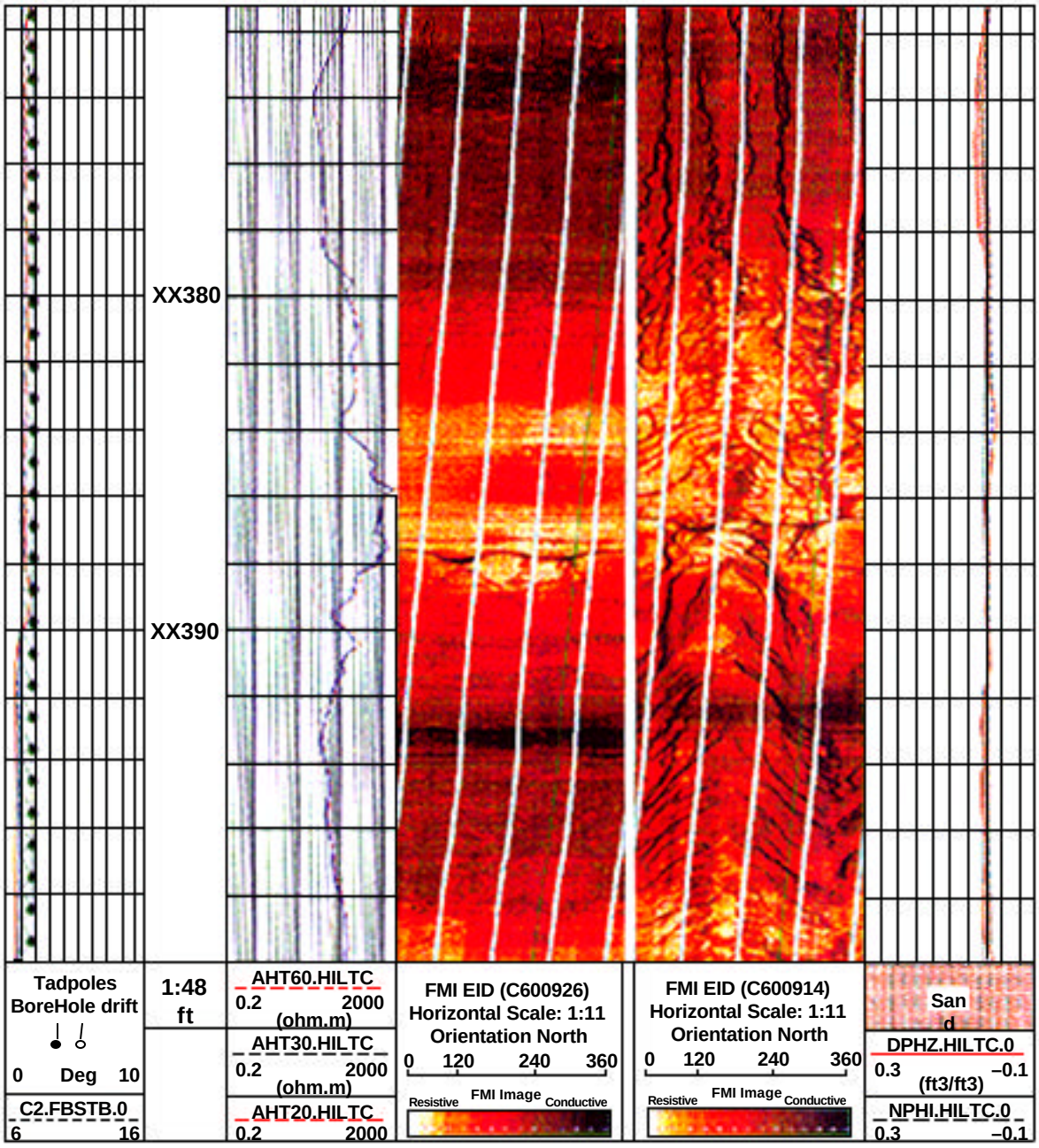

Fracture Exercise 6

Objective of this example: Fracture Characterization.
Geological Background: Carbonate.
Available Data: Resistivity Calibrated Electrical Images.
Evaluation:
Identification: ❑ Natural Vertical ❑ Polygonal (Syneresis) ❑ Mechanical Induced
Morphology: ❑ Open ❑ Partially Mineral-Filled ❑ Mineral-Filled ❑ Vuggy
Orientation: Fracture Angle: _____
Fracture Strike: _____

Carbonate

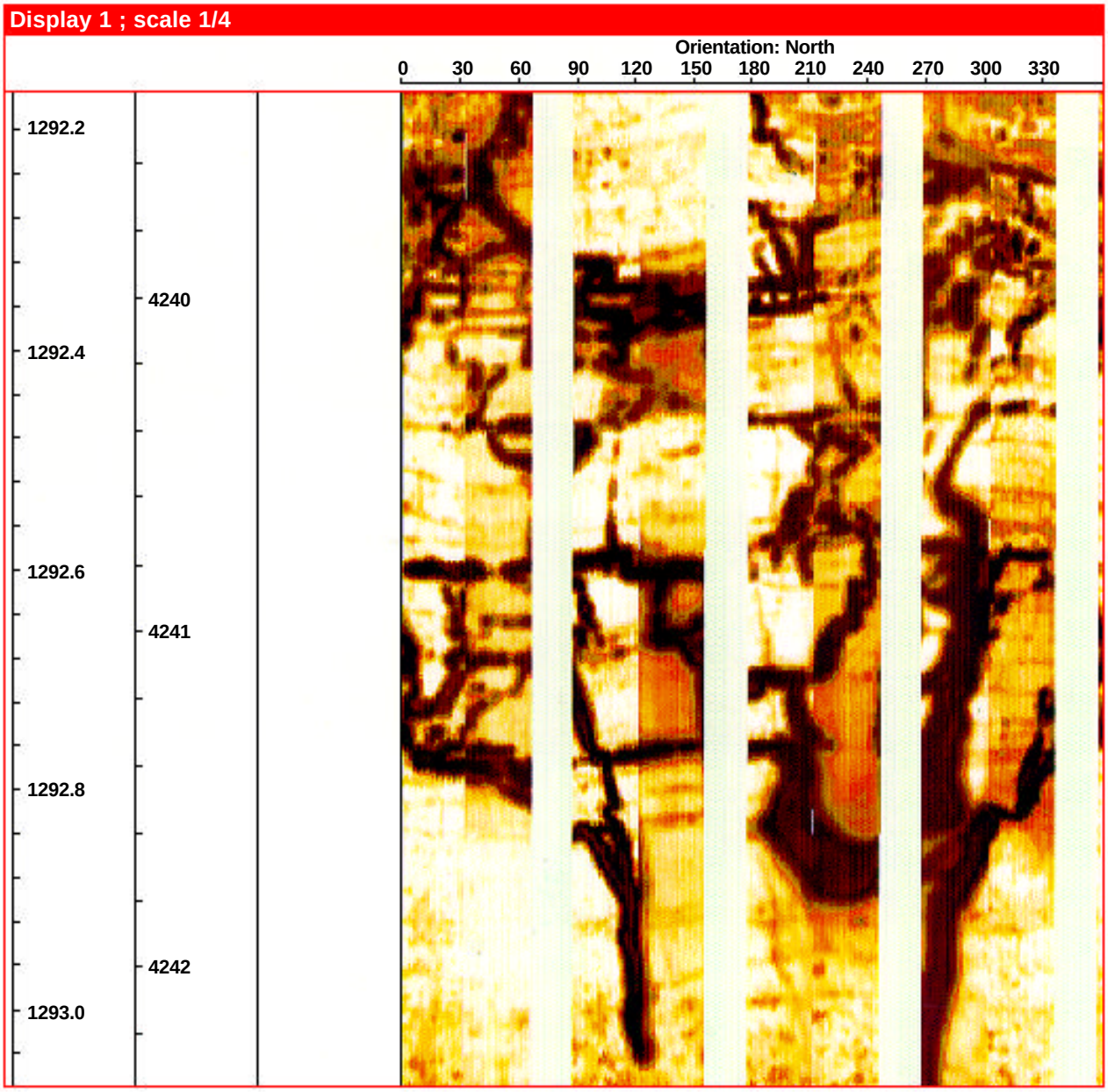

Fracture Exercise 7

Objective of this example: Fracture Characterization.
Geological Background: Carbonate.
Available Data: Resistivity Calibrated Images, Straight Borehole.
Evaluation:
Identification: ❑ Natural Vertical ❑ Polygonal (Syneresis) ❑ Mechanical Induced
Morphology: ❑ Open ❑ Partially Mineral-Filled ❑ Mineral-Filled ❑ Vuggy
Orientation: Fracture Angle: _____
Fracture Strike: _____

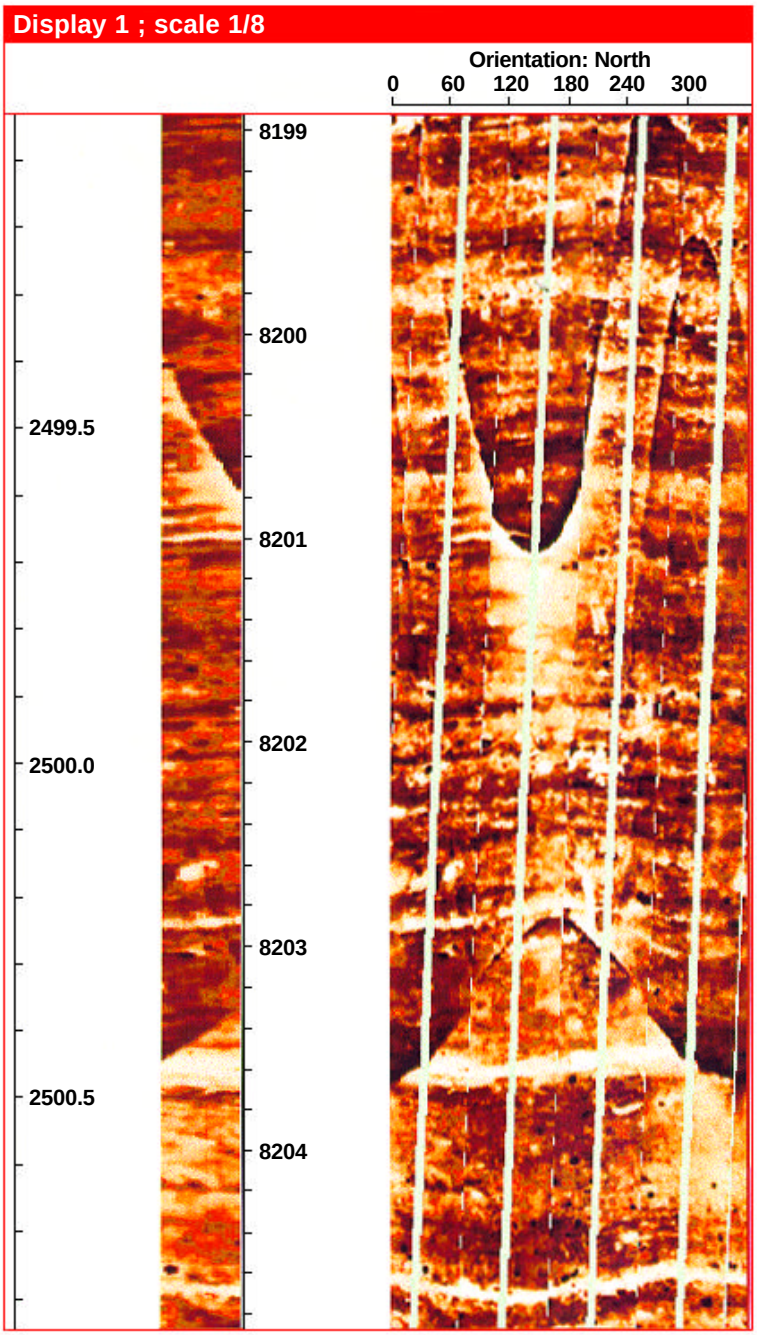

Fracture Exercise 8

Objective of this example: Fracture Characterization.
Geological Background: Carbonate.
Available Data: Resistivity Calibrated Images.
Evaluation:
Identification: ❑ Natural Vertical ❑ Polygonal (Syneresis) ❑ Mechanical Induced
Morphology: ❑ Open ❑ Partially Mineral-Filled ❑ Mineral-Filled ❑ Vuggy
Orientation: Fracture Angle: _____
Fracture Strike: _____

Azimuth Diagram:

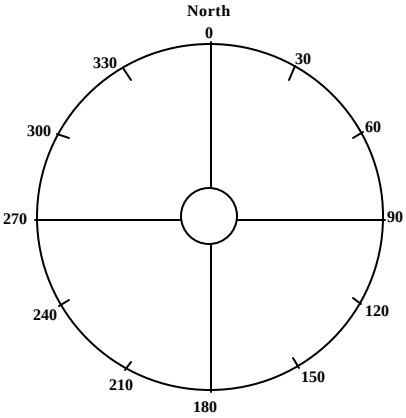

Carbonate

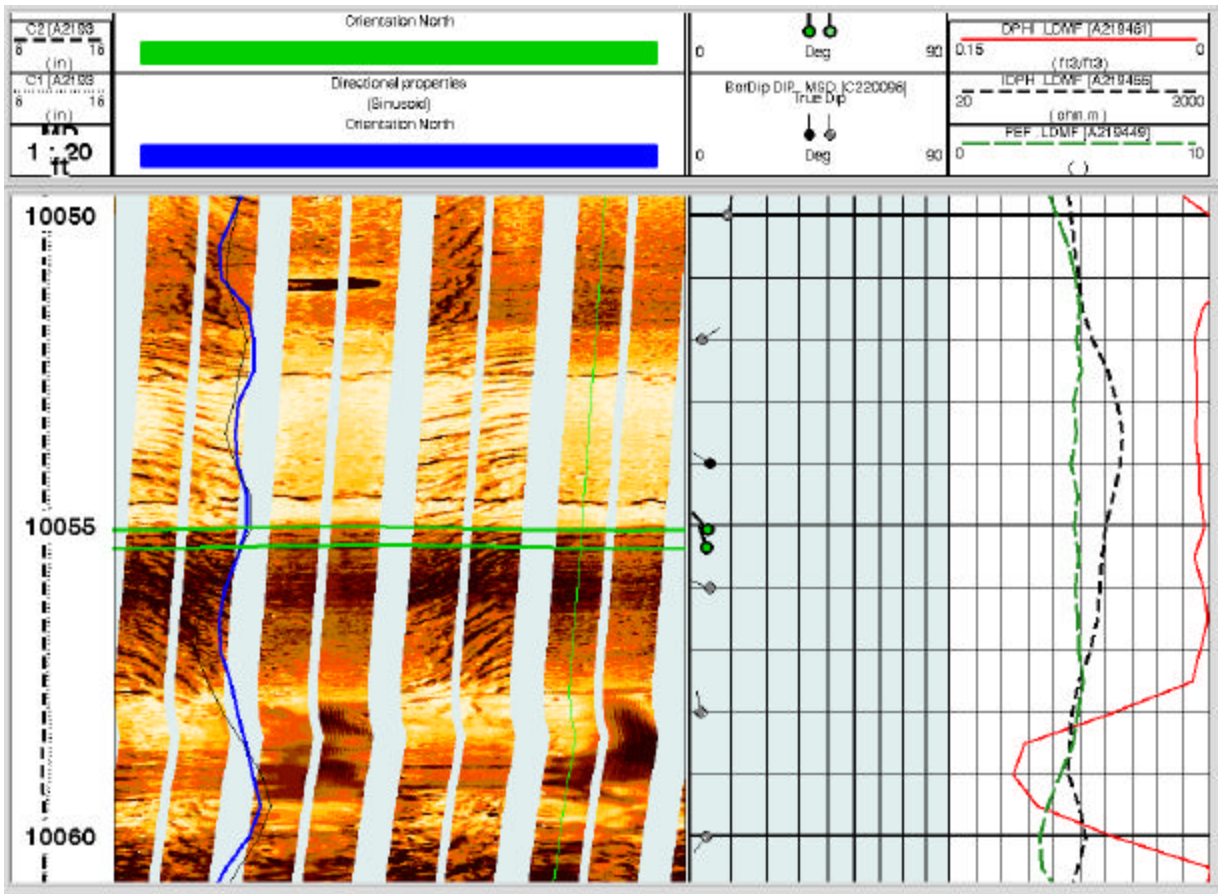

Fracture Exercise 9

Objective of this example: Fracture Characterization.
Geological Background: Carbonate.
Available Data: Resistivity Calibrated Images.
Evaluation:
Identification: ❑ Natural Vertical ❑ Polygonal (Syneresis) ❑ Mechanical Induced
Morphology: ❑ Open ❑ Partially Mineral-Filled ❑ Mineral-Filled ❑ Vuggy
Orientation: Fracture Angle: _____
Fracture Strike: _____

Ordovician Carbonate

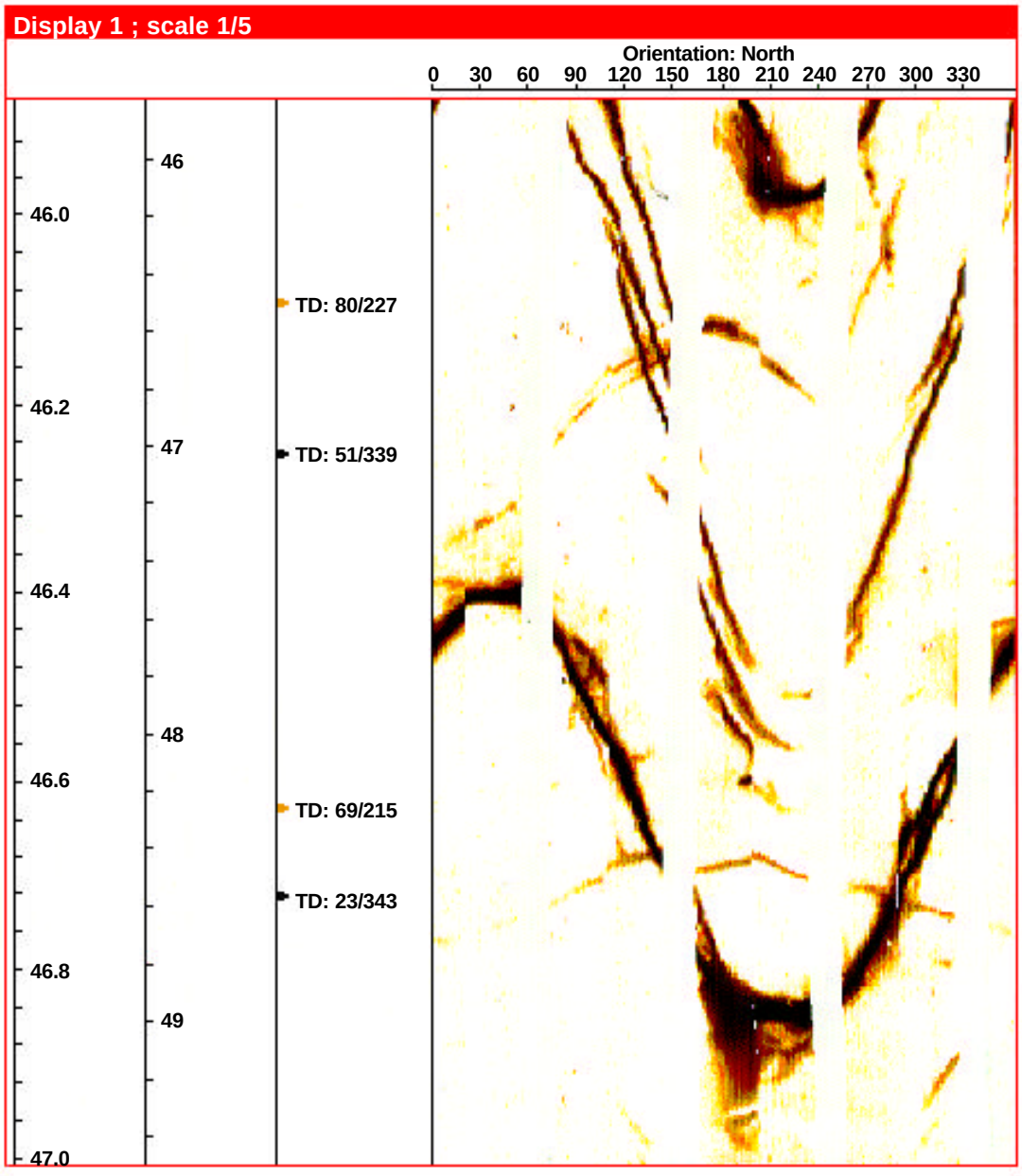

Fracture Exercise - Answers

Exercise 1

Identification: ☑ Natural Vertical ❑ Polygonal (Syneresis) ❑ Mechanical Induced
Morphology: ☑ Open ☑ Partially Mineral-Filled ❑ Mineral-Filled ☑ Vuggy
Orientation: Fracture Angle: **84°/179°**
Fracture Strike: **89° - 269° (E-W)**

Azimuth Diagram:

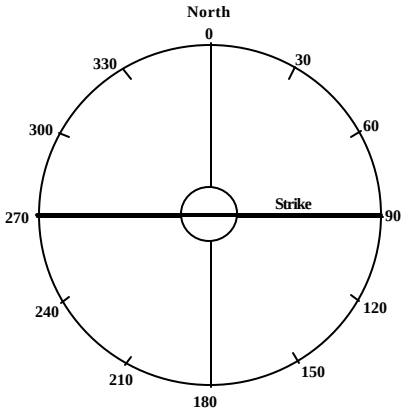

Exercise 2

Identification: ☑ Natural Vertical ❑ Polygonal (Syneresis) ❑ Mechanical Induced
Morphology: ☑ Open ☑ Partially Mineral-Filled ❑ Mineral-Filled ❑ Vuggy
Orientation: Fracture Angle: **87°/112°**
Fracture Strike: **22° - 202°**

Azimuth Diagram:

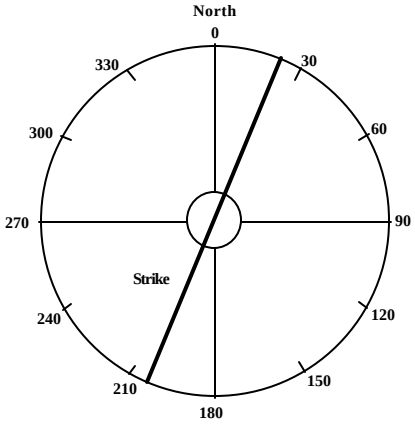

Exercise 3

Identification: ☑ Natural Vertical ❑ Polygonal (Syneresis) ❑ Mechanical Induced
Morphology: ❑ Open ❑ Partially Mineral-Filled ☑ Mineral-Filled ❑ Vuggy
Orientation: Fracture Angle: **50°/140°**
Fracture Strike: **N50°E - S50°W**

Fracture Exercise - Answers **(continued)**

Exercise 4

Identification:	❑ Natural Vertical ☑ Polygonal (Syneresis) ❑ Mechanical Induced
Morphology:	☑ Open ☑ Partially Mineral-Filled ❑ Mineral-Filled ❑ Vuggy
Orientation:	Fracture Angle: **NA**
	Fracture Strike: **NA**

Exercise 5

Identification:	❑ Natural Vertical ❑ Polygonal (Syneresis) ☑ Mechanical Induced
Morphology:	☑ Open ❑ Partially Mineral-Filled ❑ Mineral-Filled ❑ Vuggy
Orientation:	Fracture Angle: **Vertical**
	Fracture Strike: **30° - 210°**

Exercise 6

Identification:	❑ Natural Vertical ☑ Polygonal (Syneresis) ❑ Mechanical Induced
Morphology:	☑ Open ❑ Partially Mineral-Filled ❑ Mineral-Filled ☑ Vuggy
Orientation:	Fracture Angle: **NA**
	Fracture Strike: **NA**

Exercise 7

Identification:	☑ Natural Vertical ❑ Polygonal (Syneresis) ❑ Mechanical Induced
Morphology:	❑ Open ❑ Partially Mineral-Filled ☑ Mineral-Filled ❑ Vuggy
Orientation:	Fracture Angle: **High > 80°**
	Fracture Strike: **ENE - WSW**

***Note:** There is a fault at 2,500.4 meters

Exercise 8

Identification:	❑ Natural Vertical ❑ Polygonal (Syneresis) ☑ Mechanical Induced
Morphology:	☑ Open ❑ Partially Mineral-Filled ❑ Mineral-Filled ❑ Vuggy
Orientation:	Fracture Angle: **Vertical**
	Fracture Strike: **NE - SW**

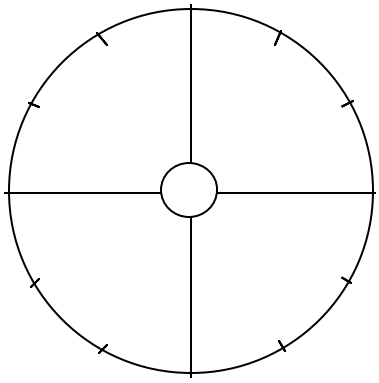

Fracture Exercise - Answers **(continued)**

Exercise 9 - Equalized Images

Identification:	☑ Natural Vertical ❑ Polygonal (Syneresis) ❑ Mechanical Induced
Morphology:	☑ Open ❑ Partially Mineral-Filled ❑ Mineral-Filled ❑ Vuggy
Orientation:	**Upper Fracture:**
	Fracture Angle: **80°/227°**
	Fracture Strike: **137° - 317°**
	Lower Fracture:
	Fracture Angle: **69°/215°**
	Fracture Strike: **125° - 305°**

Exercise 9 - Resistivity Calibrated

Identification:	❑ Natural Vertical ❑ Polygonal (Syneresis) ❑ Mechanical Induced
Morphology:	☑ Open **(very low flow rate)**
Orientation:	Fracture Angle: **Vertical**
	Fracture Strike: **NW - SE**

Comments: The figure on the following page shows both the fraction image and the computed hydraulic aperture. Normally, a minimum of 0.05 mm in gas reservoirs is required to be commercially productive. The image of a fracture is affected by the surrounding rock resistivity and the mud resistivity. The “large” fracture appearance is a result of a very resistive formation with a very conductive mud system. This allows a low aperture fracture to have the appearance of an open fracture due to the resistivity contrast.

Caution: *The only positive method of fracture evaluation is to calculate the hydraulic fracture aperture through fracture analysis programs.* This is discussed in a later chapter.

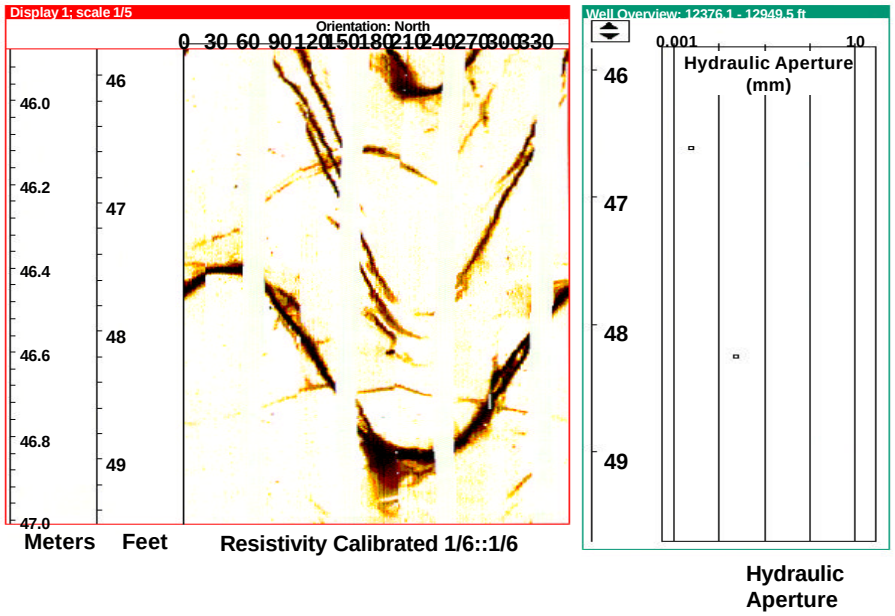

Fracture Analysis

Objectives of this Chapter:

Fracture analysis provides a quantitative evaluation of certain fracture properties. The electrical image response to fractures is a function of the fracture geometry, the flushed zone resistivity, and the mud resistivity. The fracture properties are:

- Hydraulic Aperture
- Porosity
- Density
- Length
- Statistics

Fracture Analysis

The fracture properties required for reservoir studies are the effective fracture aperture, the fracture porosity, fracture density, and the trace length of the fracture observed by the images. These are determined by the use of the program FracView. This is an interactive computer assisted program. The analyst marks a trace on the fracture image in the vicinity of the fracture. The program then searches the locality and follows the conductive, or resistive, fracture trace. From mathematical modeling of the electrical image tool, calculation of the invaded zone resistivity, and knowledge of the mud resistivity, the fracture width (aperture) can be computed. Fracture porosity is a function of the computed aperture. The width times the trace length is the area of the fracture. This is divided by the pad coverage to define the fracture porosity. The density is the number of fractures per foot or meter computed perpendicular to the fracture plane. The trace length is the actual length of the fracture observed on the image. Fractured reservoirs are the primary target for horizontal boreholes.

- ♦ Required Measurements
  - – Electrical Images
  - – Resistivity (SFL or LLS)
  - – AMS or Accurate Rm
- ♦ Processing
  - – FMSRES, “FMR” Files
  - – BORSCA, “ECS” Files
- ♦ Calculated Fracture Properties
  - – Fracture Morphology
  - – Petrophysical
    - • Hydraulic Aperture
    - • Porosity
    - • Density
    - • Trace Lengths
    - • Statistics

Fracture Aperture Calculations

As a button electrode approaches a fracture, which is filled with mud or other fluid of resistivity, Rm, an increased current will begin to flow because of the presence of this low resistivity anomaly. This increased current will continue to flow until the electrode is far enough away from the fracture that is no longer affected by the fracture. For this reason, a fracture which is physically thinner than 0.1 mm may have an electrical image which appears to be an inch or more wide. Obviously it is impossible to resolve directly a fracture using a sensor button which is many times the size of the fracture. There is however, an indirect method which provides the solution. From measurements and mathematical simulation, we know the response of the electrical image tool to fractures filled with fluids of different resistivities. Further, we know that the fracture aperture is proportional to the sum of the increased current flow, mathematically this can be expressed as:

$$W = c \bullet A \bullet Rm^{b} \bullet Rxo^{1-b}$$

Where **W** = fracture aperture

b,e = constant from tool modeling

A = excess current divided by voltage and integrated along a line perpendicular to the fracture trace

Rm = mud resistivity

Rxo = flushed zone resistivity

Fracture Aperture Calculation

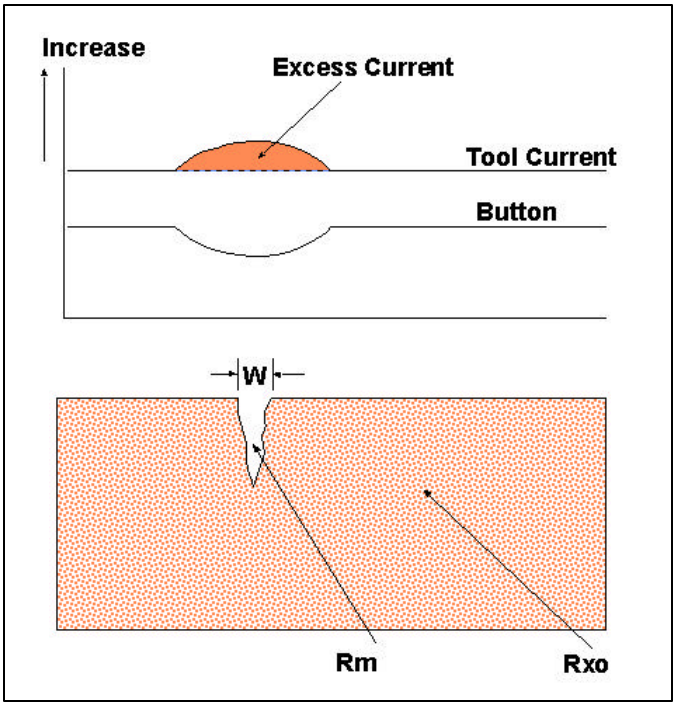

Hydraulic versus Mean Aperture

Two calculations of fracture aperture are available. The first, mean aperture, is simply the average width of the fracture along its length. The second, hydraulic aperture, is the cubic mean of the fracture width. The term hydraulic is used since this method is proportional to fluid flow through the fracture. The mean aperture provides only information about the physical size of the fracture opening. A comparison of flow capacities of different fractures is possible with the hydraulic apertures but not with the mean apertures. A numeric example of these calculations is provided in Appendix I.

Example - Production versus Hydraulic Aperture

Fracture hydraulic apertures were computed in several oil fields. There is a cubic relationship between the initial production results and the hydraulic aperture in this field. Similar results have been found in all fractured monophasic (gas or oil) reservoirs.

Production vs. Hydraulic Aperture

- 20 wells
- No water/gas production
- 3 measured Rm
- Single fractures
- Not normalized for pressure/viscosity

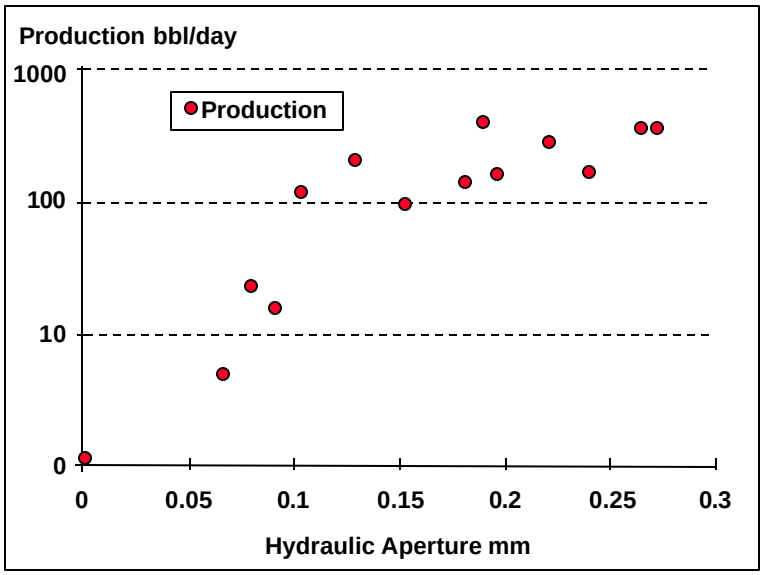

Hydraulic versus Mean Aperture

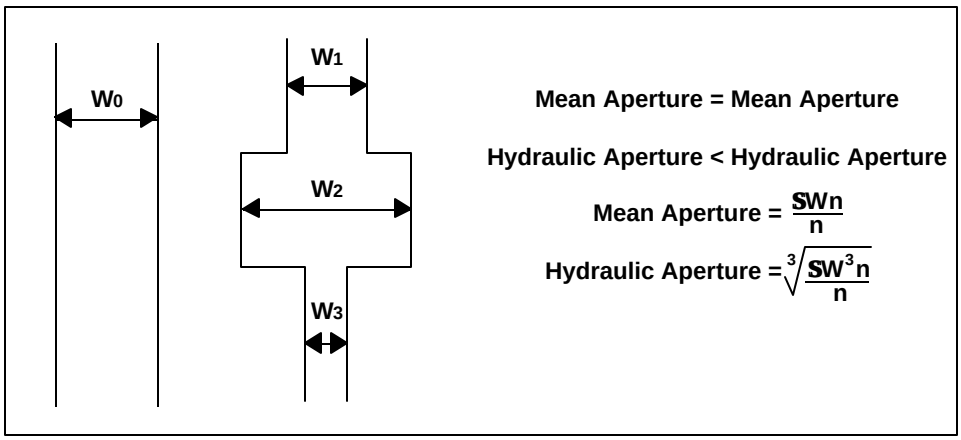

Example of Hydraulic versus Mean Apertures

This example compares the results of the hydraulic aperture calculations with mean aperture calculations on a horizontal borehole. The hydraulic apertures are larger than the mean apertures. However, there is not a consistent offset between the two results since the shape of the fracture opening is accounted for in the hydraulic aperture calculation.

The average values for hydraulic aperture and mean aperture of all the individual fractures penetrated by the borehole is shown in the lower panel.

Aperture Calculation

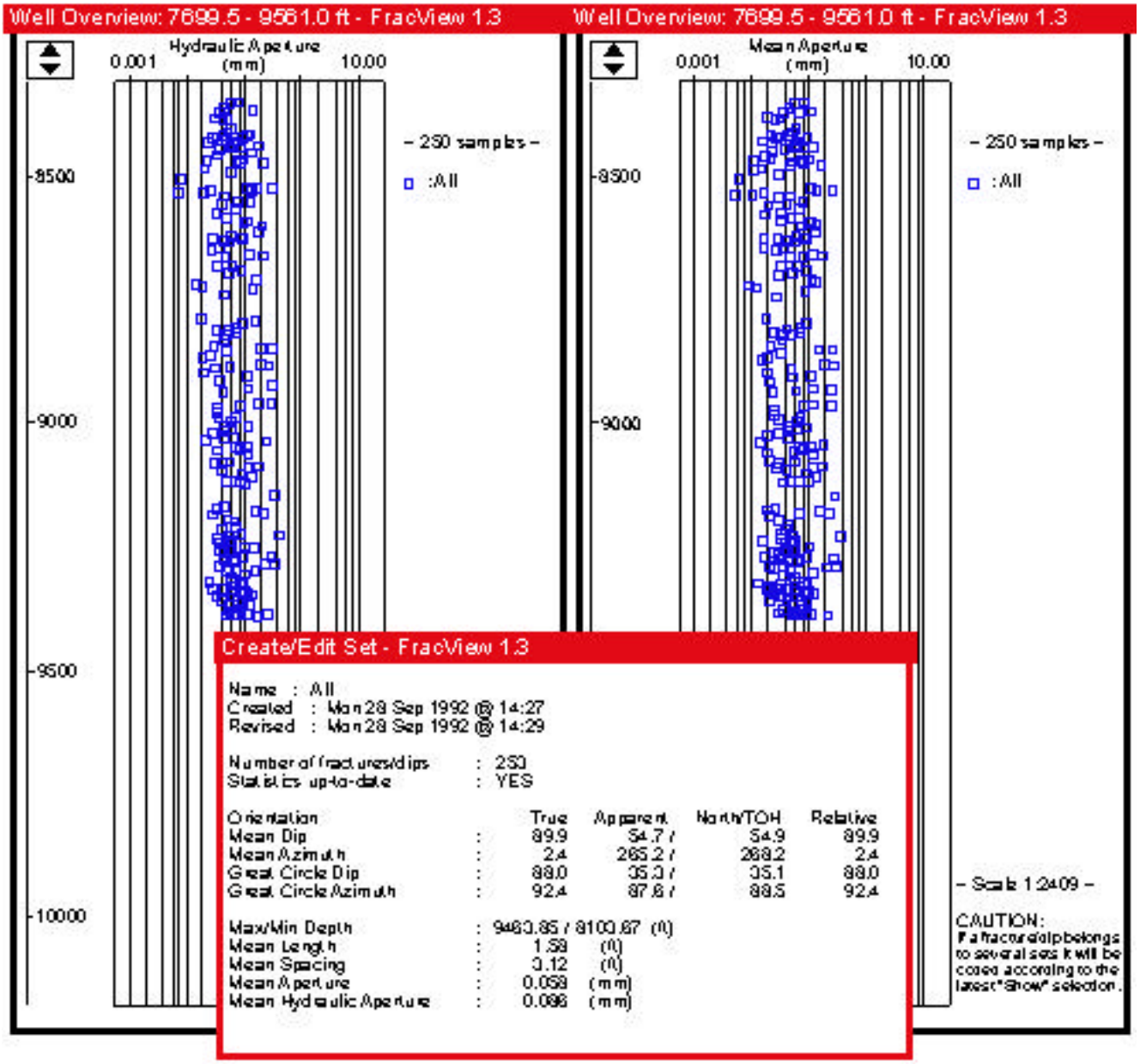

Effect of Rm and Rxo

The resistivity of the mud filling the fracture affects the images and thus the aperture calculations. A highly resistive mud, typically fresh mud, will suppress the electrical image response. A low resistivity mud, salt mud, will enhance the appearance of the fracture on the electrical images. Fracture aperture calculations account for this effect and allow for an accurate determination of the aperture.

A comparison of the effects of changing the value input for mud resistivity is shown opposite. The correct values for a horizontal borehole are shown in Figure 1. These are Rm = .15 and Rxo = 16. When an incorrect value of Rm = .5 is input, the calculated values increase. This is shown in Figure 2. Likewise, when an Fm = .05 is used, the aperture calculations decrease as shown in Figure 3.

Another important consideration is the proper calibration of the images to true resistivity. An incorrect Rxo will also cause a shift in the apparent apertures. The above calculations were based on an Rxo of 16. Figure 4 shows the effect of deliberately miscalculating the images to a value of 12. A comparison with Figure 1 shows the apertures have been shifted to a higher value.

Incorrect values of mud resistivity and calibrated image resistivity will produce the following changes in calculated fracture apertures:

Input	**Apertures**
Rm too high	*Increase*
Rm too low	*Decrease*
Rxo too high	*Decrease*
Rxo too low	*Increase*

Effects of Rm and Rxo

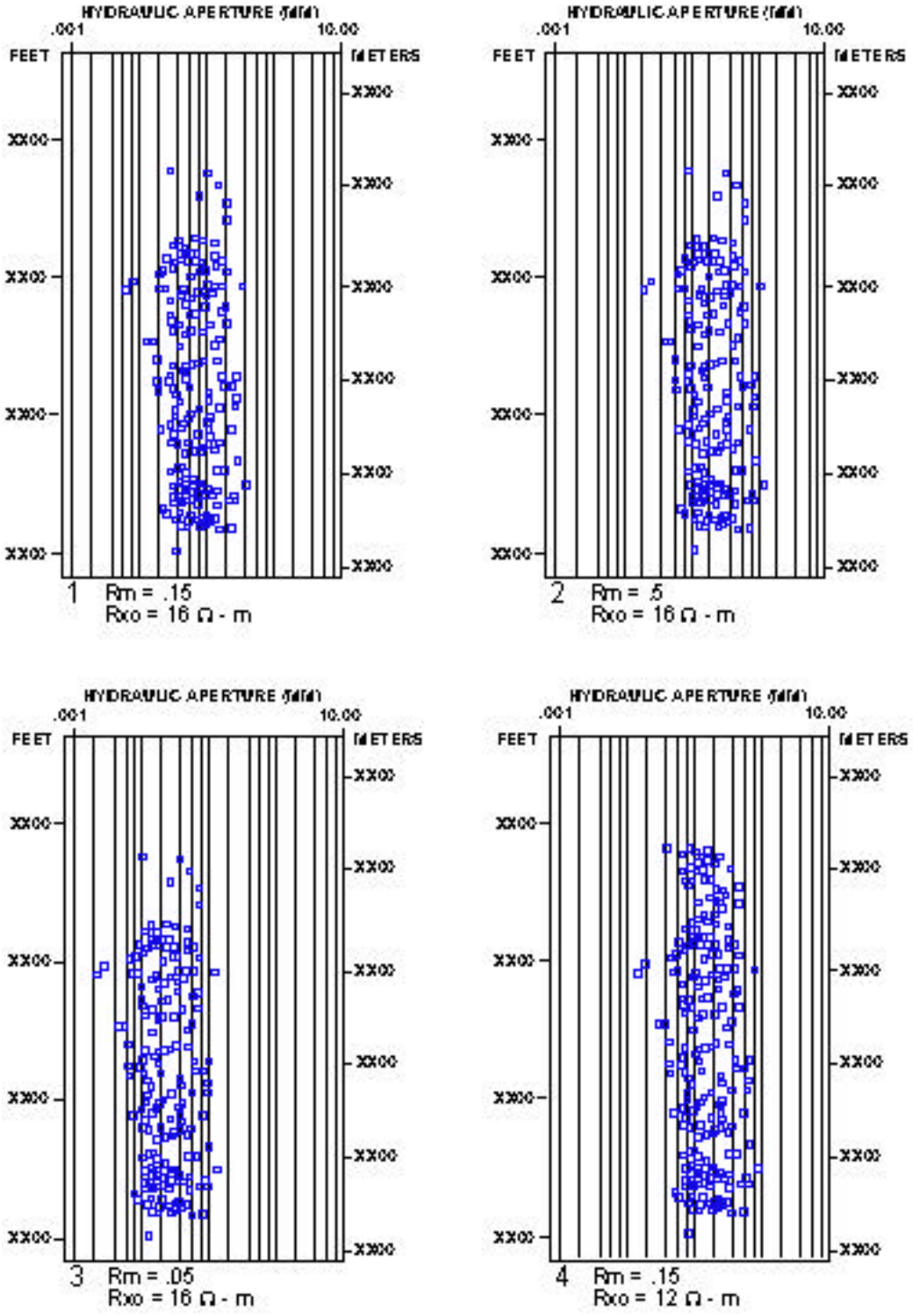

Fracture Porosity

Fracture porosity is defined as the percentage of the borehole wall which is represented by the fracture. This porosity is derived from the fracture aperture, trace length, and the borehole coverage of the images. It should be noted this fracture porosity value applies only to the fracture void space and not with matrix porosity.

Fracture Density

There are two available fracture density calculations. The **raw fracture density** is the number of fractures per foot or meter selected along the borehole. The **corrected fracture density** is the number of fractures per foot or meter selected along a line perpendicular to the fracture plane.

Trace Length

The segment of the fracture as observed by the images in the borehole is the **trace length.**

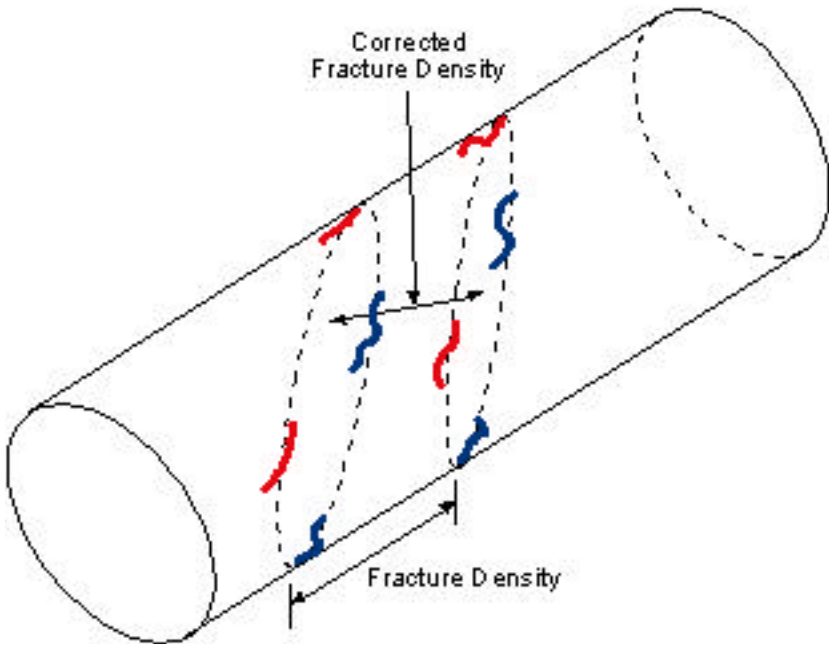

Porosity = Width x Length

For Image Analysis:

Fracture Porosity = Width x Trace Length x 1/Coverage

Raw Fracture Density = Number of Fractures/Foot Along the Borehole

Corrected Fracture Density = Number of Fractures/Foot Along a Line Perpendicular to the Fractures

Trace Length = Length of Fracture as Seen on the Images

Fracture Log Example

The fracture log computation attempts to summarize the information from the individual fracture calculations into a continuous log presentation. This allows comparison with other log data. The ***FVDC*** curve is the corrected fracture density. ***FVAH*** is the hydraulic aperture while ***FVPA*** is the fracture porosity.

Fracture Log

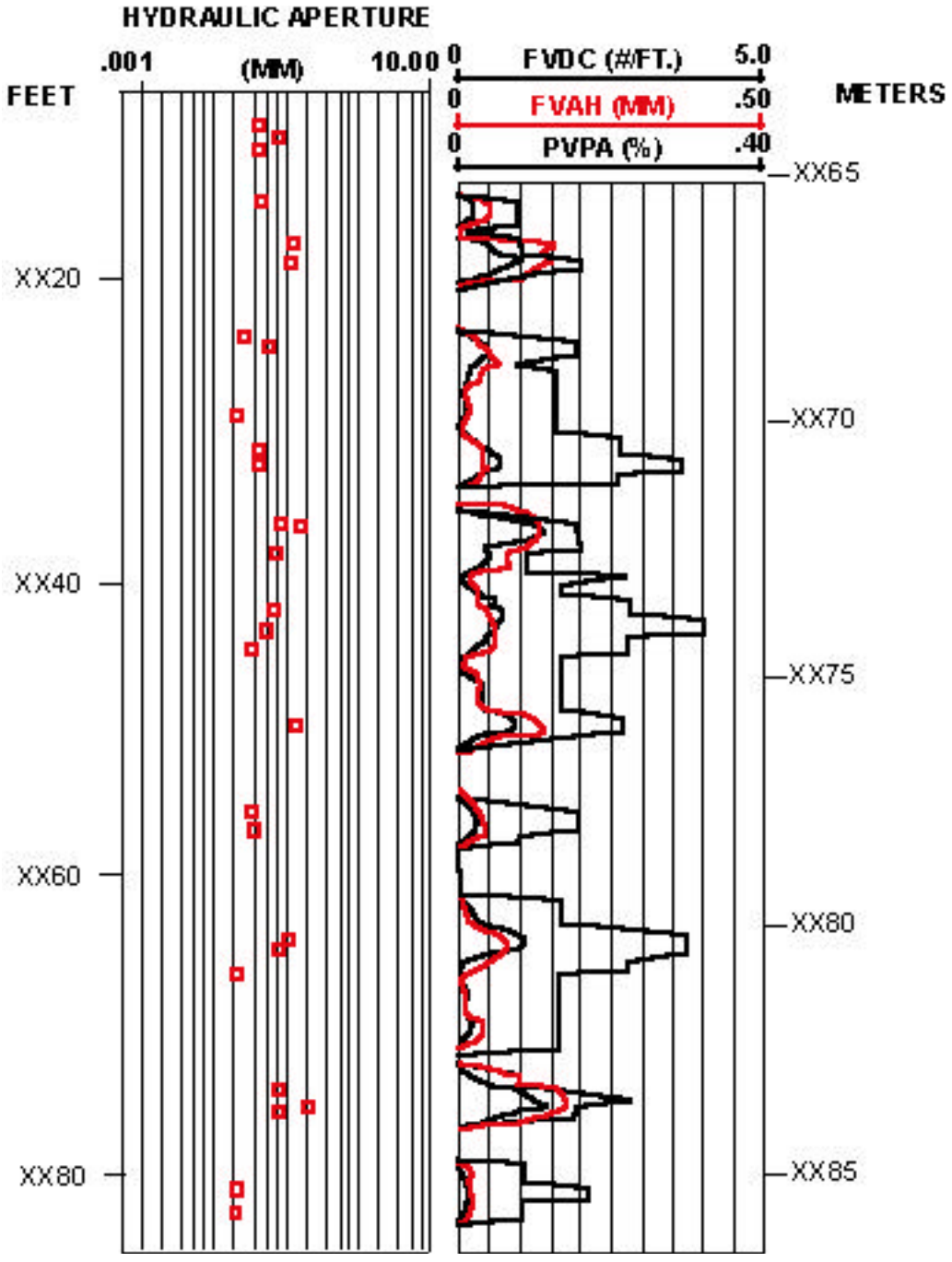

Fracture Analysis Exercise 1

Objective of this Exercise: Fracture analysis in a deviated borehole.

Geological Background: This is a 45 degree deviation borehole which is a pilot hole for a horizontal well in a fractured carbonate.

Available Data: Electrical Images and a Fracture Log

Question: What should be the target zone for the horizontal borehole?

Cretaceous Carbonate (45° Deviation - Pilot Hole)

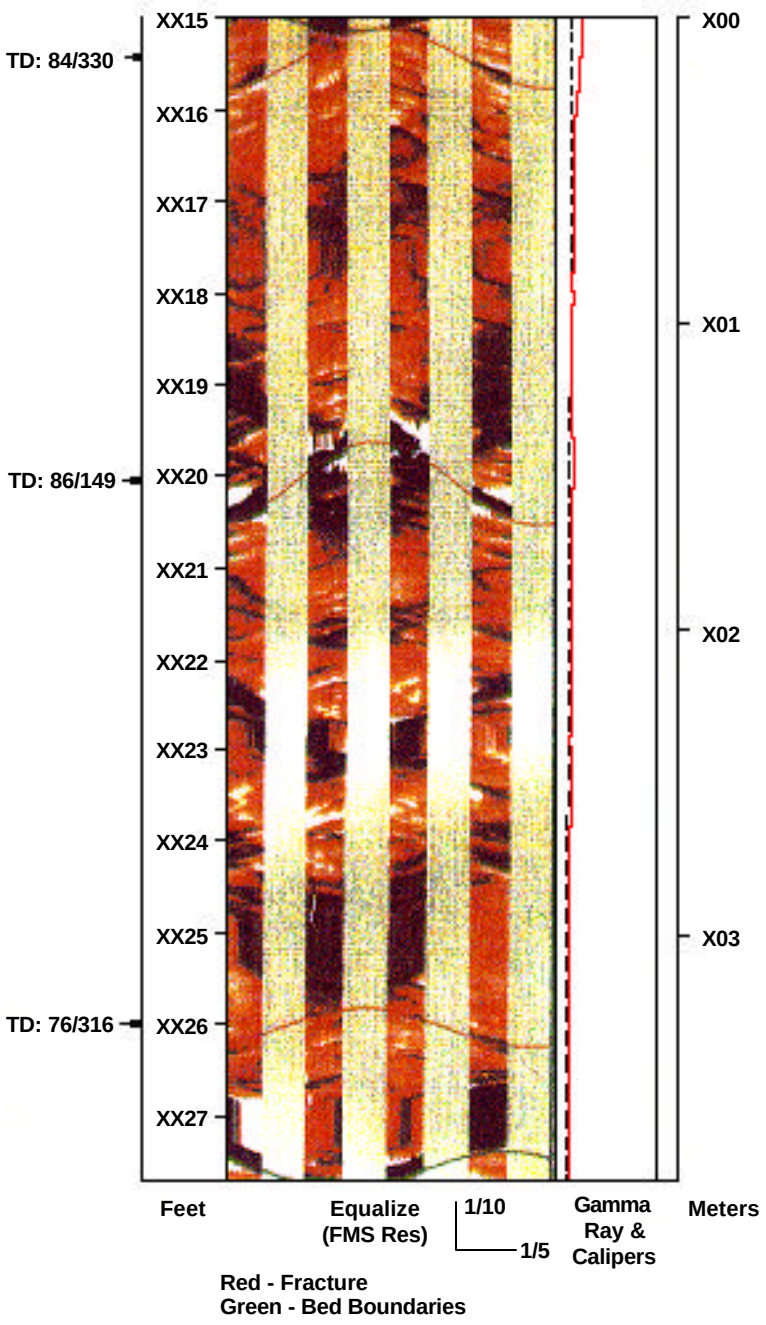

FracView Cretaceous Carbonate (45° Deviation - Pilot Hole)

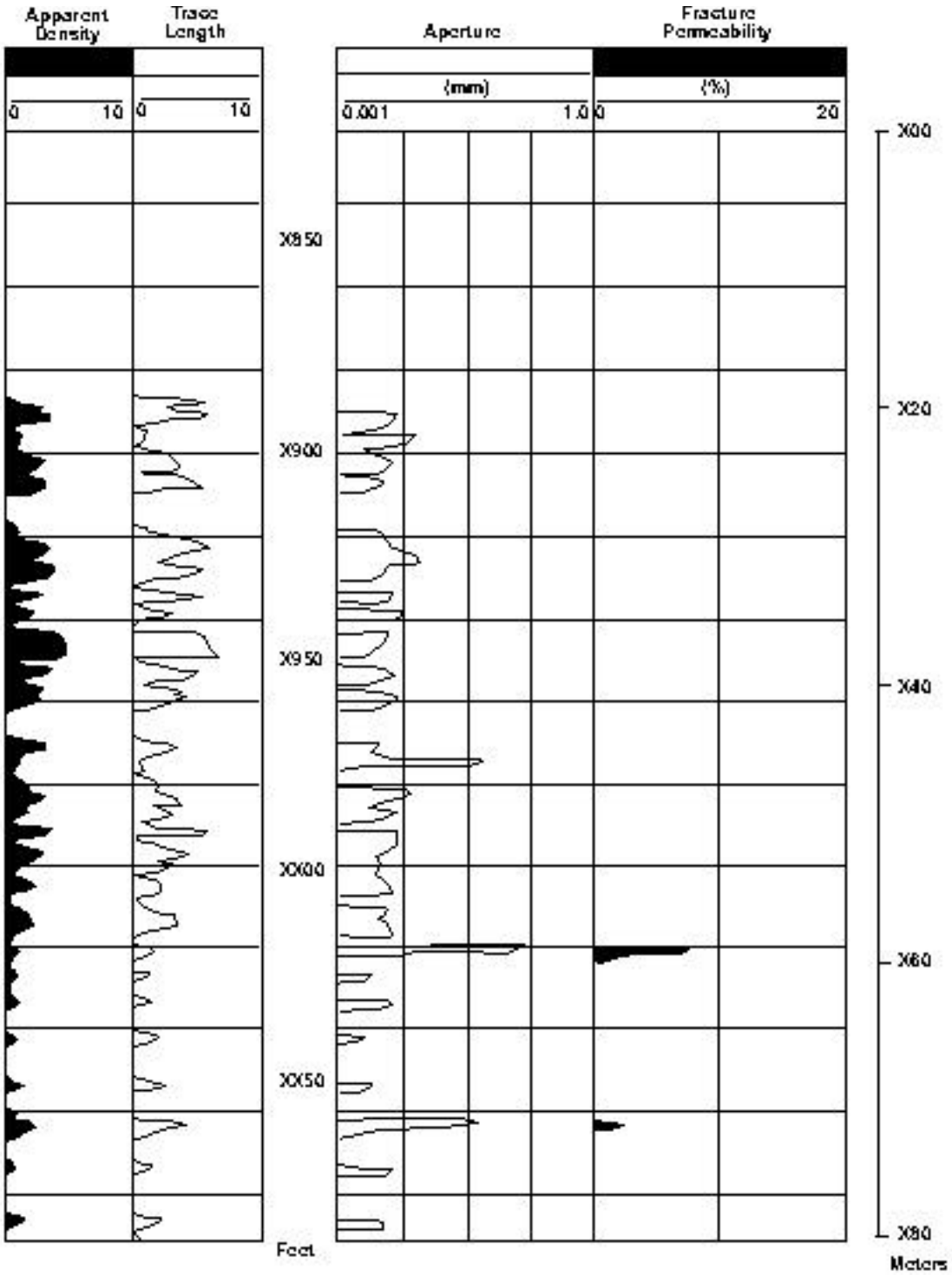

Fracture Analysis Exercise 2

Objective of this Exercise: Fracture analysis in a vertical borehole.

Geological Background: This is a carbonate. There were no shows or drilling breaks and no porosity indicated on the porosity logs.

Available Data: Electrical Images and a Fracture Log

Question: Casing was set on this well for a lower interval. Should the indicated interval be perforated? Why? Should other intervals be perforated?

Polygonal Fractures Carbonate

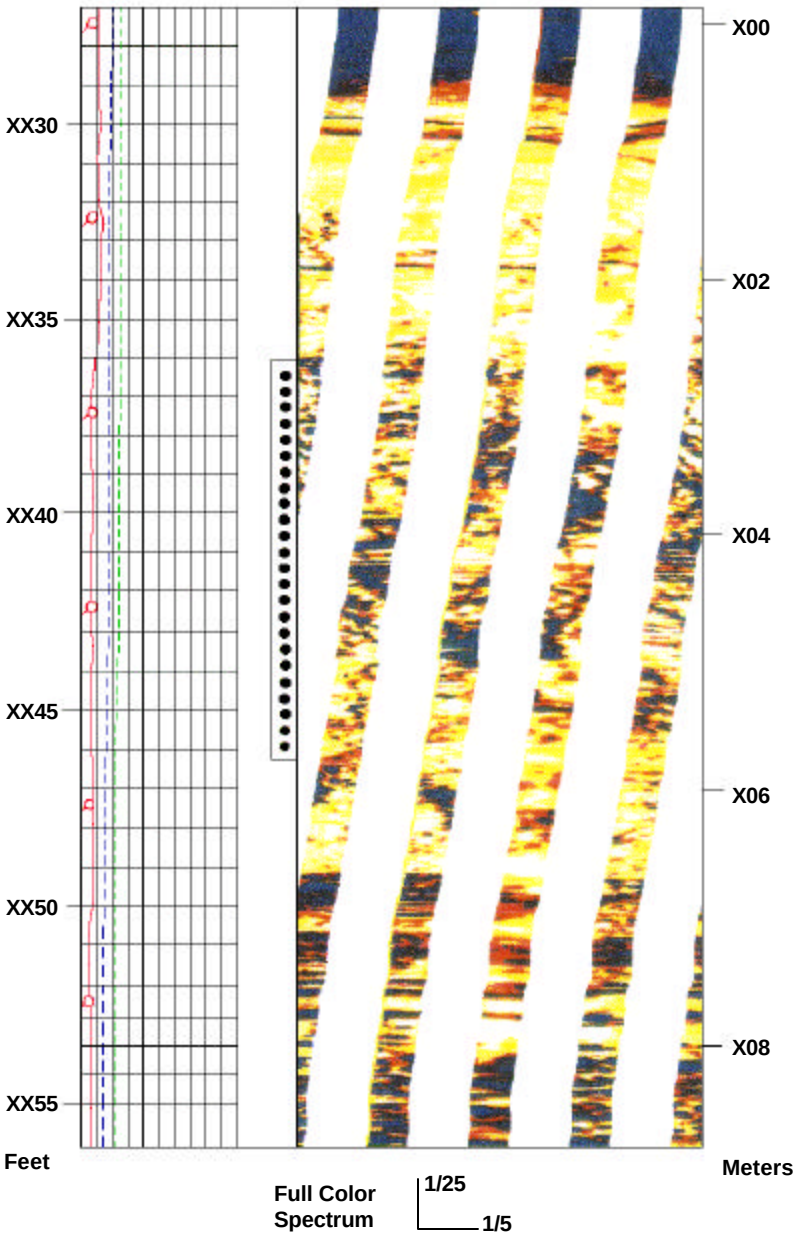

FracView Carbonate Polygonal Fractures

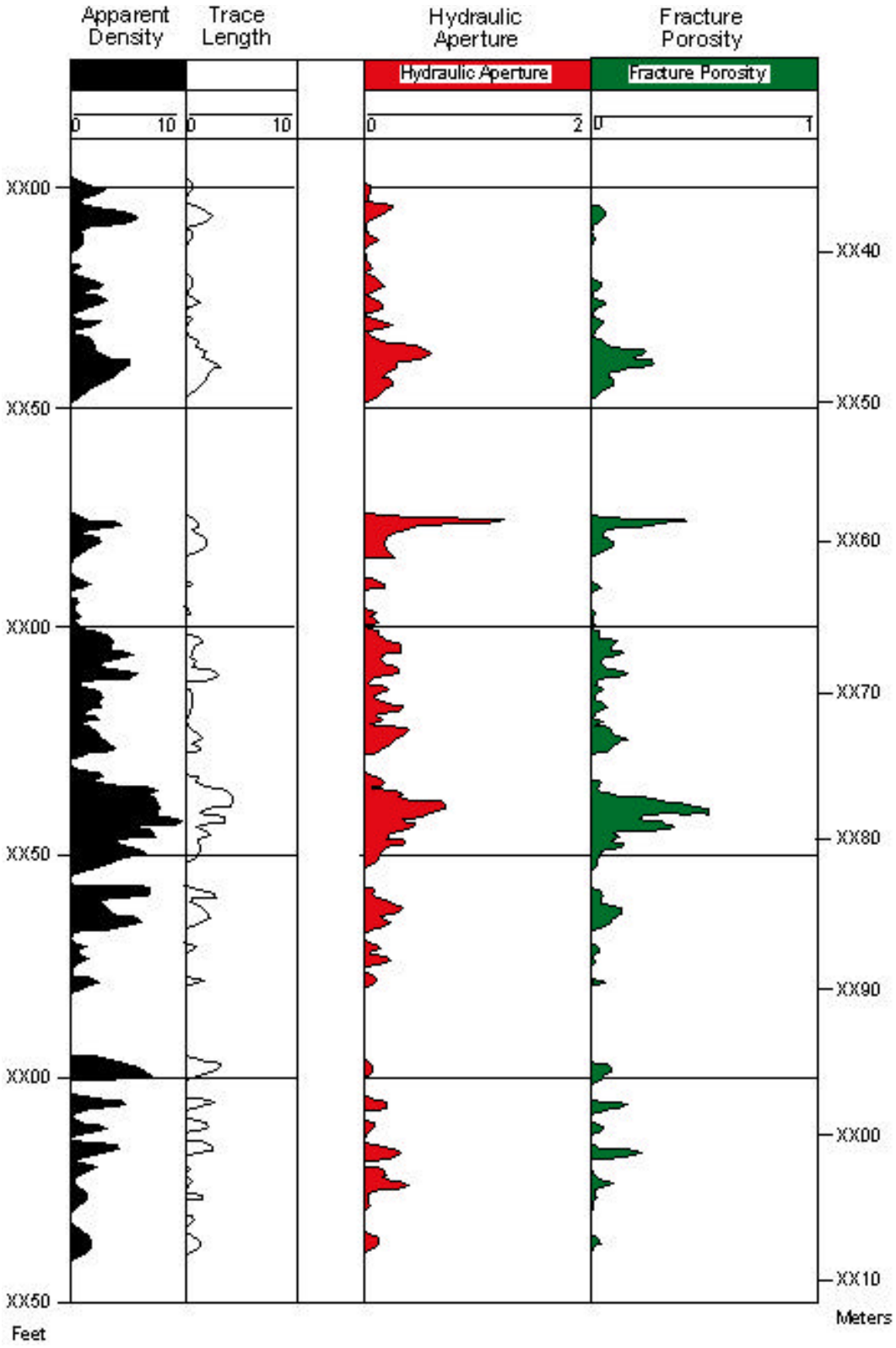

Fracture Analysis Exercise 3

Objective of this Exercise: Fracture analysis in a vertical borehole.

Geological Background: This is a carbonate. There were no shows or drilling breaks and no porosity indicated on the porosity logs.

Available Data: Electrical Images, Hydraulic Apertures, and a Neutron-Density Log.

Question: **Should this well be perforated?** _____

Where should this well be perforated?

_____

Neutron/Density Log

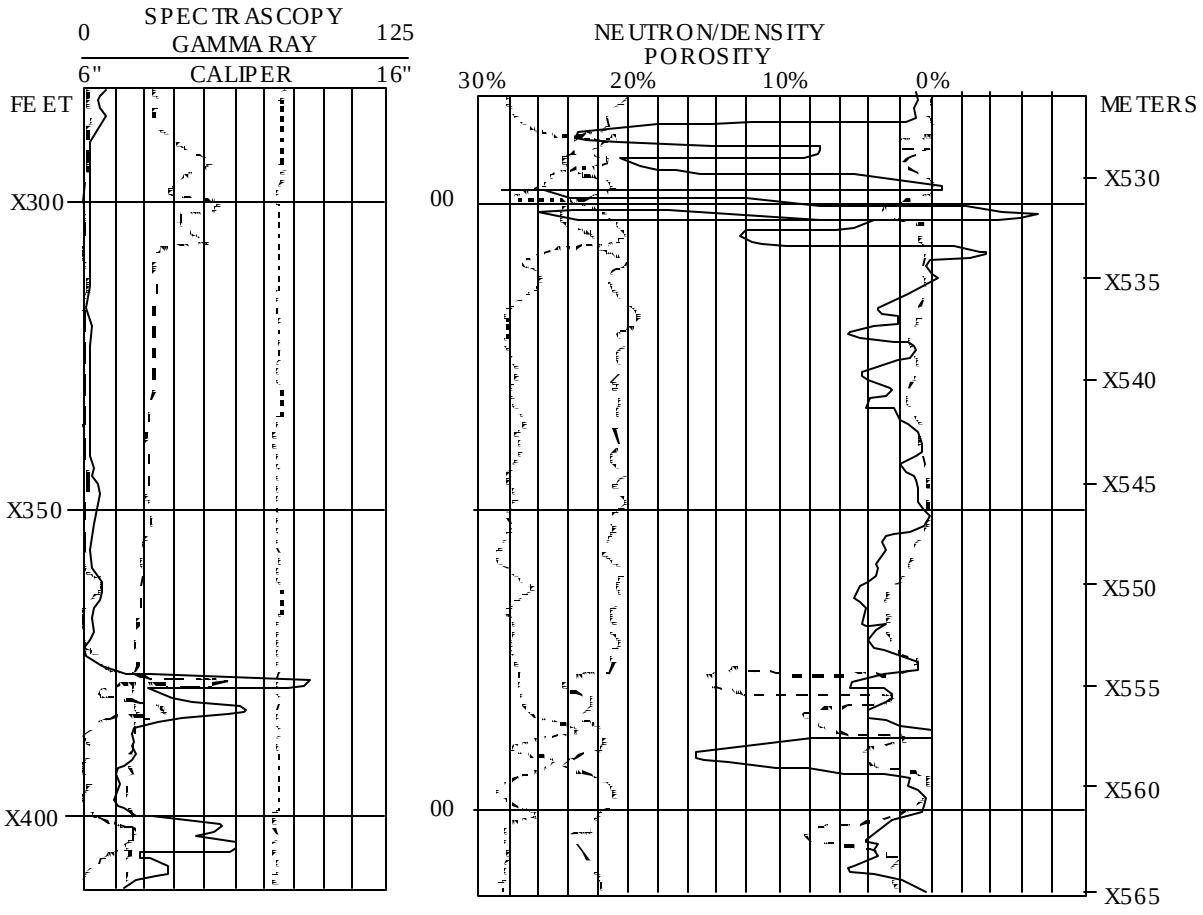

Carbonate

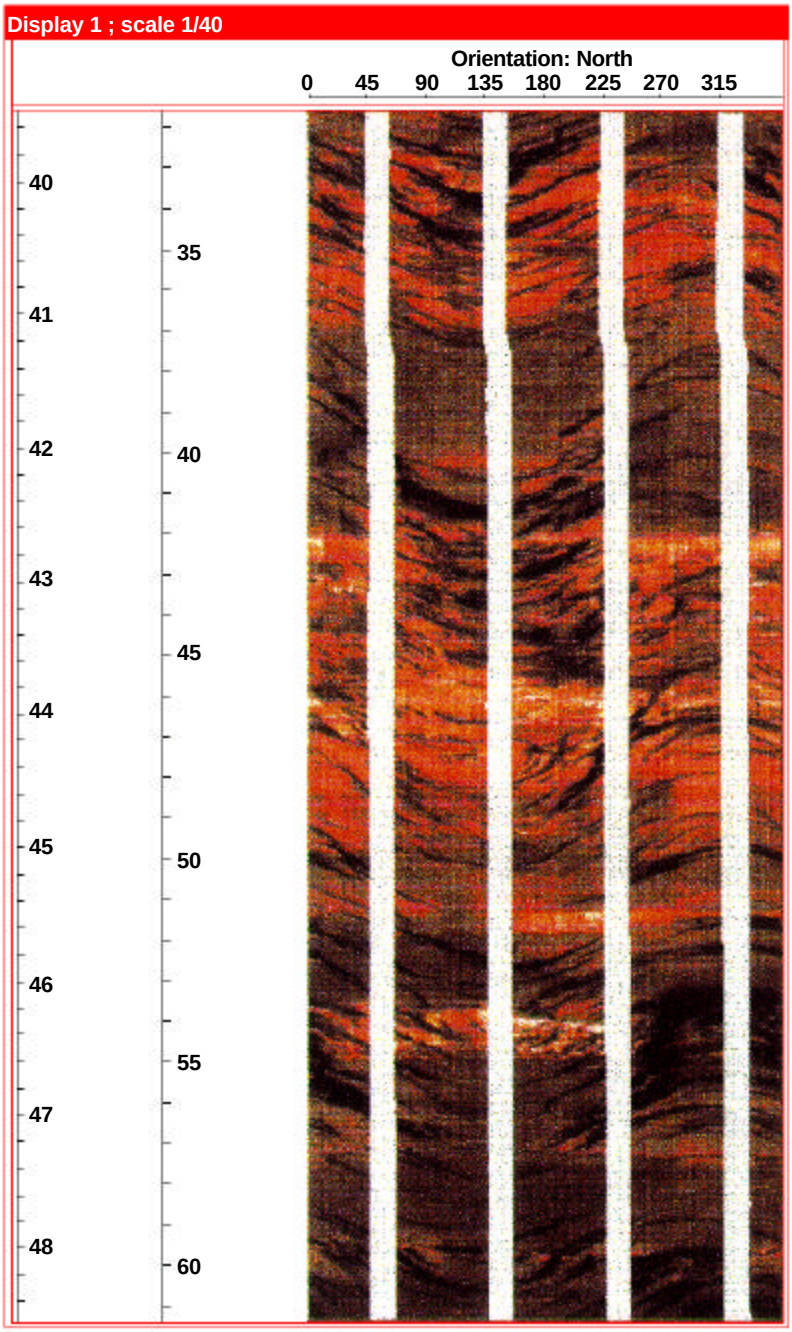
Display 1 ; scale 1/40
Orientation: North
0 45 90 135 180 225 270 315
40
41
42
43
44
45
46
47
48
35
40
45
50
55
60
Meters
Feet
Equalized Images

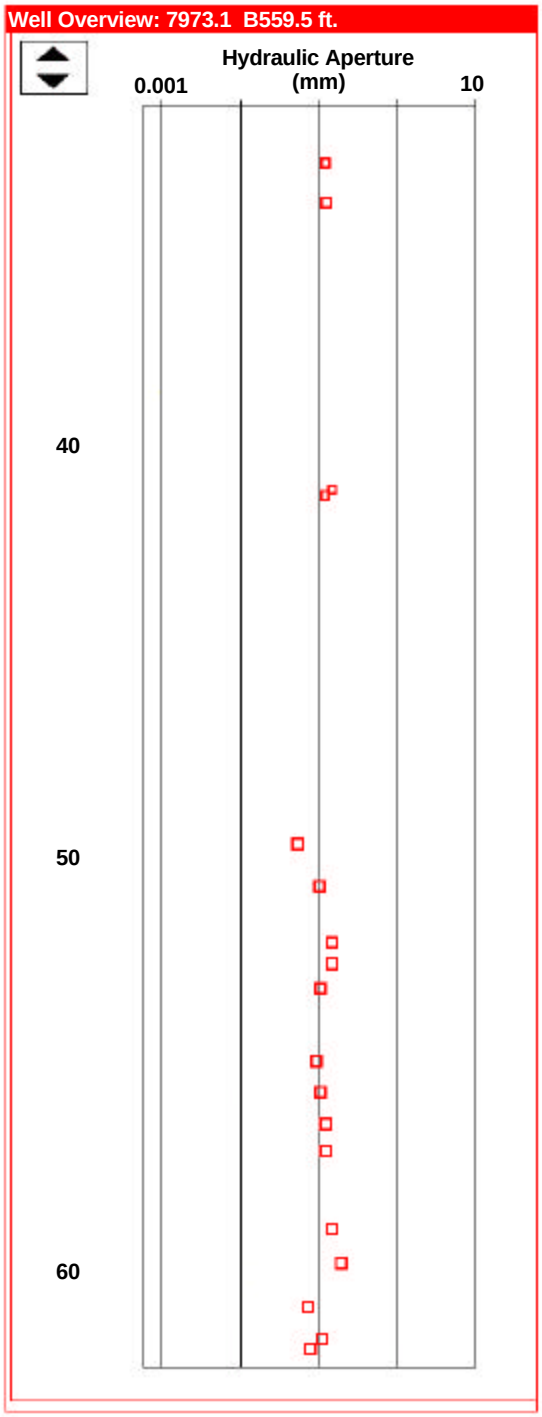
Well Overview: 7973.1 B559.5 ft.
Hydraulic Aperture
(mm)
0.001
10
40
50
60
Feet
Hydraulic Aperture

Fracture Analysis Exercise - Answers

Exercise 1

1. The best fracture is at xx20 feet (59.5 meters). This is the target interval.

Exercise 2

1. Yes. There are polygonal fractures present. The fracture Log indicates good aperture and porosity in this interval. There are other sections at xx58 meters and at xx47 meters.

Exercise 3

1. Yes. Hydraulic apertures are greater than 0.1 mm.
2. The highest aperture fractures are from x50 ft. - x60 ft. This well flowed 511 BOPD from this perforated interval.

Vugs

Objectives of this Chapter:

- The characterization of vugs from electrical images. This includes the classification of vugs into:
  - open-interconnected;
  - open-isolated; and
  - mineral-filled.

Vuggy Porosity

Secondary porosity in carbonates includes vugs and fractures. Vugs are cavities which form naturally in carbonates. Producibility can be greatly enhanced if the vugular porosity is interconnected.

Vugs can be identified by electrical images and classified into open or mineral-filled as well as interconnected or isolated.

Interconnected Vugs

Vugs which are interconnected will appear as a dark smudge on the electrical images. This is due to the depth of investigation of the image tools. The interconnected vugs form a path of diffusion for the electrical current and cause the smudged appearance. The equalized images should be used to identify the connectiveness of the vugs. The hilited images are helpful to identify vuggy porosity when the images are very blurred.

Isolated Open Vugs

Isolated vugs do not contribute to production. These are recognized as individual vugs with no blurring.

Mineral-Filled Vugs

As vugs become mineral-filled, the permeability is greatly reduced or even reduced to nothing. Mineral-filled vugs have a “white” appearance since the common filling minerals are calcite and anhydrite which are resistive.

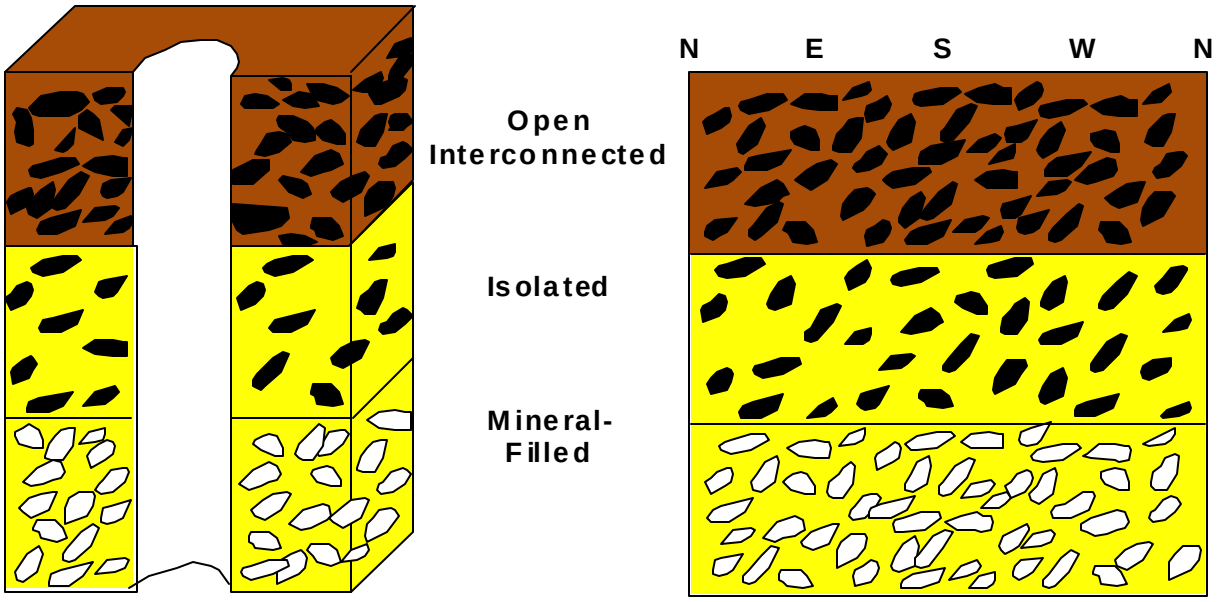

Pyritic Shale

A caution is required for the case of pyritic shale. Due to their conductive properties, even extremely small pyrite crystals will show up as dark patches.

Pyritic Shale

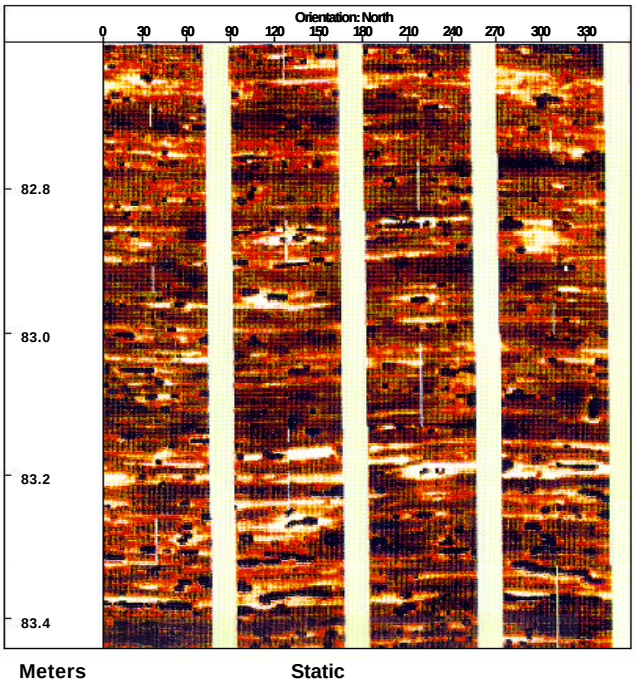

Gas Entry

This images shows a gas entry into the wellbore. Gas, or oil, is resistive and gives a resistive smeared appearance.

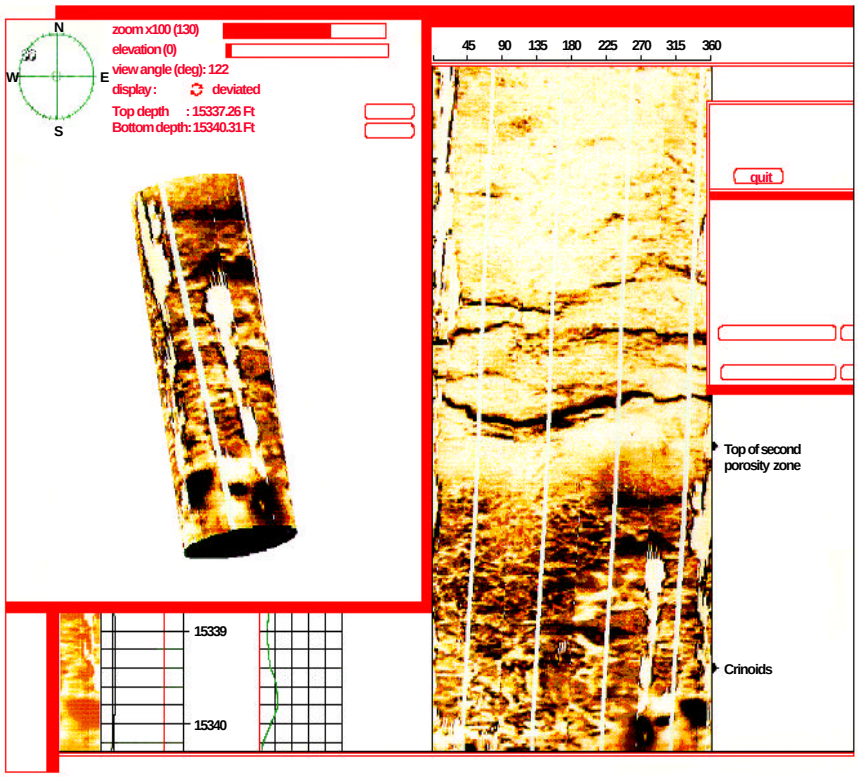

Vuggy Porosity - Calcite Filled Vugs

Secondary porosity must be open to be productive. Filling material such as calcite effectively plugs the pore space. Shown in upper figure below is the result of vugs filled with calcite. Images alone cannot determine the lithology of the filling material but can indicate the presence of such resistive material. Shown in the lower figure below is the the image of anhydrite inclusions.

Calcite Filled Vugs

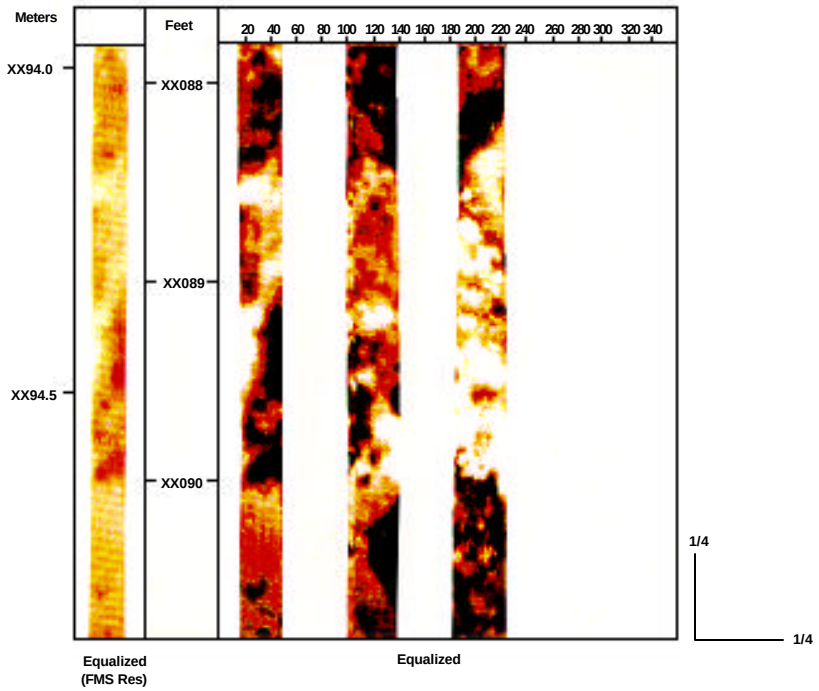

Anhydrite Inclusions

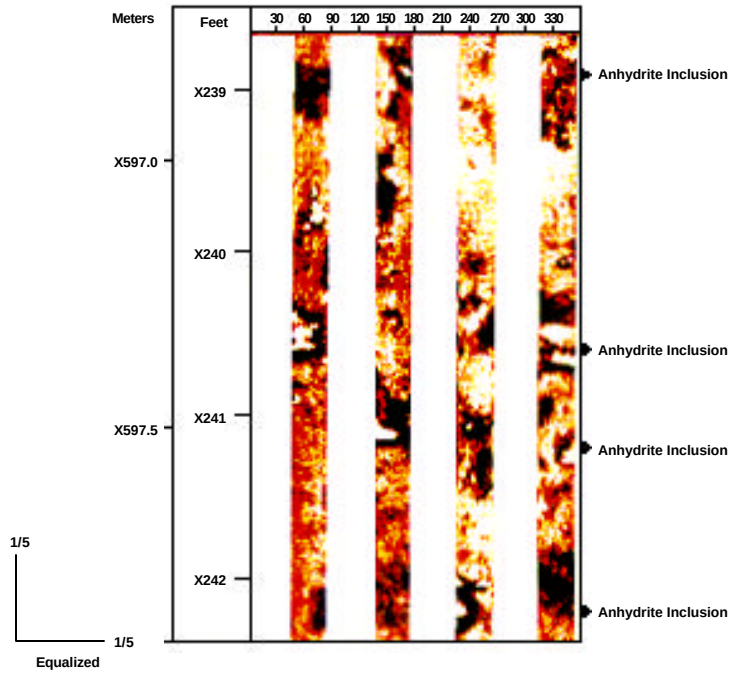

Vugs Exercise 1

Objective of this exercise: Vug Characterization.
Geological Background: Carbonate.
Available Data: Electrical Images, computed log.
Question: What type of vuggy porosity is present in zones A and B?

____ Open/Interconnected
____ Open/Isolated
____ Mineral-Filled

Carbonate (Computed Log: Elan)

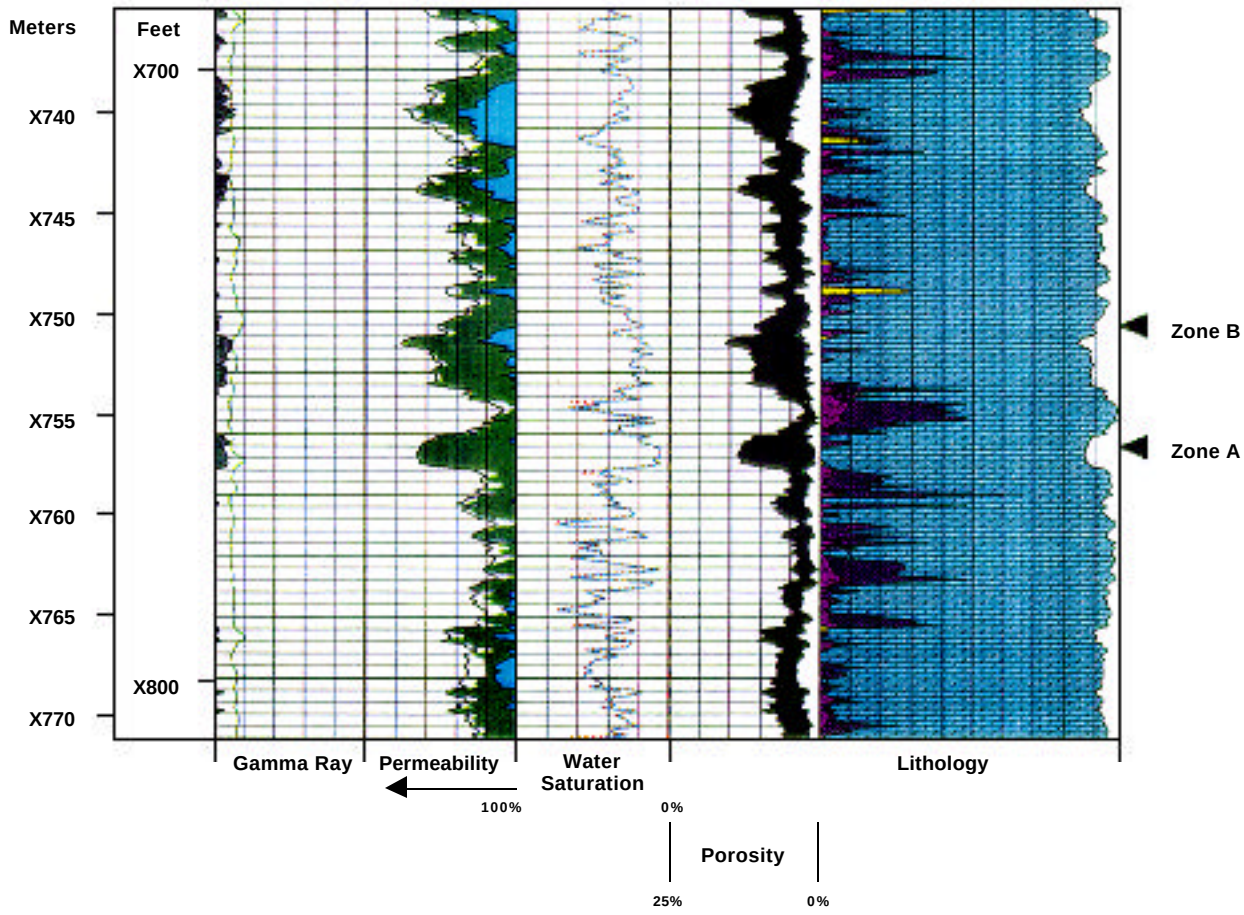

Carbonate

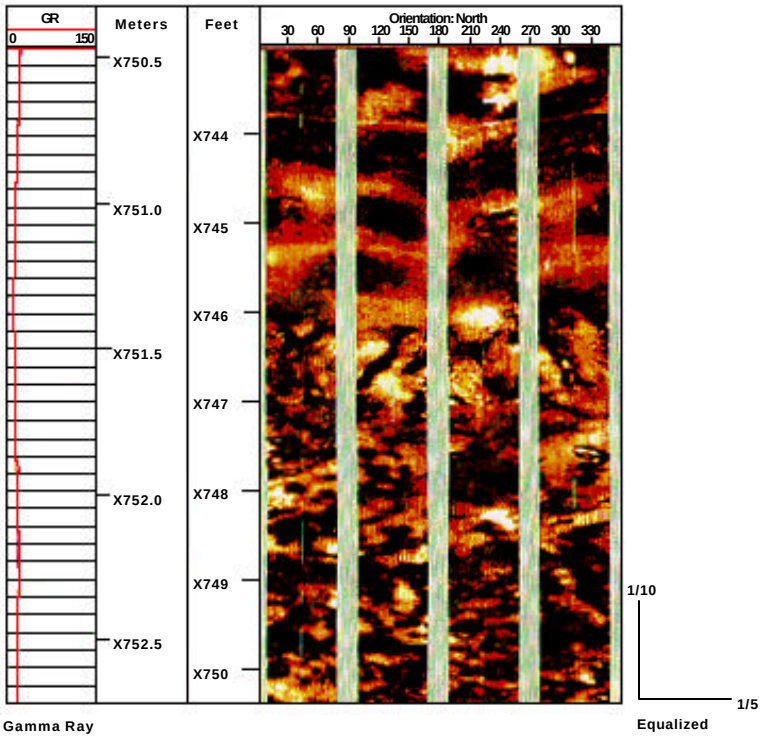

Carbonate

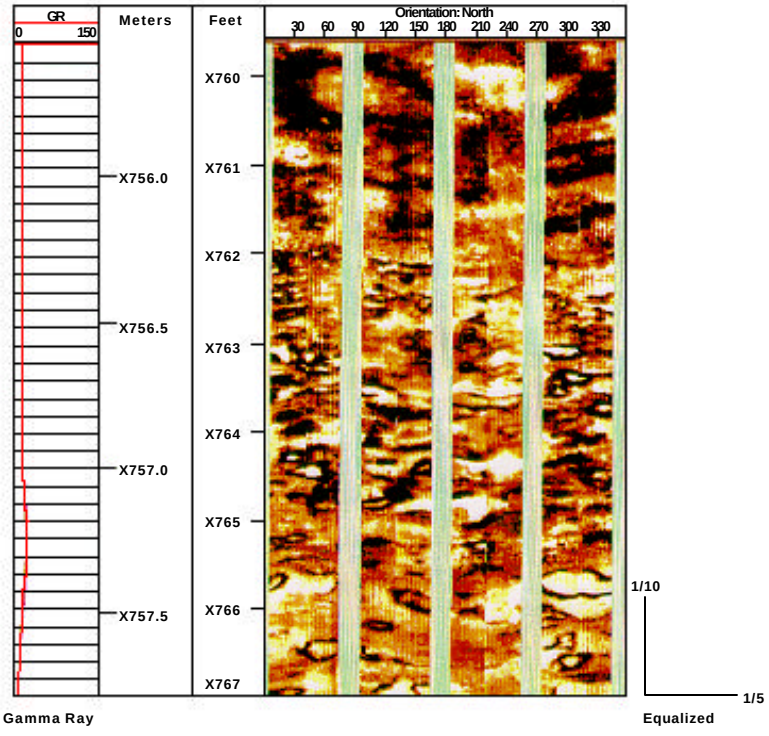

Vugs Exercise 2

Objective of this exercise: Vug Characterization.
Geological Background: Permian Carbonate, Anhydrite in samples.
Available Data: Electrical Images.
Question: What type of vuggy porosity is present?

____ Open/Interconnected
____ Open/Isolated
____ Mineral-Filled

Permian Carbonate

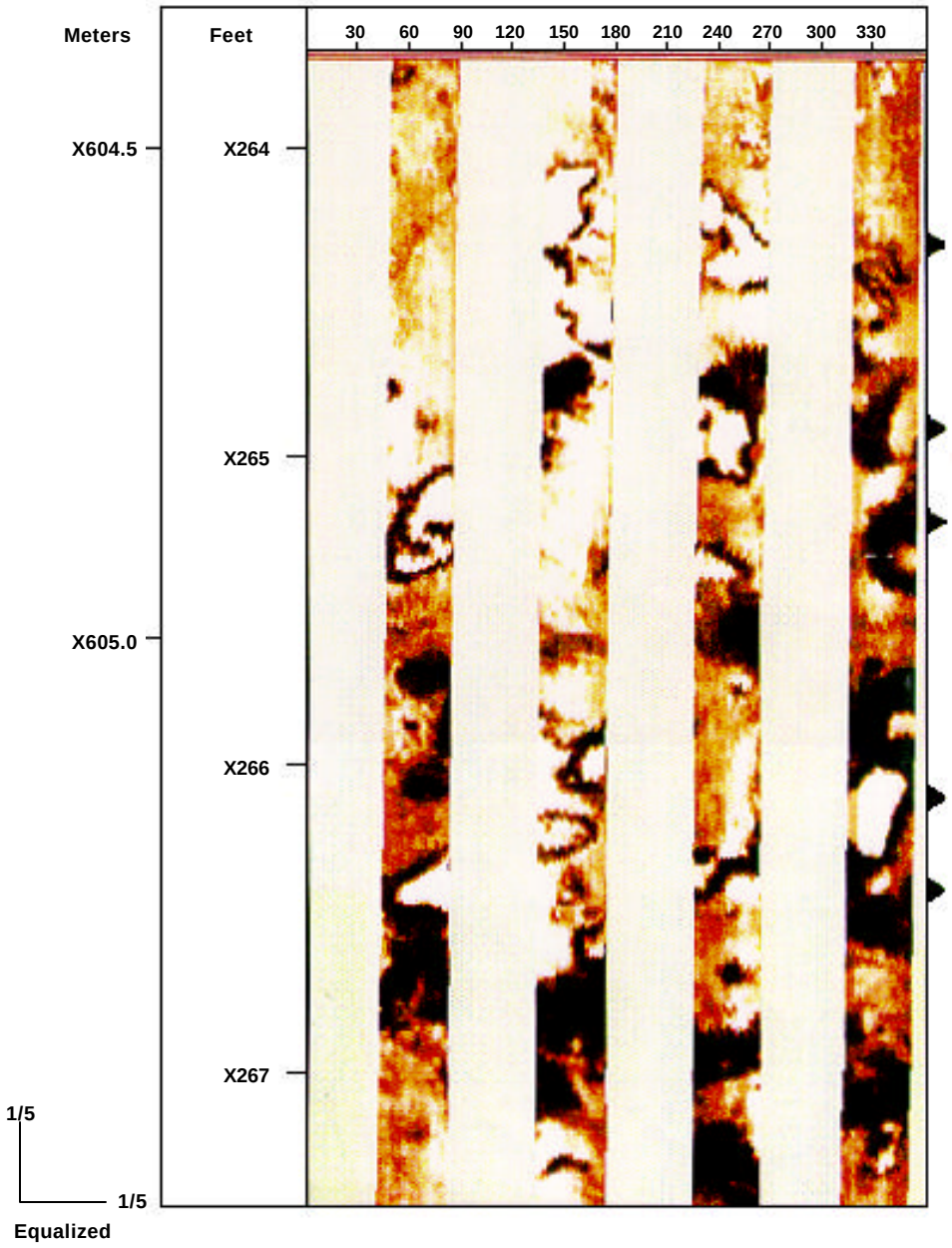

Vugs Exercise 3

Objective of this exercise: Vug Characterization.
Geological Background: Devonian Carbonate.
Available Data: Electrical Images.
Question: What type of vuggy porosity is present?

____ Open/Interconnected
____ Open/Isolated
____ Mineral-Filled

Devonian Carbonate

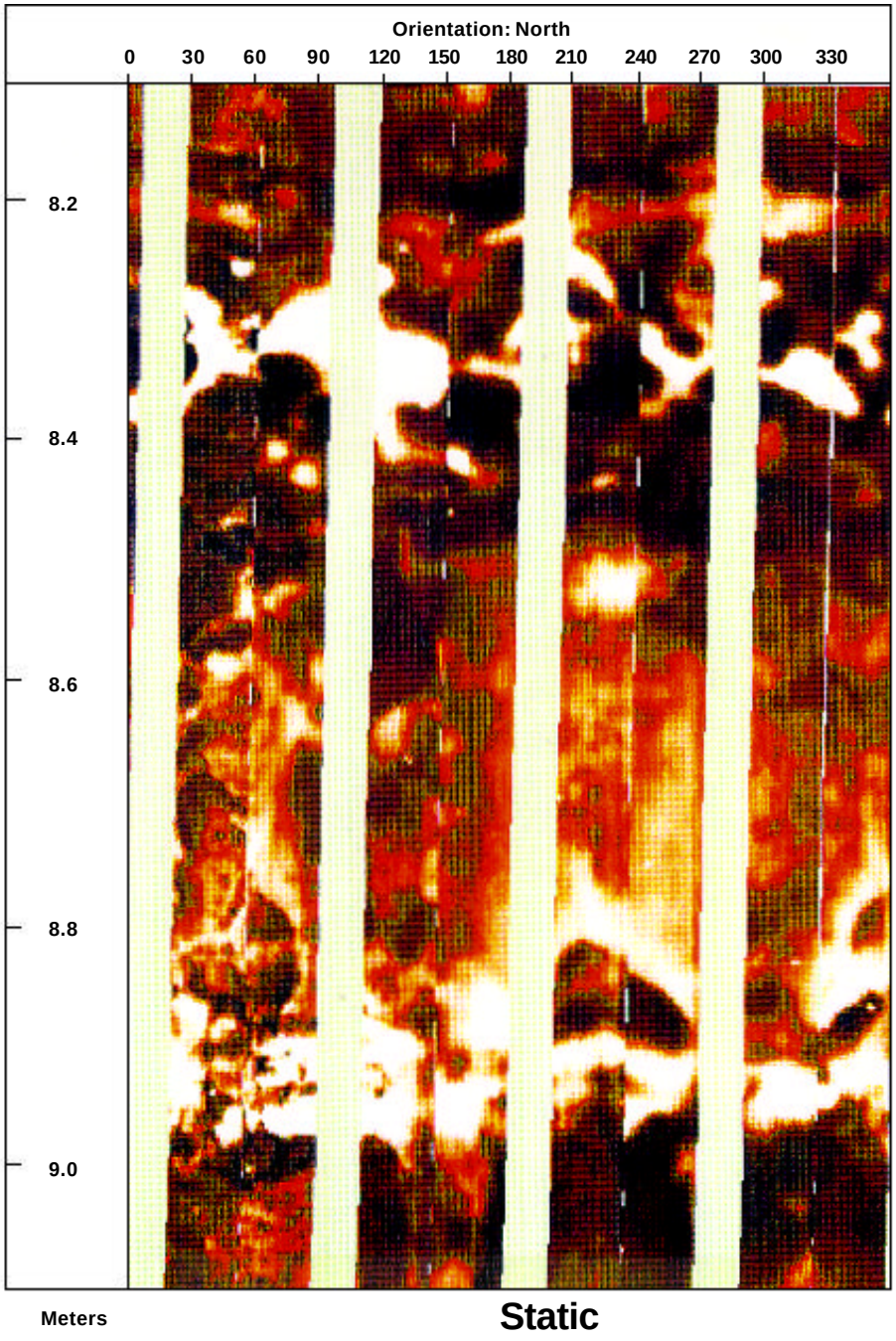

Vugs Exercise 4

Questions: What type of vuggy porosity is present?

____ Open/Interconnected
____ Open/Isolated
____ Mineral-Filled

A.

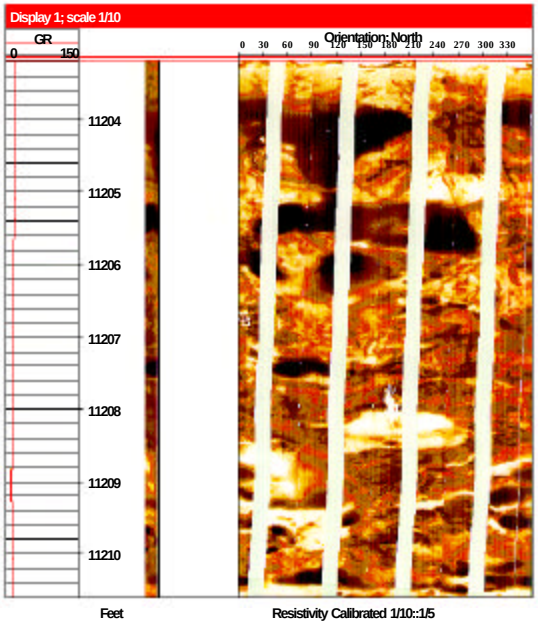

B.

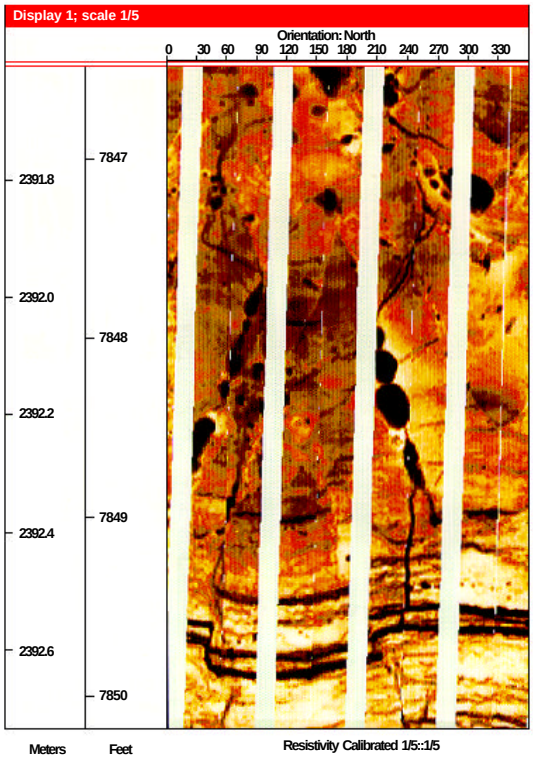

C.

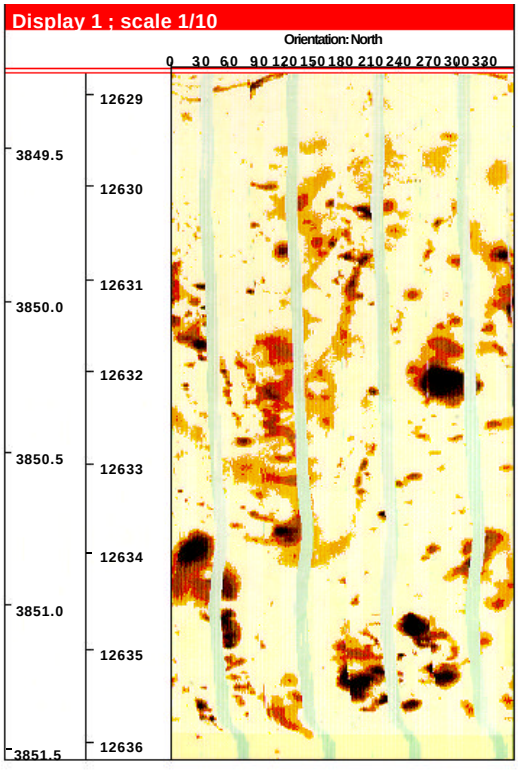

D.

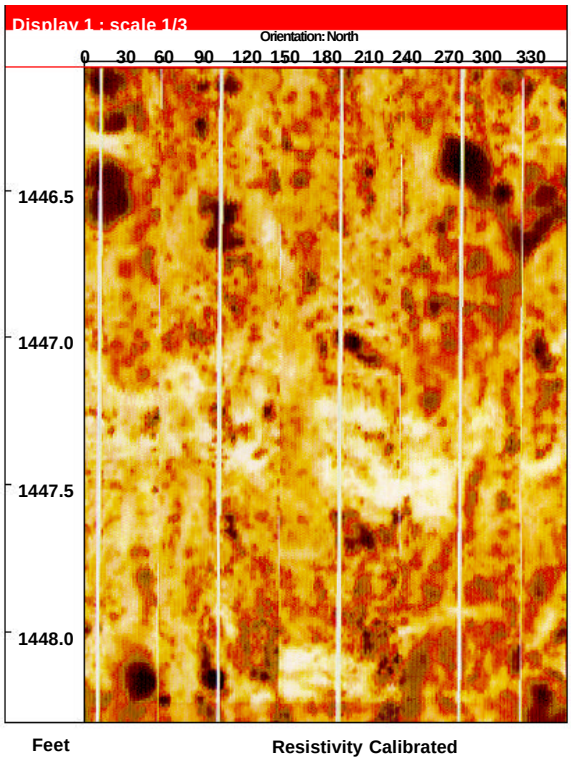

Vugs Exercise - Answers

Exercise 1

1. Open/Interconnected - Zone B
   Mineral-Filled - Zone A

Exercise 2

1. Mineral-Filled.

Exercise 3

1. Open/Interconnected
   Open/Isolated
   Mineral-Filled.

Exercise 4

A. Open, interconnected and mineral-filled vugs

B. Vuggy fractures with micro-fault.

C. Open/Interconnected vugs; the vugs are developed along a partly mineralized fractured plane. Fractures of this type tend to be interconnected and should not be ignored. This well is productive from this interval.

D. Mineral-filled and open isolated vugs.

Vug Analysis

Objectives of this Chapter:

The quantitative characterization of carbonate intervals containing vuggy and patchy porosity in order to locate the most productive zones and to provide better information for petrophysical analysis. This includes the determination of:

- Vug Size
- Number of Vugs
- Distribution of Secondary Porosity

Vug Analysis

In order to fully analyze the effects of vuggy porosity on reservoir volume and flow potential, it is necessary to do more than recognize and type the vugs. A method to quantify the vug characteristics is provided by a program called **"SPOT"**. This software analyzes the images to extract either resistive or conductive features from the data. Extensive processing is performed to precisely contour the edges of each feature and to determine the degree to which these features are interconnected. These individual results are then combined to give summary curves of the answers on a foot by foot basis. The information output includes the area of the borehole wall covered by vugs (which is directly relatable to porosity), the median size of the vugs, the density or number of vugs per wellbore foot, and a measure of the connectedness of the vugs.

The images displayed to the right have the edge contours of each vug superimposed on the FMI images along with the median vug size, "SIZE", the connectedness index, "CONN', and the conductivity of the host rock, "BCKG", curves. This example shows large and small vugs, some of which are well connected while others are poorly connected or isolated.

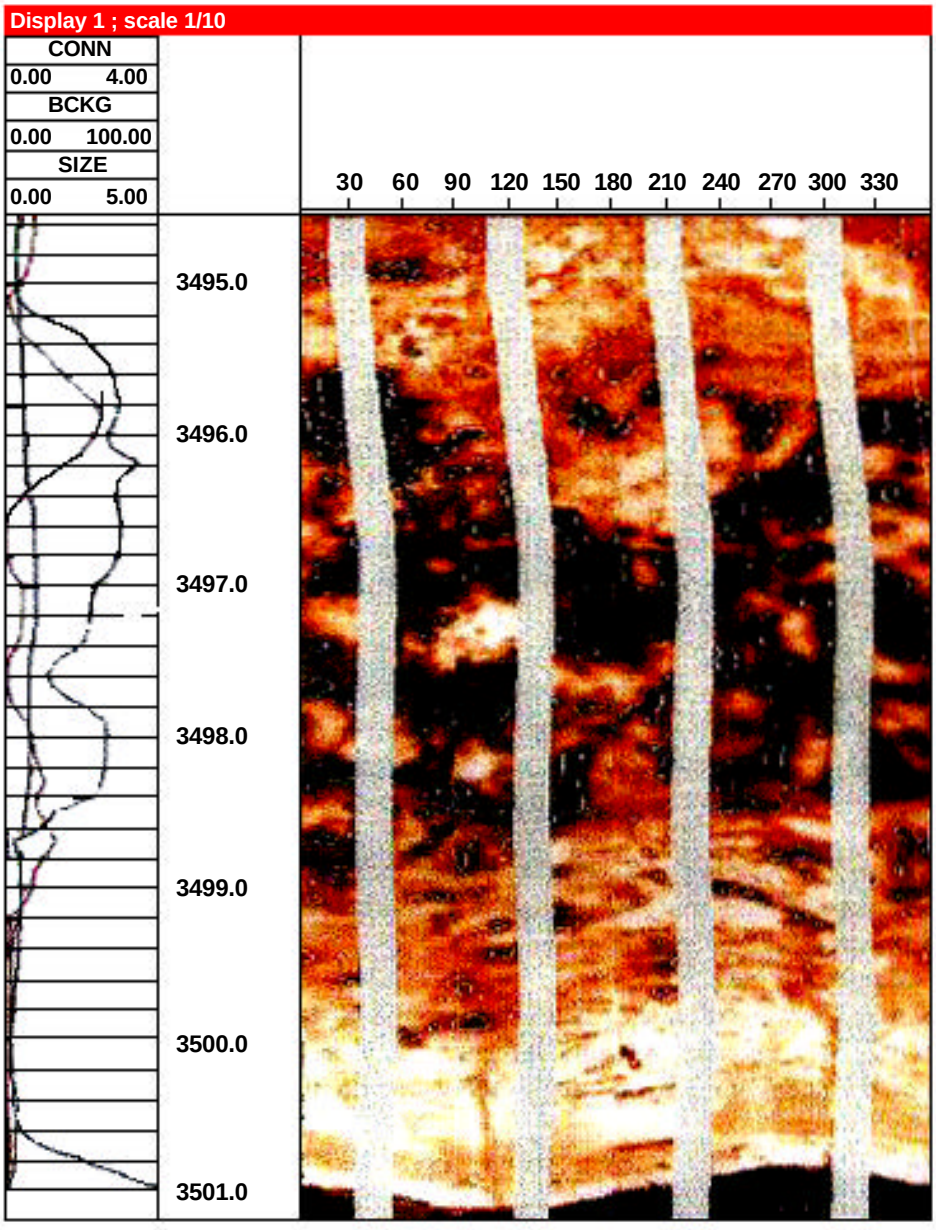

This example shows a more extensive display of the curves output by **SPOT**.

ISOD - Number of unconnected spots per meter or foot
NBCO - Median number of mutually connected spots
DENS - Number of spots per meter or foot
SIZE - Median spot size in mm2 or in 2
AREA - Percentage of images covered by spots
CONN - Connectedness index related to paths/background contrast
CIND - Connectivity index (= (NBCO * SIZE * DENS) / 144)

The first curve track contains “ISOD”, “NBCO”, “DENS” curves. The separation between ISOD and DENS gives the density of connected vugs while NBCO gives a measure of how interconnected they are.

Track two shows “SIZE” and “DENS”. The SIZE curve indicates what the median size of the vugs are and “DENS” shows how numerous they are. These curves are useful for observing the changes in distribution of vugs. We see sections which have large numbers of small vugs, sections with a small number of large vugs with variations between these extremes.

Track three contains “AREA” and “CONN”. AREA gives the percentage of the borehole surface which is covered by vugs. Statistically, this is directly related to porosity or more precisely secondary porosity since SPOT is relatively insensitive to primary, intergranular type porosity. The CONN curve indicates how well connected is the system of vugs.

Track four contains “NBCO” and “CIND”. While NBCO calculates the number of interconnected vugs, CIND tries to calculate a connectivity index which includes the effects of variations in size and density of the vugs.

An important point to keep in mind is that when very large vugs are present small values of connectedness are sufficient for good fluid flow. Smaller vugs would require more extensive interconnection of the vugs to achieve the same fluid flow.

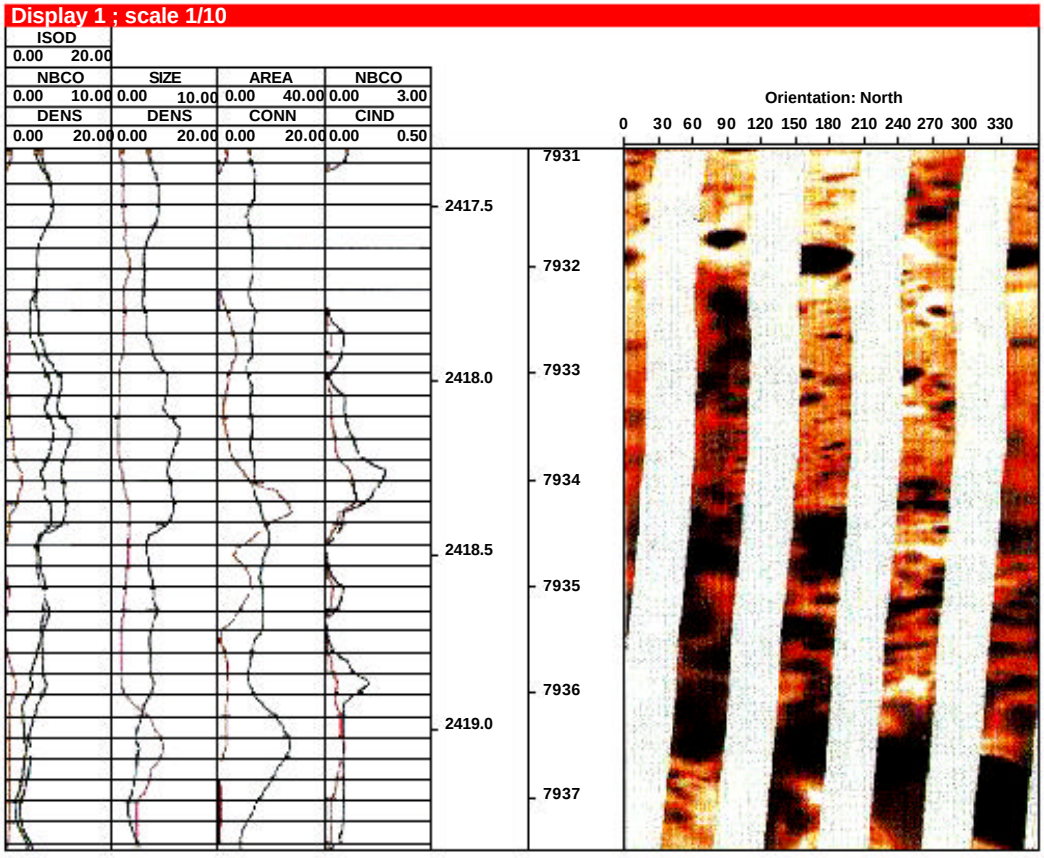

•Quite often vuggy porosity is observed on electrical images which is not seen on standard neutron/density logs. The accompanying display shows this effect. Although some large, well connected vugs are seen on the images, the standard porosity curves show a relatively poor correlation through this section. The images along with the **SPOT** results provides a more realistic analysis in this type of environment.

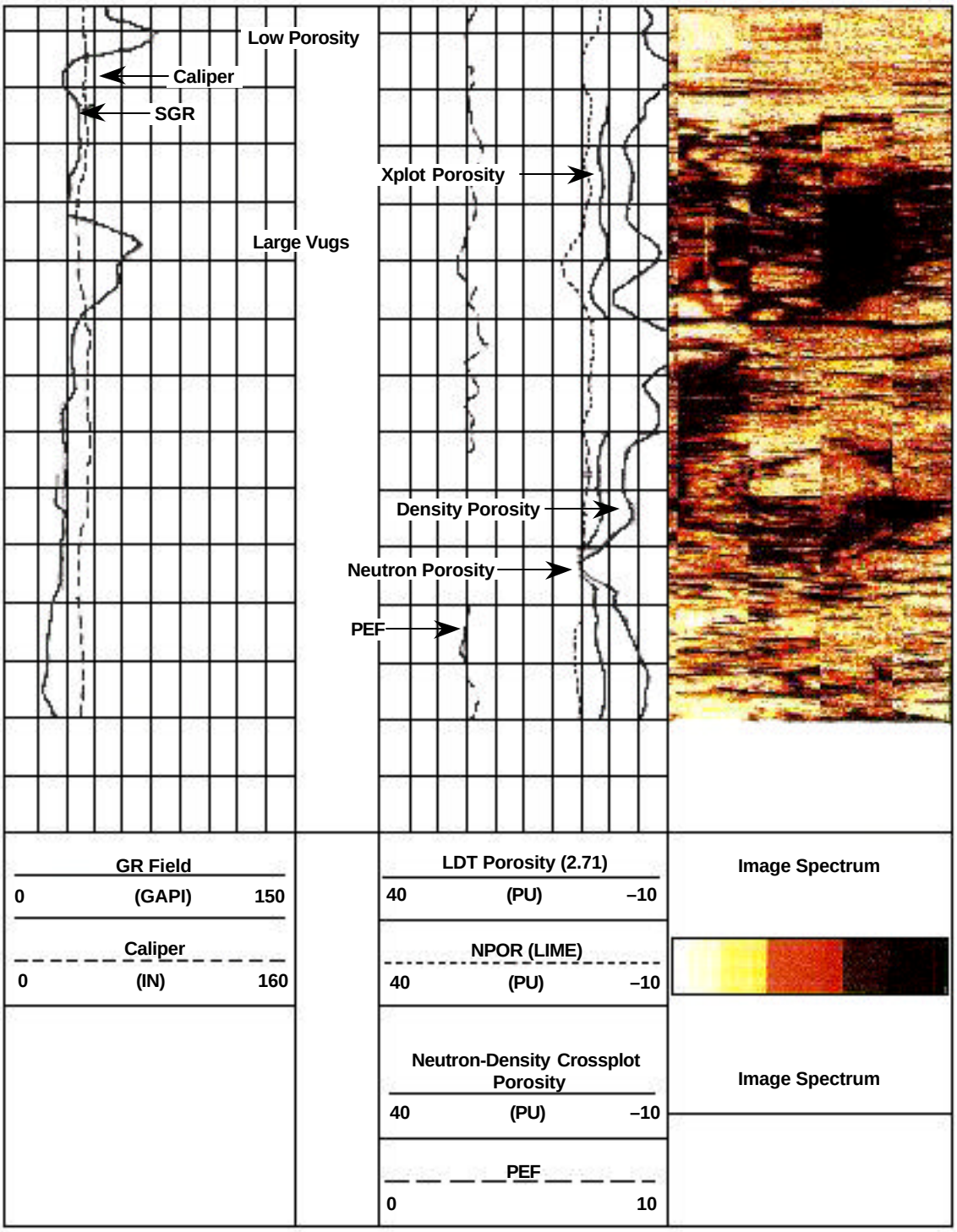

This example shows a potential problem of which the interpreter must be aware. Since the **SPOT** program is designed to locate conductive anomalies, it will respond to such features as thin conductive beds and stylolites. It is always a good practice to confirm "vuggy" sections seen on the summary curves with the images in order to eliminate such zones.

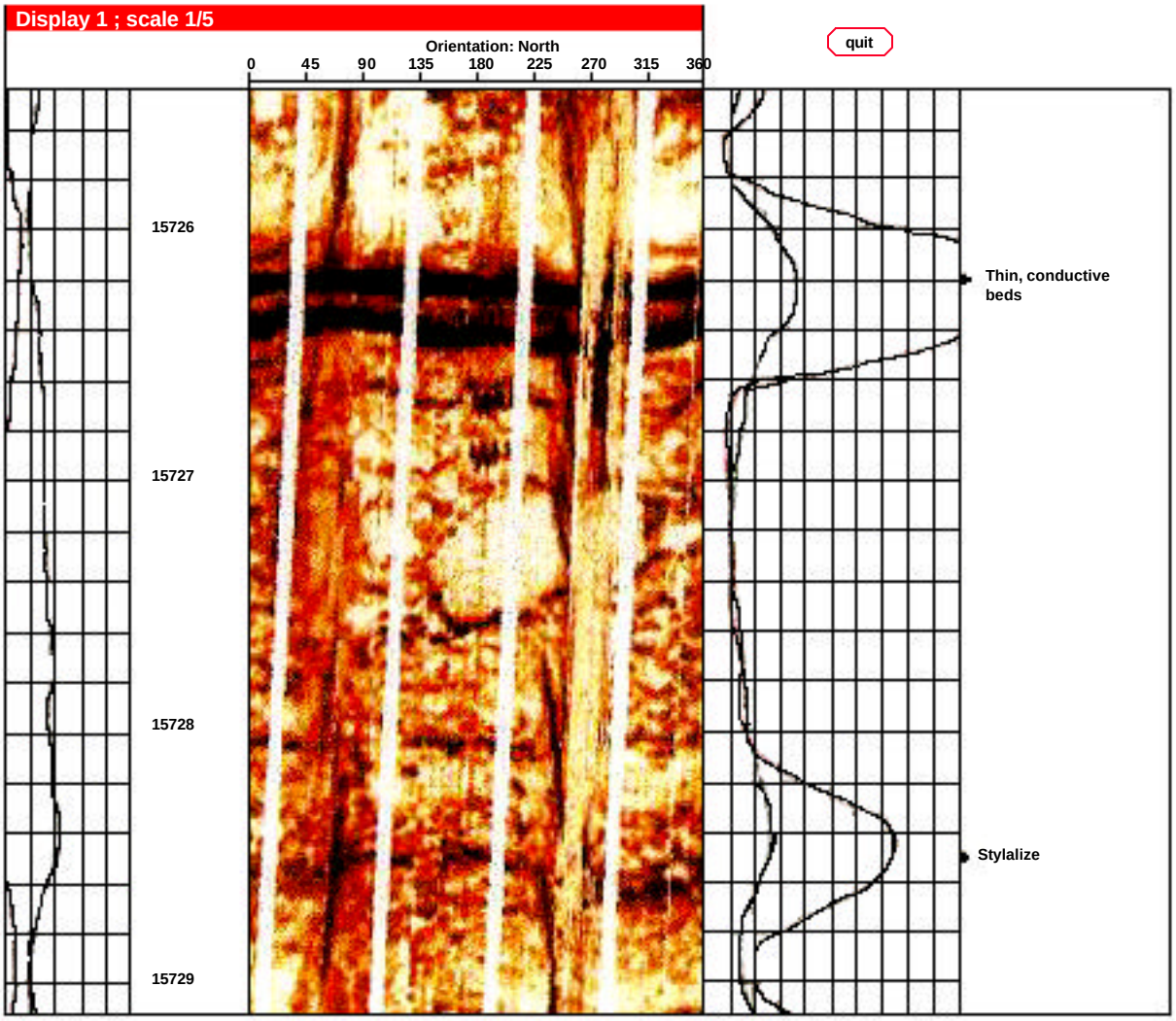

This crossplot shows some preliminary results from over 30 wells of comparing only the connectedness values from **SPOT** analysis with initial production from those wells. A good correlation is evident although there is considerable scatter to the data. There appears to be a threshold value of vug connectedness below which no flow can be expected. Increased connectedness correlates to increased production. Further work to include the effects of vug size and density variations needs to be done to refine this type of analysis, but it is very encouraging to see such good agreement of predictions versus production in what has been traditionally a difficult interpretation environment.

SPOT Connectivity vs Production

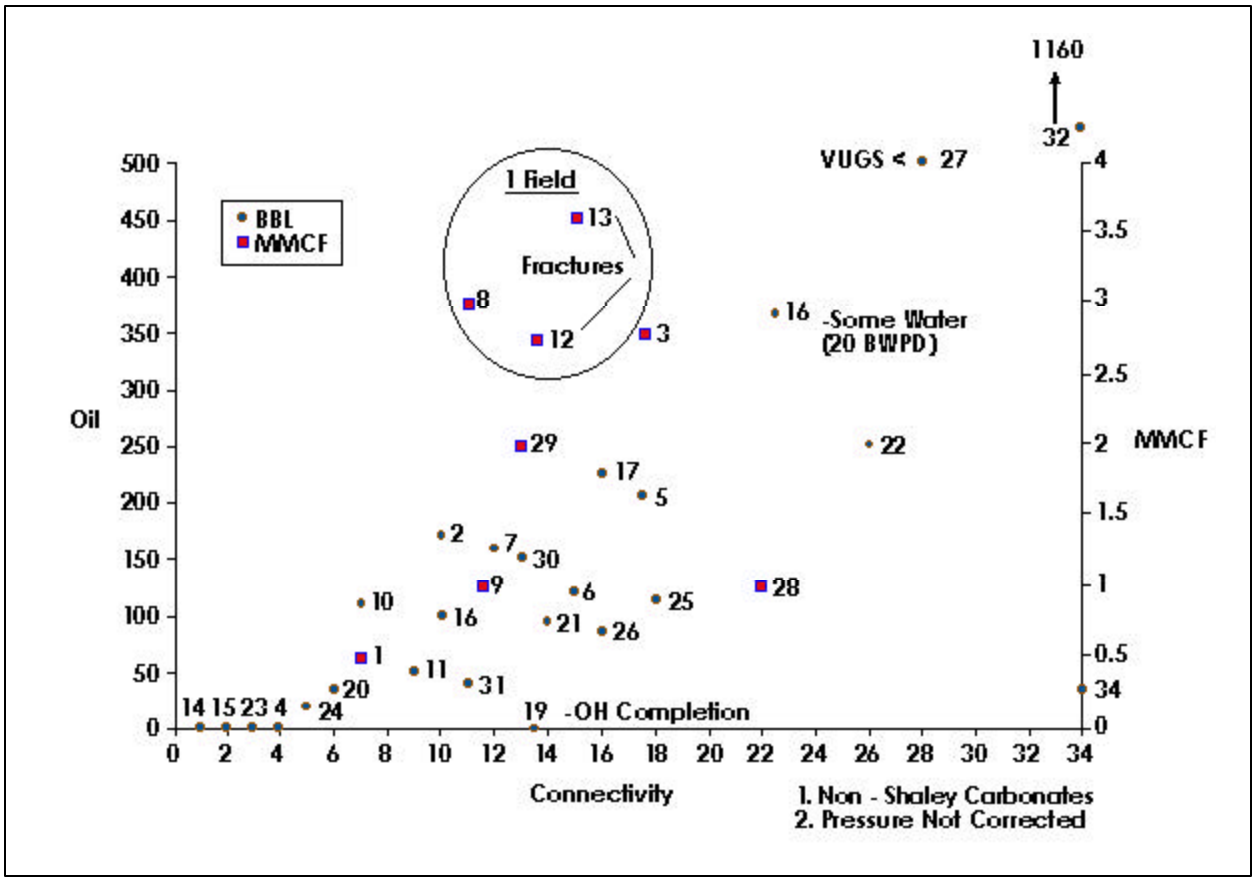

The following pages show the results of ELAN computations over a carbonate section. The first, a "standard" ELAN, relies on the neutron/density data to obtain formation porosity. The second ELAN adds porosity information derived from the "AREA" curve from the SPOT computation. Since SPOT is rather insensitive to primary porosity, the higher of the two porosity inputs is used in the ELAN. In this way we rely on the neutron/density data for primary porosity information and SPOT data to give a better estimate of the secondary porosity. This enhanced ELAN much better correlates to the well's production as well as to shows during drilling than does the ELAN without the aid of inputs from SPOT.

Standard ELAN

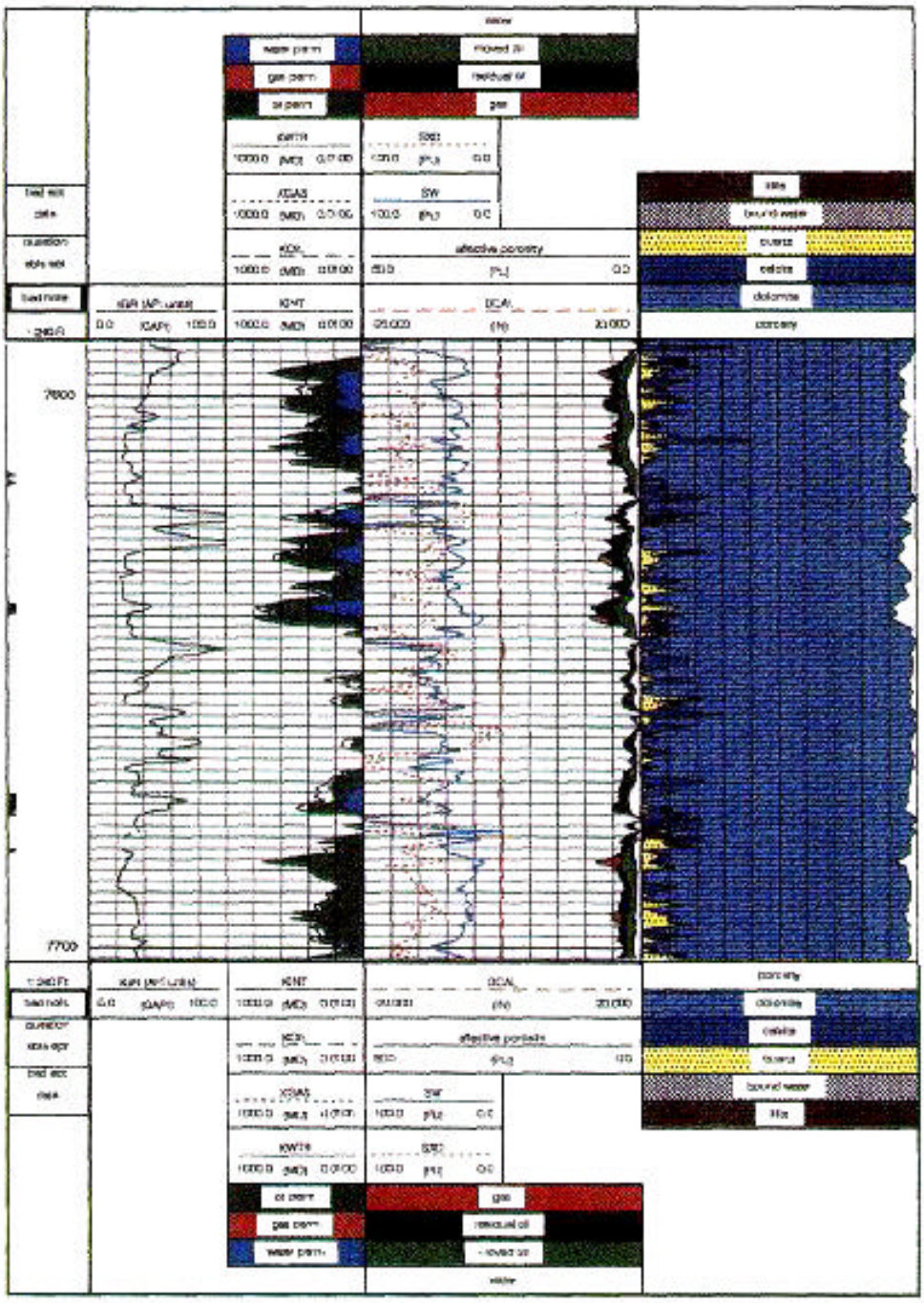

Petrophysical Analysis Utilizing SPOT Outputs

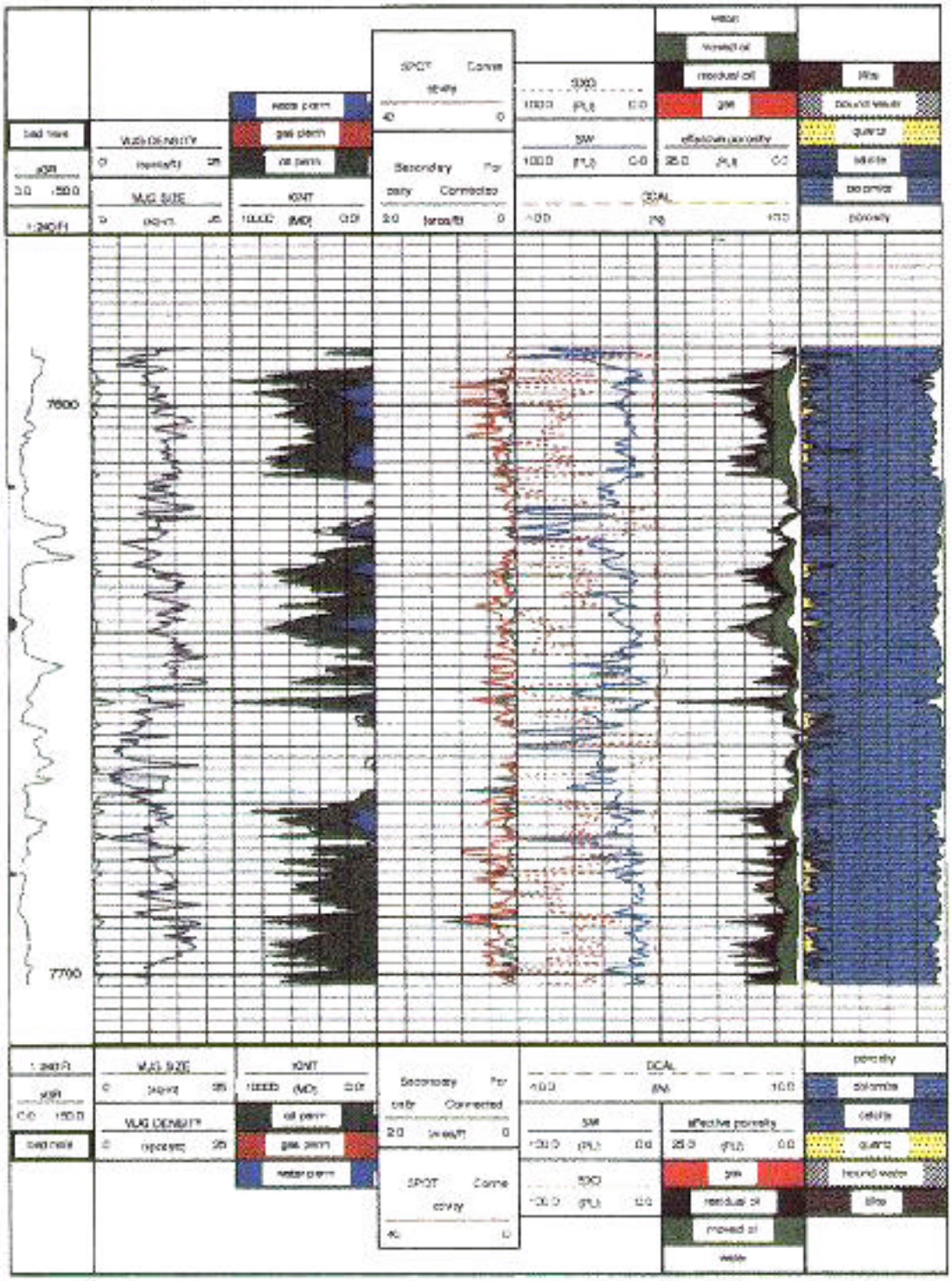

SPE 35158

Analysis of Carbonate Dual Porosity Systems from Borehole Electrical Images

B.M. Newberry, SPE, Schlumberger GeoQuest; L.M. Grace, SPE, and D.D. Stief, Schlumberger Wireline and Testing

This paper was prepared for presentation at the Permian Basin Oil & Gas Recovery Conference held in Midland, Texas 27-29 March 1996.

Abstract

Many productive carbonates have dual porosity systems with widely varying proportions of primary and secondary porosity. The secondary porosity may contain vugs, molds and fractures. Most interpretation methods rely on traditional resistivity and porosity logs. These often fail to produce results consistent with production because of the complex nature of the dual-porosity carbonate. Borehole electrical images provide both the small-scale resolution and azimuthal borehole coverage to quantitatively resolve the heterogeneous nature of the porosity components. The primary assumption for this technique is that the resistivity data from the electrical images are measured in the flushed zone of the borehole. Then, the electrical images can be transformed into a porosity map of the borehole. Automated analysis of this porosity map, windowed over short intervals, provides a continuous output of the primary and secondary porosity components. This method has been applied to a variety of carbonate formations where conventional log analysis has usually failed. The predicted results compare accurately with the actual production.

Overview

Historically, for many carbonate reservoirs, the correlation between hydrocarbon production and neturon-density logs has been inconsistent. Good production has been obtained from intervals showing low log porosity whereas zones having higher porosity have not produced. Also, total production from carbonate reservoirs in mature fields has often been greater than expected from standard porosity logs. Although carbonate porosity often appears somewhat uniformly distributed (**Fig. 1**), many carbonate sections observed on high-resolution borehole electrical images exhibit a texture that is apparently vuggy or dominated by patchy porosity (**Fig. 2**). The prototype software program PoroSpect*, Porosity Spectrum Analysis, which transforms the conductive regions seen on electrical images into equivalent porosities and provides facilities for examining the distribution of porosity values, was developed as a means of better quantifying this patchy porosity.

Technique

Calibrated electrical images from the FMI* Fullbore Formation MicroImager, are essentially a conductivity map of the borehole wall, primarily from within the flushed zone. The classic Archie saturation equation in the flushed zone is

$$S_{xo}^{n} = \frac{aR_{mf}}{\Phi^{m} R_{xo}}$$

By setting S_{xo} = 1.0, a = 1.0 and $m = n$ = 2.0, the FMI images can be transformed into a porosity map,

$$\Phi = \sqrt{\frac{R_{mf}}{R_{xo}}}$$

A reasonable accurate value for mud filtrate resistivity, R_{mf}, is usually available, and the flushed zone resistivity, R_{xo}, is the numerical value of the electrical image at any particular point. By statistically examining the distribution of porosity over a short vertical window (1.2 in.), it is possible to locate the porosity value that separates the matrix porosity fraction from that of the secondary porosity in that local region. It is then possible to count the sections that contribute to primary porosity and those that contribute to secondary porosity, (**Fig. 3**). Summing the primary and secondary components then yields the total porosity. For intervals having homogeneous porosity the comparison to neutron/density logs is normally excellent. However there is often little correlation over zones having a heterogeneous distribution of porosities. This discrepancy is due to the fact that the nuclear measurements are highly azimuthal in nature whereas the PoroSpect results are derived from data which covers most of the circumference of the borehole thereby providing a more consistent answer.

Automated analysis of the porosity map, windowed over short intervals, provides a continuous output of these results. Similarly, porosity values can be extracted for various percentiles (20, 40, 60, 80) of the distribution and displayed as curves. Converting these histograms of porosity into an image also produces a convenient display for visualizing the distribution. Little separation of the percentile curves or the histogram images would imply that the porosity is rather homogeneous with most of the porosity confined to a narrow range of values. Extensive separation indicates that there is a heterogeneous mixture of porosities.

This type of analysis is subject to some basic caveats; i.e., conductive minerals and shale can produce erroneous results. Also, in the presence of high porosity or large vugs, the FMI button current may saturate, resulting in pessimistic porosity values. This condition is easily recognized on the histogram image display.

Examination of these porosity maps leads to some interesting observations. Many intervals that would normally be interpreted from the images as containing large interconnected vugs do not appear to contain voids. The “vugs” are generally sections of patchy porosity that are significantly more porous than the surrounding rock. These patchy sections are usually the remnants of diagenetic channels developed in the host matrix. Such channels can form extensive networks, honeycombing the lower porosity rock. In terms of flow characteristics, this is analogous to an extensive fracture network with the diagenetic channels providing an efficient permeability path into which the lower porosity matrix rock can produce. The nuclear porosity logs give a statistical view of the formation. This usually provides sufficient resolution where porosity is distributed generally uniformly around the borehole. Porosity that occurs as heterogeneous patches or vuggy sections is usually not adequately described by neutron-density logs. When a porous patch is not aligned azimuthally with the tool detectors, it is not seen on the logs. Conversely, when pointed directly at vugs or porous patches the nuclear logs will read too high, giving an optimistic view of the formation. Even at high resolution the density log provides only a single data point over a 1.0 in. interval. Over the same interval the FMI log provides almost 2000 samples. Only with this density of data is it possible to

recognize and quantitatively analyze the heterogeneous mixture that makes up carbonate porosity. Further, because the higher porosity patches may represent only a small fraction of the porous surface, their contribution to the total porosity as seen by the nuclear tools is often relatively small. For instance, a zone having 75% of 4 p.u. porosity and 25% of 20 p.u. porosity would be seen by the nuclear logs as an 8 p.u. formation. However such a zone would produce much better than one would expect from an 8 p.u. zone. The higher porosity fraction will dominate the permeability and flow characteristics of the rock. Likewise, such a dual-porosity zone would have to be treated differently when doing reserves calculations. Because of the more efficient drainage system, lower porosity cutoff values and higher recovery factors would be called for than in a similar zone having only a single porosity system. Using these concepts, it is then easy to reconcile most of the discrepancies between log porosity and production results.

Program Logic

The PoroSpect program takes calibrated FMI image files as input. The image resistivity values are internally converted to porosities using the above relationship. A sliding 1.2 in. vertical window is applied. The data from all input pads over this window generate a histogram of porosities, (**Fig. 4**). For sections that contain only evenly distributed "matrix" type porosity, only the first peak (primary) will be seen on the histogram. However for a complex porosity system, multiple peaks are seen on the histogram. It is then possible to statistically locate the value of porosity that marks the separation of the values into primary and secondary porosity. By locating the porosity value on each histogram that separates the primary and secondary fractions, it is possible to examine each porosity value and assign it to one of the porosity types. Continuous curves are then output of the primary and secondary porosity as well as their sum, which equals the total porosity. In addition to finding the break point between primary and secondary porosity, various percentiles (20, 40, 60, 80) of the data distribution are found (**Fig. 5**). These percentiles represent the porosity values for each of these fractions of the rock.

For purposes of visualization, the histogram data are converted into an image for display (**Fig. 6**) by generating a variable density representation of each histogram. This is equivalent to looking down on the histogram from the y-axis with darker colors representing higher peaks and with each histogram displayed as a single horizontal line on the image. For such large quantities of data it is more convenient to use a variable density type of display than to examine numerous histograms (**Fig. 7**).

The lower section in **Fig. 7** shows predominantly primary-type porosity. Hence, we would expect relatively low permeability and a low recovery factor for this zone. The upper section indicates a dual-porosity system. Here the initial production should be good owing to the high-permeability channels, and because these channels tend to honeycomb the formation and allow the low-porosity sections to be drained efficiently, the ultimate recovery should be high. Also, the lower zone would be a better candidate for water flooding because a more consistent sweep would be achieved than in the upper section, where the high-permeability channels would cause early water breakthrough.

Many factors can be measured precisely when calculating reserves. One factor that cannot usually be determined accurately is "recovery factor." As we have seen from **Fig. 7**, it is necessary to understand the nature of the porosity (and hence, drainage) system of the particular formation.

Example Well #1

Extensive full-diameter core was available over this carbonate section. The total porosity curve from the PoroSpect analysis, labeled "TPOR" in the first track of **Fig. 8**, shows reasonable agreement with the neutron-density logs. In the second track, the PoroSpect total porosity curve is compared with the porosity from whole-core analysis.

The "PHIS" curve in the third track represents the results of an interesting experiment on the core. The slabbed core was polished, and then photographed using an inclined light source. The idea was to try to get the vugs to stand out on the photographs, which were scanned into a computer as a digital image. Imaging software was then used to count the fraction of vugs seen on the core photographs. Comparison of the photographed fraction, "PHIS," with the secondary porosity, "SPOR," from PoroSpect analysis, shows a good correlation.

Example Well #2

The original well was making 100 BOPD when the hole was lost as a result of casing collapse. PoroSpect analysis of this zone in the replacement well indicated low matrix porosity with little evidence of channels or vugs (**Fig. 9**). Perforations in this interval of the replacement well, drilled 100 ft away from the original producer, produced a flow of 5 BOPD. An upper zone, which had tested tight in the original well and hence was not considered a target, looked promising on the PoroSpect analysis with a large number of high porous channels (**Fig. 10**). This interval produces 250 BOPD.

Conclusions

Measurements obtained from nuclear porosity logs have a large azimuthal dependency. Porosity in zones having significantly heterogeneous porosity development are more reliably and consistently determined by analysis of electrical images using PoroSpect methodology. The extremely complex and varying nature of carbonates requires careful evaluation. Simple correlation of zones even in closely-spaced offset wells is not sufficient. The location and analysis of intervals containing enhanced, well-connected porosity systems are critical to the efficient production of many reservoirs. Electrical images, with proper processing and analysis, provide an efficient, cost-effective means of interpreting dual-porosity carbonate systems.

Nomenclature

R_{mf} = mud filtrate resistivity

R_{xo} = flushed zone resistivity

S_{xo} = flushed zone water saturation

ϕ = porosity

Acknowledgments

We thank Bob Young of Schlumberger Wireline and Testing for performing much of the core analysis and Darrel Cannon of Schlumberger Wireline and Testing for valuable discussions concerning logging tool responses.

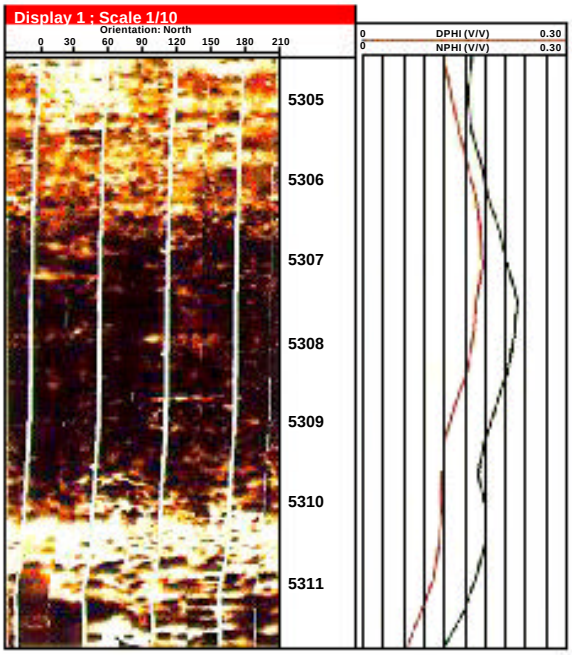

Figure 1. Carbonate section with relatively homogeneous porosity development.

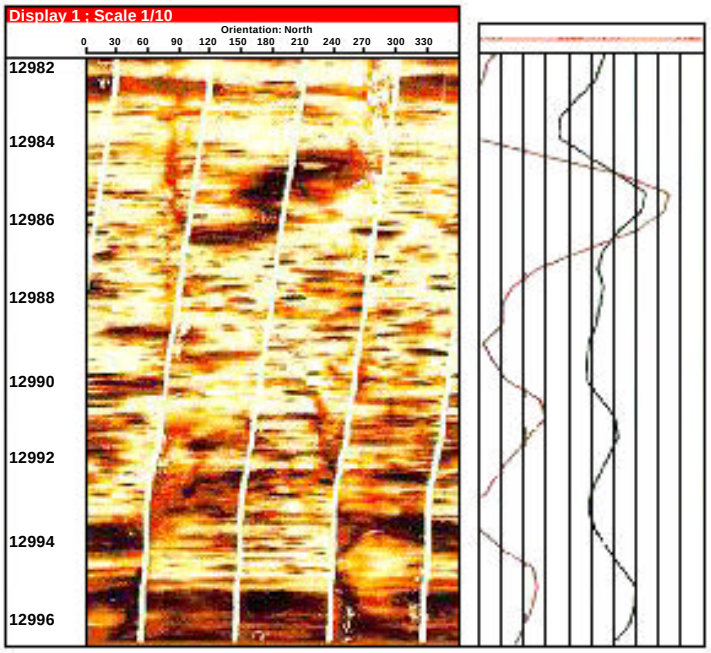

Figure 2. Vuggy and patchy porosity sections.

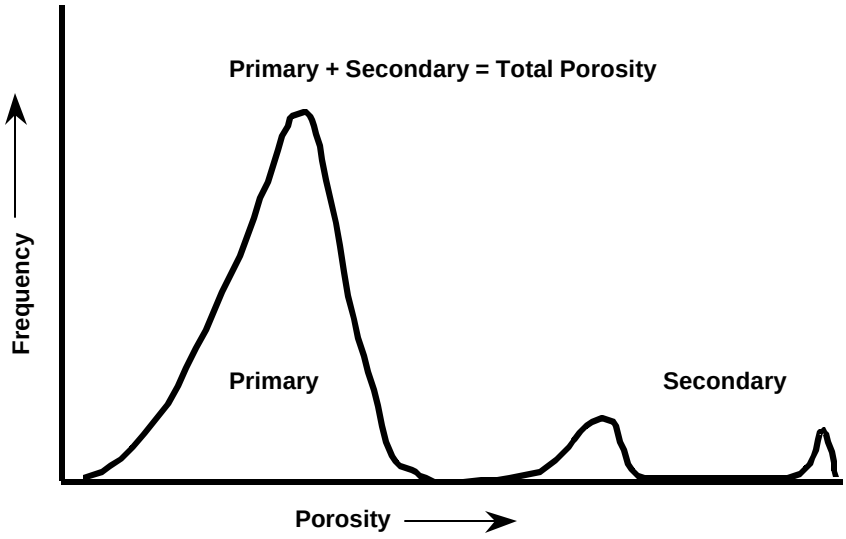

Figure 3. Typical histogram of porosity from electrical images in a dual-porosity carbonate.

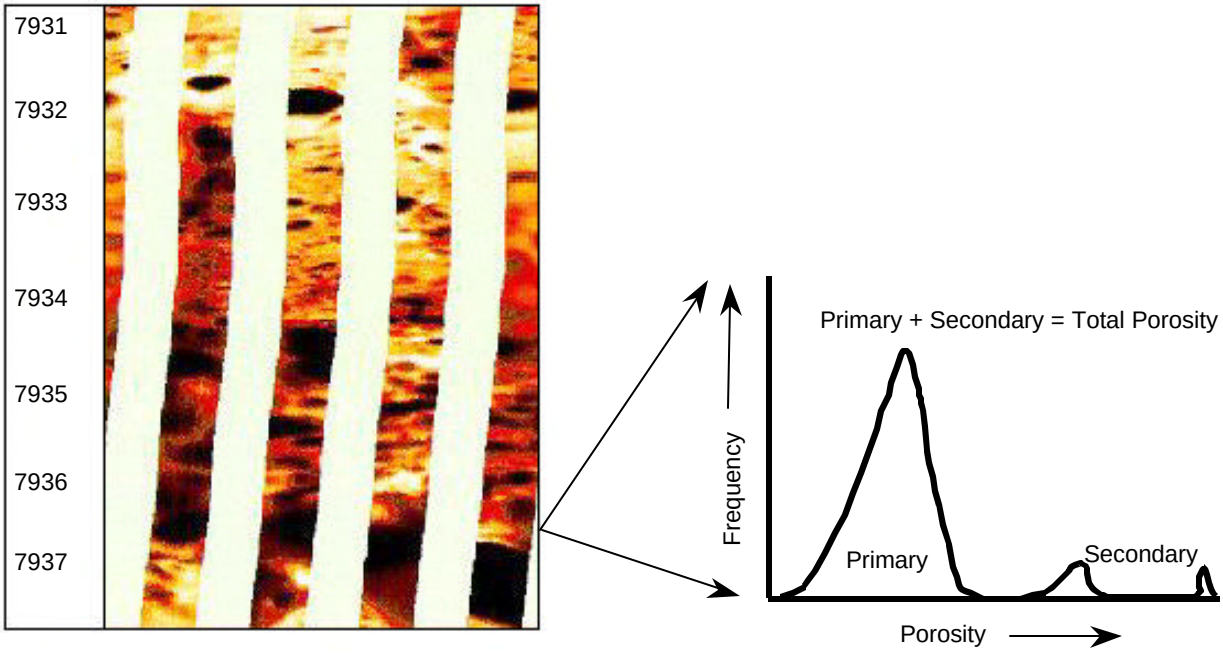

Figure 4. Local variations in porosity distribution produce distinct histograms.

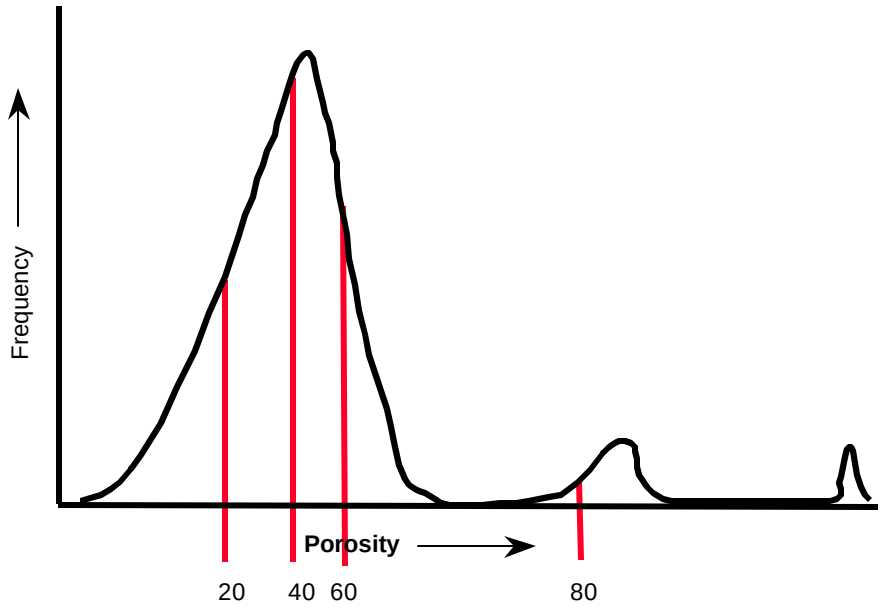

Figure 5. Example of 20th, 40th, 60th, and 80th percentile location.

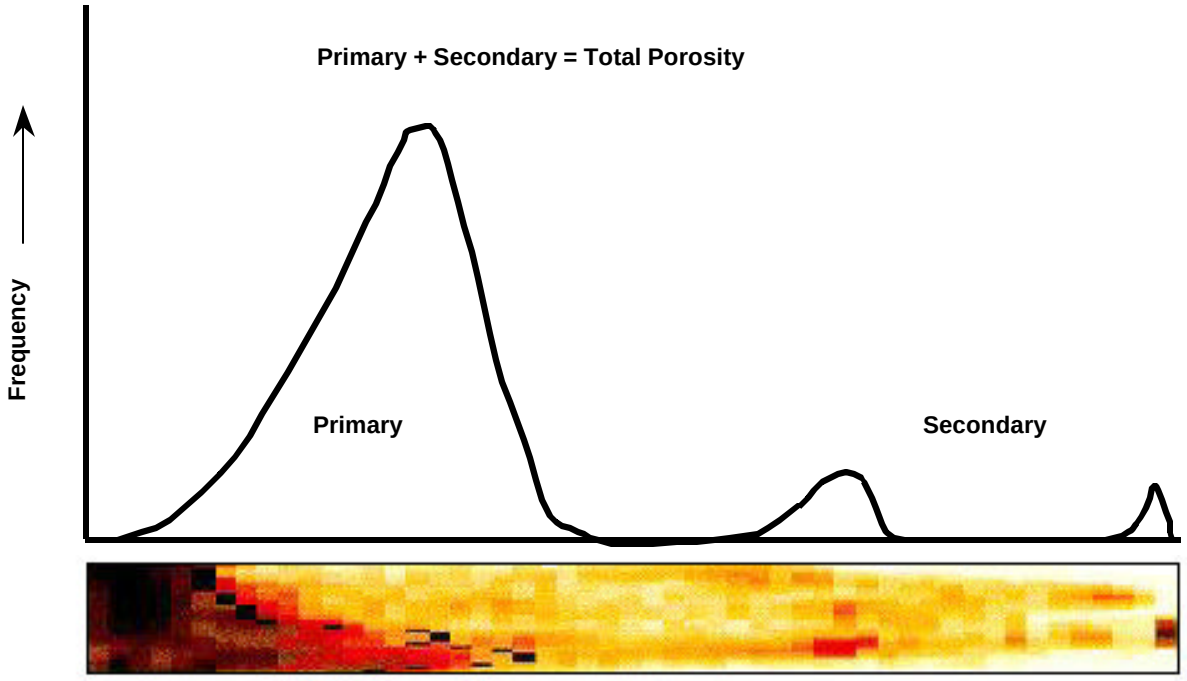

Figure 6. Series of histograms transformed into a variable density display.

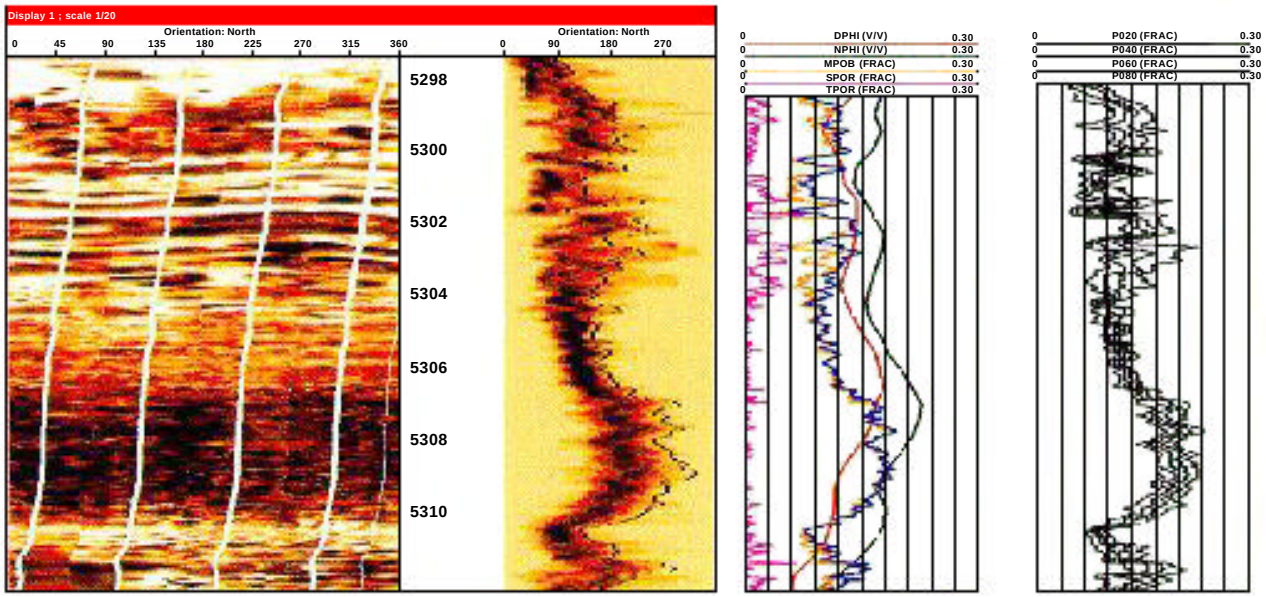

Figure 7. The lower section is relatively homogeneous whereas the upper section shows considerable spread in porosity values.

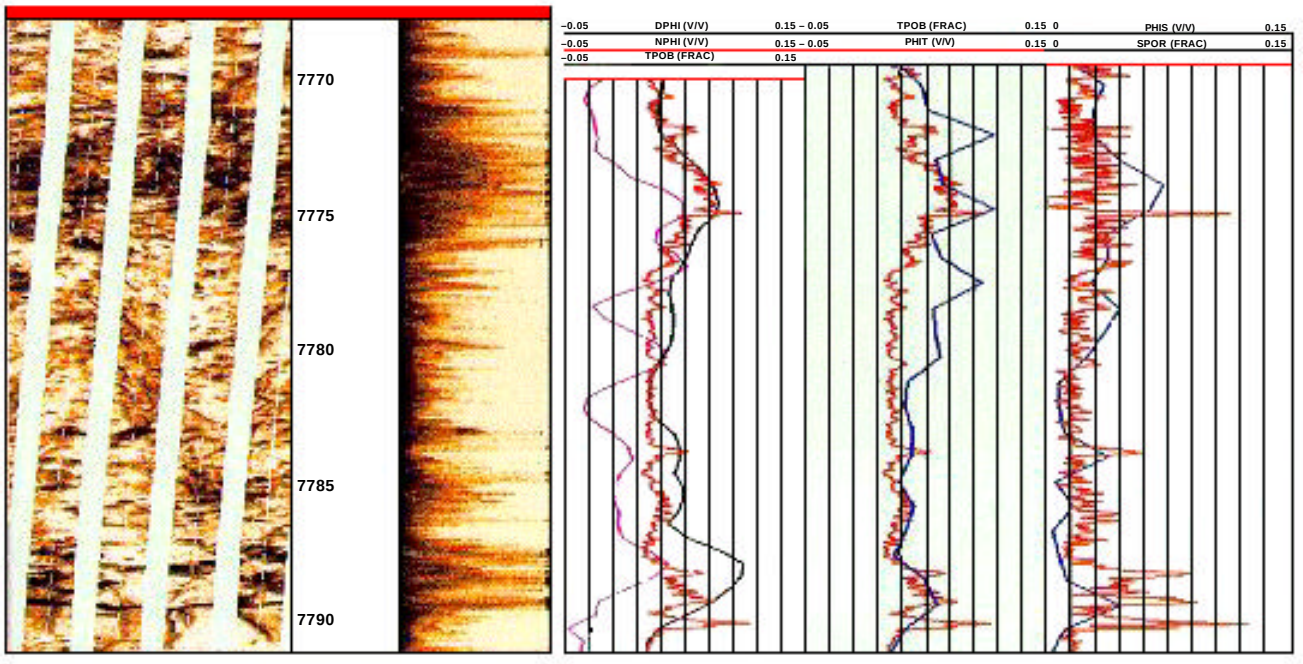

Figure 8. Section with considerable homogeneous porosity. FMI images are shown with porosity spectrum. PoroSpect porosity is compared to neutron/density porosities and with whole-core porosities. Secondary porosity from PoroSpect is shown with the results of photographic analysis of slabbed core surface.

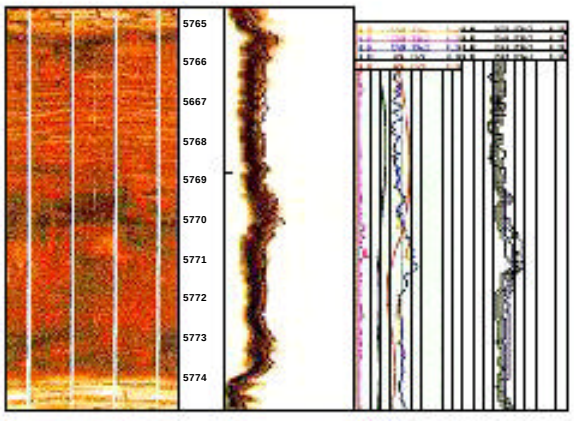

Figure 9. Section with small porosity variations.

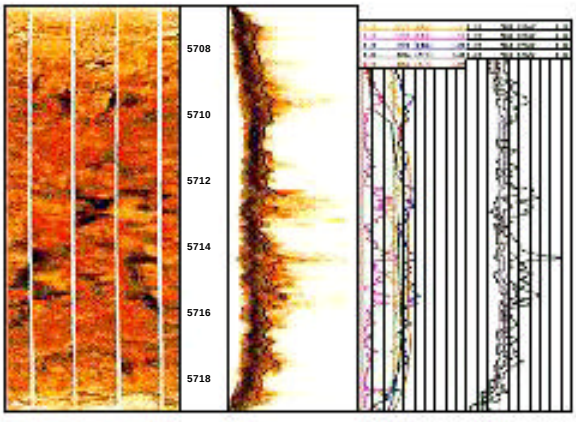

Figure 10. Section with heterogeneous porosity. Some patches of porosity are quite large compared with the overall section.

Deviated Boreholes

Deviated boreholes have historically been used because of surface restrictions. There are several production reasons for deviated boreholes:

Maximize the Penetration of Fractures

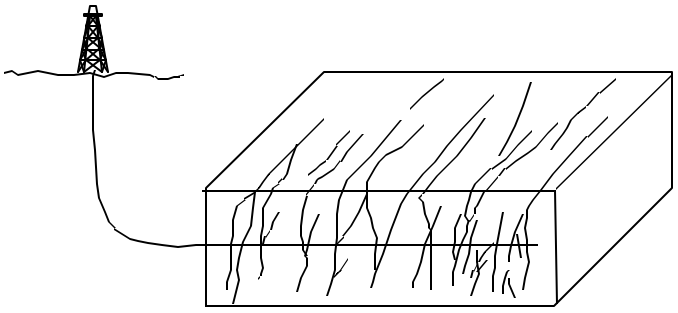

Minimize Water Production

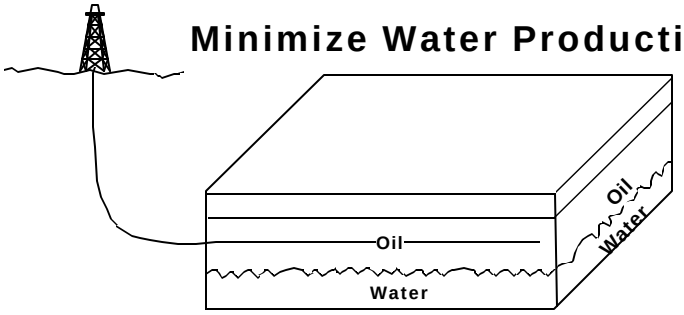

Penetrate Multiple Topographic Features

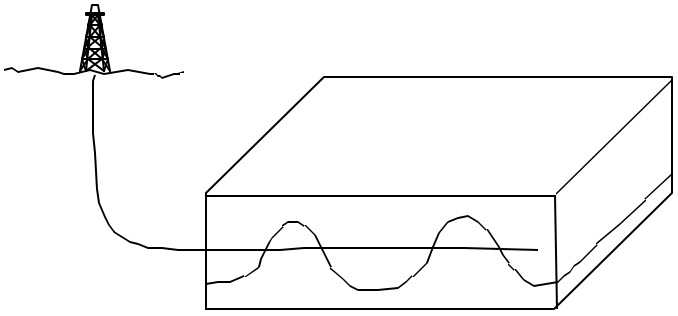

Deviated Boreholes

There are many production and drillsite location reasons for deviated boreholes. Drilling platforms are common in offshore areas and in cities to minimize drilling expense. The advent of horizontal drilling for production purposes has caused many marginal exploration programs to become successful.

Fractured reservoirs are the primary target for horizontal boreholes. The borehole is drilled horizontally perpendicular to the fractures. This technique allows the maximum number of fractures per length of lateral borehole.

Reservoirs with a high vertical permeability and on active water drive are important horizontal candidates. The borehole is drilled as near the top of the zone as possible. This causes the water coning to be much less severe.

Viewing Perspective

Electrical images are observed on the presentation as recorded in the borehole. This does require an adjustment in the viewing perspective.

Vertical fractures are observed in a vertical borehole as high amplitude sine waves. The horizontal bedding planes are low amplitude sine waves.

As the borehole is deviated to 45°, the bedding planes and fractures may both be medium amplitude sine waves. This is due to the relative position of the borehole to the events.

For horizontal boreholes, the perspective has changed completely. The vertical fractures cross the borehole as low amplitude sine waves. While the bedding planes create high amplitude sine waves.

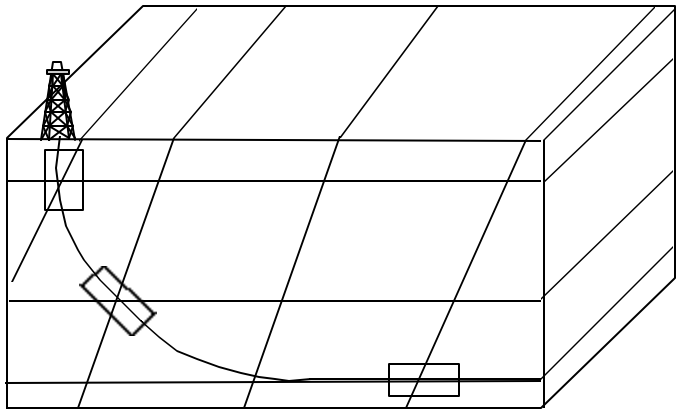

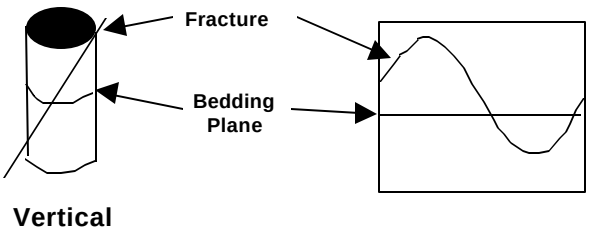

Vertical

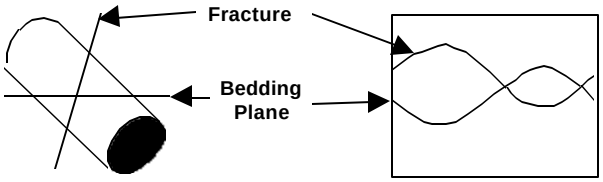

45° Deviation

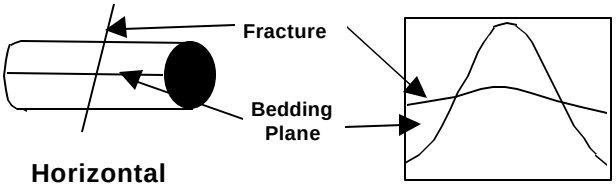

Horizontal

Deviated Boreholes - Example 1

Objective of this Example: To demonstrate the viewing perspective in a 45° deviation borehole.

Geological Background: Carbonate.

Available Data: Electrical Images.

Comments:

1. There is a bedding plane at xx 57-1/2. The dip of this bed is 7° at N 22° E.
2. There are several fractures with a general NW dip. This is a NE-SW strike.
3. This well was drilled as a pilot hole to determine the target zone and the lateral deviation . The target zone will be shown in the fracture analysis chapter. The lateral deviation is perpendicular to the fracture strike to the SE or NW.

Cretaceous Carbonate (45° Deviation - Pilot Hole)

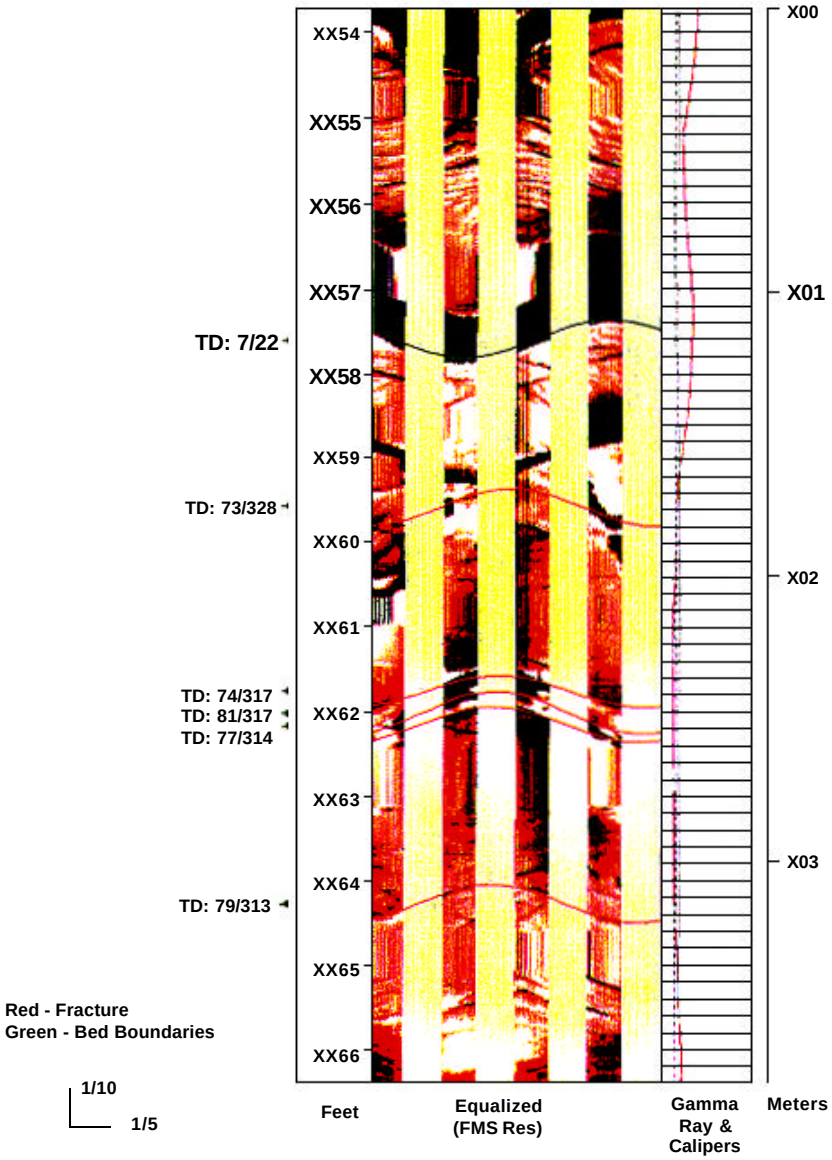

Maximize Fracture Penetration

There are two important fracture properties to consider when planning a horizontal borehole. The maximum number of fractures are crossed by the borehole if the well is drilled perpendicular to the fracture strike and into the dip. For example, if a borehole is drilled 20° from the fracture strike, then the lateral will cross 44° of the fractures for a 6° loss. An equally important loss is when the borehole is not drilled into the fracture.

- **Drill horizontal wells perpendicular to fracture strike**

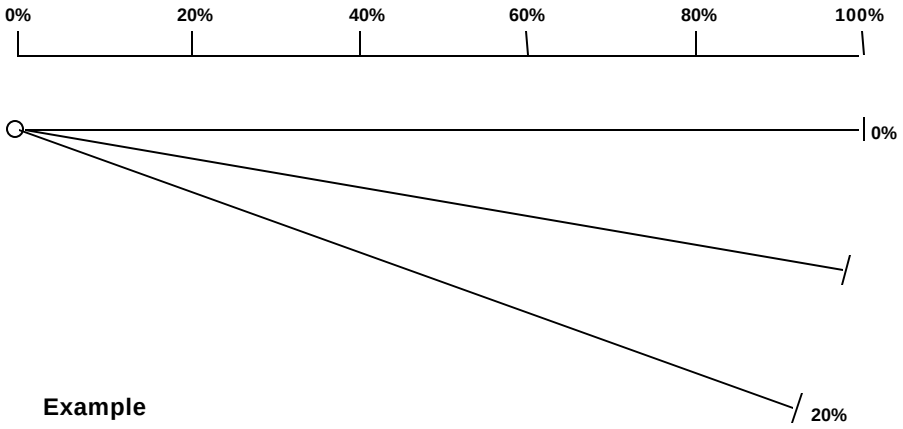

Example
3000 ft. of horizontal boreholes yields

0°	**- 3000 ft -**	**100%**
10°	**- 2954 ft -**	**98%**
20°	**- 2819 ft -**	**94%**
30°	**- 2698 ft -**	**87%**

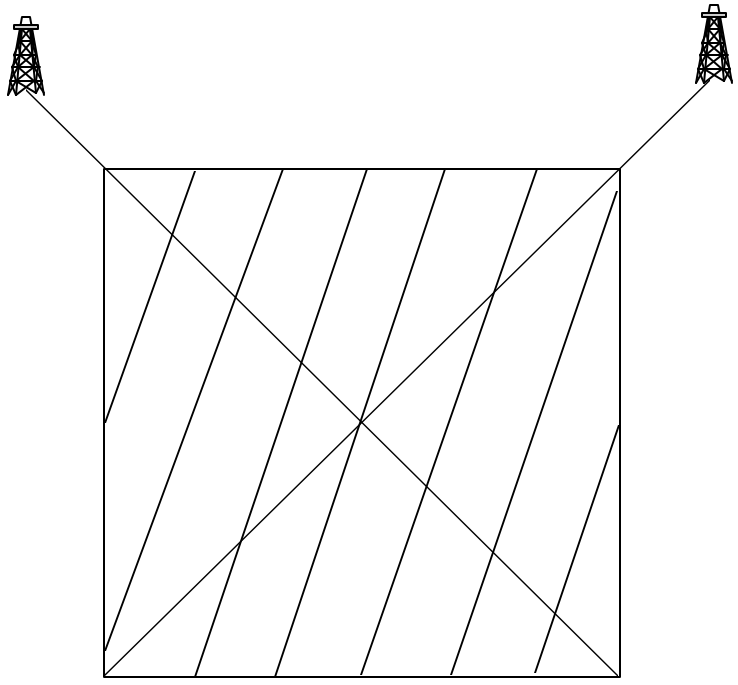

- **Drill deviated wells into fracture dip**

Borehole Reference

A borehole reference of North is the standard for vertical boreholes. This loses meaning in horizontal wells. A more useful reference is the top of hole. The top of the borehole is on the edges of the presentation which the bottom of the hole is in the center of the presentation.

Borehole Reference

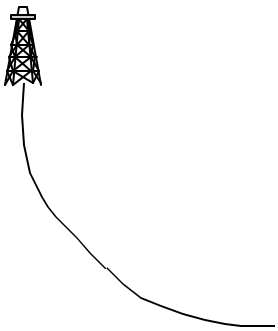

Vertical Wells

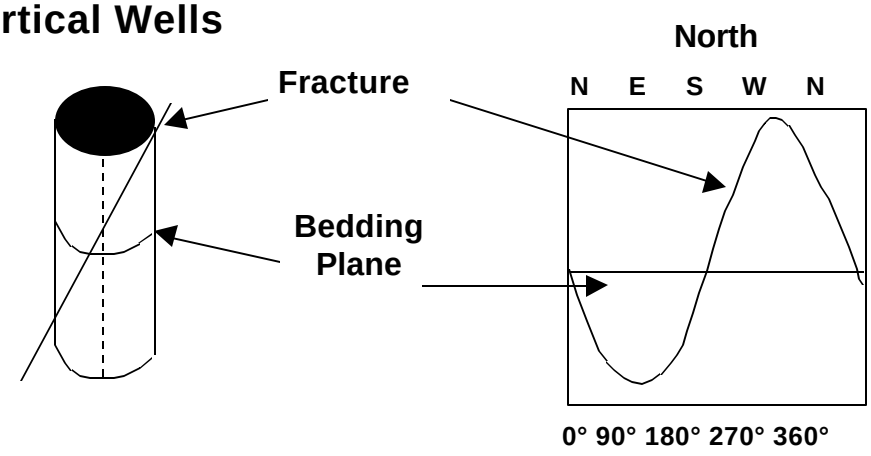

Horizontal Wells

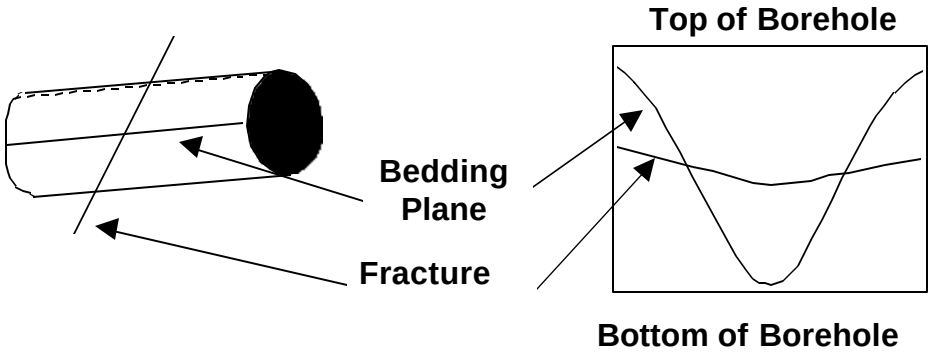

Deviated Boreholes - Example 2

Objective of this Example: To demonstrate the top of hole borehole reference.

Geological Background: Carbonate.

Available Data: Electrical Images.

Comments:

1. The low amplitude sine waves are fractures
2. There are two fracture zones which are commonly called “super fractures”. This is where several fractures occur in an close spacing.
3. There is oil in the top of the borehole which causes the poor image on the right pad.

Cretaceous Carbonate - Horizontal Well

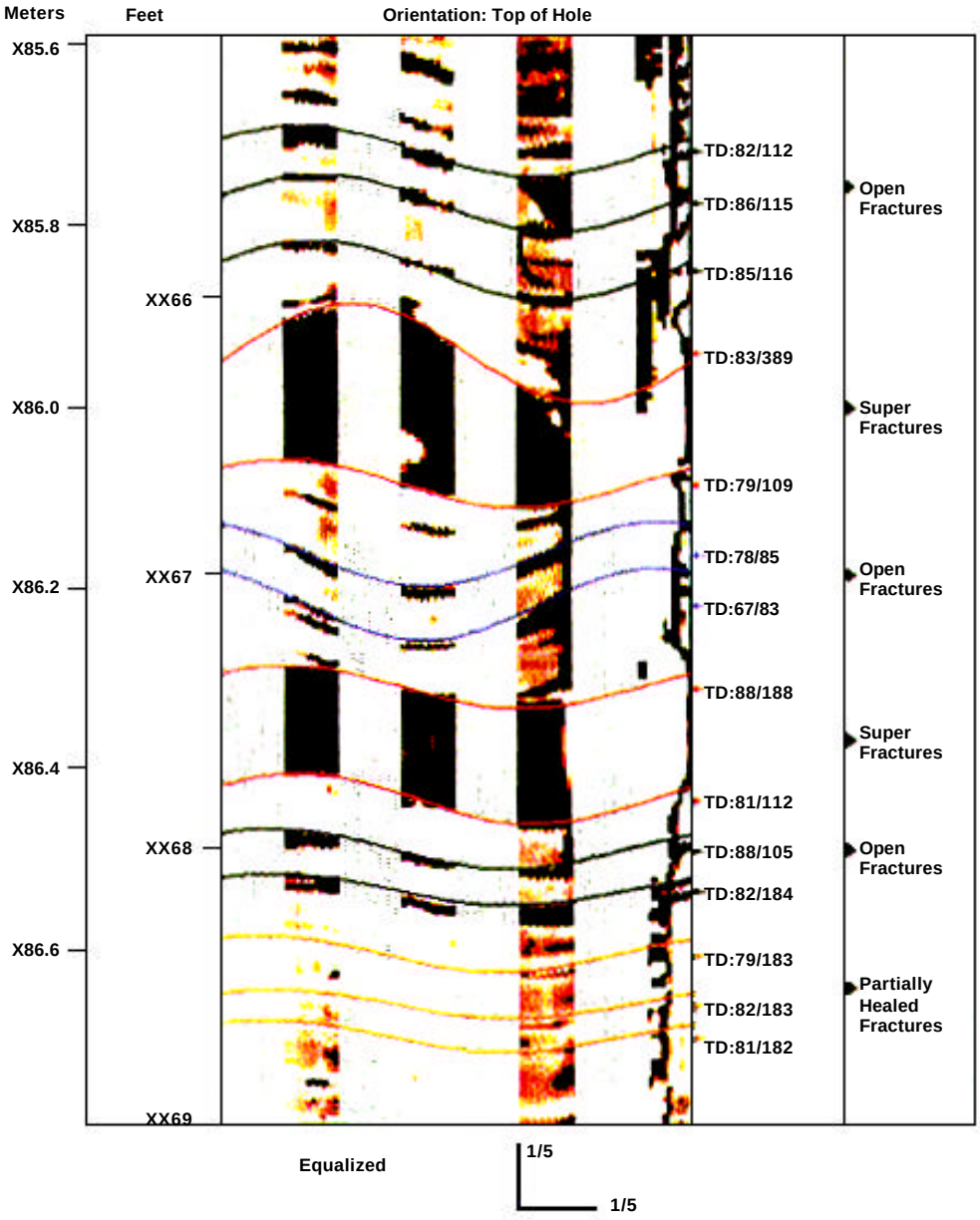

Horizontal Well Advisor

Log data (particularly FMS images) from horizontal wells have proven to be difficult to display in a concise understandable manner. The Horizontal Well Advisor package was developed to answer this need. Essentially, this package provides the tools needed to create a customized display of horizontal log data which mimics the geometry of the well trajectory, i.e., log channels and images are plotted alongside the curving track of the well. It is often much easier to locate fluid entries or highly fracture intervals when the information is presented in such a condensed form.

In effect, the view presented is that of the vertical plane which contains the well path. The horizontal reach of the well is shown along the long axis of the plot while displacement along the short axis represents the vertical drop of the well. Calipers from the FMS are plotted along the well path to show the changing nature of borehole. Most any available log data can be plotted either along the well path or in a straight track along the edges of the plot.

The accompanying example shows a short section of a horizontal well where the bit is actually travelling upward, i.e. hole deviated is greater than 90 degrees, for about 250 feet and then moves slightly downward again. This produces a “hump” in the well profile. The most interesting thing about this section is that the hump is filled with produced oil. The measured mud resistivity, displayed in color to the right, increases from blue to green to brown to red. The section of increased mud resistivity correlates well with the “up flag” and the washed out appearance of the images.

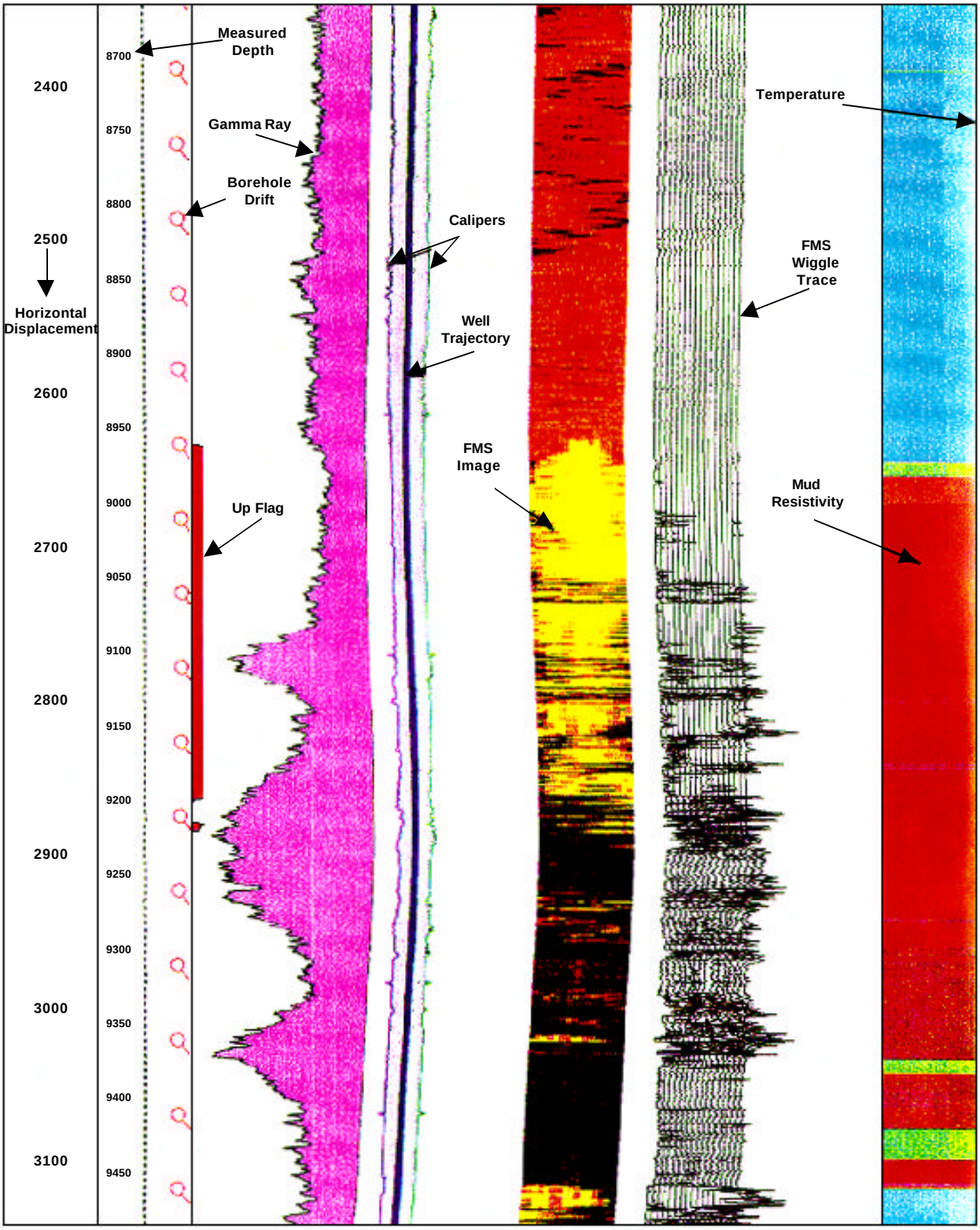
Measured Depth
Gamma Ray
Borehole Drift
Calipers
Well Trajectory
FMS Image
Up Flag
Temperature
FMS Wiggle Trace
Mud Resistivity
Horizontal Displacement
2400
2500
2600
2700
2800
2900
3000
3100
8700
8750
8800
8850
8900
8950
9000
9050
9100
9150
9200
9250
9300
9350
9400
9450

Deviated Boreholes - Exercise 1

Objective of this Exercise: Analysis of geologic features in a horizontal borehole.
Geological Background: Carbonate.
Available Data: Electrical Images in a horizontal borehole.
Question: What geological features are present?

Horizontal Borehole Vuggy Porosity

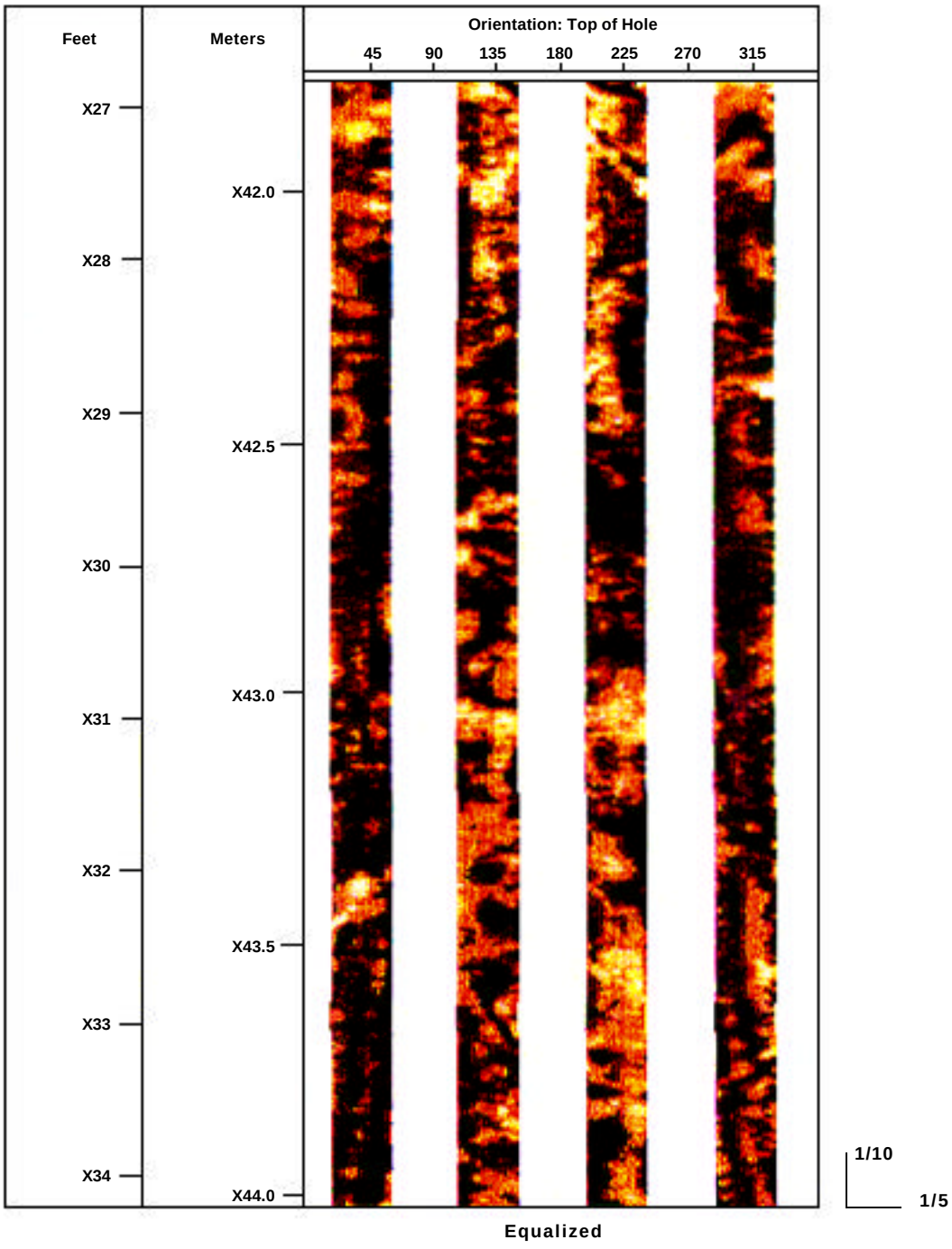

Deviated Boreholes - Exercise 2

Objective of this Exercise: Analysis of geologic features in a horizontal borehole.
Geological Background: Carbonate.
Available Data: Electrical Images in a horizontal borehole.
Question: What geological features are present?

Horizontal Borehole

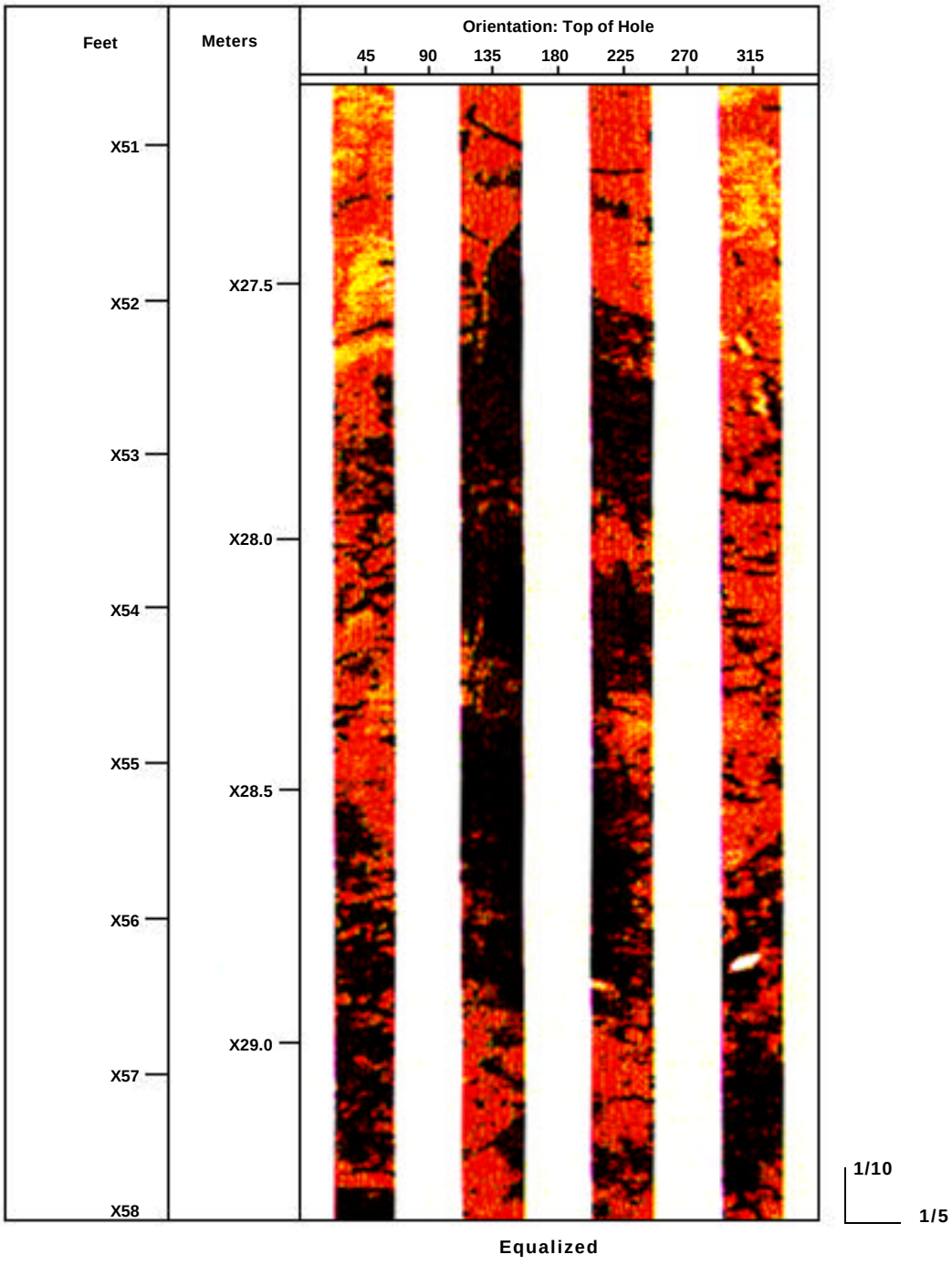

Deviated Boreholes - Exercise 3

Objective of this Exercise: Analysis of geologic features in a horizontal borehole.
Geological Background: Carbonate/Shale.
Available Data: Electrical Images in a horizontal borehole.
Question: What geological features are present?

Horizontal Borehole

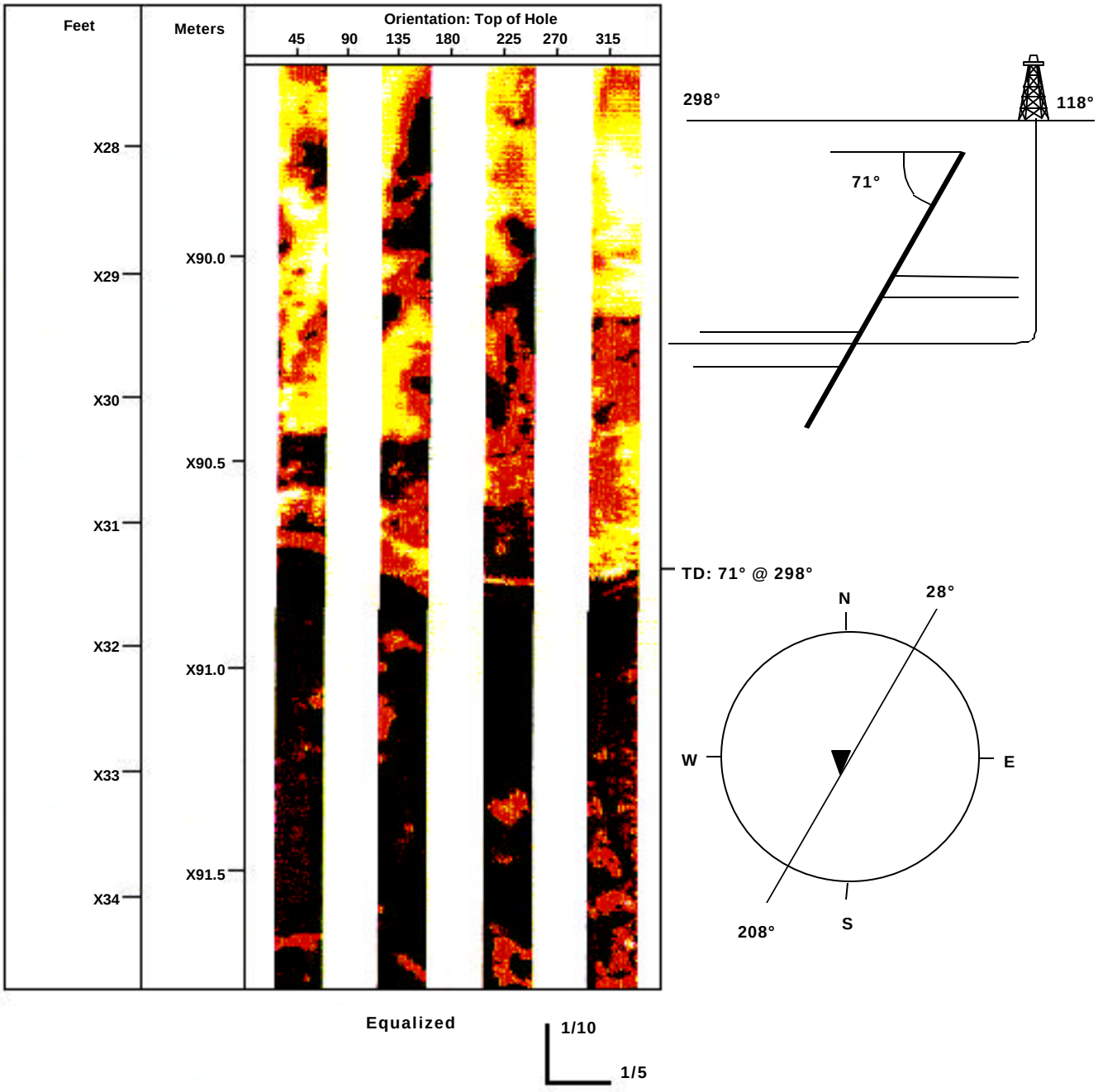

Deviated Boreholes - Exercise 4

Objective of this Exercise: Analysis of geologic features in a horizontal borehole.
Geological Background: Carbonate/Shale.
Available Data: Electrical Images in a horizontal borehole.
Question: What geological features are present?

Horizontal Borehole

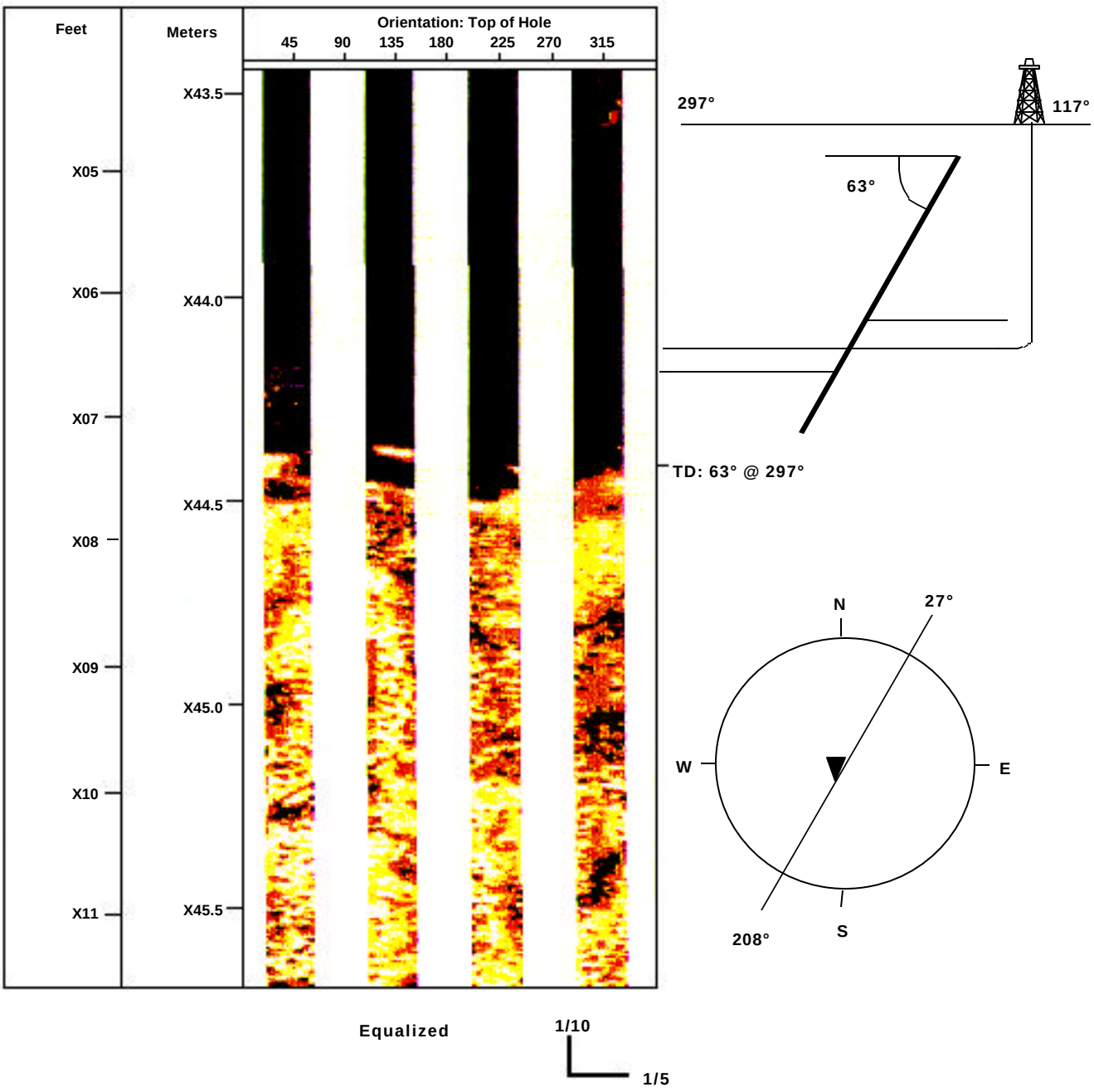

Deviated Boreholes - Answers

1. Vuggy porosity is present. The vugs are interconnected. These are polygonal fractures at 43.6 meters and at 42.6 meters.

2. Polygonal fractures are present from 27.5 meters to 29.3 meters.

3. Since this is a horizontal borehole, the abrupt lithology change is a fault.

4. Again, since this is a horizontal borehole, the lithology change is a fault.

Structure and Pattern Recognition

Objective of this Chapter:

- Recognition the basic dip patterns of:
  - Red - downdip thickening
  - Blue - downdip thinning
  - Green - constant section

These patterns will be used to define:

- Structural dip from the green patterns.

Structural Analysis

Structural analysis consists of defining the structural dip and the evaluation of unconformities and faults.

Dipmeter Processing

Dipmeter processing of the data recorded with the electrical images is an excellent "quick look" for determining structural dip as well as for locating some faults and unconformities. Dipmeter processing is very useful in resolving low structural dip.

Structural Dip

Dip computation of either the borehole images or dipmeter processing is a measurement of structural dip and not regional dip. Regional dip, as determined from multiple well logs is an area, can be different from structural dip resolved from a single well. Dips computed from either borehole images or from dipmeter can be influenced by compaction or structural changes. The figure opposite illustrates the influence of compaction and structural uplift.

Structural dip is an average of many dip computations; therefore, a dipmeter plot will yield the structural dip more accurately than a point by point manual computation in low structural dip situations. A long correlation length, eight feet, will usually yield an accurate dip. In higher structural dips, image analysis can provide higher confidence data. The two types of processing do compliment each other. Structural dip and mega-patterns from dipmeter processing will be presented first.

Regional Dip vs. Structural Dip

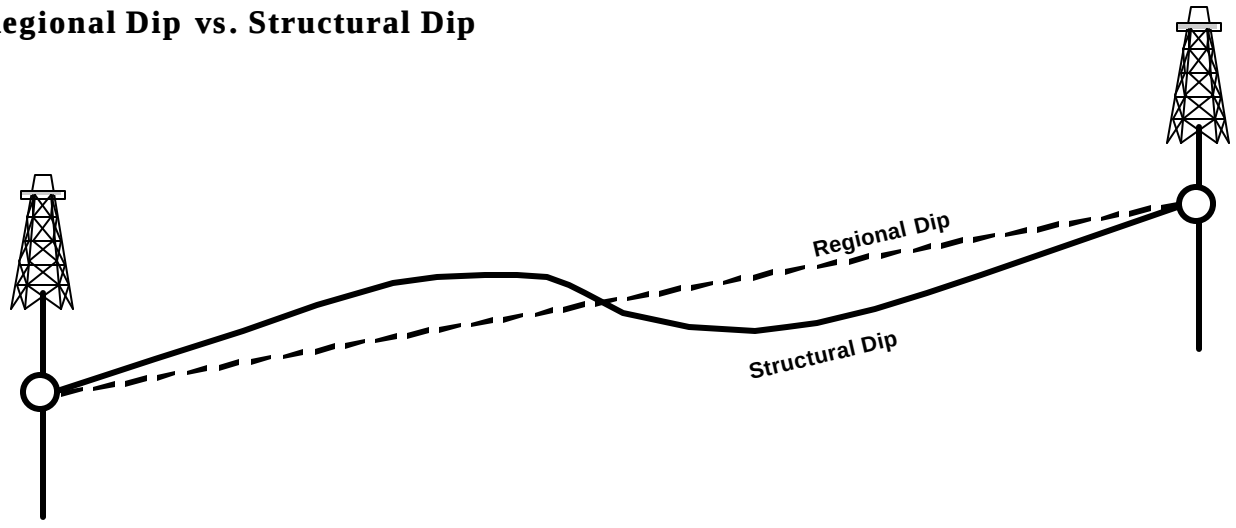

Rule : Structural dip may be projected horizontally as far as the green pattern extends vertically.

Structural Dip vs. Regional Dip Example

An example opposite illustrates the importance of structural dip determination. Well No. 1 penetrated a carbonate at –3814 ft. There was a strong oil show. Regional dip was 1°SSW. Well No. 2 was located 2210 ft to the NNE and did penetrate the carbonate in a much better structural position as –3754 ft. This was the expected depth from regional dip projection. Well No. 2 produced oil at the rate 55 BOPD but with 120 BWPD. A dipmeter was run in Well No. 2. The structural dip was determined to be 2° NNE. This indicated a closure to the SSW, which is regionally downdip. Well No. 3 was located 736 ft WSW of Well No. 2 and along the WNW-ESE structural strike. Final well location was 100 ft to the ESE of Well No. 2. (A well located only 736 ft from a marginal well was not deemed to be politically sound). Well No. 3 produced oil at the rate of 200 BOPD with no water production. Structural dip determination is very important in locating potential closures.

Example of Regional vs. Structural Dip

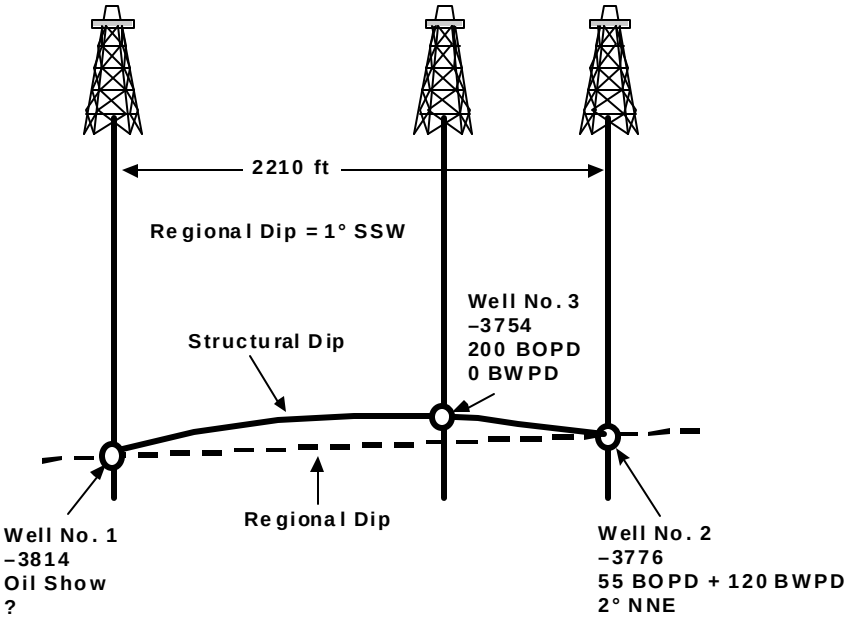

Subsea at Pay Zone Production Structural Dip

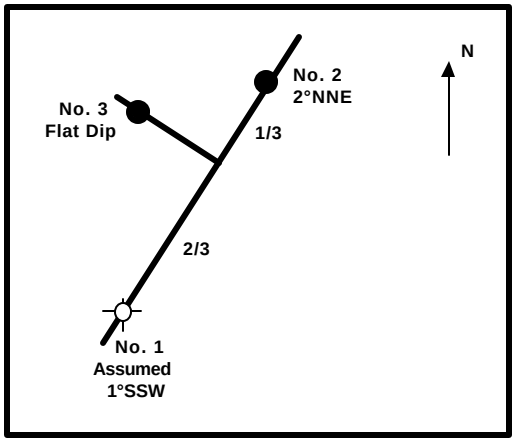

Dip Patterns

There are four basic groups of dip patterns defined by Al Gilreath:

- ♦ Downdip thinning Blue
- ♦ Constant downdip Green
- ♦ Downdip thickening Red
- ♦ Random Bedding Yellow

All patterns must have a constant azimuth, but the dips either increase upward, decrease upward, or remain constant.

Green:
Constant Thickness

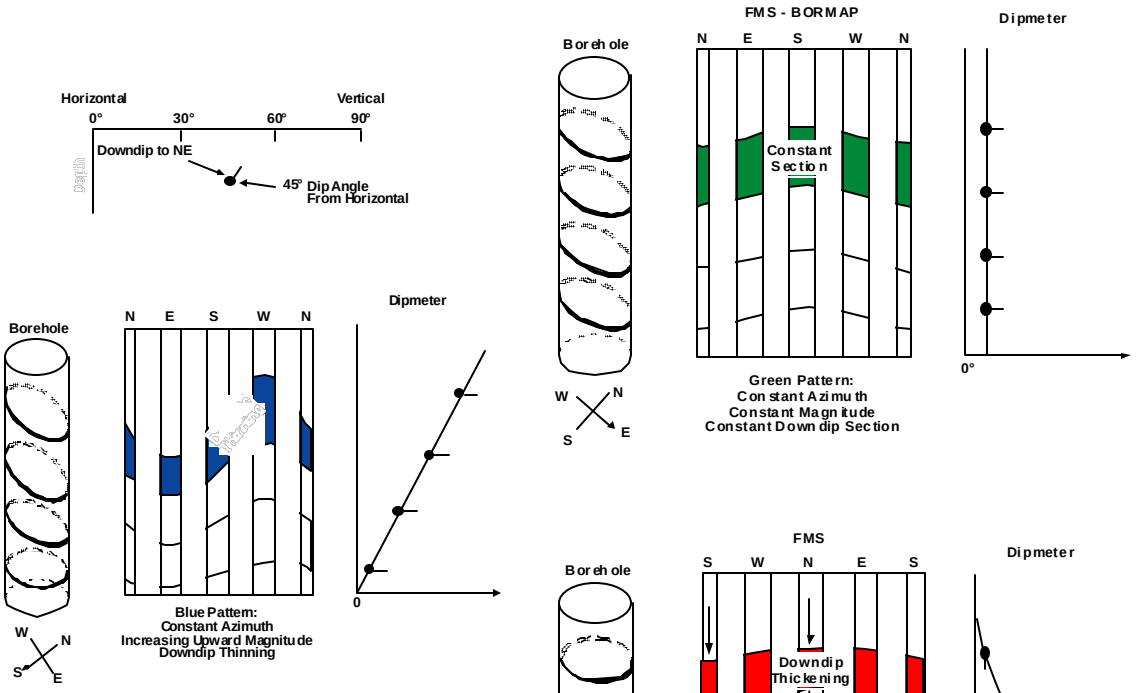

Blue:
Downdip Thinning

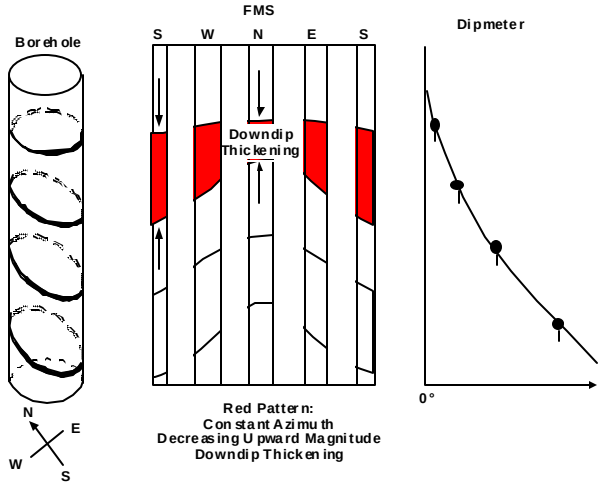

Red:
Downdip Thickening

Pattern Recognition Exercise 1

Objective: Determination of dips and mega-patterns from arrow plots.

Questions: Complete the blanks opposite.

Pattern Recognition Exercise 1

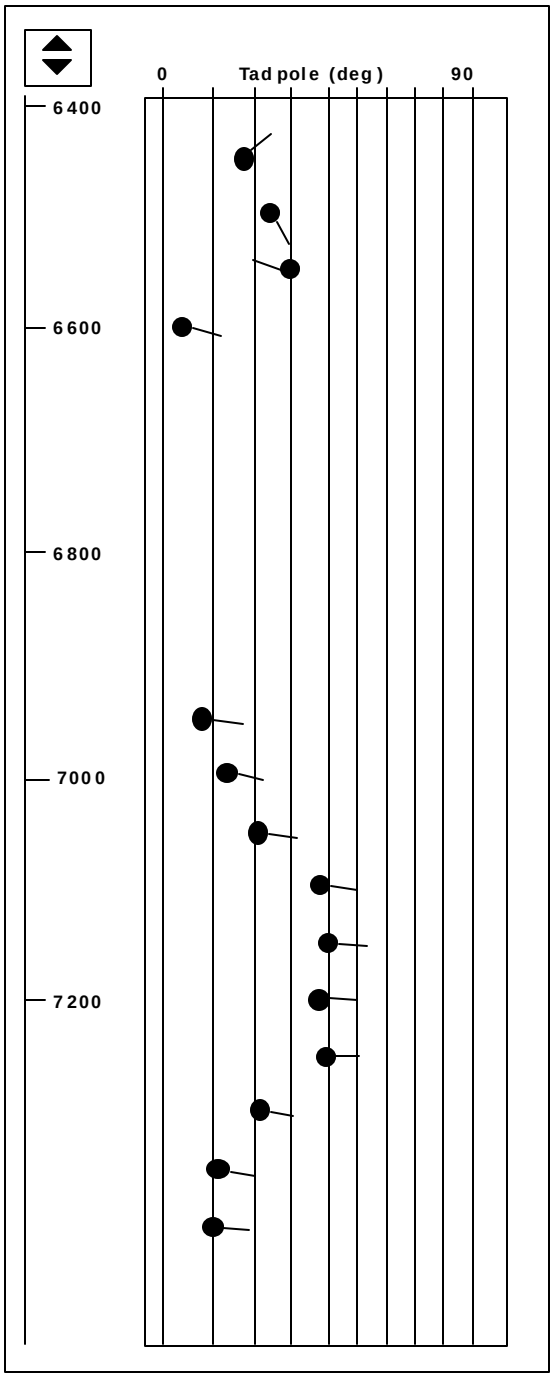

Magnitude	Azimuth

Construct Arrow Plot of

45°	100°
17°	345°
75°	335°

Mark the patterns (red, blue, green)

Borehole Drift

Unless controlled, the magnitude and direction of borehole drift is a useful indication of structural events. The borehole deviation is presented much as the dipmeter arrow plot. The body of the tadpole indicates the magnitude of the borehole deviation and is measured with reference to gravity. The arrow points in the direction of borehole drift and is measured with reference to magnetic north but presented as true north.

Borehole drift in a consolidated formation will vary with the structural dip and with the borehole fluid. The bit will drift updip in mud drilled boreholes and downdip in air drilled boreholes. The magnitude of drift reflects the structural dip in the lower dip ranges but does not respond when the structural dip exceeds approximately 60°.

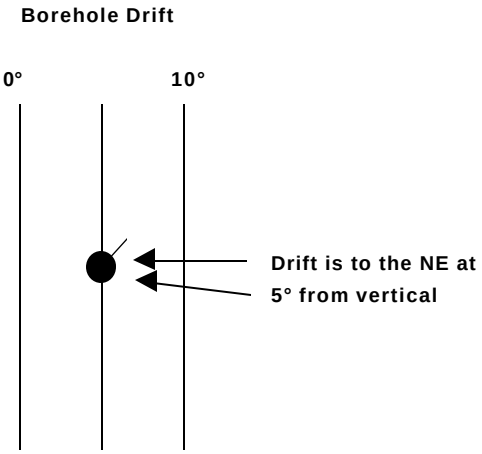

Borehole Deviation

- Borehole Drifts - Consolidated
  - Updip in mud drilled boreholes
  - Downdip in air drilled boreholes
- Borehole Drifts - Unconsolidated and Flat Dip
  - Tend to spiral
- Doglegs may occur at
  - Faults
  - Unconformities
  - Structural dip changes

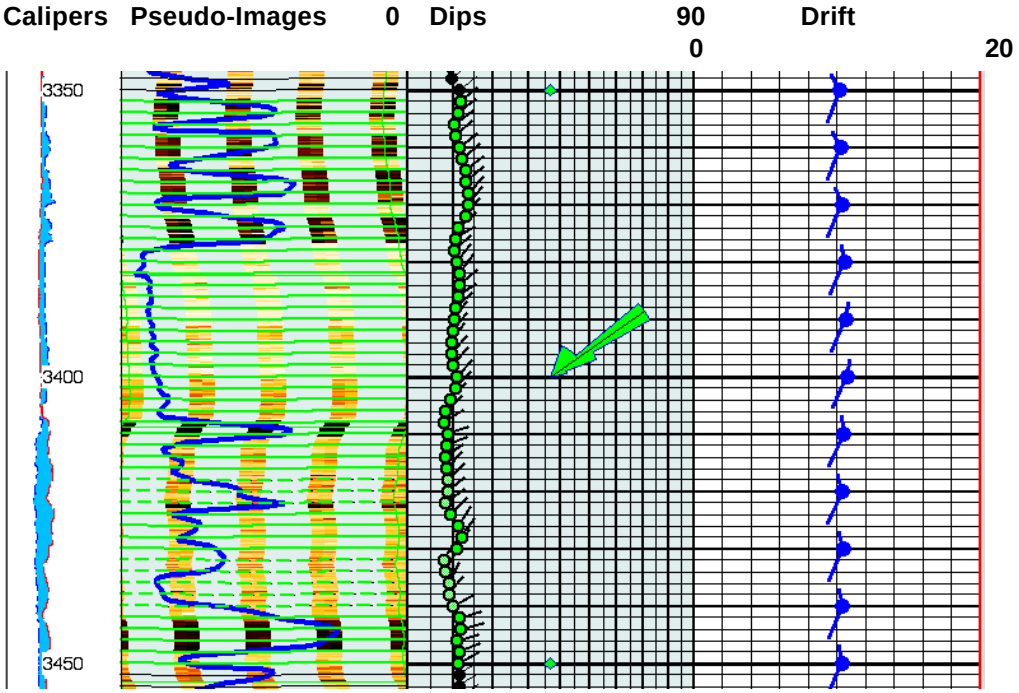

Pattern Recognition Exercise 2

Objective: Pattern recognition.

Questions: Mark the dip patterns.

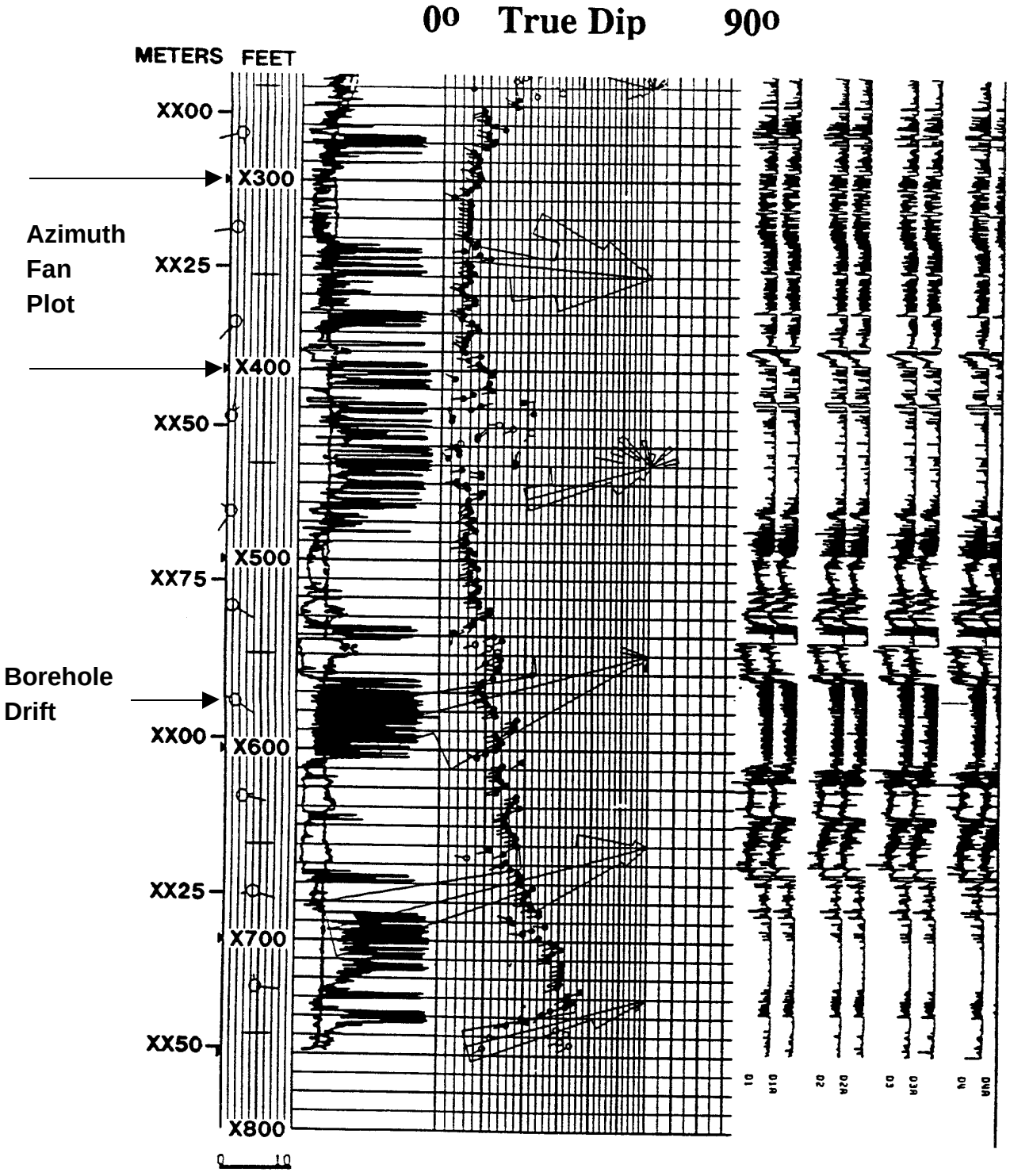

Pattern Recognition Exercise 3

Objective: Pattern recognition.

Questions: Mark the patterns.

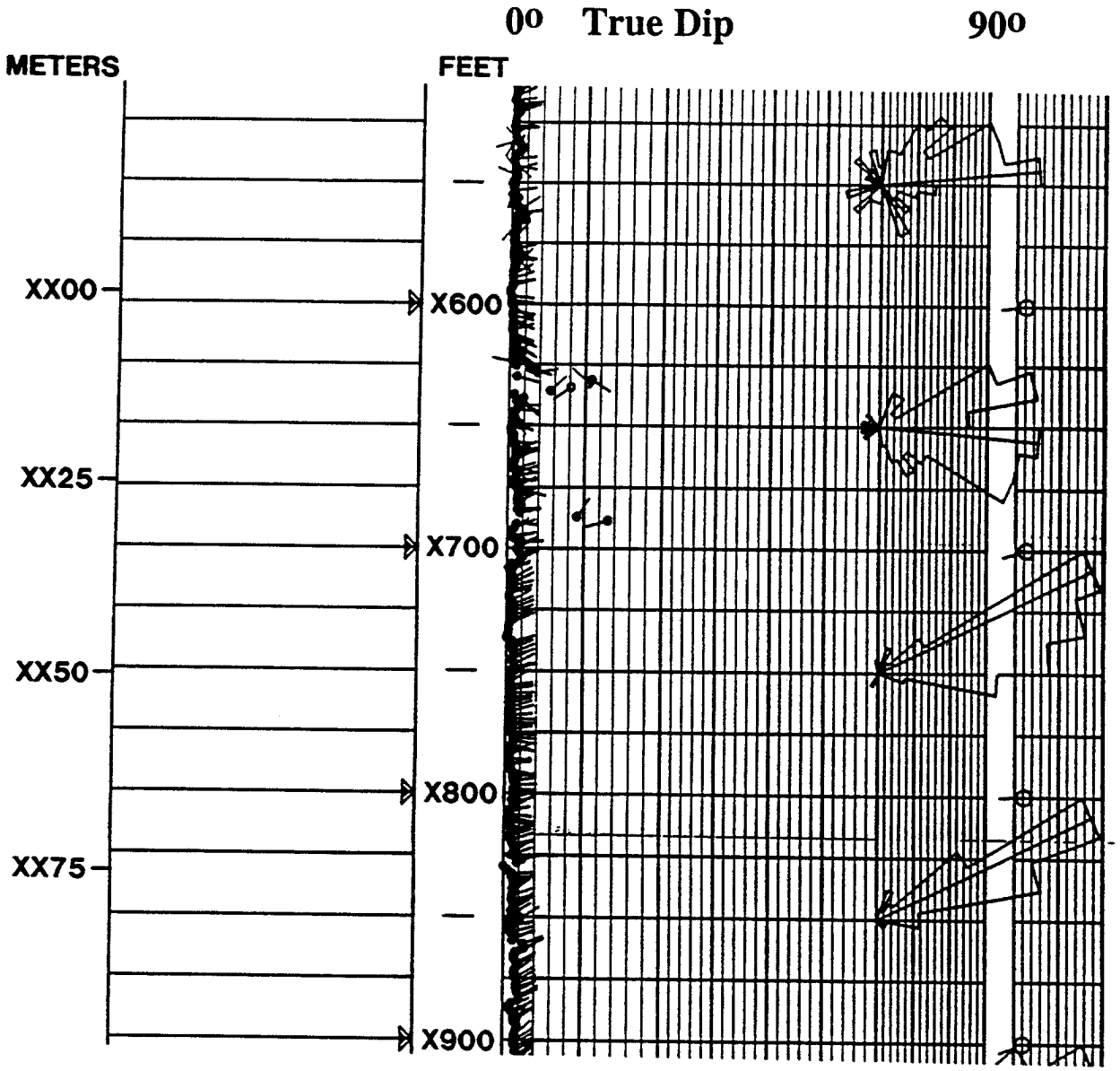

Pattern Recognition Exercise 4

Objective: Pattern recognition.

Questions: Mark the patterns.

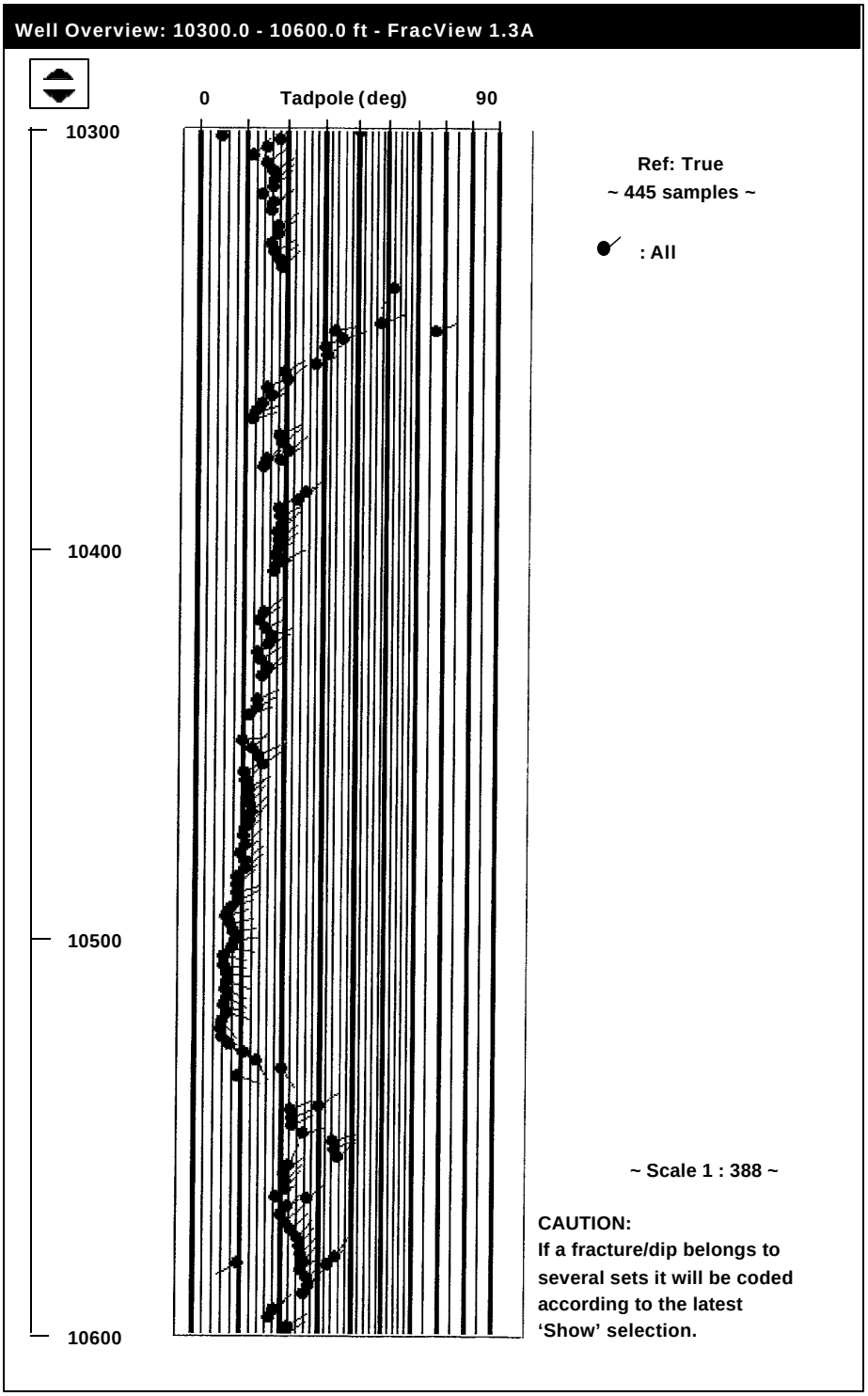

Pattern Recognition Exercise 4

Objective: Pattern recognition with structural dip.

Questions: Mark the patterns.

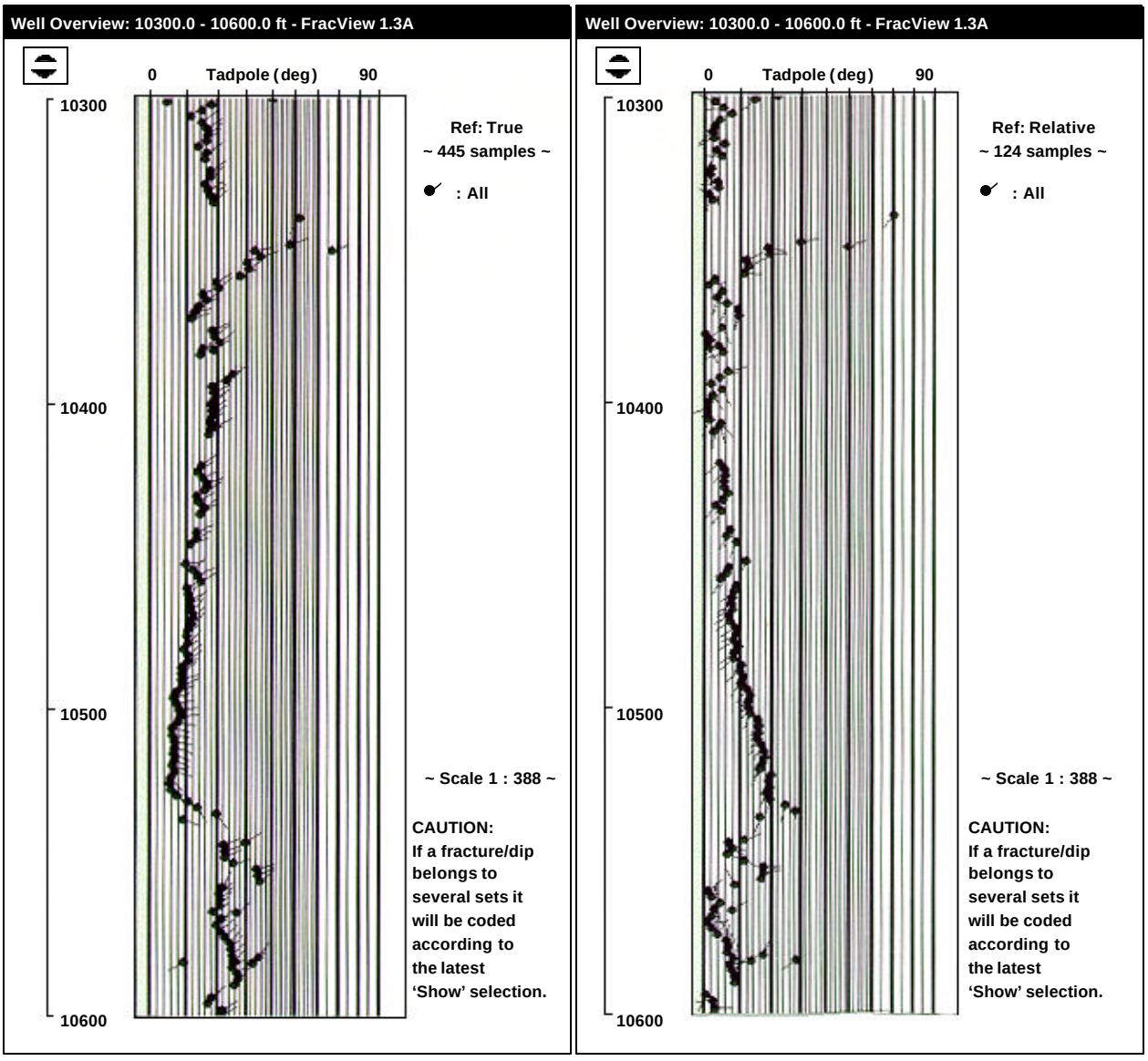

- If structural dip greater than 4° then always use the structural dip subtract (relative) when marking dip patterns.

Structural Dip Exercise 1

Objective: Determination of structural dip from arrow plots.

Questions: What is the structural dip?

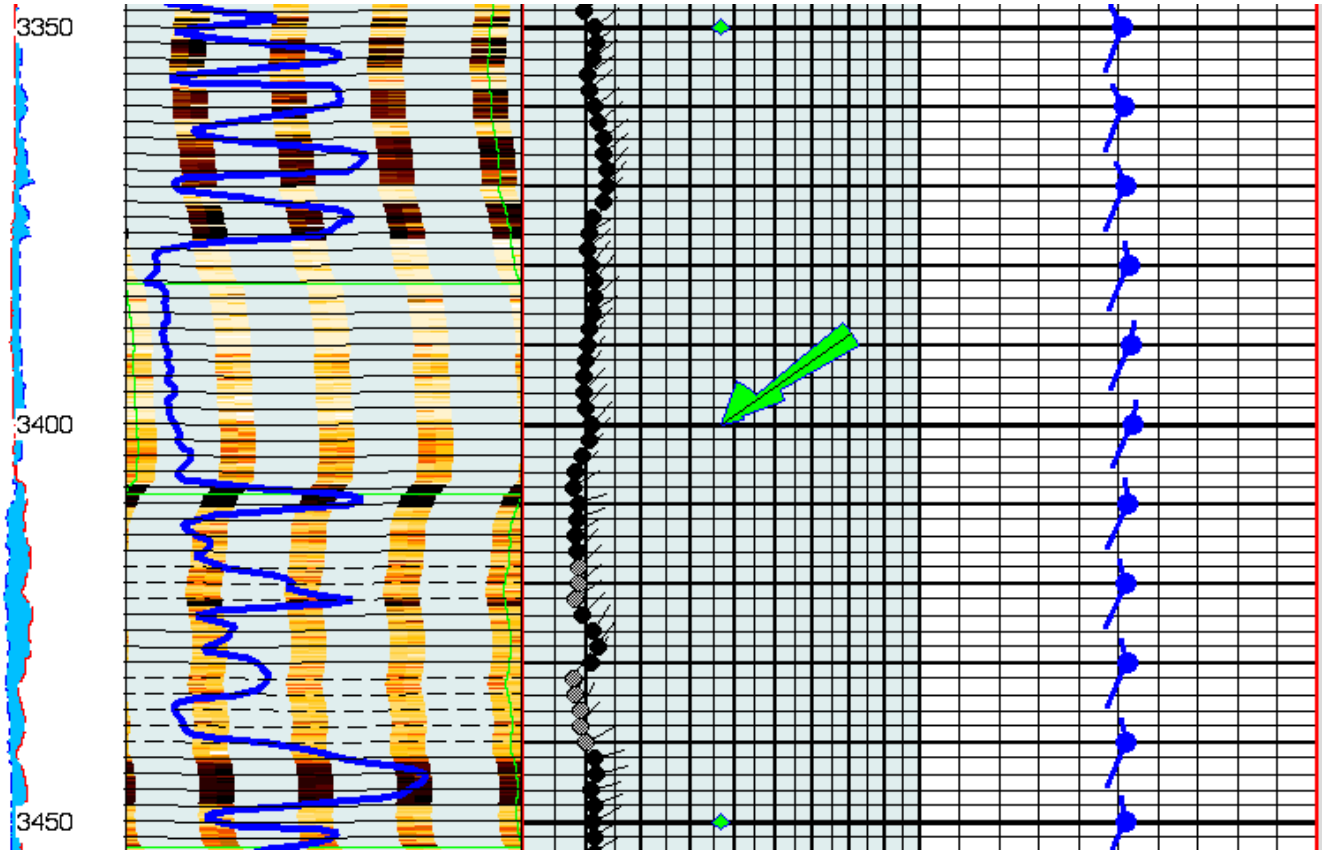

An offset located 1000’ structurally up dip should gain _____ feet.

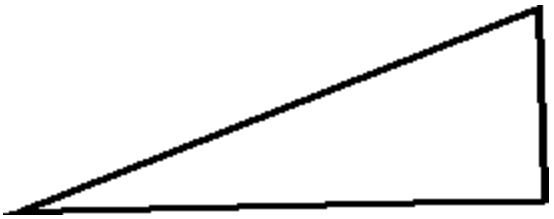

Structural gain = _____ ft.

1000’

Structural Dip Exercise 2

Objective: Determination of structural dip from arrow plots.

Questions: What is the structural dip?

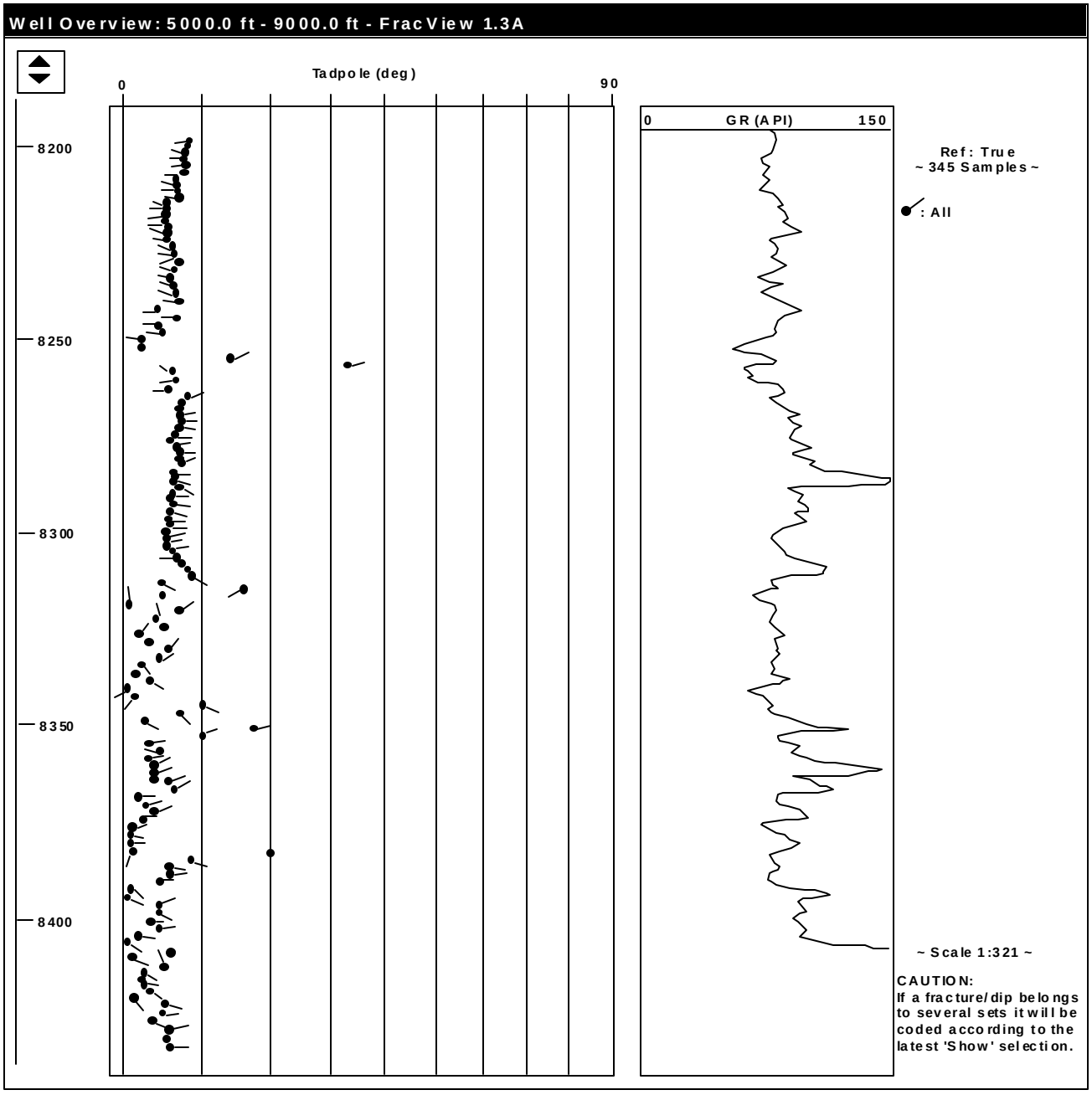

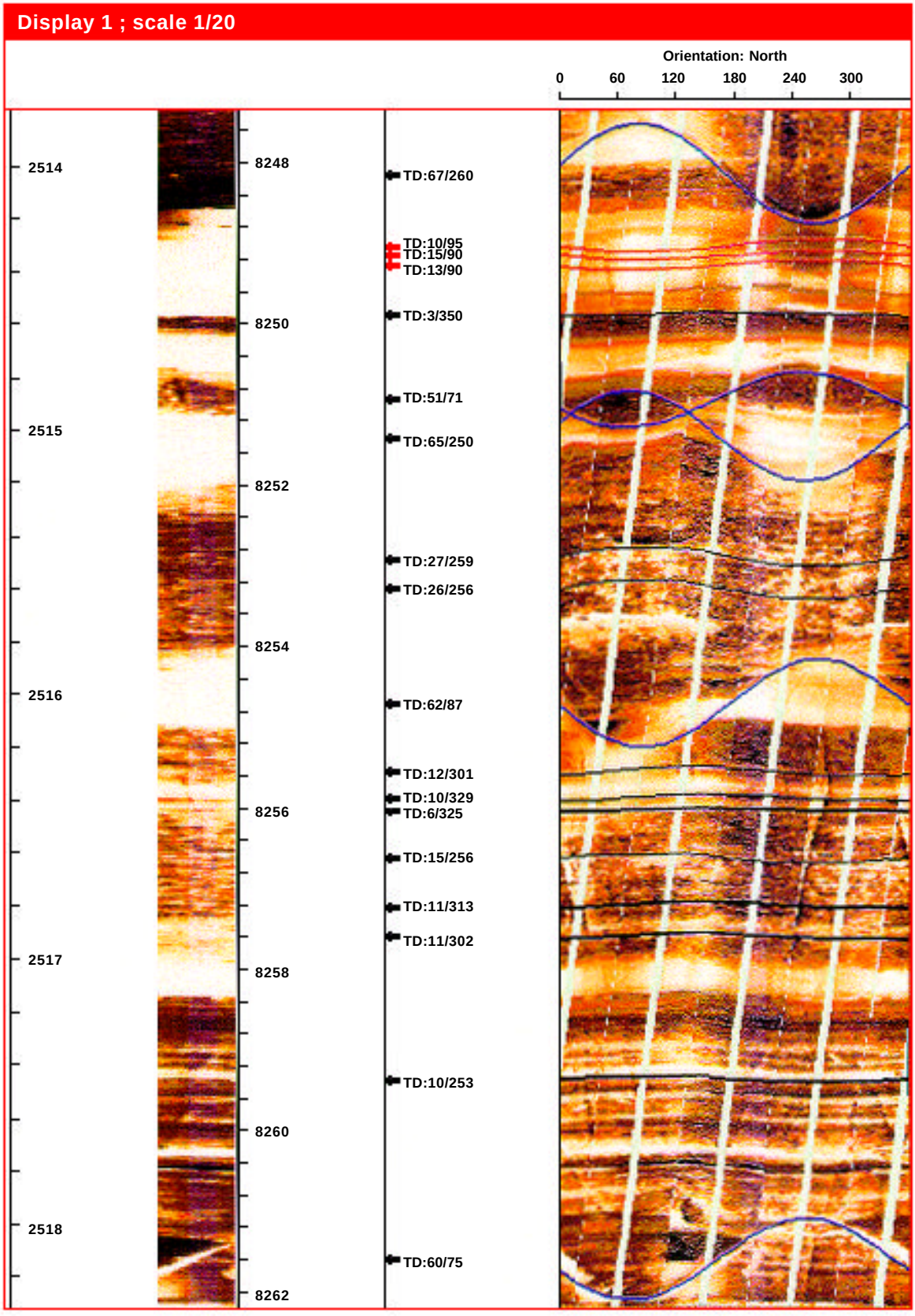
Display 1 ; scale 1/20
Orientation: North
0
60
120
180
240
300
2514
2515
2516
2517
2518
8248
8250
8252
8254
8256
8258
8260
8262
TD:67/260
TD:10/95
TD:15/90
TD:13/90
TD:3/350
TD:51/71
TD:65/250
TD:27/259
TD:26/256
TD:62/87
TD:12/301
TD:10/329
TD:6/325
TD:15/256
TD:11/313
TD:11/302
TD:10/253
TD:60/75

Structural Dip Exercise 3

Objective: Determination of structural dip from arrow plots.

Questions: What is the structural dip?

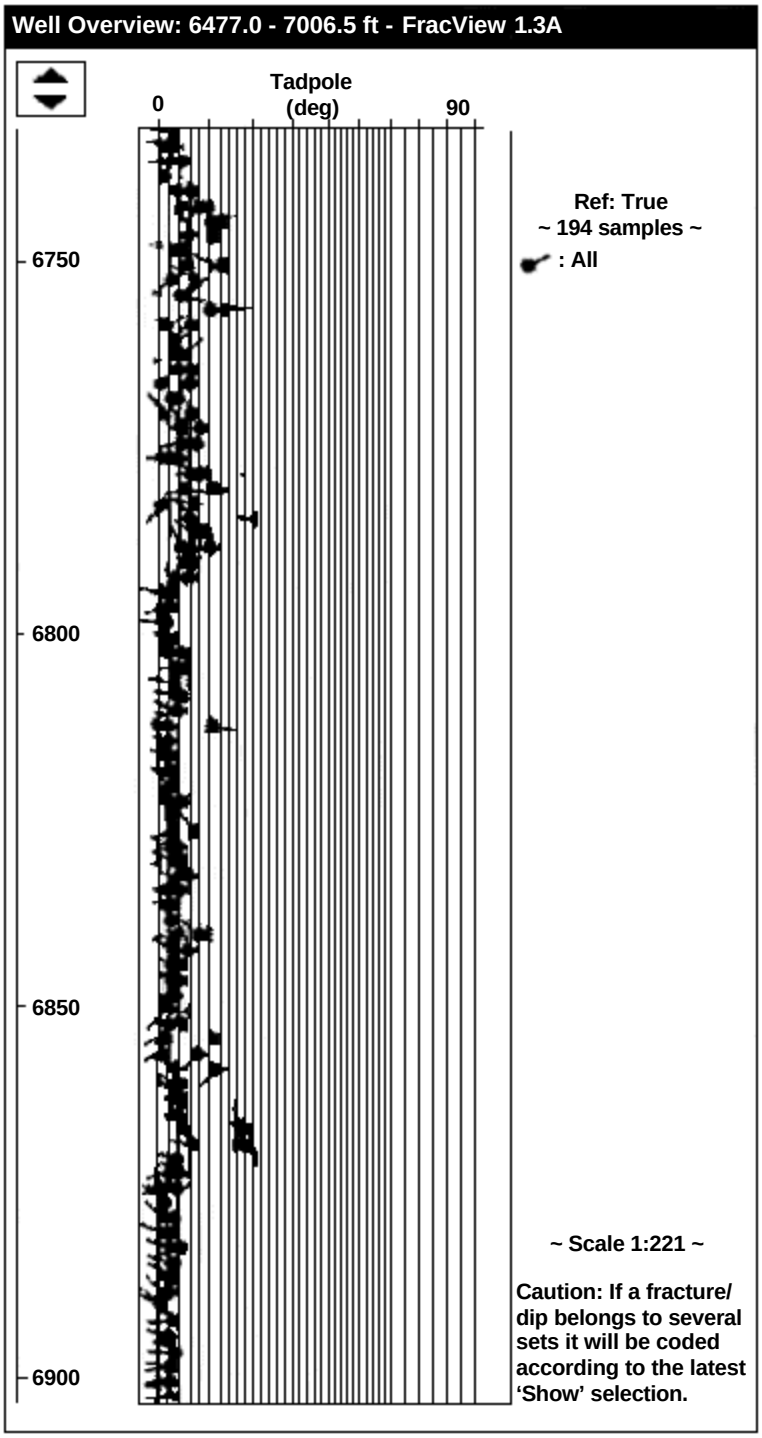

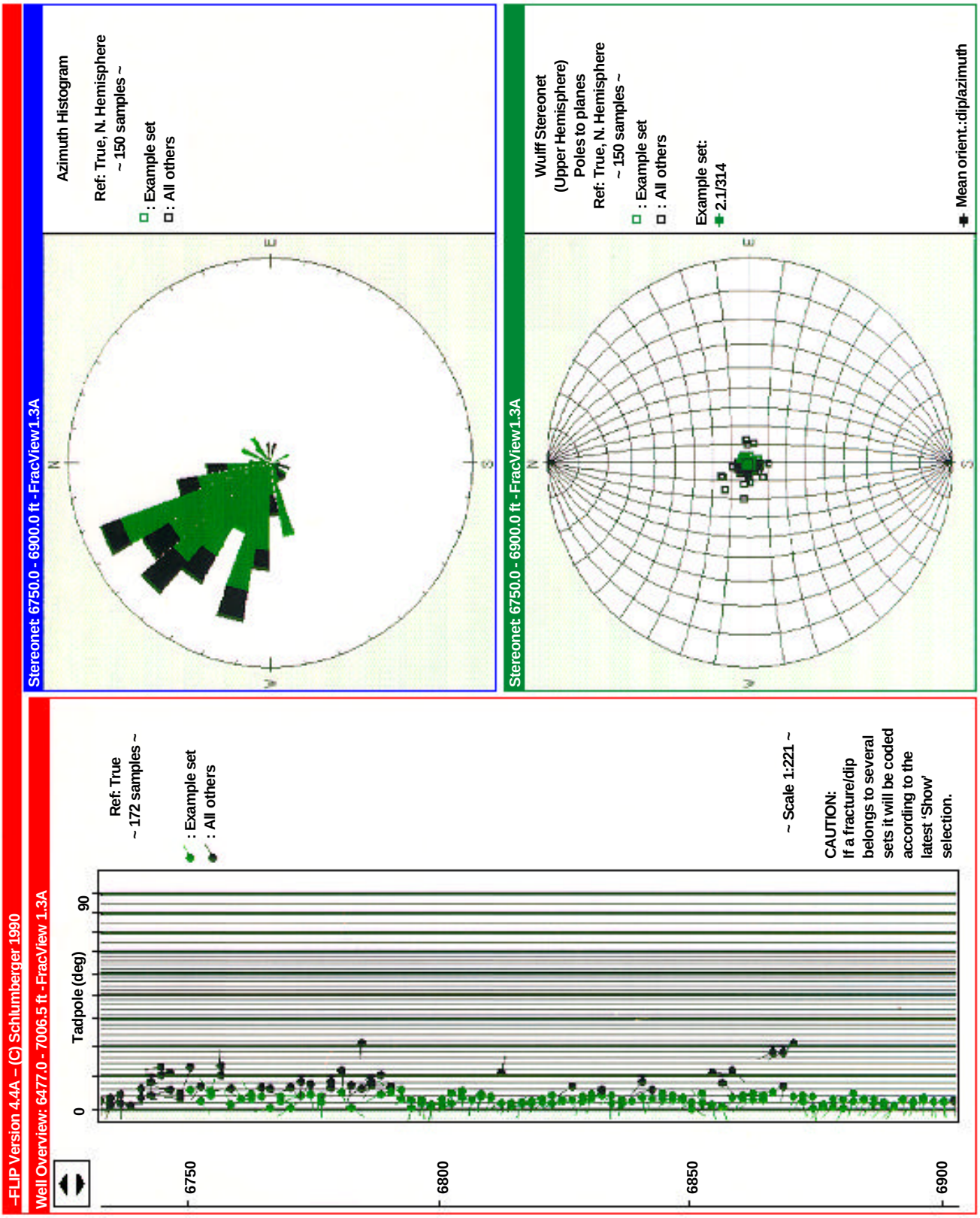
-FLIP Version 4.4A – (C) Schlumberger 1990
Well Overview: 6477.0 - 7006.5 ft - FracView 1.3A
Tadpole (deg)
0
90
6750
6800
6850
6900
Ref: True
~ 172 samples ~
: Example set
: All others
~ Scale 1:221 ~
CAUTION:
If a fracture/dip
belongs to several
sets it will be coded
according to the
latest 'Show'
selection.
Stereonet 6750.0 - 6900.0 ft - FracView 1.3A
Azimuth Histogram
Ref: True, N. Hemisphere
~ 150 samples ~
: Example set
: All others
N
E
S
Stereonet 6750.0 - 6900.0 ft - FracView 1.3A
Wulff Stereonet
(Upper Hemisphere)
Poles to planes
Ref: True, N. Hemisphere
~ 150 samples ~
: Example set
: All others
Example set:
2.1/314
Mean orient.:dip/azimuth
N
E
S

Structural Dip Exercise 4

Question: What is the structural dip?

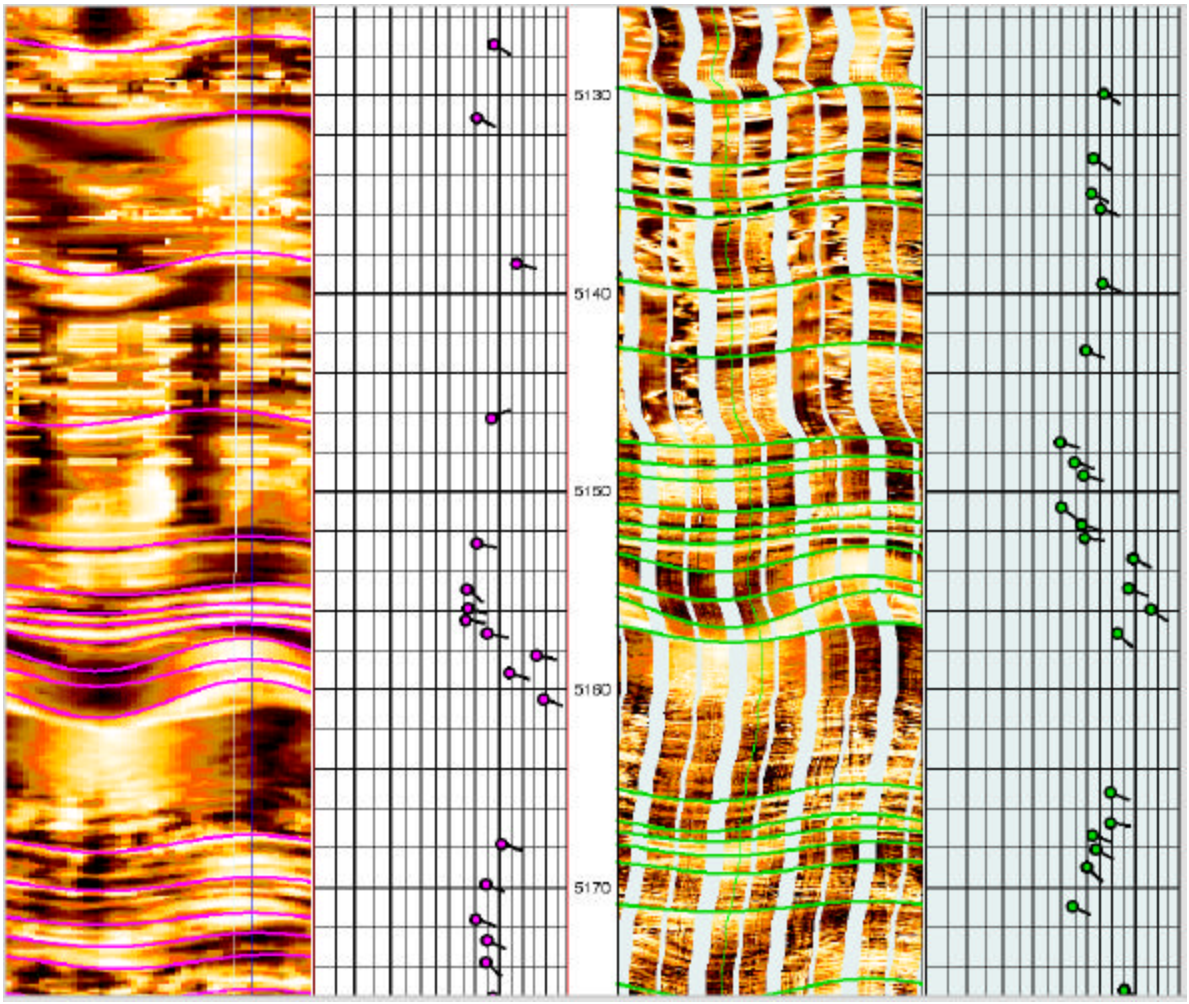

RAB Images / Dips **Electrical Images / Dips**

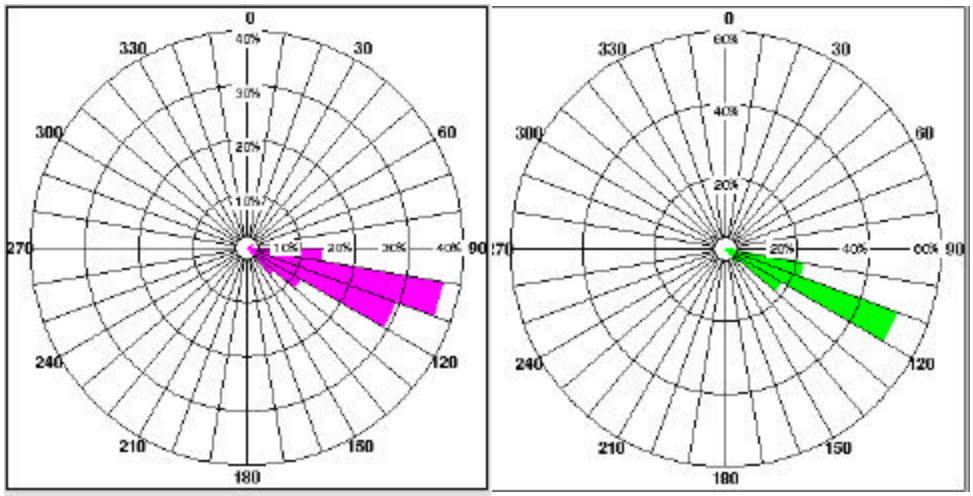

Structural Dip Exercise 5

Question: What is the structural dip?

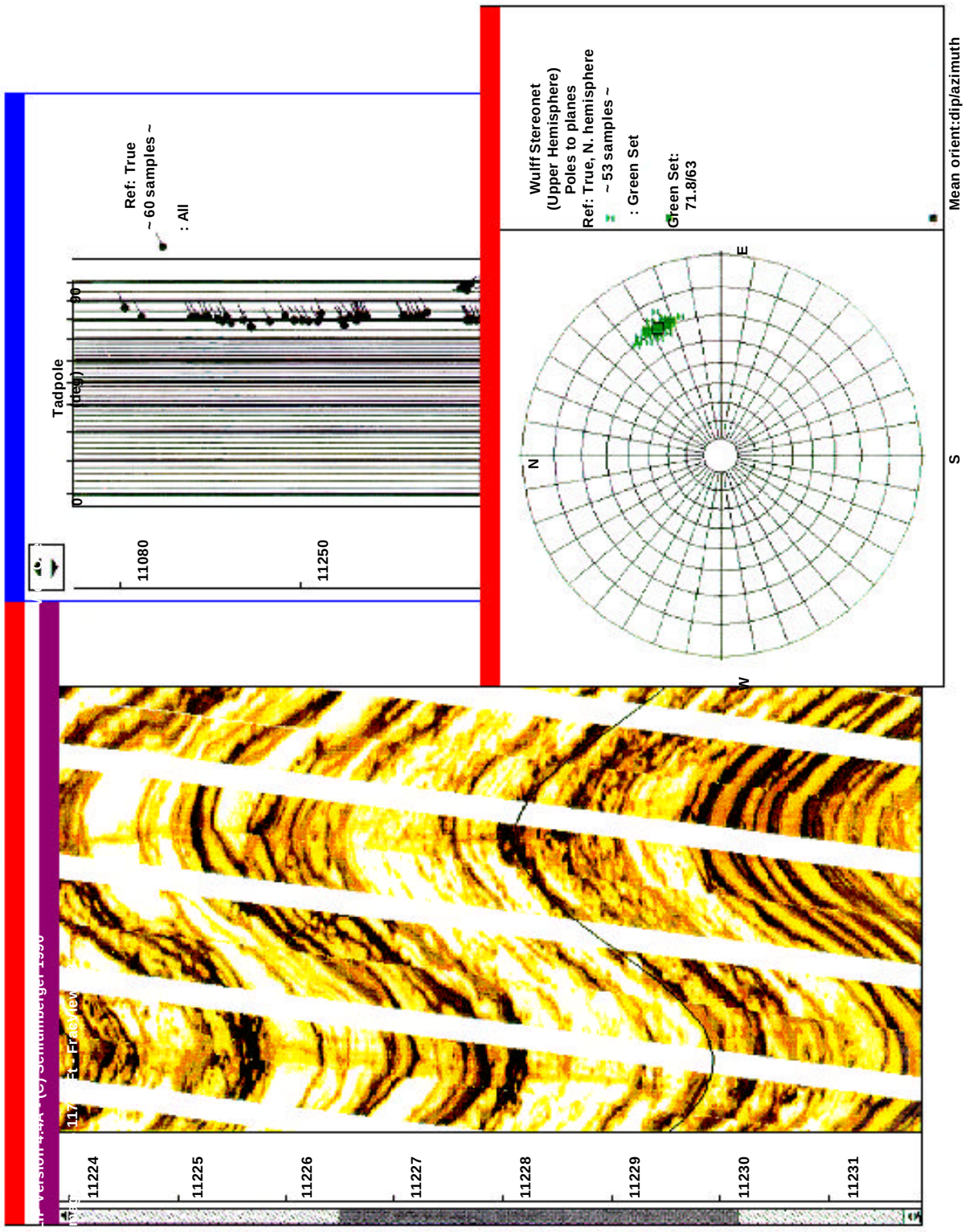

Structural Dip Exercise 5 (continued)

Question: If the following information is used

1. Vertical wellbore; and
2. Measured thickness of pay sand is 202 ft.

then

1. What is the true sand thickness?
2. If 50 ft is a minimum thickness, is this a commercial well?

Structure and Pattern Recognition Exercise - Answers

Pattern Recognition

Exercise 1

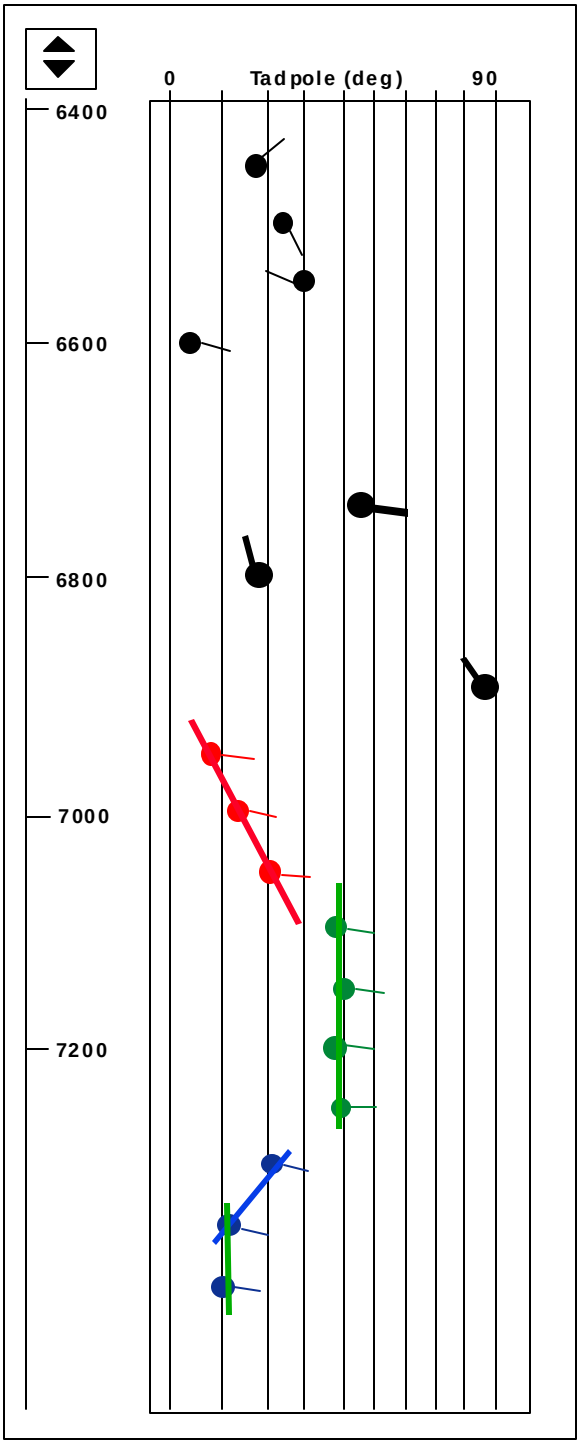

Magnitude	Azimuth
17°	45°
25°	140°
29°	285°
4°	105°

Construct Arrow Plot of

45°	100°
17°	345°
75°	335°

Mark the patterns (red, blue, green)

Exercise 2

a. Structure Interpretation:
   – Blue from top to 320 ft
   – Green from 320 ft to 530 ft
   – Red from 530 ft to TD

b. Stratigraphic Interpretation
   – Many red/blue/green patterns

Exercise 3

1. Red Pattern.

Exercise 4

1. Major red from 10400 ft to 10540 ft.

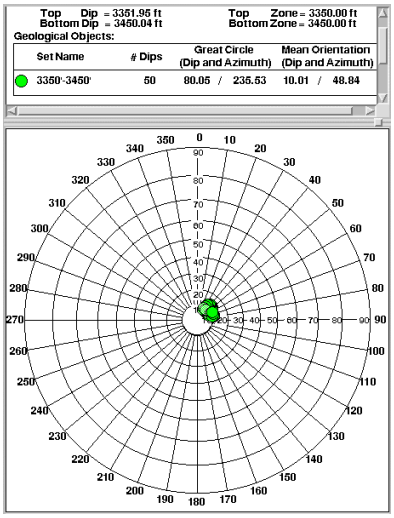

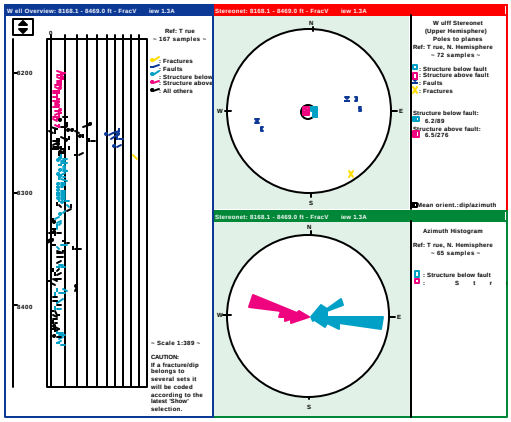

Structural Dip

Exercise 1

1. 10.1° at 48.84°; gain = tan 10.1*1000= 178’

Exercise 2

1. 6.5° at 276° above 8248 ft
   6.2° at 39° below 8248 ft

Exercise 3

1. 2.1° at 314°

Exercise 4

1. FMI: 56.97 magnitude at 115.55 azimuth, RAB: 59:25 magnitude at 110.26 azimuth.

Exercise 5

1. 70.8° at 63°
   Yes, thickness is 66.43 ft

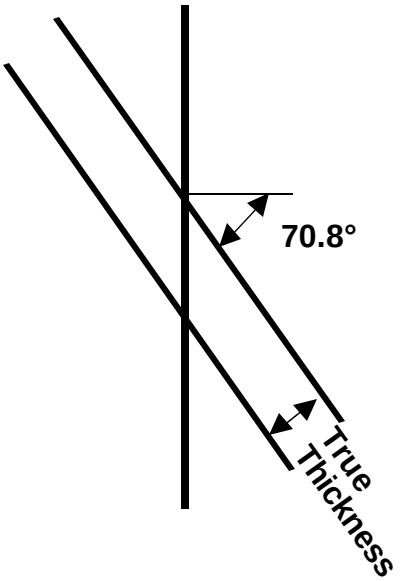

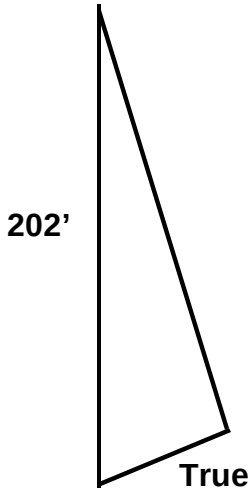

Cos 70.8° = True thickness/ 202’
= 66.43’

If 80°, then = 35.1’

Unconformities

Objective of this Chapter:

- Recognition and analysis of unconformities from arrow plots and electrical images.

Photo by J.A. Gilreath

Rule: Structural Dip is usually higher *below* an unconformity and higher *above* a fault

Unconformities

An unconformity is the erosional surface which represents a geological hiatus between younger and older rock units. Unconformities are created when there is non-deposition on previously deposited sediments or when there is erosion of the previously deposited sediments.

The Process

The process for the interpretable types of unconformities is shown below. The original shale-line sequence can be altered by either structural tilting or by faulting. Subsequent erosion causes changes in dip magnitudes and azimuths or in loss of section. These dip changes and the resulting unconformity surfaces are the subject of this section.

Unconformities - The Process

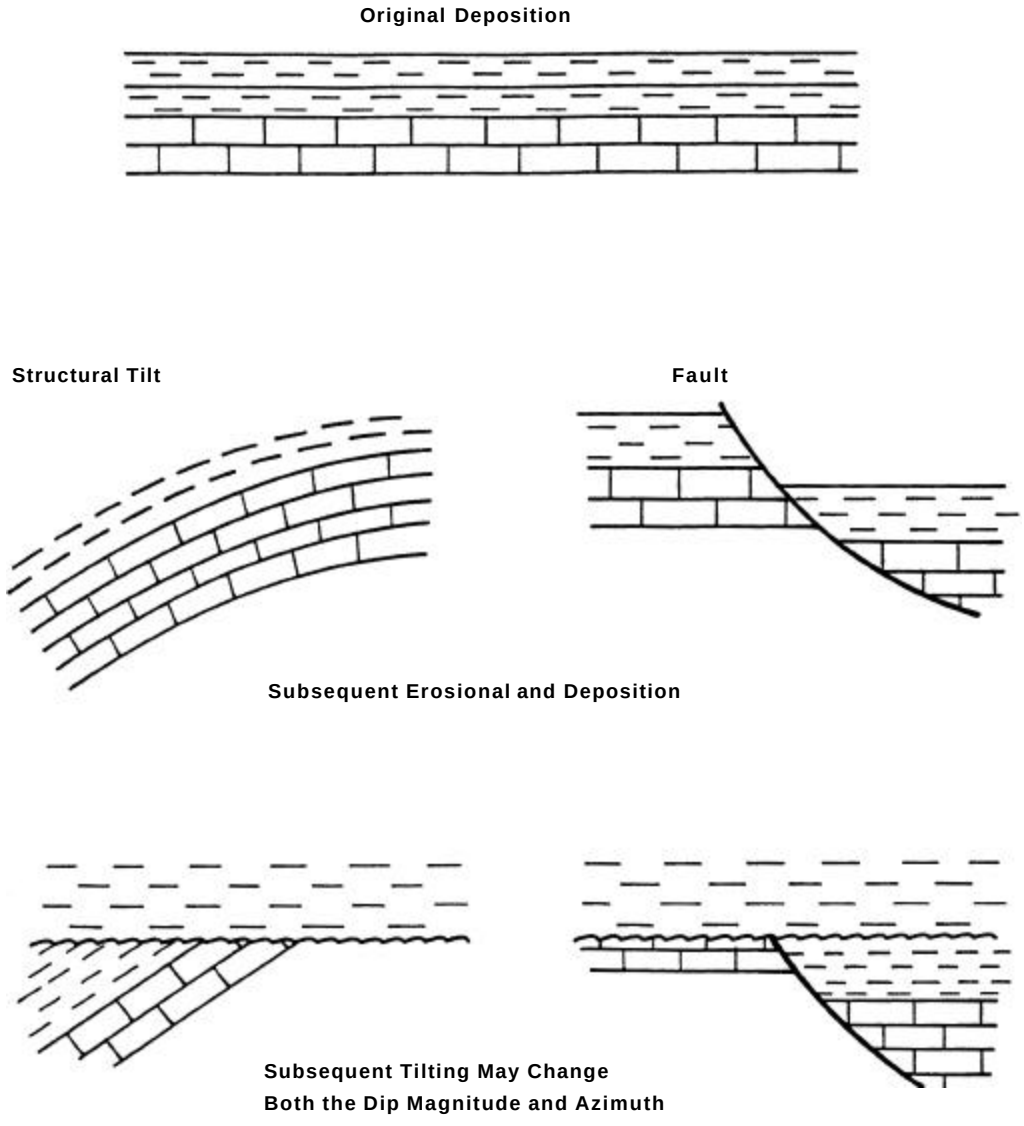

Unconformity Classification

A unconformity is the result of non-deposition or the erosion of inclined beds. These may be located from arrow plots by changes in:

- ♦ dip density
- ♦ dip magnitude
- ♦ dip density

The figure below illustrates these types. The lower unconformity, between A and M, is a change in dip azimuth. The dip magnitude is constant over the contact by the dip azimuth shifts from West to East.

The next unconformity, between M and D, is a change in dip magnitude. The dip azimuth remains constant over the contact, but there is a share *decrease* in dip magnitude.

The unconformity between D and N is very difficult to recognize. The dip magnitude and azimuth remain constant over the unconformity but there is a difference in the frequency of computed dips. This is the result of a well bedded versus a poorly bedded formation.

The upper unconformity does not possess any dip changes and cannot be determined from arrow plots. This type of unconformity may often be recognized on the electrical images.

Classification of Unconformities

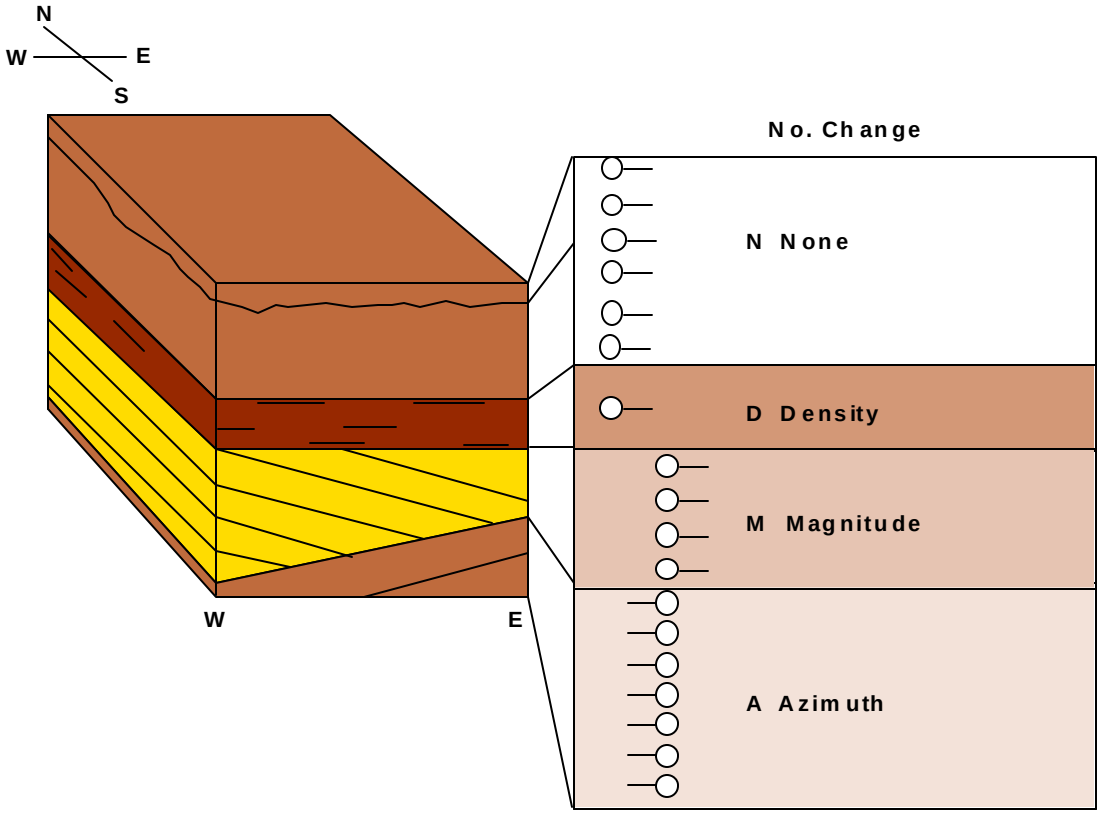

Location of Unconformities with Weathered Zones

The dip plot can accurately locate the exact depth of the structural dip change if there is no weathering at the unconformity. Weathering at unconformity surfaces can cause blank zones or dip patterns on arrow plots. The blank zones may be due to random bedding or could be caused by biogenic processes such as bioturbation. Borehole images can be used to determine the cause of the blank zone.

If the weathered zone is blank and other input (samples, etc.) is not available, then select the depth at the top of the blank zone.

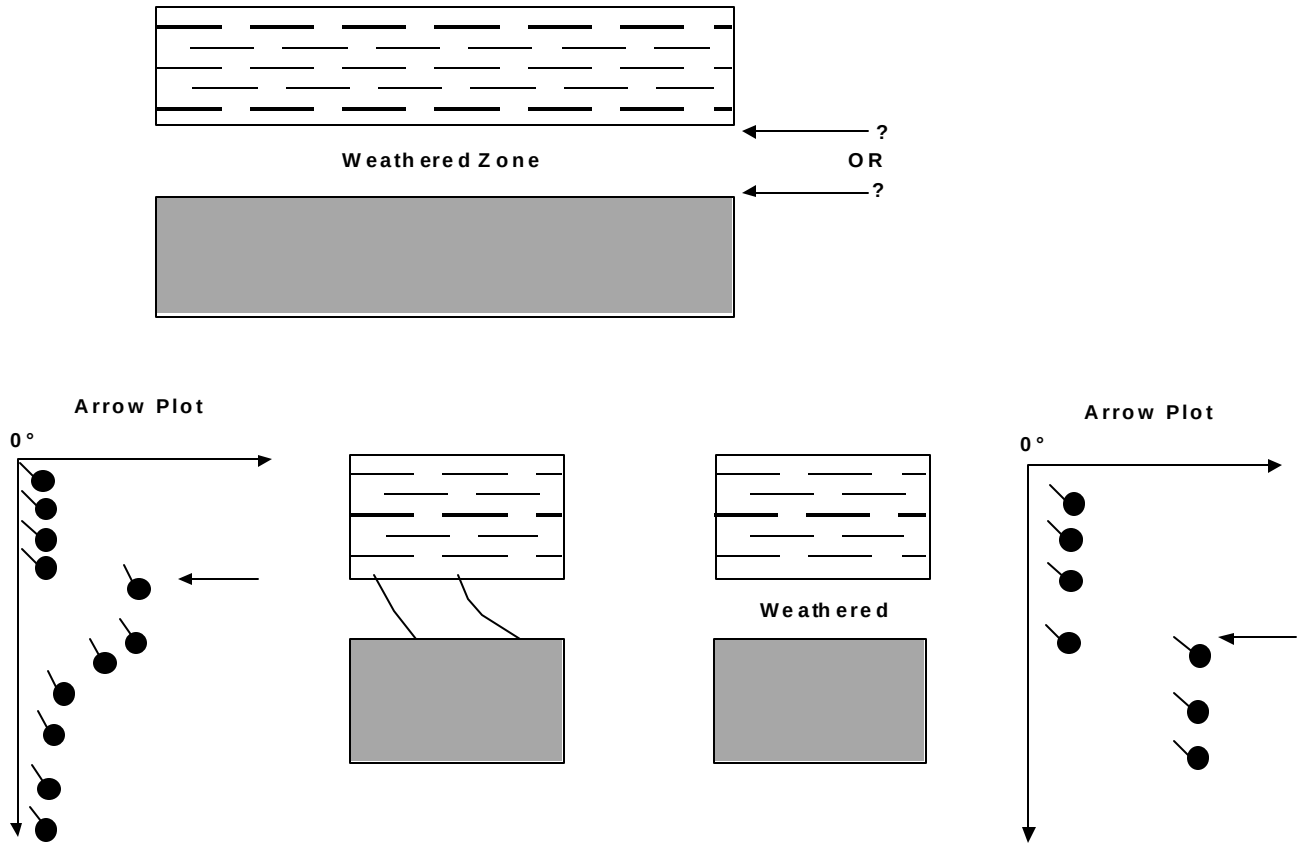

If weathered zone is blank and other input (samples etc.) is not available, then select the depth at the top of the blank zone.

Unconformity Example

The dipmeter below shows a structural dip change from 45° below 8924 ft to 10° above 8906 ft. The top of the blank zone is picked as the depth of the unconformity. This is confirmed by correlation with offset wells.

Dipmeter - 8 ft x 2 ft x 70° x 1 MSD, Unconformity

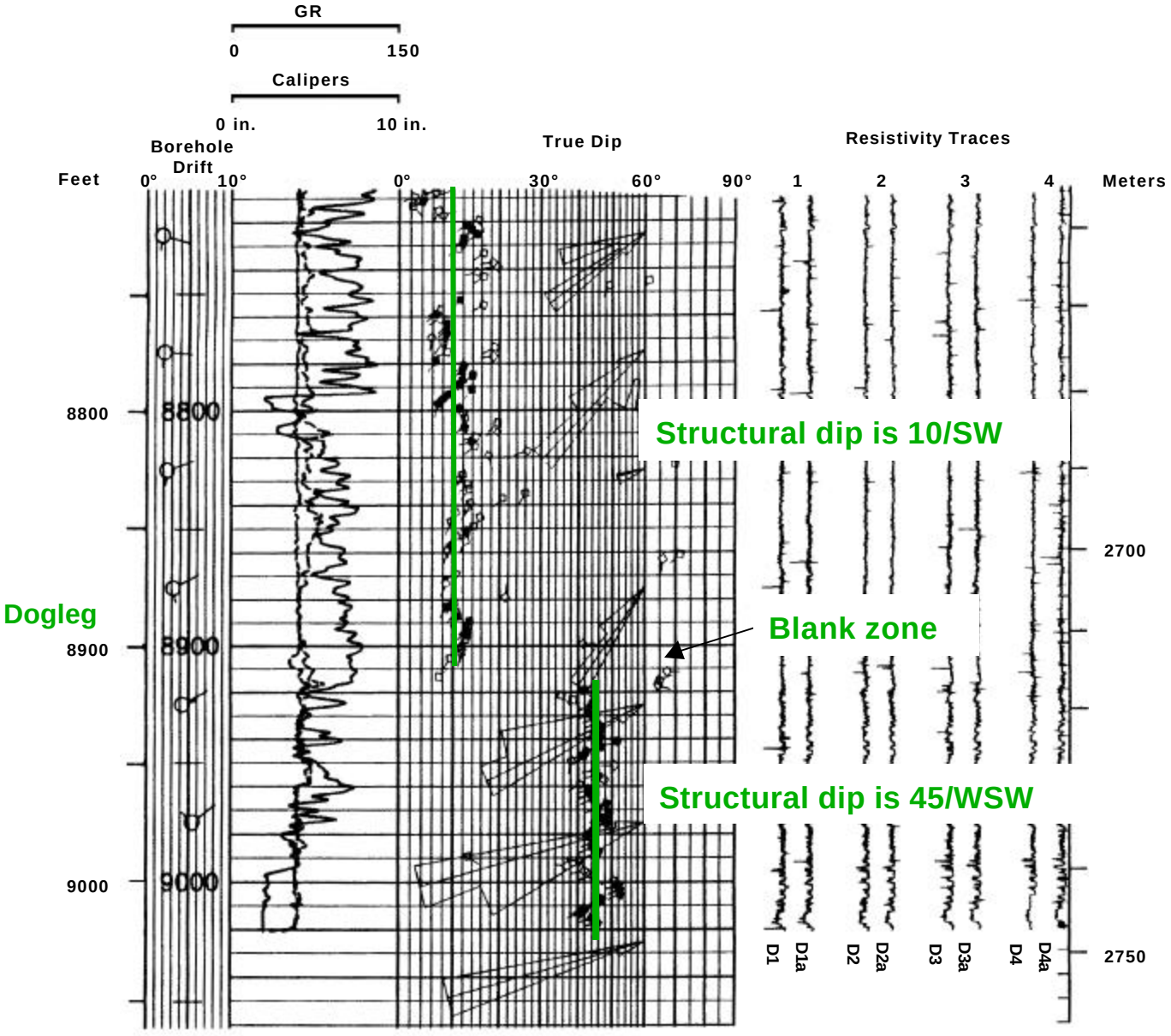

Unconformity Exercise 1

Objective: Evaluation of an unconformity from arrow plots.

Questions:
1. Depth of the unconformities are: _____
2. Is a weathered zone present? _____
3. Is a dogleg present? _____
4. What are the structural dips? _____

Dipmeter 4 ft x 2 ft x 30° x 2 MSD

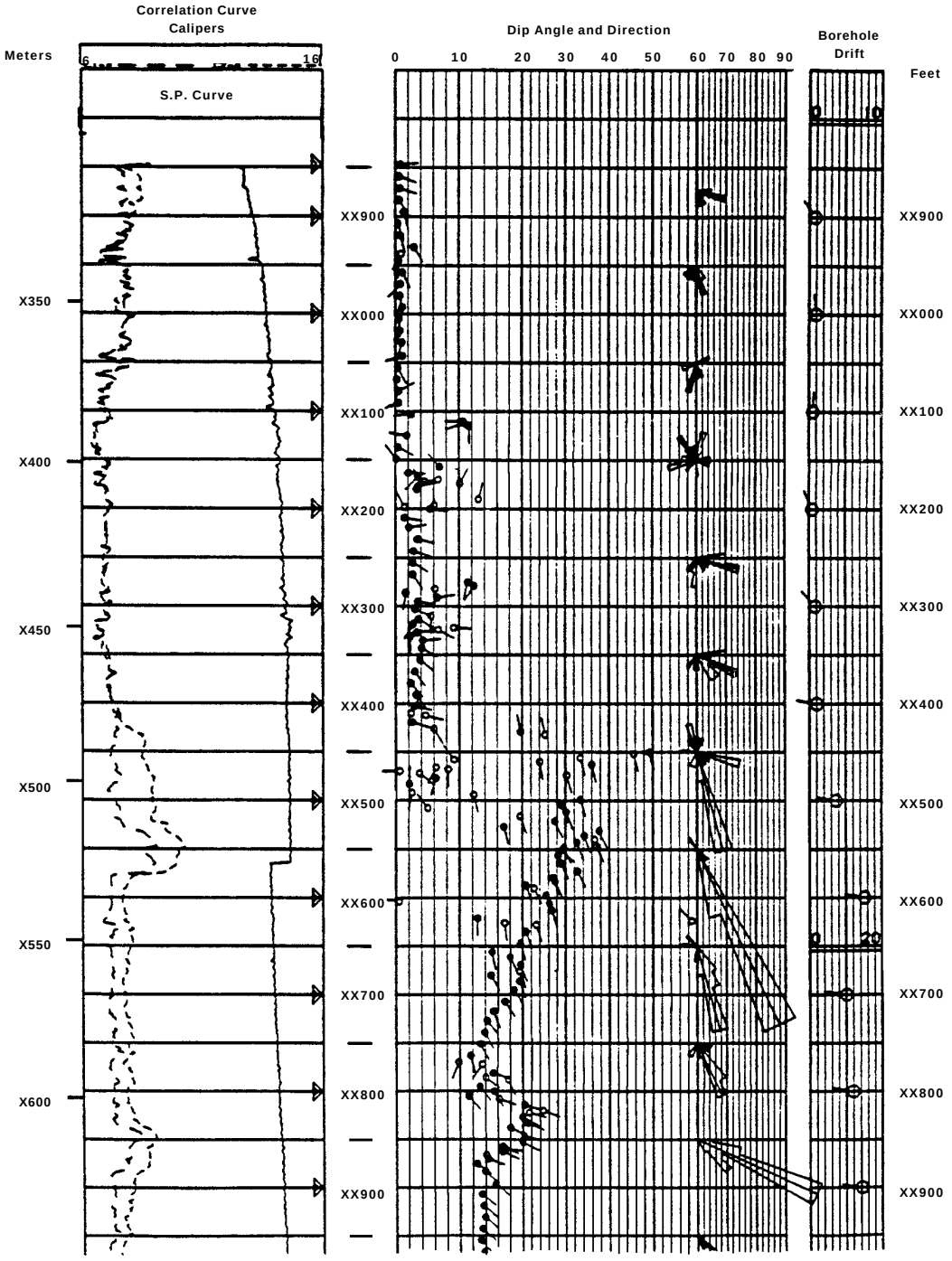

Unconformity Exercise 2

Objective: Evaluation of an unconformity from arrow plots.

Questions:

1. Depth of the unconformities are: _____
2. Is a weathered zone present? _____
3. What are the structural dips? _____

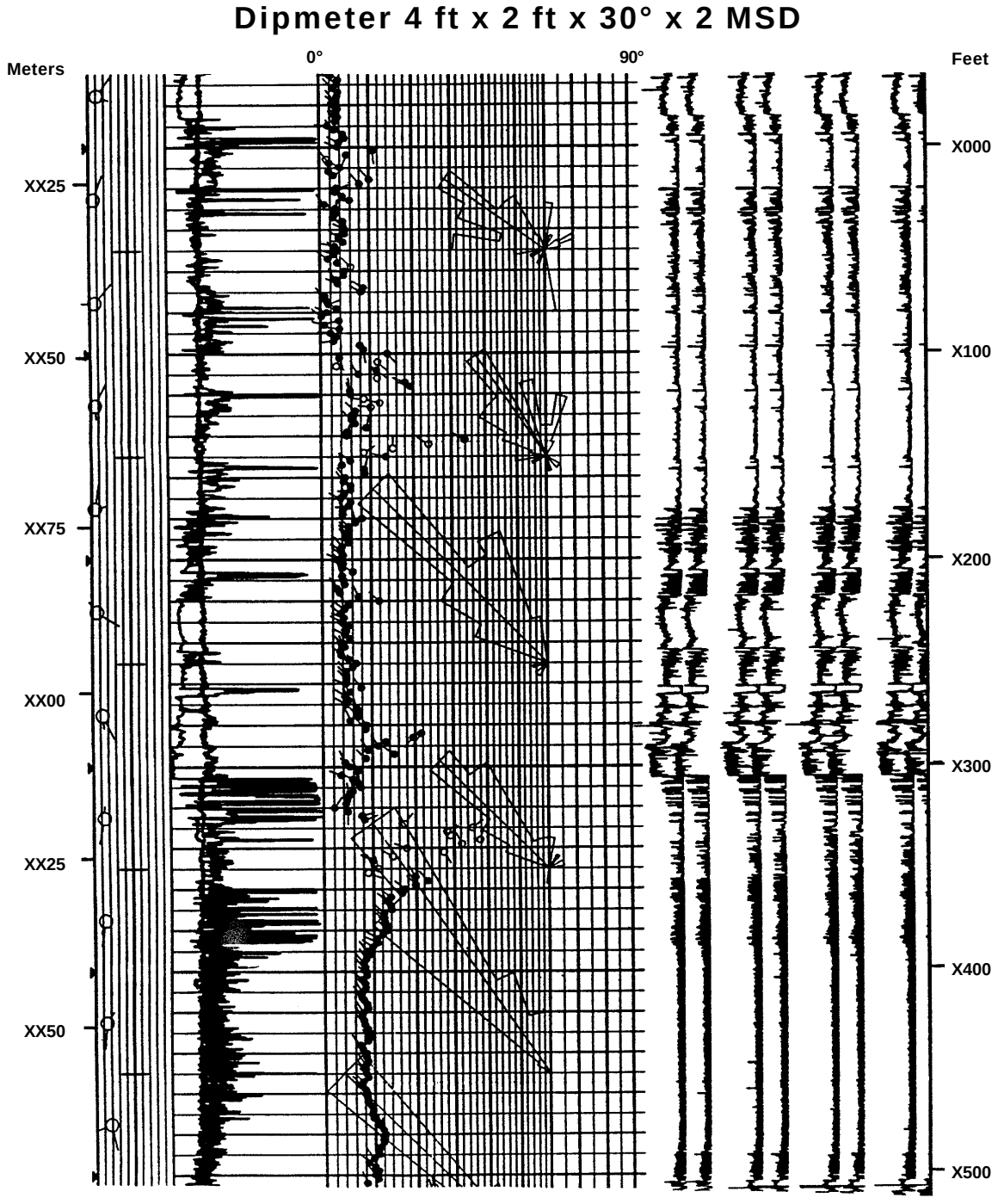

Planar vs. Non-Planar Contacts

The interface between formations at an unconformity may be either planar or non-planar. This difference is important in the recognition of some types of unconformities such as karsted surfaces. Dipmeter arrow plots cannot be used to determine this. If the contact is planar, then a good fit sine wave may be constructed through points on the erosional surface. See figure below.

Non-planar contacts are more difficult to obtain as representative dip through the contact. See figure below. One method to resolve this is to fit a sine wave through opposite pads.

All unconformity contacts must be considered as local events. This should not be extrapolated to any great extent. Structural dip above and below the contact may be used to define the strike of the unconformity.

Unconformity Contacts

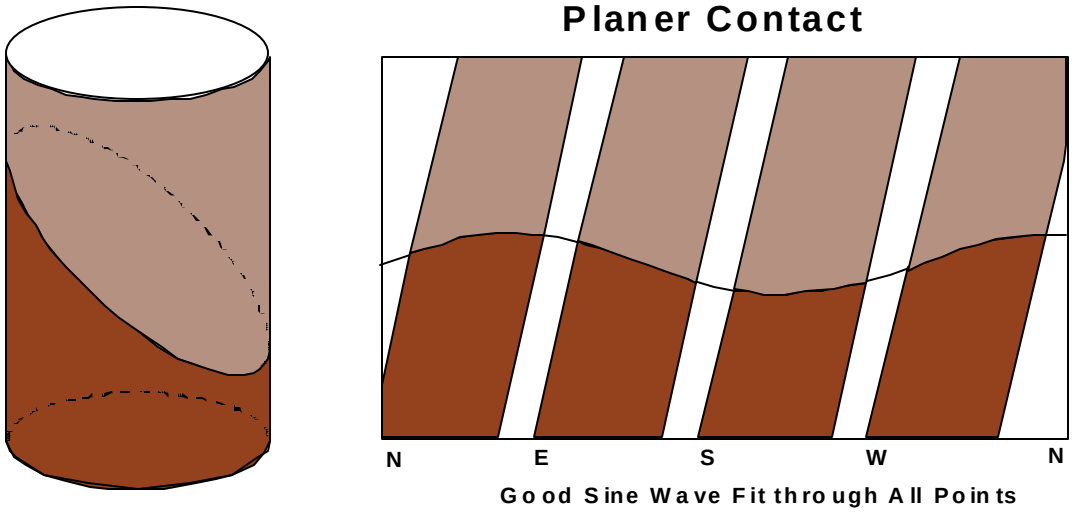

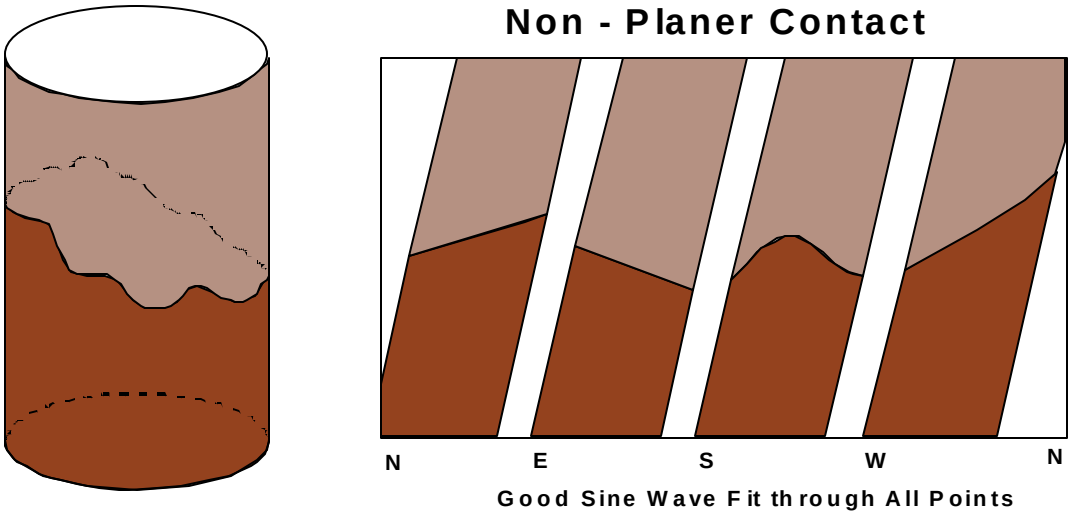

Unconformity Exercise 3

Objective: Evaluation of an unconformity from arrow plots and electrical images.

Questions:

1. Depth of the unconformities are: _____
2. Is the unconformity surface planar? _____
3. What are the structural dips? _____

Sand/Shale

Electrical Images

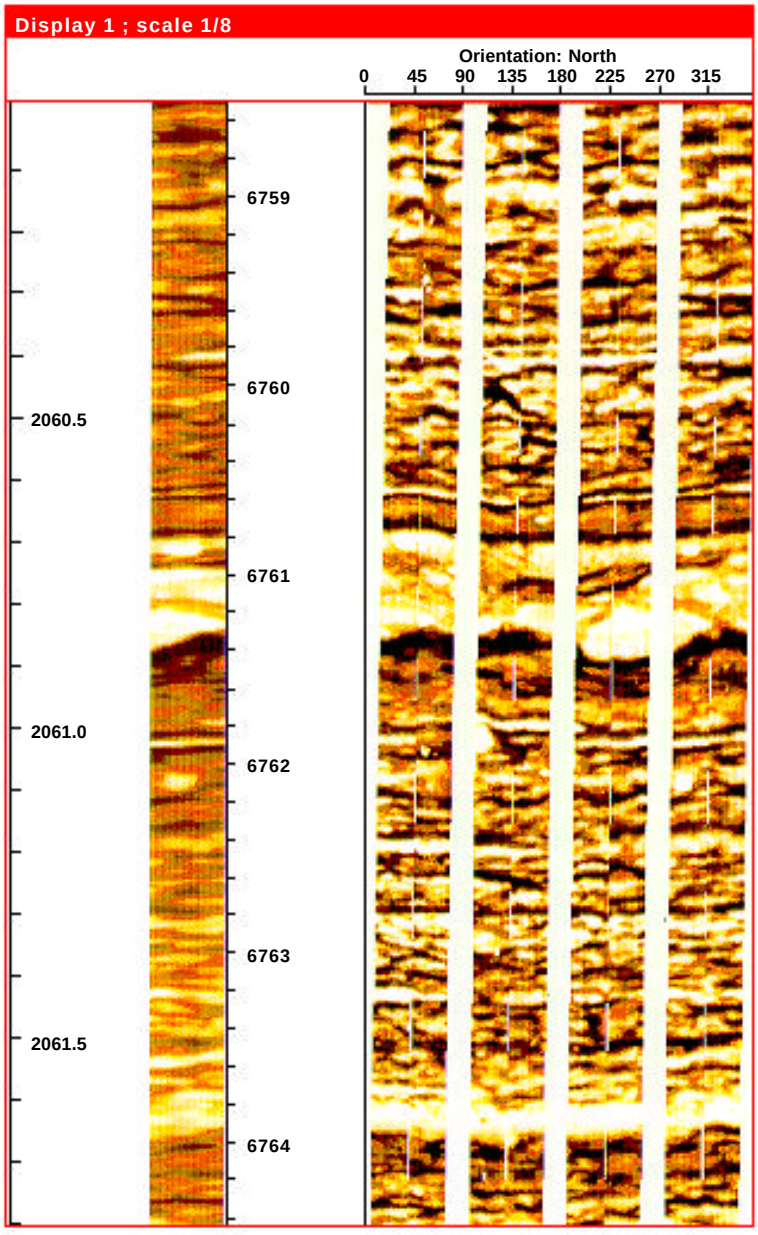

Dipmeter
4 ft x 2 ft x 30° x 2 MSD

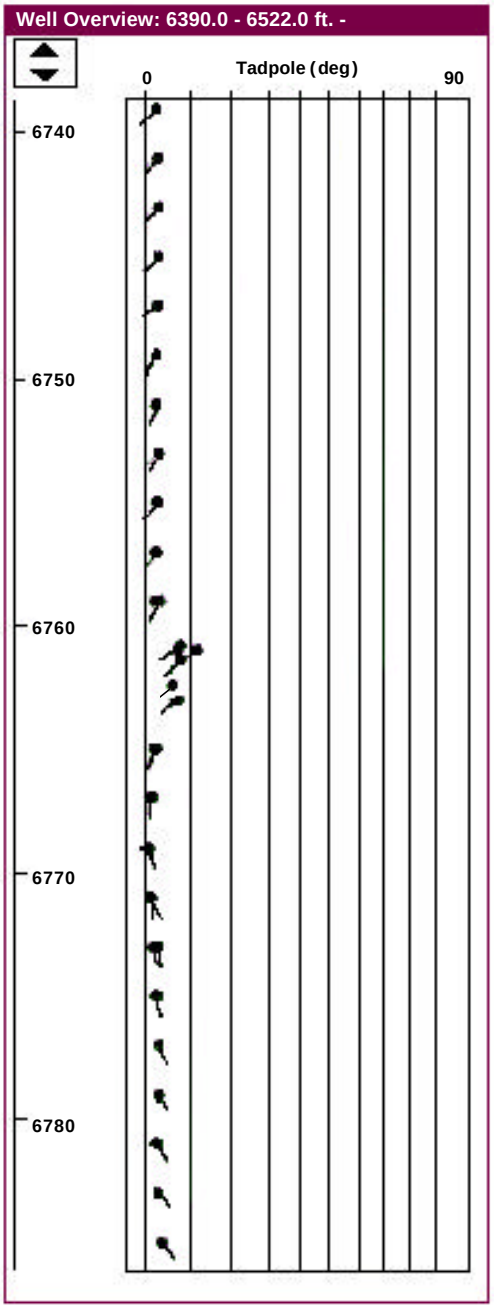

Unconformity Exercise 4

Objective: Classification of contacts from electrical images.

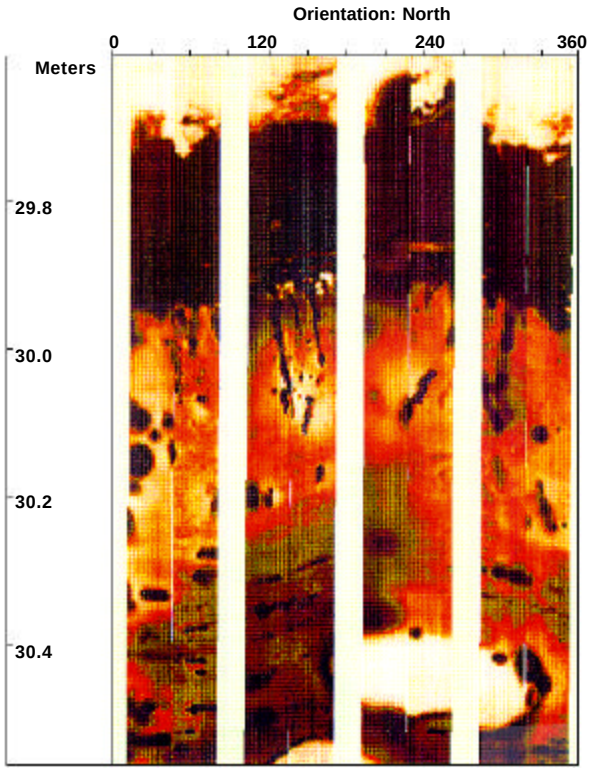

A. _____

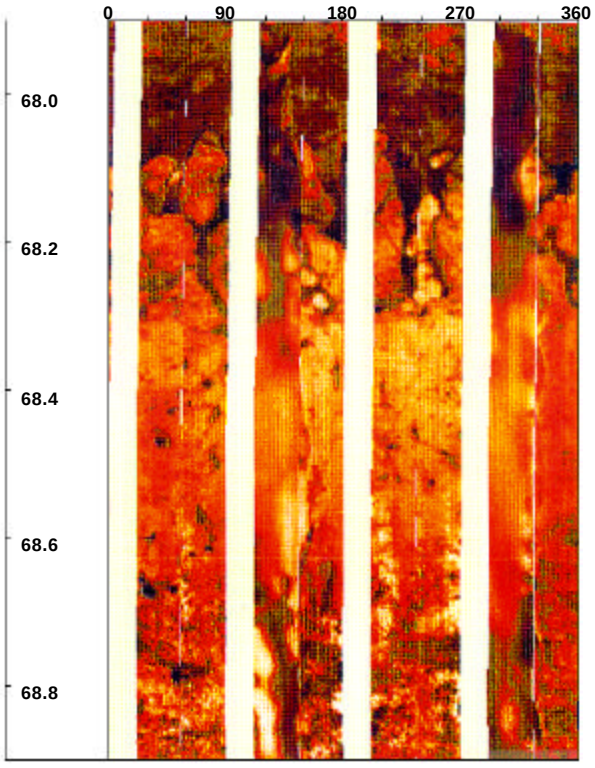

B. _____

Unconformity Exercise 5

Objective: Evaluation of unconformities.

Geological background: Pennsylvanian.

Available Data: Electrical images and dipmeter.

Questions:

1. What is the structural dip?_____

2. Interpret the data? _____

Dipmeter - 4 ft x 2 ft x 30° x 2 MSD

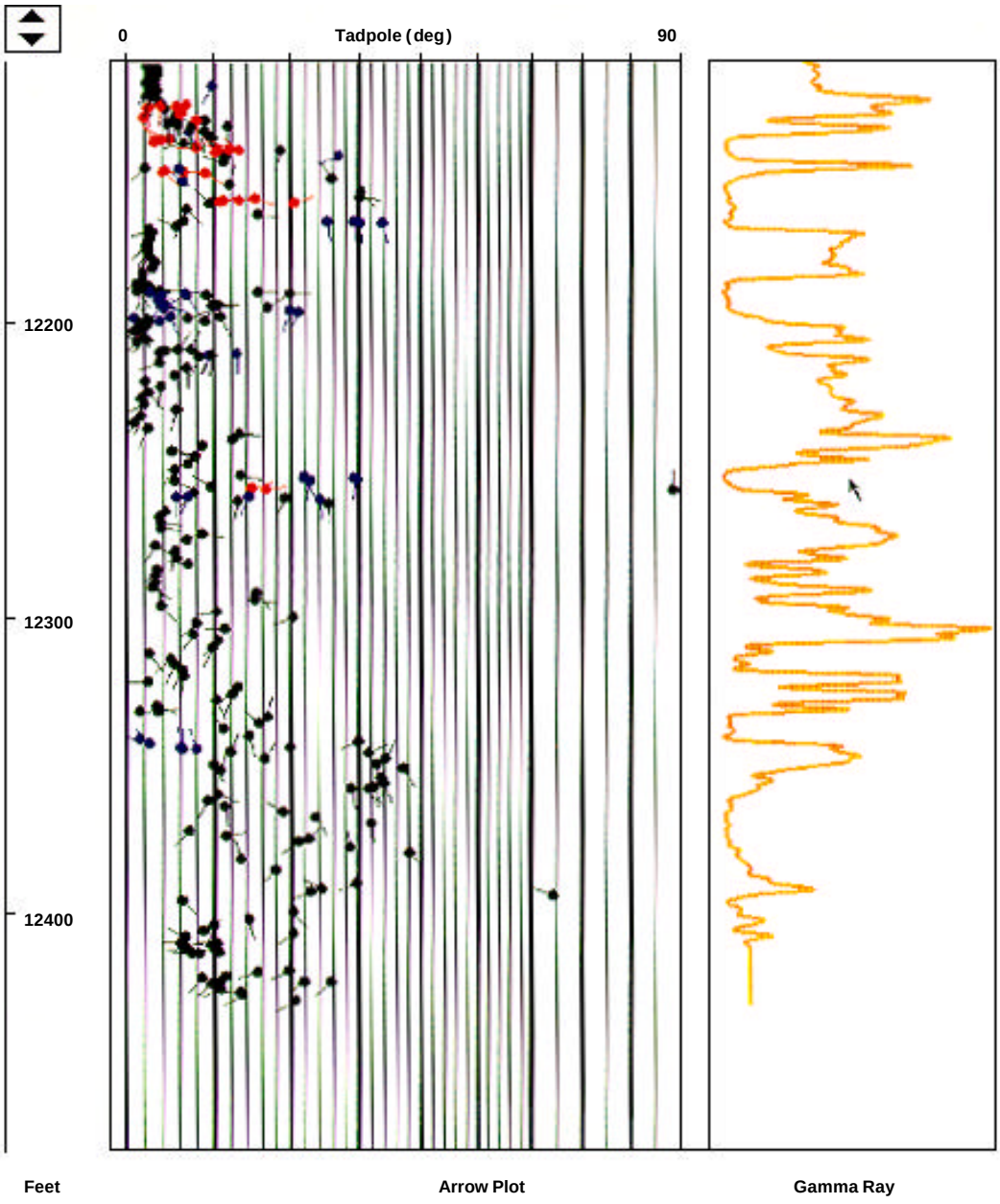

Pennsylvanian

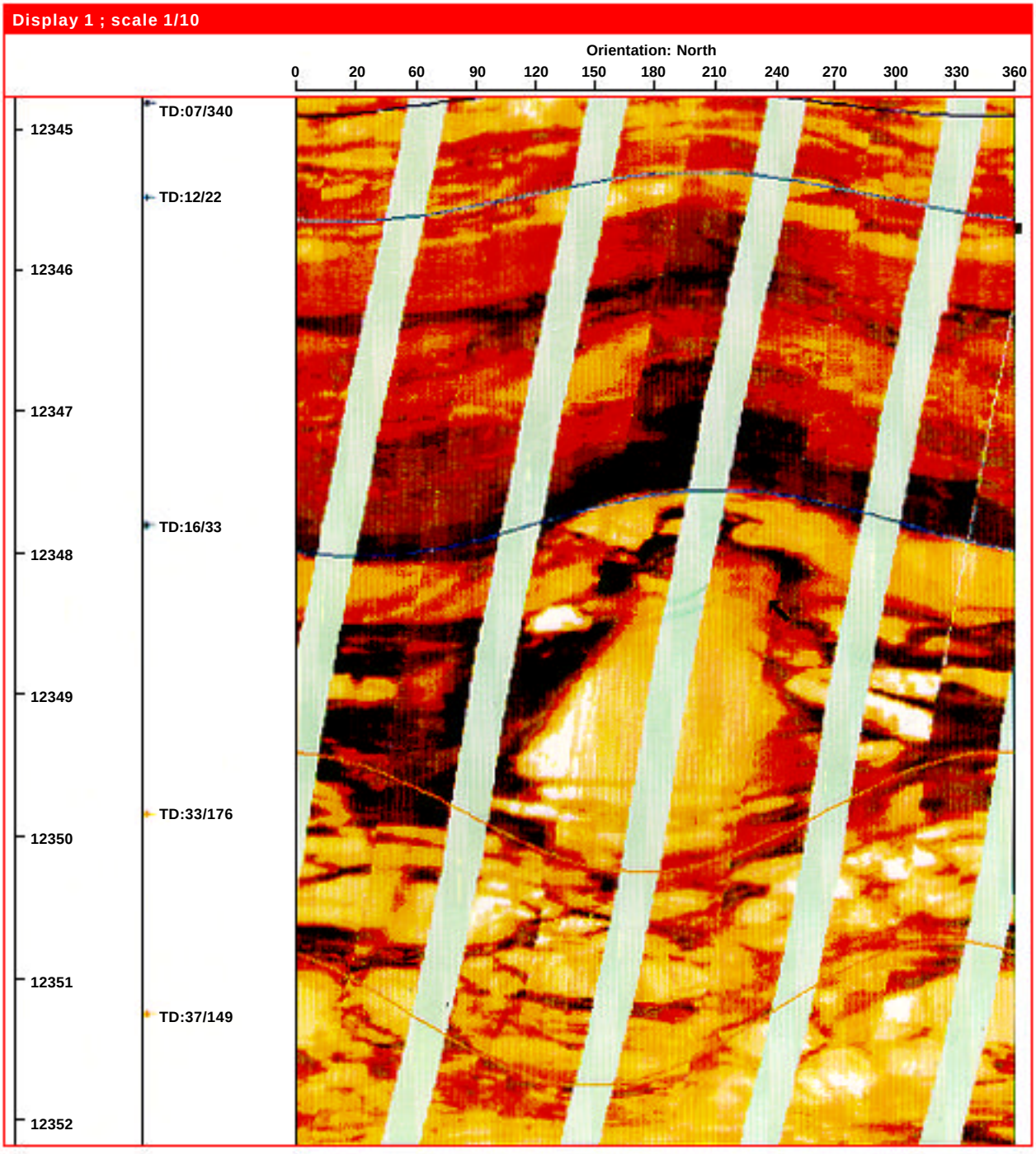

Unconformity Exercise 6

Objective: Evaluation of an unconformity from arrow plots and electrical images.

Questions:

1. Depth of the unconformities are: _____
2. Is the unconformity surface planar? _____
3. What are the structural dips? _____

_____

Dipmeter - 4 ft x 2 ft x 30° x 2 MSD

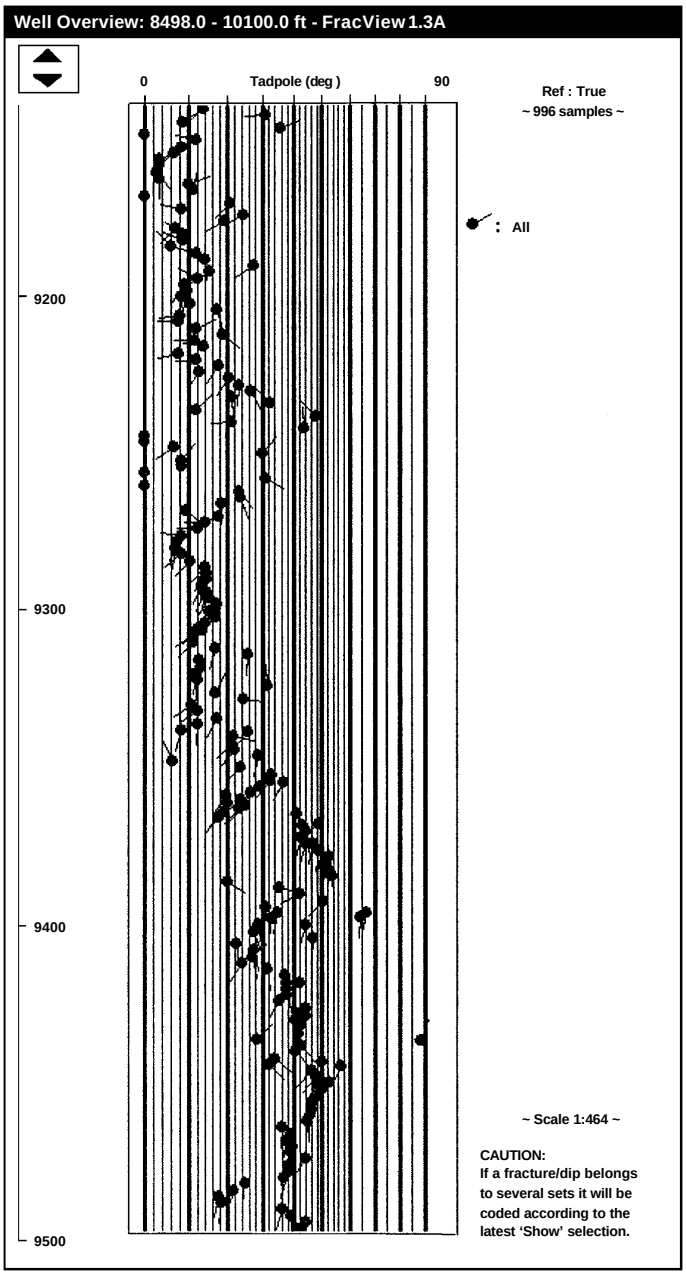

Electrical Images

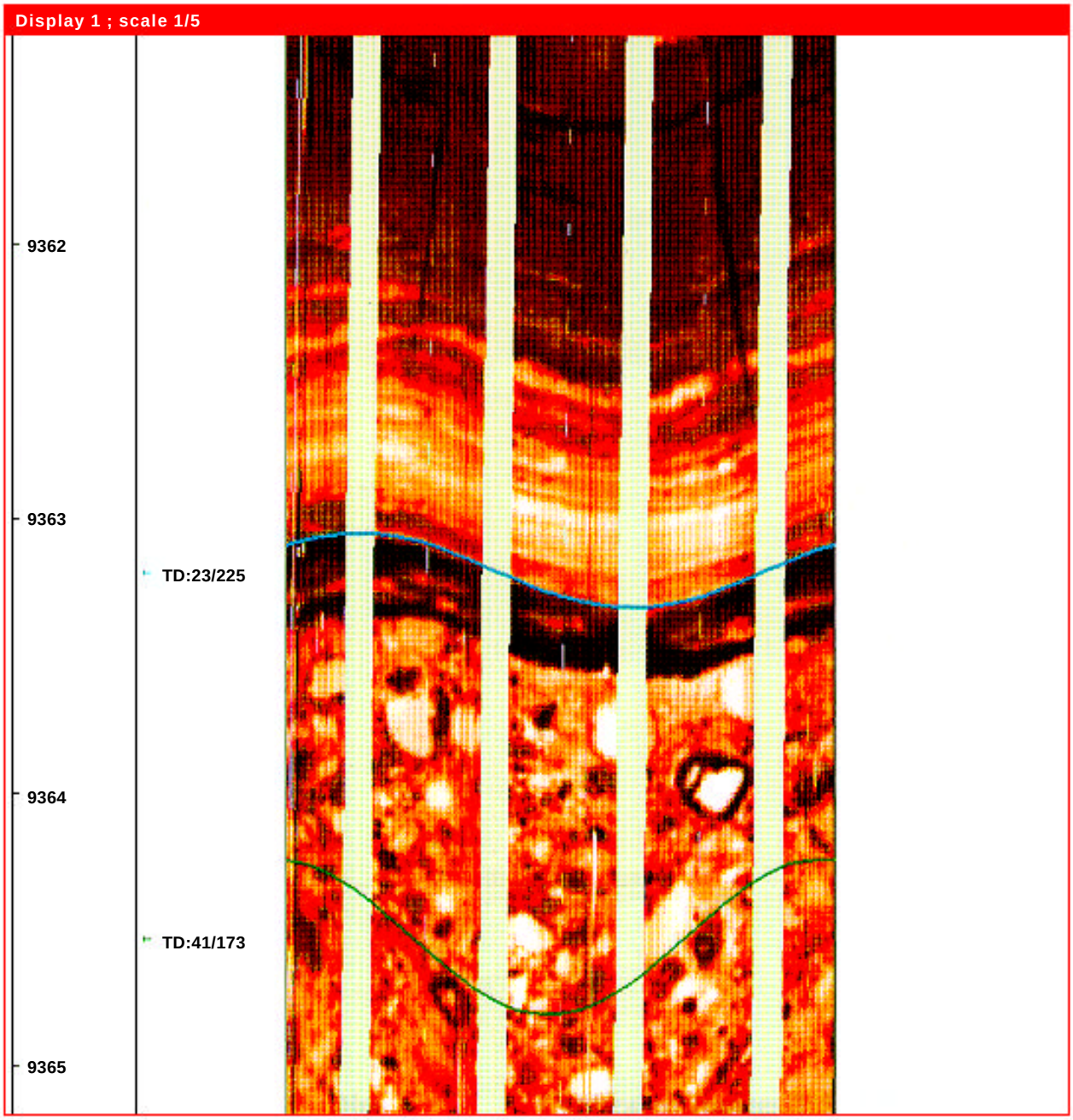

Unconformity Exercise 7

Objective: Evaluation of unconformities.

Geological background: Missing section.

Available Data: Dip plot, Electrical Images, Logs.

Questions: 1. Where is the unconformity

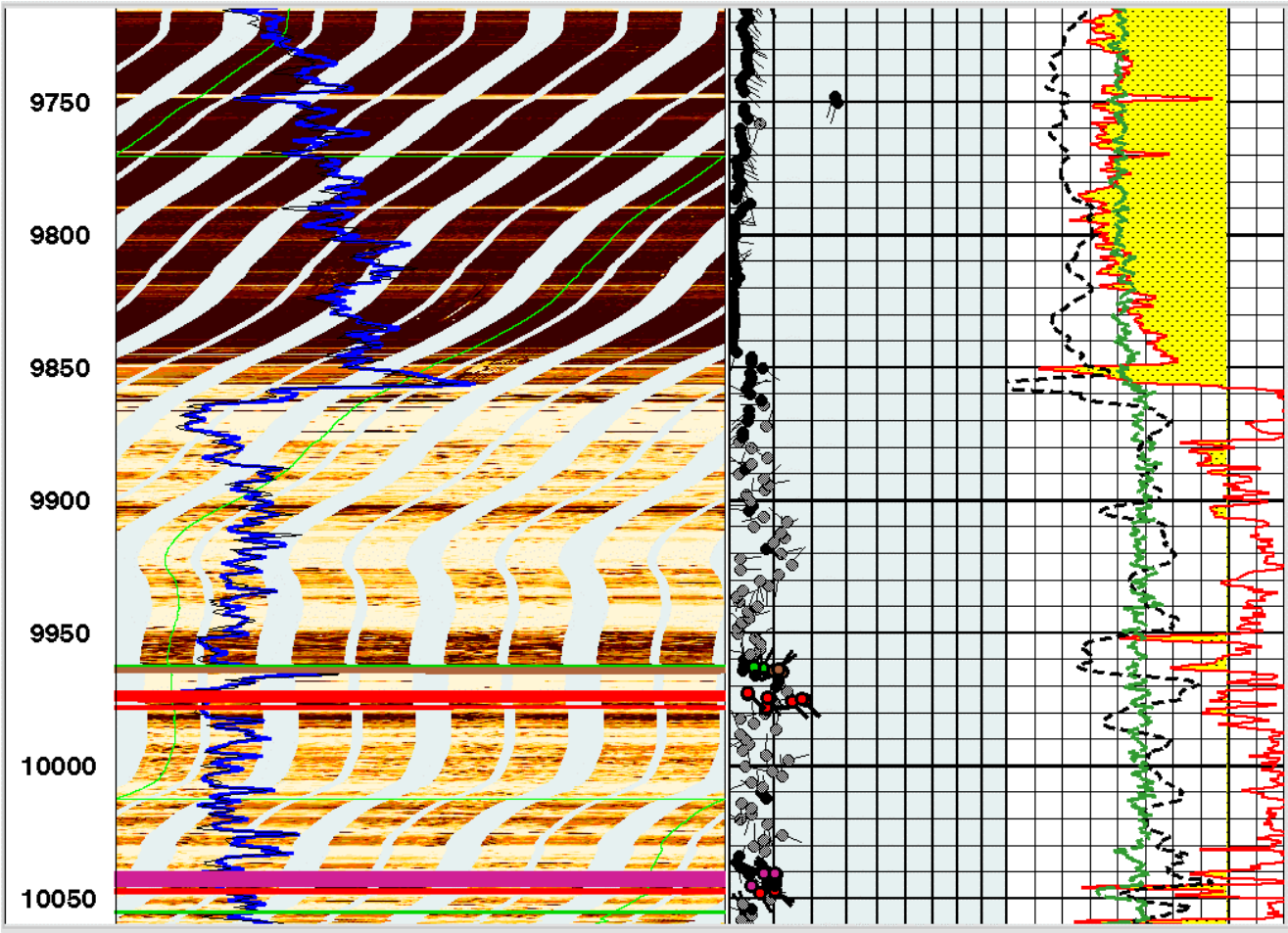

Structure and Pattern Recognition Exercise - Answers

Exercise 1

1. XX, 450 ft and at XX, 150 ft
2. Yes, at both.
3. Yes, at XX, 450 ft.
4. 14°SE from XX, 950 ft to XX, 450 ft
   3°ESE from XX, 450 ft to XX, 150 ft
   Flat above XX, 150 ft.

Exercise 2

1. X320 ft and X095 ft
2. Yes, at both.
3. 8°NW X500 ft to X400 ft.
   4°NW X320 ft to X150 ft.
   3°NW X095 ft to X960 ft.

Exercise 3

1. 6761-1/2 ft.
2. No, the surface is non-planar.
3. The structural dip above the unconformity is 3°SW and is 3°SE below.

Exercise 4

A. The contact between the shale at 29.8m and the underlying sandstone contains several root traces.
   The disconformity therefore is at the top of the shale.
   Periodic exposure and inundation, bioturbation, burrowing, all indicate a shallow marine environment of deposition most likely in a tidal flat setting.

B. Non-planar, No angular unconformity exists, these are desiccation cracks.

Exercise 5

1. Structural dip is 2°SW above 12350 ft.
   Structural dip is 9°SW below 12350 ft.
2. The structural dip change indicates this is an unconformity. The structural dip is higher below the change. The electrical images show a weathered unconformity at 12348 ft where the structural dip change occurs.

Exercise 6

1. 9363 feet.
2. Yes.
3. 36 degrees SSW below the unconformity and 11 degrees WSW above the unconformity.

Exercise 7

1. 9864 feet.

Faults

The Objectives of this Chapter are:

- Analysis of normal, reverse, and combination fault planes from electrical images to obtain:
  - Depth of the fault;
  - Strike of the fault;
  - Angle of the fault plane;
  - The fault model and well position relative to the fault.

Rules:

- **The depth of a fault is at the base of the breccia zone.**
- **Structural dip is usually higher above a fault.**
- **Structural dip is usually higher below an unconformity.**

Faults

Faults occur when external forces cause displacement of rock mass along a fracture plane. There are three primary fault types: normal, reverse, and lateral.

Normal faults occur when a rock mass is displaced downward along a fracture plane. Normal faults are primarily dip-slip and include fault types of rollover, growth drag, hybrid, step, and no distortion. When a borehole penetrates a normal fault, a missing vertical section will normally occur.

Reverse faults occur when a rock mass is displaced upward along a fracture plane. Reverse faults are, by definition, also dip-slip. The fault types include reverse, thrust, overthrust, flower, and no distortion. When a borehole penetrates a reverse fault, a repeated vertical section will normally occur.

Lateral faults occur when rock masses are displaced along strike with respect to each other. Lateral faults are strike-slip. The fault types include dextral and sinistral. Dextral is displacement to the right and sinistral is displacement to the left. When a borehole penetrates a lateral fault, there is no change in the vertical section.

Oblique-normal and oblique-reverse faults are a combination of dip-slip and strike-slip movements.

Rotational-slip is often coupled with vertical and strike slip in either hinge or pivot faults.

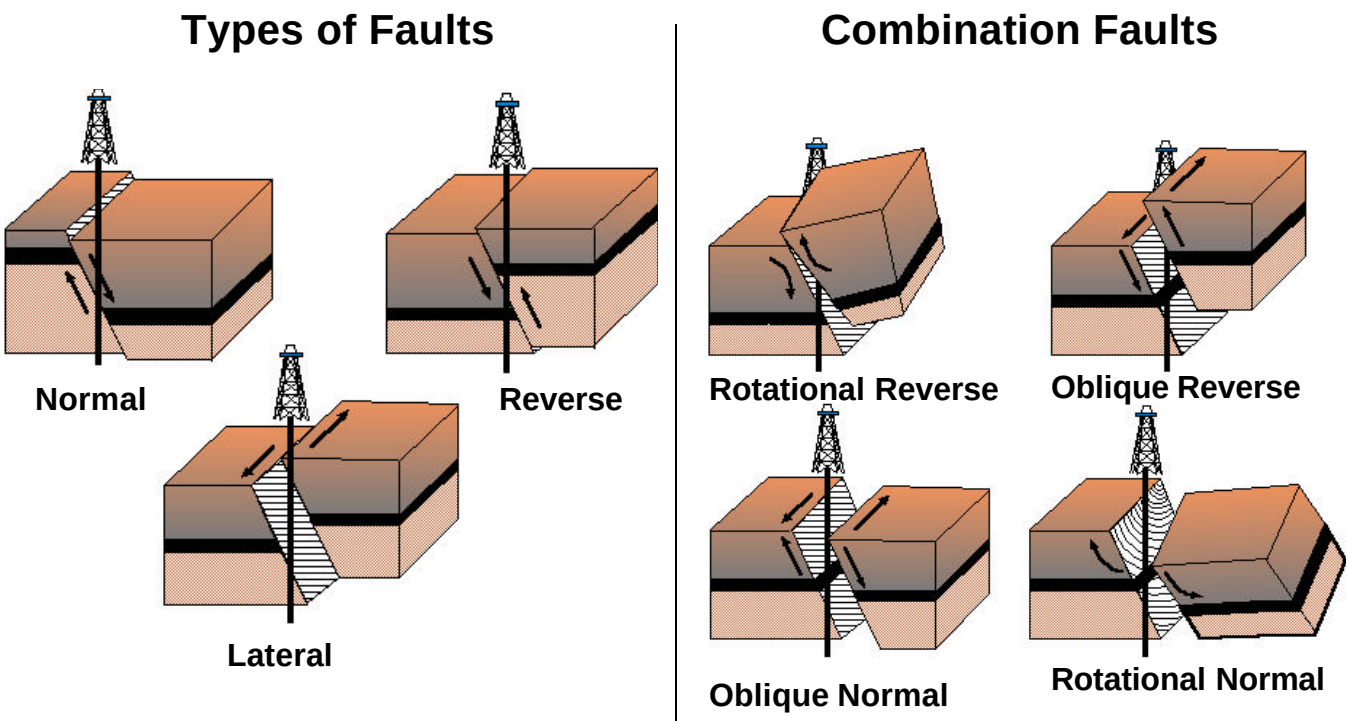

Objectives of Fault Analysis

The primary objective of fault analysis by formation imaging is the evaluation of the fault plane and bedding place distortion surrounding the fault. The following parameters can be determined independent of the fault model:

- Depth the borehole intersects the fault plane
- Strike of the fault
- Angle of the fault plane
- Distortion of the adjacent fault blocks

A fault breccia zone may occur in many faults. The base of the breccia is defined as the depth of the fault. Strike of the fault is perpendicular to the fault azimuth. (Add ±90 degrees to the fault plane azimuth.) The angle of the fault is the dip computed at the fault plane. Mega-red and blue patterns computed from the electrical images or a dipmeter are used to determine the distortion of the adjacent fault blocks.

A normal fault and a reverse fault may exhibit the same fault plane and distortion characteristics. An outside input such as local geology or log correlation's is required to determine whether there is missing or repeated section in order to define the fault model.

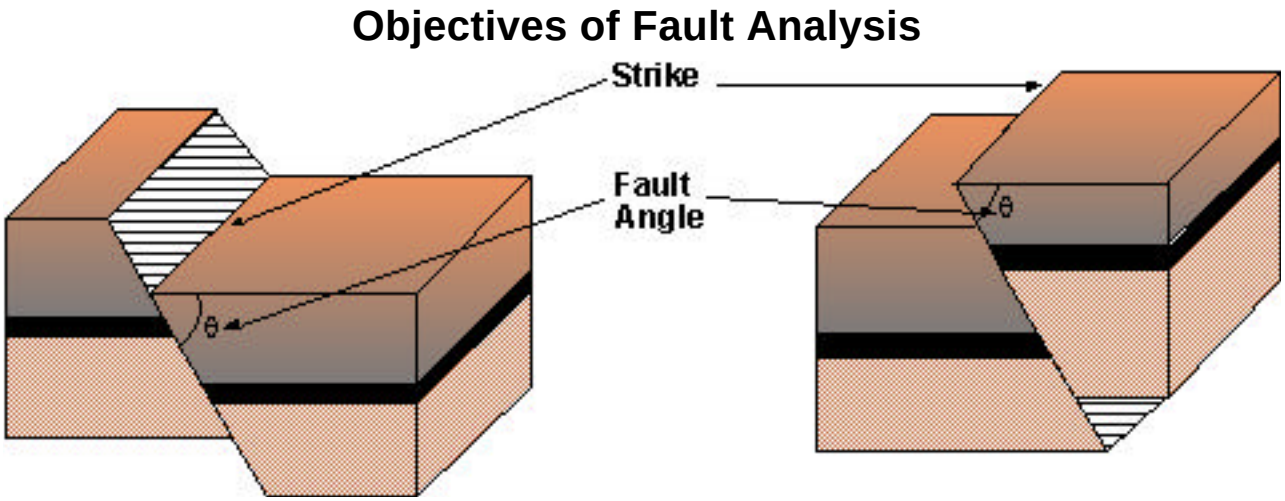

- Fault Plane Analysis: (From Images)
  - Depth of fault
  - Strike of fault
  - Angle of fault
  - Azimuth of fault
  - Sealing of fault
- Fault Model
  - Geologic Input
  - Missing Section
  - Repeated Section
  - No change of section
  - Adjacent bedding plane analysis: (from dips)
  - Upthrown block
  - Downthrown block

Fault Plane Analysis

A fault plane will have the appearance of a very large fracture. The distortion of the beds may conform to the fault plane or there may be no distortion of the surrounding beds. Bedding planes will not correlate across a fault but will correlate across a fracture.

The base of the fault plane is the depth of the fault. A best fit sinewave at the base or top of the fault plane will yield the fault azimuth and angle. Strike of the fault is perpendicular to the fault azimuth. The fault angle is the angle between the fault plane and horizontal.

A resistive (white) fault plane is normally a sealing fault while a conductive (black) fault plane may be sealing or non-sealing. It may be difficult to observe a very thin fault plane. However, the same halo effect as observed in fractures also is apparent in mineral-filled fault planes.

• Identification

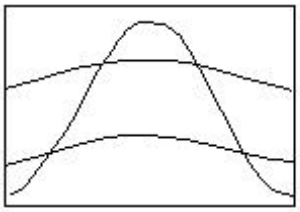
Fracture

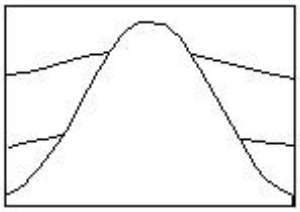
Faulting

• Depth of the fault is the base of the fault zone.
• Strike of the fault is perpendicular to the fault plane azimuth.
• Fault angle is the angle between horizontal and the fault plane.

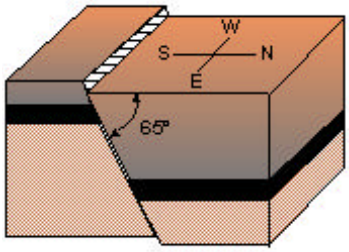

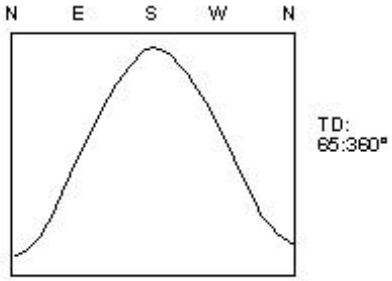

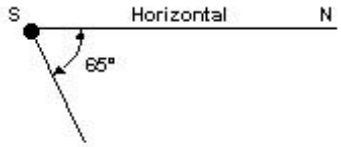

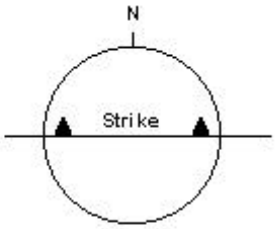

• Sealing of the fault plane.

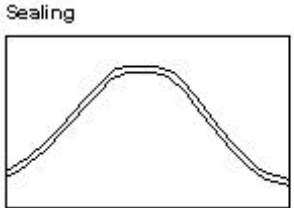

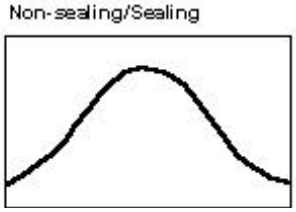

Fault Plane Analysis Example

Objective of this Exercise: Analysis of a fault plane.
Geological Background: This well has repeated section.
Available Data: Equalized Images.
Questions:

1. Depth of fault? **24.0 M, although several other faults were present above this level.**
2. Strike of fault? **NNE-SSW**
3. Fault Angle? **Approximately 70°SE**
4. Sealing fault? Why? **Yes - resistive fault plane.**

Fault - Repeated Section

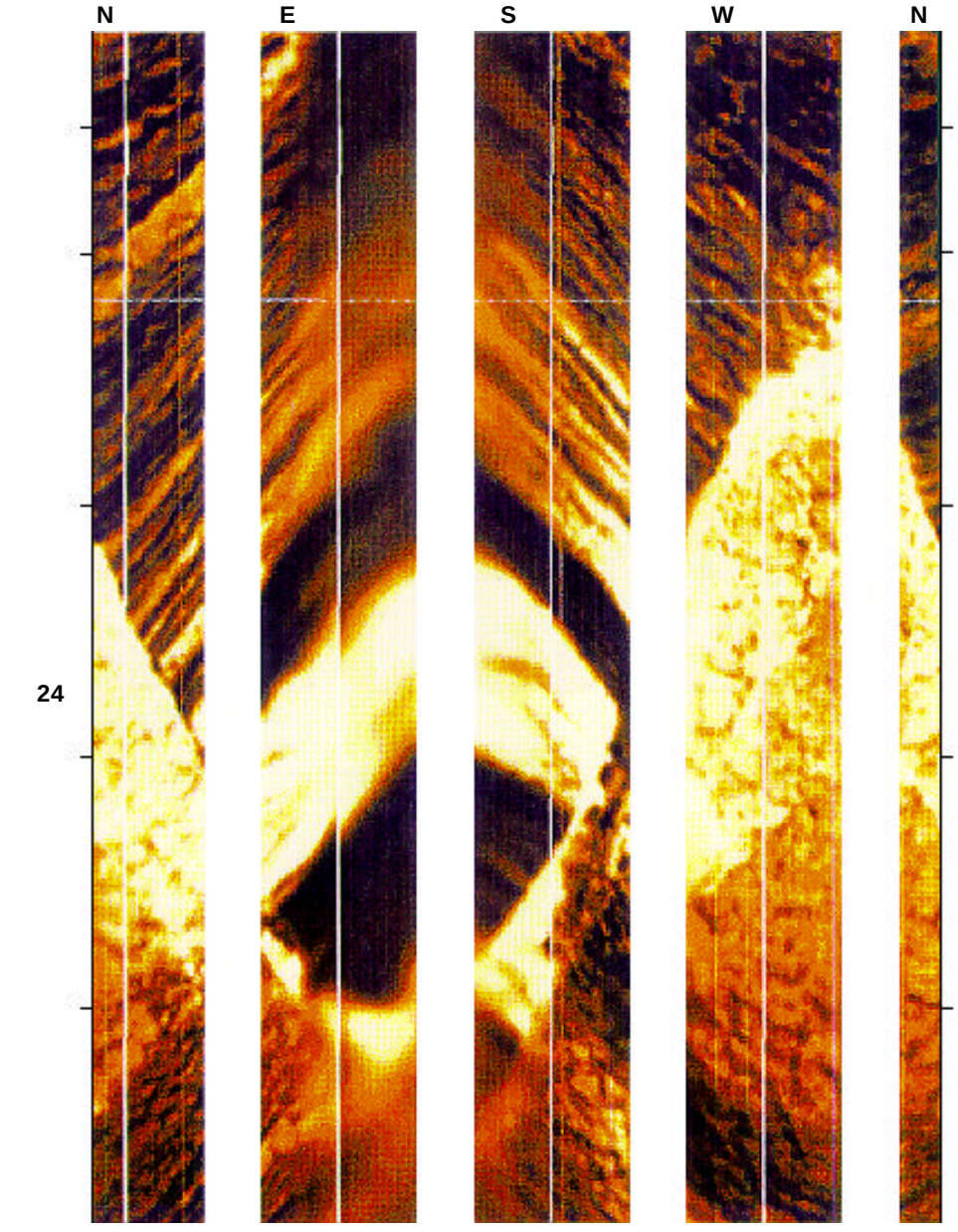

Faults - Exercise 1

Objective of this Exercise: Analysis of a fault plane.
Geological Background: Sand/shale with 208 ft.(63m) missing section.
Available Data: Equalized Images.
Questions:

1. Depth of fault? _____
2. Strike of fault? _____
3. Fault Angle? _____
4. Sealing fault? Why? _____

Sand/Shale - 208 ft.(63m) of Missing Section

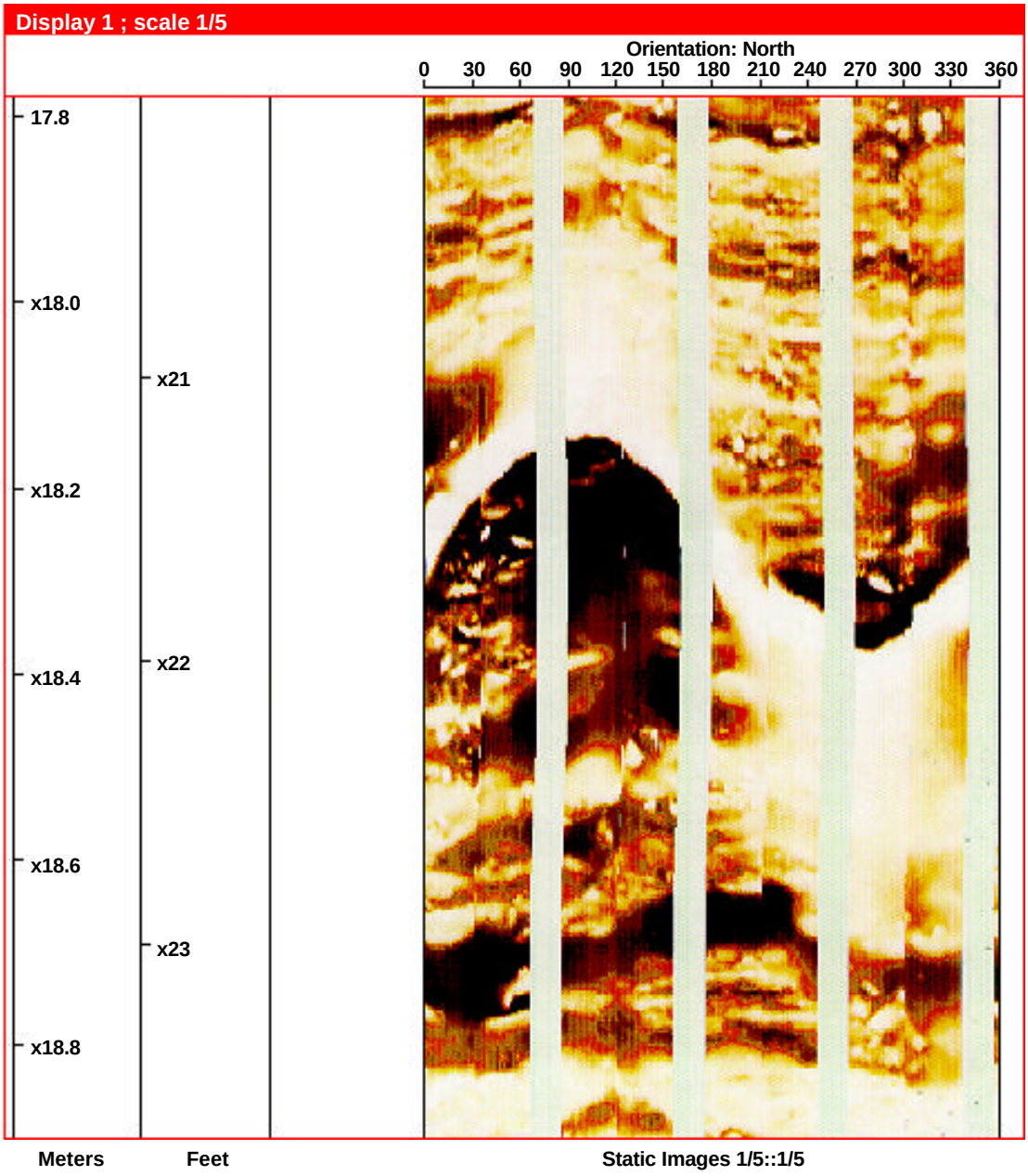

Faults Exercise 2

For the following faults:(all are static images)

1. Strike?: a._____b._____c._____d._____

2. Sealing?: a._____b._____c._____d._____

3. Fracture?: a._____b._____c._____d._____

A.

Mesozoic Sand/Shale-
120 ft. (36.5m) Missing Section

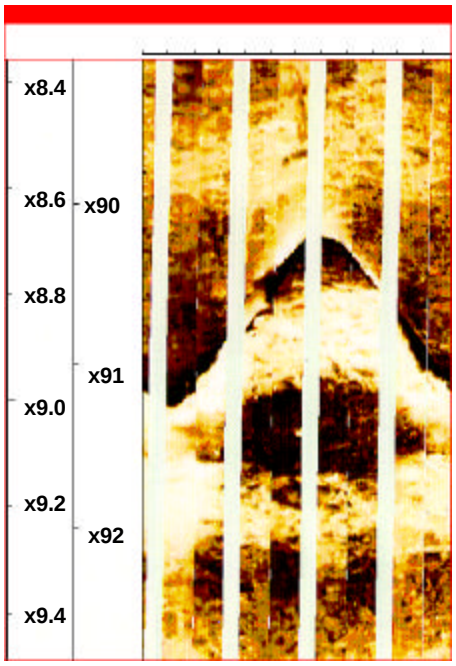

B.

Pennsylvanian Sand/Shale -
0 ft.(0m) Missing Section

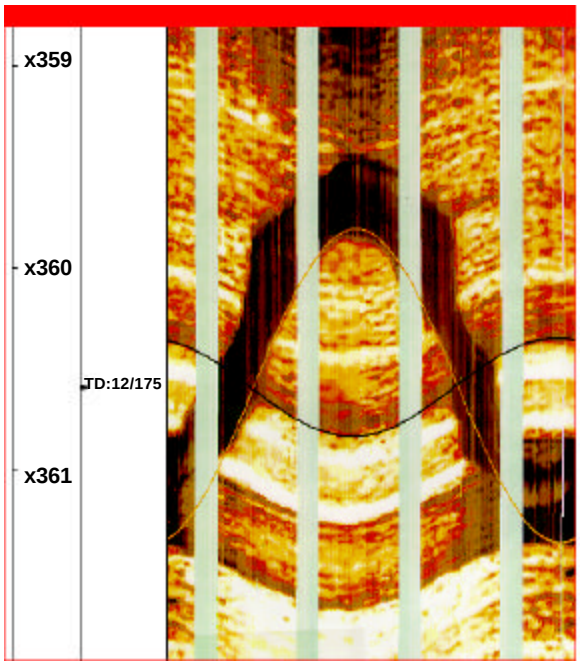

C.

Mesozoic Sand/Shale -
70 ft.(21m) Missing

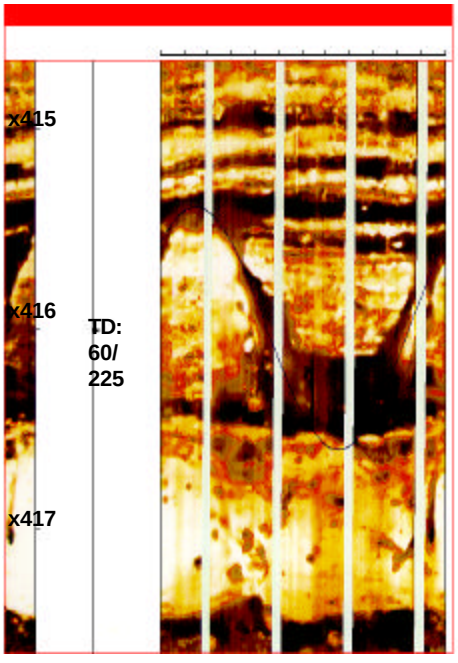

D.

Mesozoic Sand/Shale -
220 ft.(67m) Missing

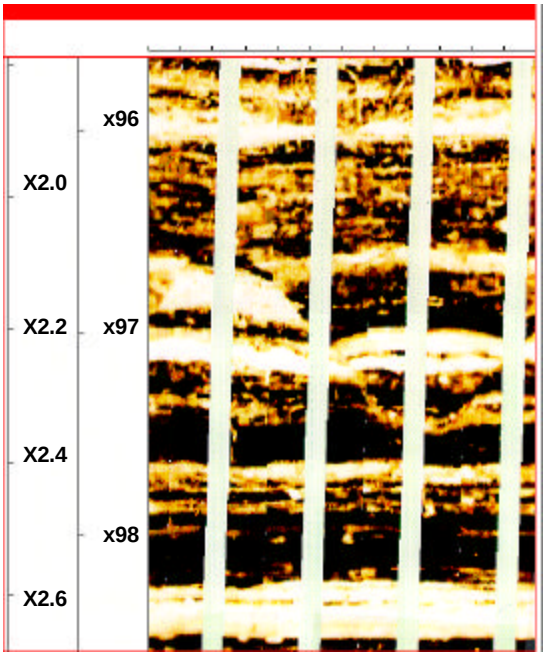

Faults - Exercise 3

Objective of this Exercise: Fault plane analysis and offset location.

Geological Background: Missing pay sand; 95 feet missing section; An offset well located 1/2 mile to the SW has produced 5 BCF from the pay sand.

Available Data: Electrical Images.

Questions:

1. Depth of fault?
2. Strike of fault?
3. Fault Angle?
4. Sealing fault?
5. If the sand has a NE-SW trend, then what is the optimum offset direction?
6. How far?

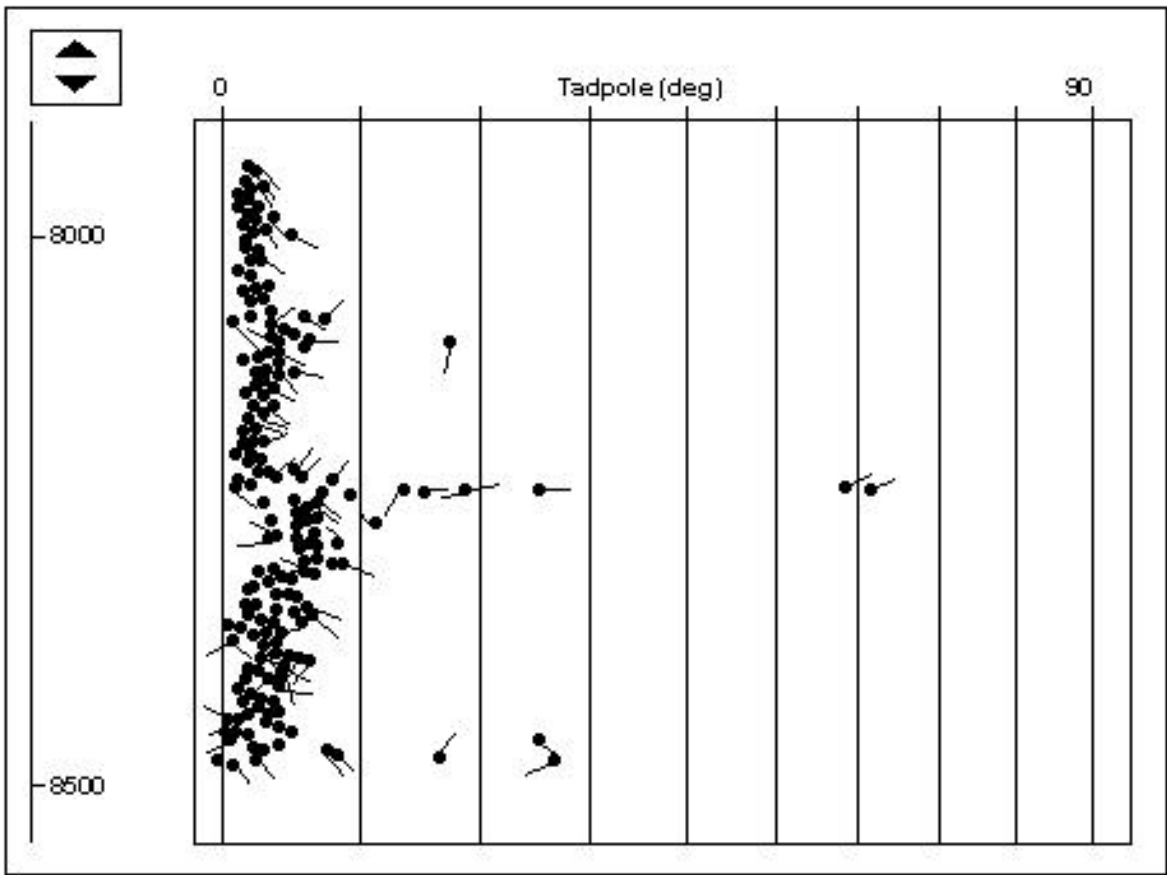

Missing Pay Sand
(95 feet Missing Section)

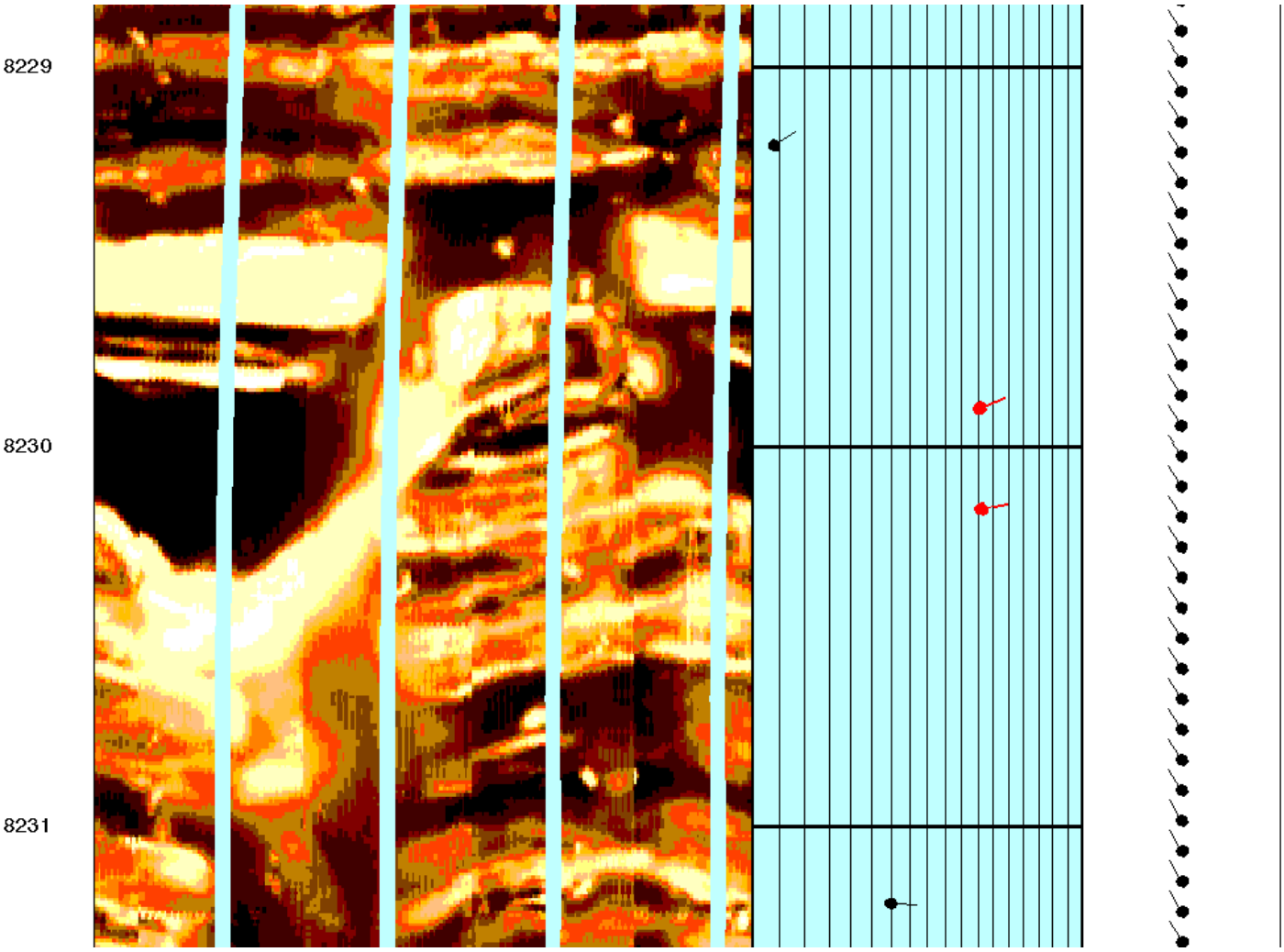

Buried Faults

Sealing faults may have traps either above or below the fault. Non-sealing faults may not have trapping either block since hydrocarbon migration is not blocked.

The anticlines formed by the fault distortion of bedding planes may cause trapping, but the presence of an unconformity is required in many non-sealing faults to form a trap. A fault must terminate. Some faults will gradually die out and other will extend to the surface. A vertical displacement fault which extends to the surface will cause a topographic feature. As this feature is eroded and subsequent bedding occurs, a buried fault is created.

The process is shown opposite. The fault extends to the surface. A portion of the upthrown block is removed by erosion. Subsequent bedding occurs and buries the fault. For a trap to occur, the overlying bedding must be impermeable. The process may be repeated several times.

Creation of a Buried Fault

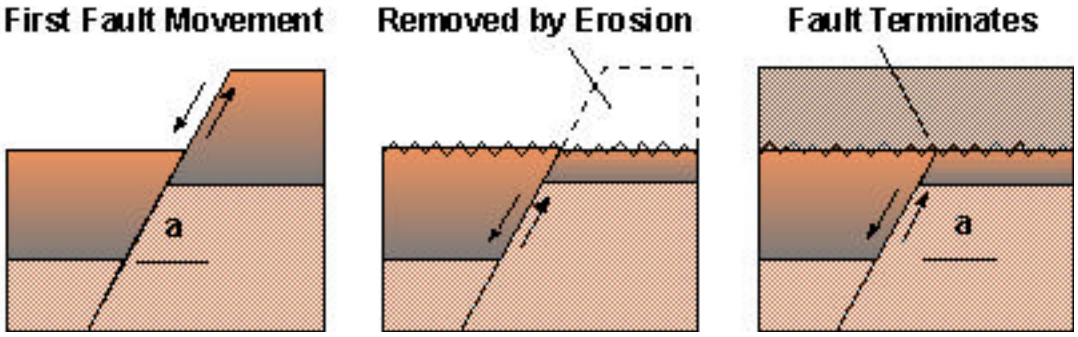

Effect of a non-sealing fault

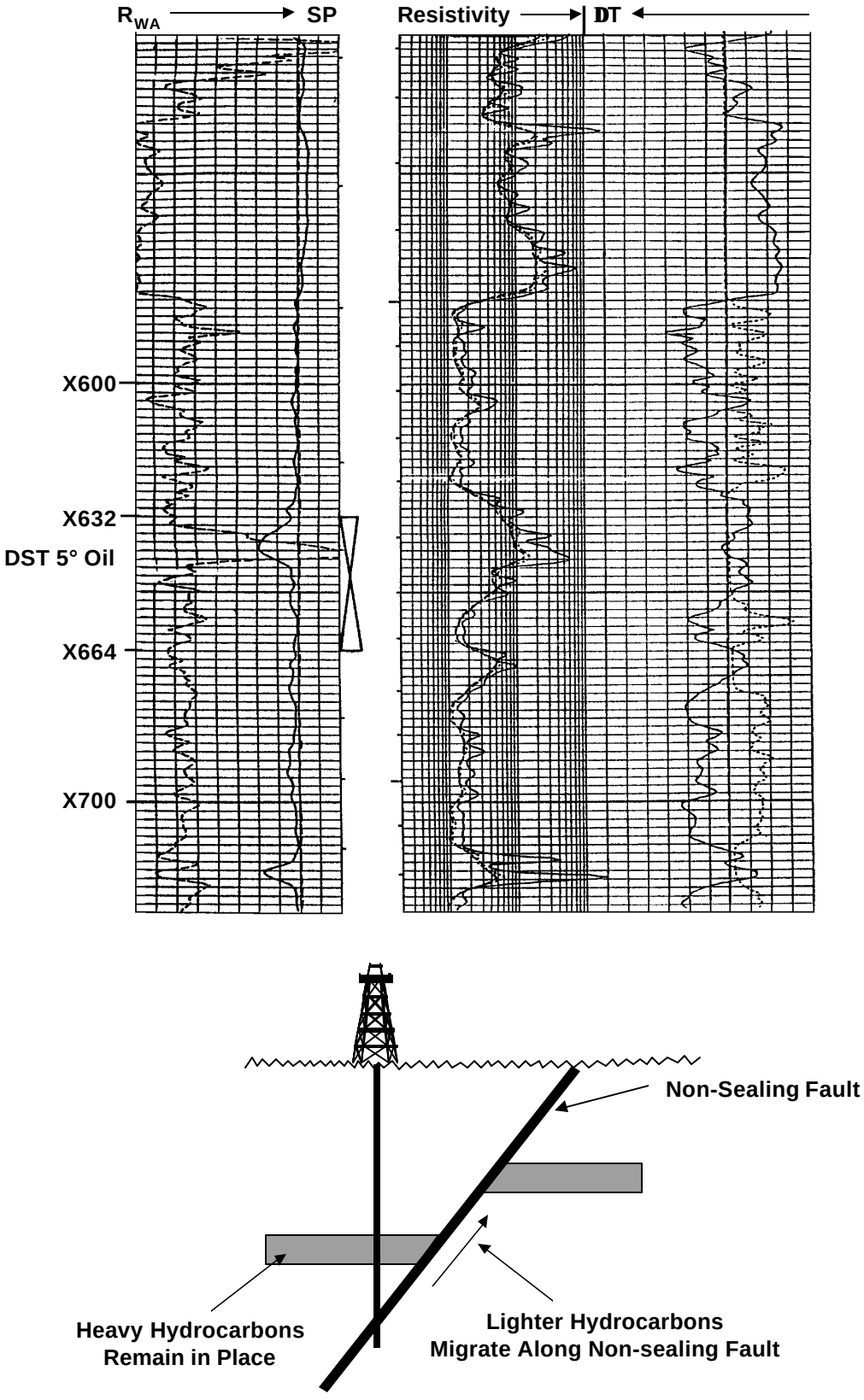

Faults Exercises - Answers

1. A. x18.2 meters/ x21.6 ft.; B. NNE-SSW C. 45° down to the WNW; D. Yes, the fault plane is resistive.

2. | | | | | |
   |---|---|---|---|---|
   | 1. Strike?: | a. WNW-ESE | b. East-West | c. NW-SE | d. North-South |
   | 2. Sealing? | a. Yes | b. Open fracture | c. ? | d. ? |
   | 3. Fracture?: | a. No | b. Yes | c. No | d. No |

3. The depth of the fault is at 8330 ft; the strike of the fault is NNW-SSE; the fault angle is 53@N62E; the fault plane is resistive so this is a sealing fault; there are two offset directions: to the SW to sidetrack into the upthrown block or to the NE to the downthrown fault block; the distance should be at least 400 ft. to penetrate the sand in a favorable location. The sidetrack was directionally drilled 400 ft. to the NE and penetrated the downthrown fault block which was at virgin pressure.

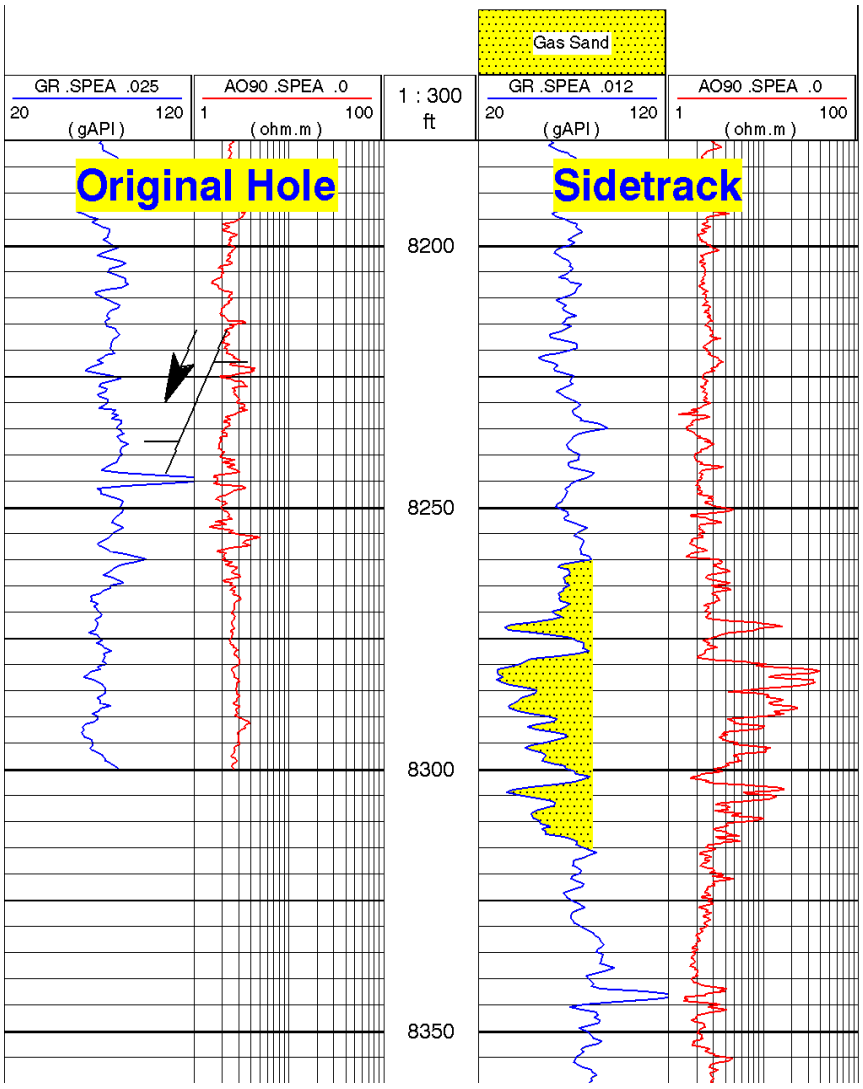

Fluvial Channels

Objectives of this Chapter are to learn the:

- Stratigraphic interpretation principles for fluvial channels. The sedimentary structures most commonly observed in fluvial channels are:
  - Current bedding, Lateral accretion, Scour surface
- These are used to determine the sand body geometry, type of channel, and the well position in the elongated sand bars of fluvial channels.

Commonly Preserved Fluvial Features and Their Associated Dip Patterns

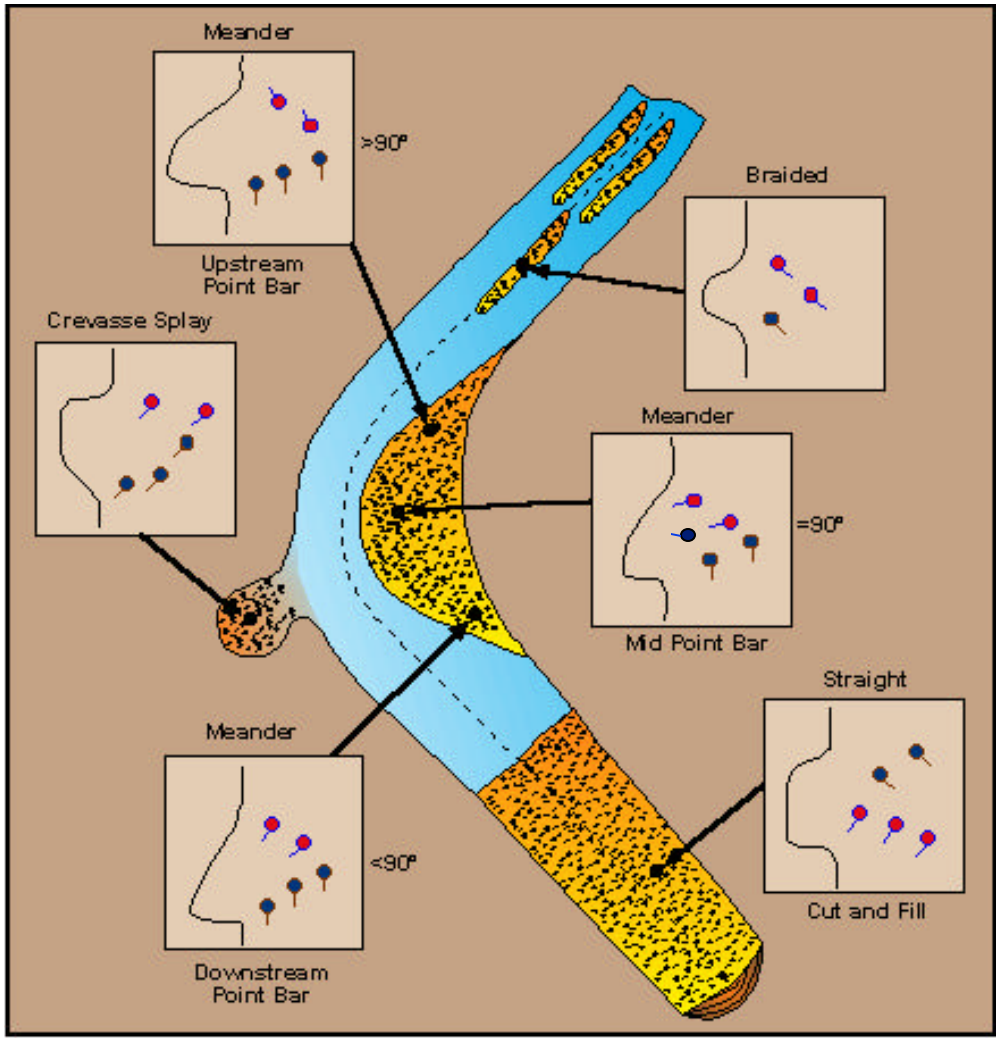

Fluvial Channels

Continental fluvial channels are an important petroleum exploration objective in many basins due to their high sand quality and excellent trapping mechanisms. Fluvial channels can be classified into four broad categories for image and dipmeter analysis: ***braided, anastomosed, straight, and meander.*** This classification by Rust separates the channel types by sinuosity and the degree of braiding. Braided and anastomosed channels are multi-channels while straight and meander channels are single channel systems. Braided and straight channels are non-sinuous; meander and anastomosed channels are sinuous. Most river contain each of these channel types. The type of river system which evolves is a function of several factors including stream gradient, consistency of discharge rate, transported sediment grain size, type of the scour surface, and the effects of vegetation and natural levees.

Objectives of Fluvial Channels

The primary input to sedimentology from either images or dipmeter analysis is the identification and orientation of sedimentary structures. ***The most common sedimentary structures present in fluvial channels are paleocurrent, lateral accretion, and scour surfaces.*** When these sedimentary structures are identified in the vertical sequence and combined with texture, the type of fluvial channel can be inferred as well as the orientation of the sand body elongation.

Method for Stratigraphic Interpretation of Fluvial Channels

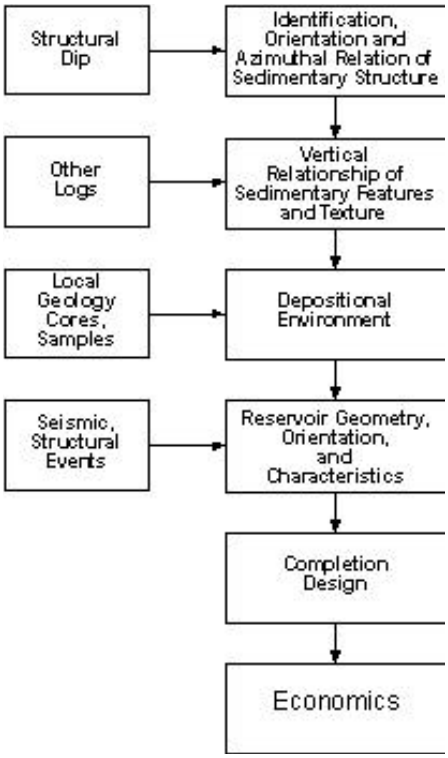

- **Current beds**
  - **identified by a rippled, truncated top**
  - **oriented parallel to the sand body elongation**
  - **located usually in the lower section of the sand**
  - **tangential current beds are the highest priority**
- **Lateral accretion**
  - **identified by a downdip thickening over thinning**
  - **oriented perpendicular to the sand body elongation**
  - **located usually in the top section of the sand**
  - **youngest lateral accretion is highest confidence**
- **Scour surfaces (much lower priority)**
  - **identified and located at the base of the sand**
  - **oriented perpendicular to sand body elongation**
  - **use only if magnitude is greater than 15 degrees**
- **Current beds and lateral accretion azimuths are generally perpendicular**
- **Texture is usually fining upward**
- **For coalescing channels, use the youngest channel for orientation**
- **Better sand quality is usually near the channel thalweg**

Depositional Environments

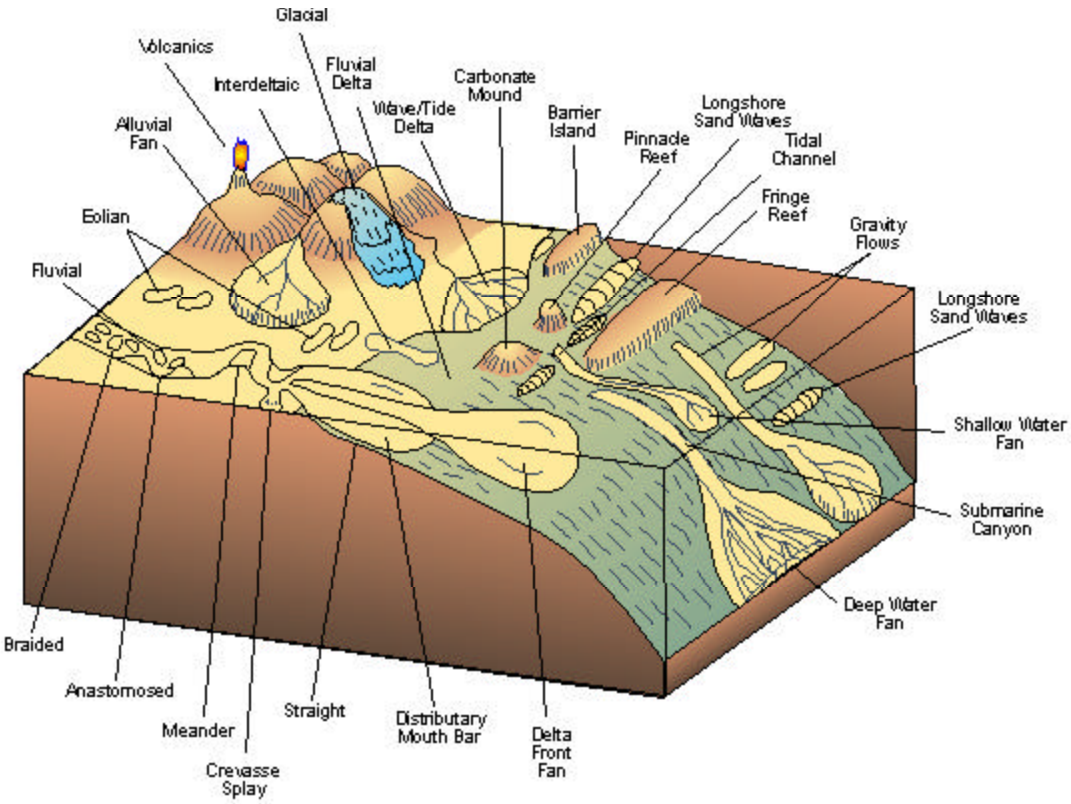

Fluvial Channel Systems

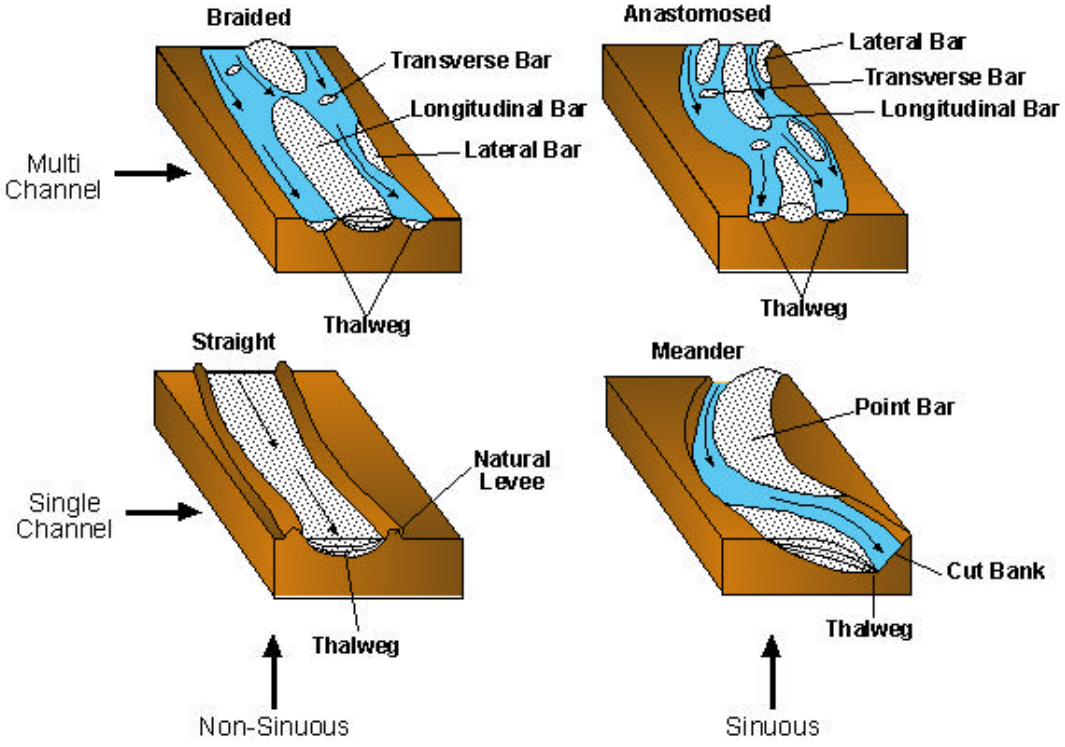

Paleocurrent

Current bedding is the most common sedimentary structure observed in stratigraphic interpretation. In fluvial channels, the identification and orientation of current bedding is particularly important. Current bedding is created by the migration of sand waves in a channel. The slip faces of the sand waves are the high angle, inclined bedding recognized as current bedding. Dip magnitudes may vary from flat to as high as 42 degrees. This is greater than the angle of repose for dry sand but the effect of clays can cause the higher magnitudes. The most common types of current bedding interpreted from electrical images are *concave, tangential, angular,* and inclined ripple.

The azimuths of the paleocurrent indicators are oriented parallel to the channel trend. Concave and tangential current bedding are high energy events and the azimuth of the tangential current beds may be directly used for channel orientation. Concave beds often have a curved base which influences the azimuths of the dips. Angular current bedding is lower energy which creates a sinuous leading edge to the sand wave. Since there may be a minor azimuth variation from the channel trend, statistical plots of the angular and concave current bed azimuths may be required. Inclined ripple bedding occurs on the stoss face of the sand wave and major azimuth variations occur. The inclined ripple beds are used for approximate orientation and to verify the identification of the other types of current bedding.

Migration of a Sandwave

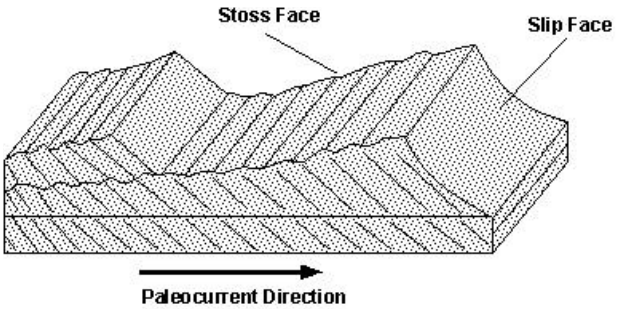

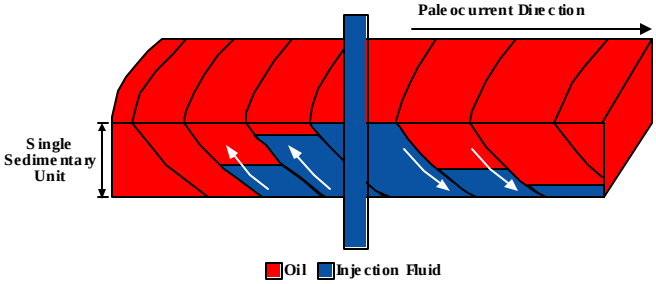

Optimum Position for Injection Well

Channels are elongated reservoirs and tend to be favorable candidates for secondary recovery. Injection wells may be located either on the upstream or the downstream end of the longitudinal sand bar. If structural dip is negligible, then consider the effect of the slip faces on the injected fluid. The slip faces tend to direct the injection fluid downward in the current direction and upward along the upstream slip faces. This provides the most optimum sweep efficiency for secondary recovery.

Paleocurrent Direction in Channel Systems

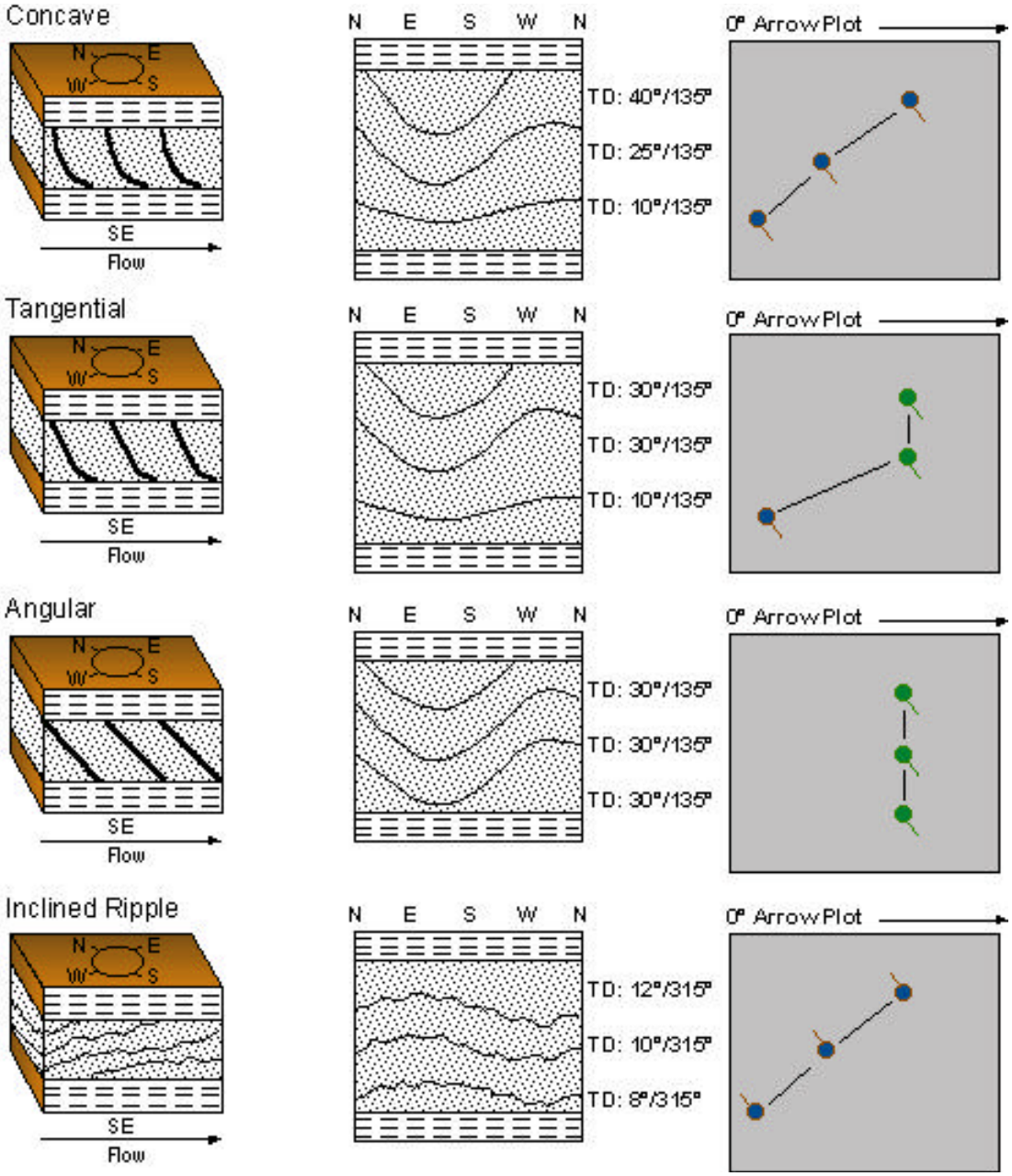

Interpretation Rules - Current Bedding

- Use the uppermost dips azimuths of each current bedding set.
- Tangential current bedding are the highest priority.
- Concave and angular bedding - use statistics
- Inclined ripples should not be used for orientation.
- Current bedding usually found in base of fluvial channels.
- Single arrow tadpoles are common responses for current bedding from dipmeters.

Fluvial Channel Exercise 1

Crossbedding in a point bar of the Brazos River near Glen Rose, Somerville County, Texas. Section is perpendicular to current flow. (Photo by L.M. Grace, June 1992.)

1. What is the paleocurrent direction?
2. What type of current bedding is present?
3. Construct the arrow plot.

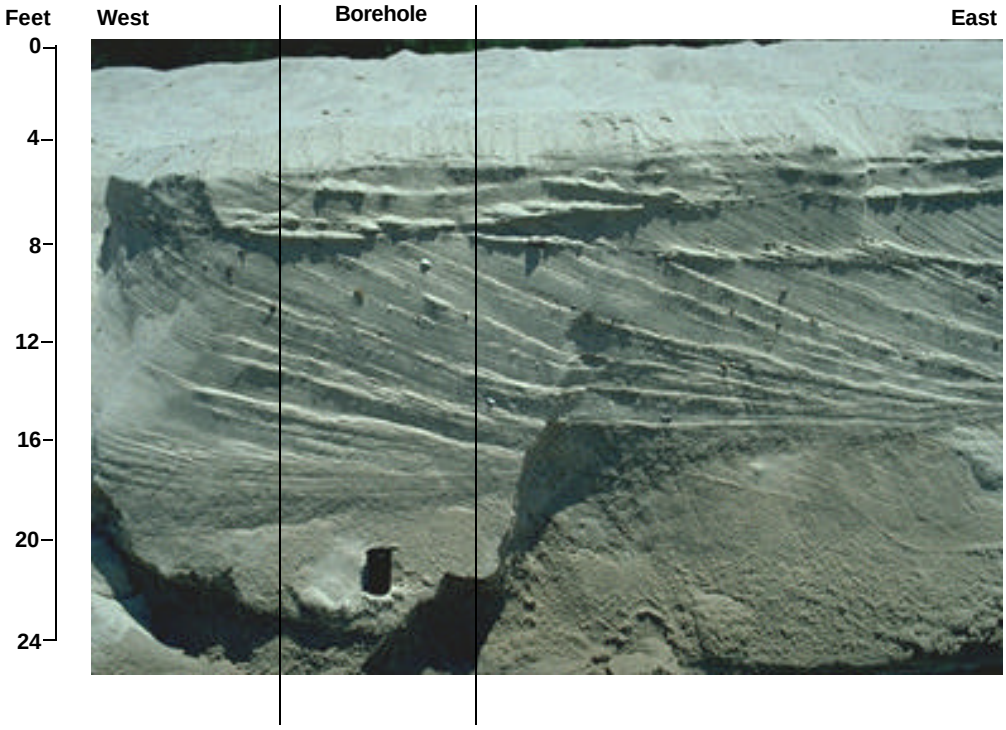

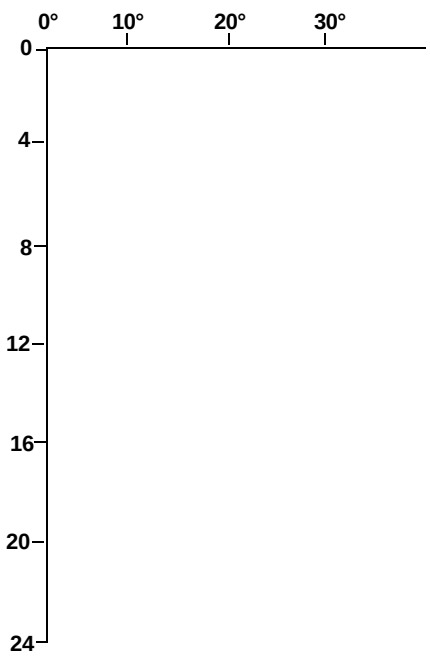

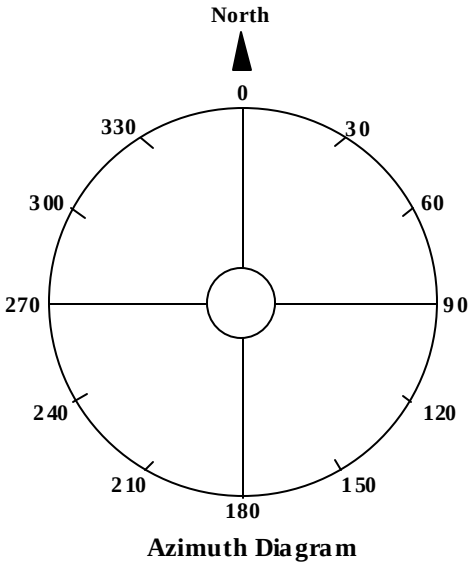

Azimuth Diagram

Fluvial Channel Exercise 2:
All are fluvial channels.

Sketch the channel orientation and paleocurrent direction.

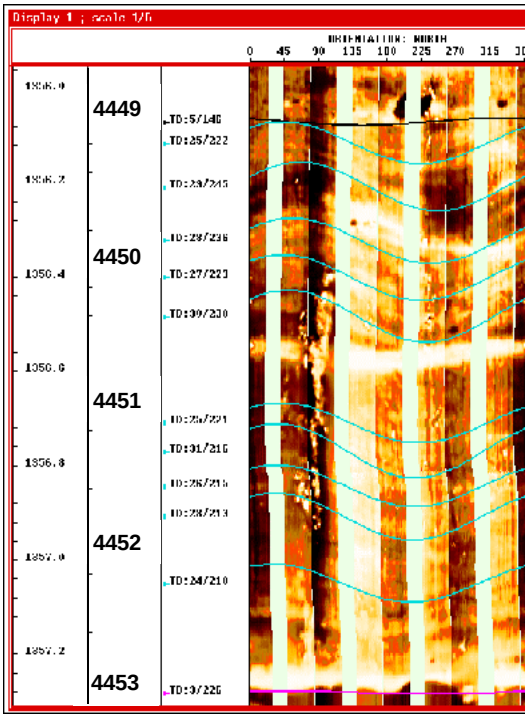

True Dips:
5/140
25/222
28/245

28/236

27/223
30/230

26/227
31/216

26/216
28/213

24/210

3/226

Meters Feet Static (Enhanced) Images 1/4:1/4

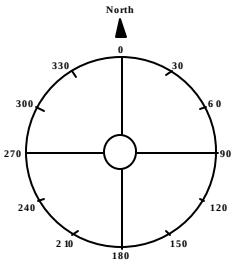

Azimuth Diagram

Types of current beds:
Angular
Tangential
Concave

Type of current bed: A._____

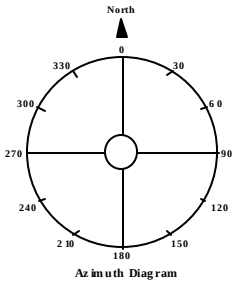

Azimuth Diagram

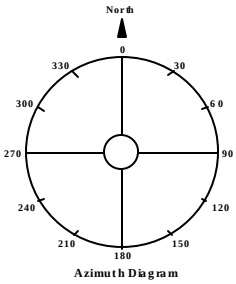

Azimuth Diagram

B._____

C._____

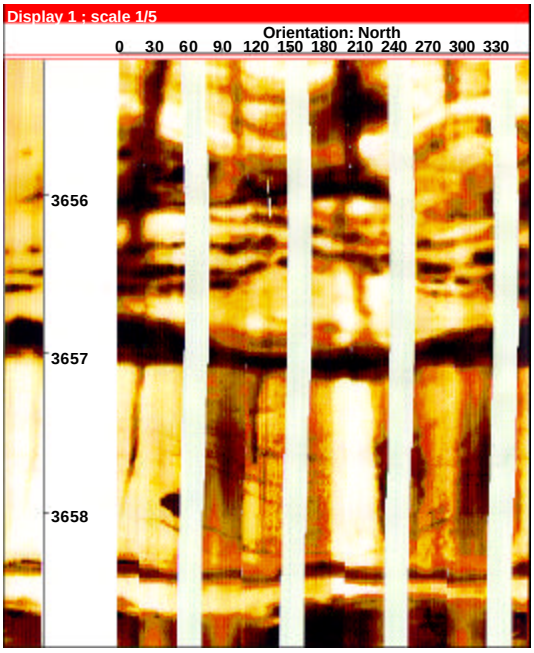

Static Feet Static (Enhanced) Images 1/4:1/4

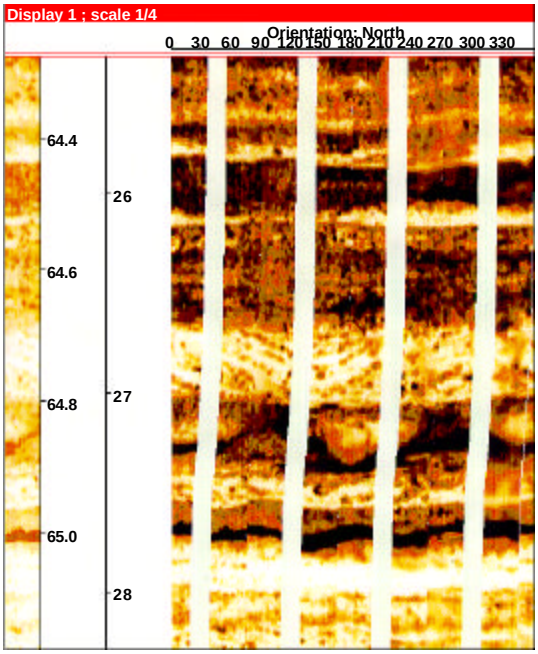

Meters Feet Static (Enhanced) Images 1/4:1/4

Lateral Accretion

The lateral accretion features is the most important thalweg indicators in both braided and meander channels. Lateral accretion is identified from the images as a thickening section over a thinning section with the same azimuth. If two lateral accretion features are found in a sand, the youngest feature is the most important; it indicates the thalweg position at time of abandonment.

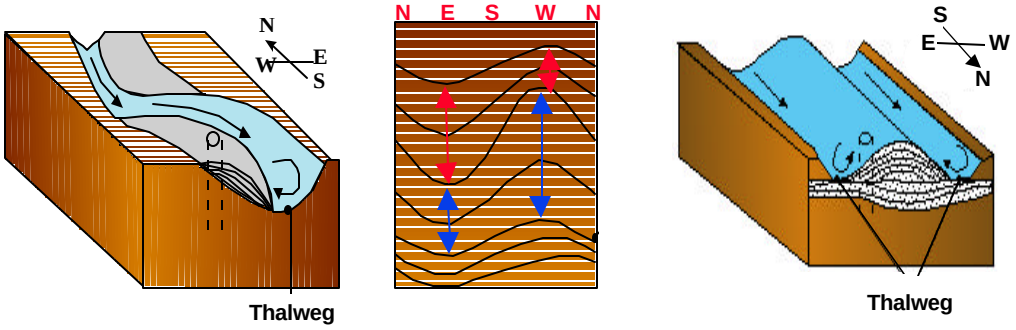

Lateral Accretion

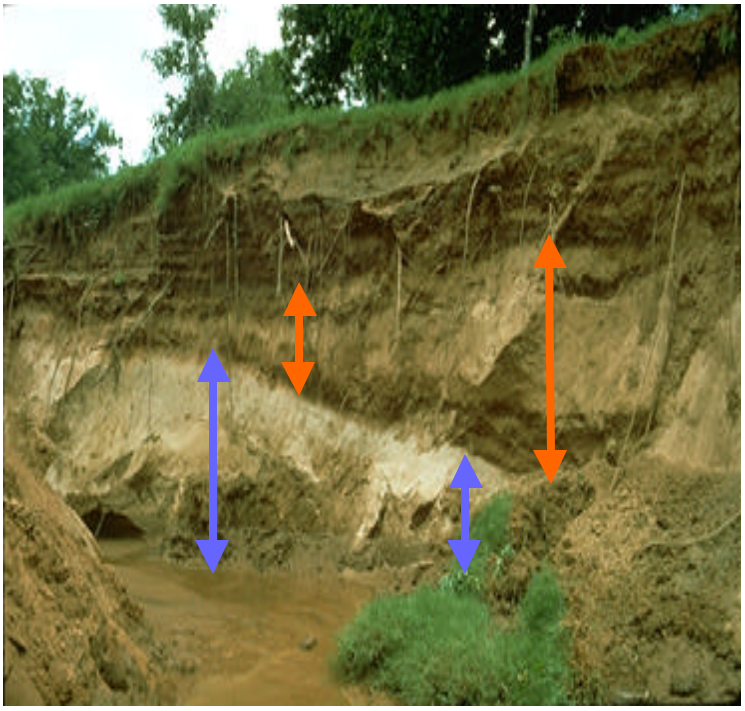

Downdip thickening

Downdip thinning

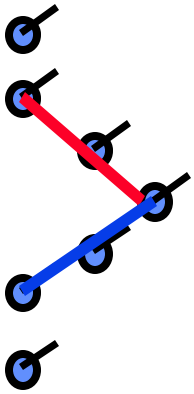

General Rules for Channel Interpretation

- Paleocurrent direction is aligned with current flow and parallels reservoir elongation.
- **Lateral accretion direction is toward the channel thalweg and is generally perpendicular to reservoir elongation.**

Fluvial Channel Exercise 3

Objective of this exercise: Stratigraphic Interpretation.
Geological Background: Fluvial Channel Sand.
Available Data: Static Images.
Stratigraphic Interpretation:

1. **What is the direction of lateral accretion? A._____B._____**
2. **Mark the channel orientations on the azimuth plots.**

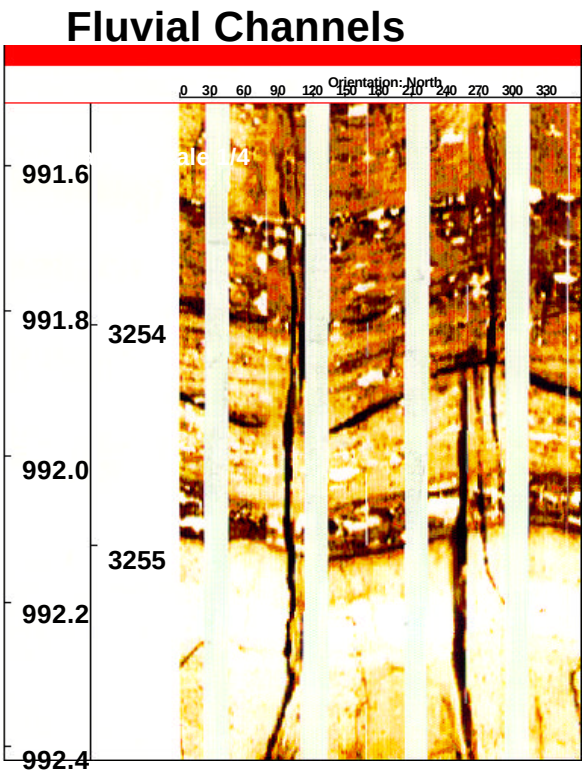

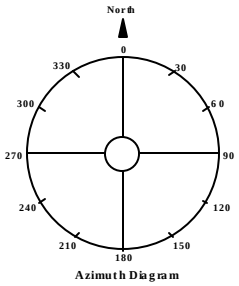

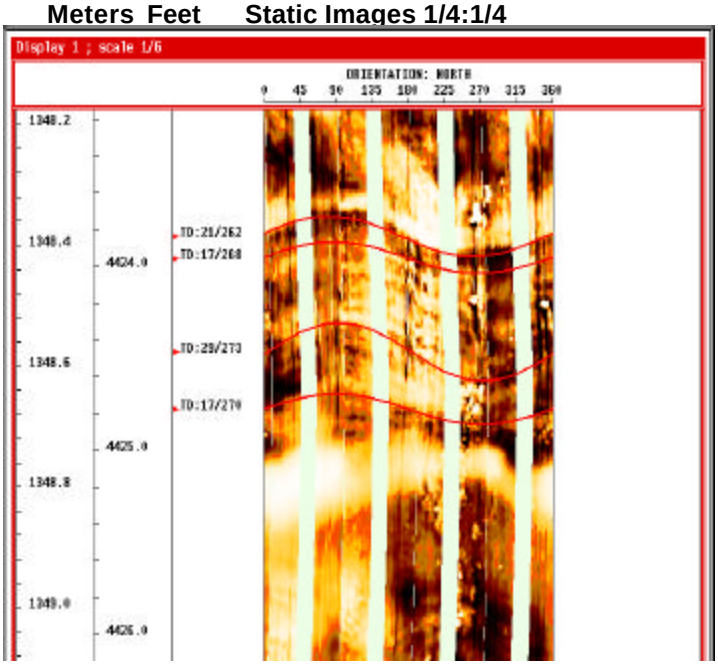

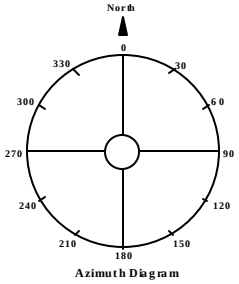

Scour Surfaces

The erosional contact between the channel and the underlying formation is the scour surface. The scour surface points toward the channel thalweg and is generally perpendicular to the sand body elongation. This sedimentary structure should be rarely used.

Fluvial Channel Exercise 4

Draw the arrow plot of the scour surface at the indicated boreholes. (Photo by P.E. Potter).

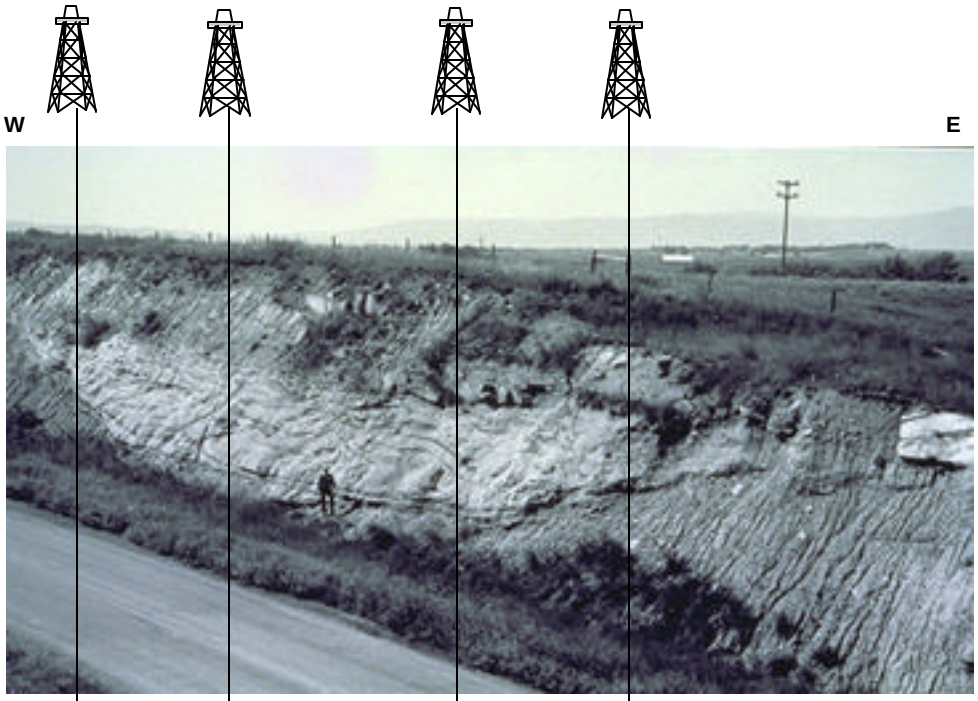

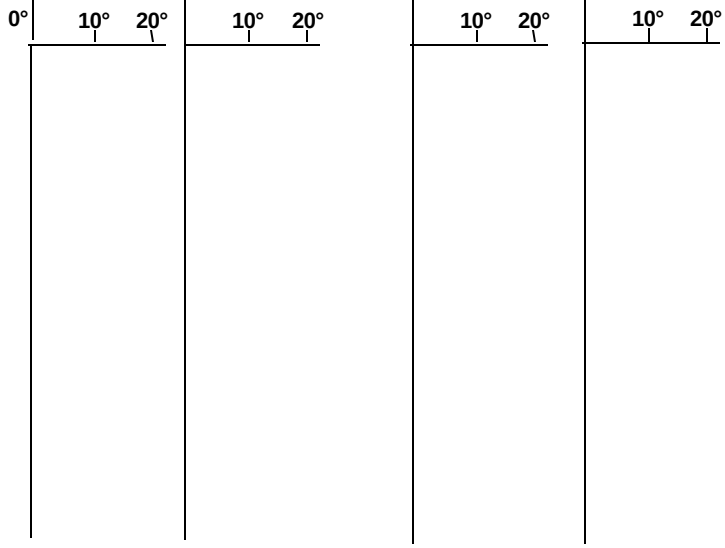

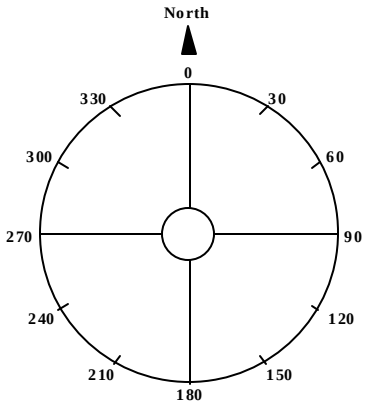

Azimuth Diagram

Fluvial Channel Exercise 5

Objective of this exercise: Stratigraphic Interpretation.
Geological Background: Fluvial Channel Sand.
Available Data: Static Images.

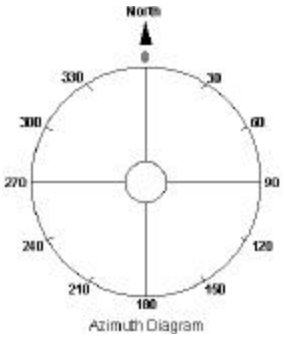

Azimuth Diagram

Stratigraphic Interpretation:

1. What is the azimuth of the scour surface? _____
2. What is the channel orientation? _____
3. What dip pattern is present in the base of the sand? _____

_____

Fluvial Channel

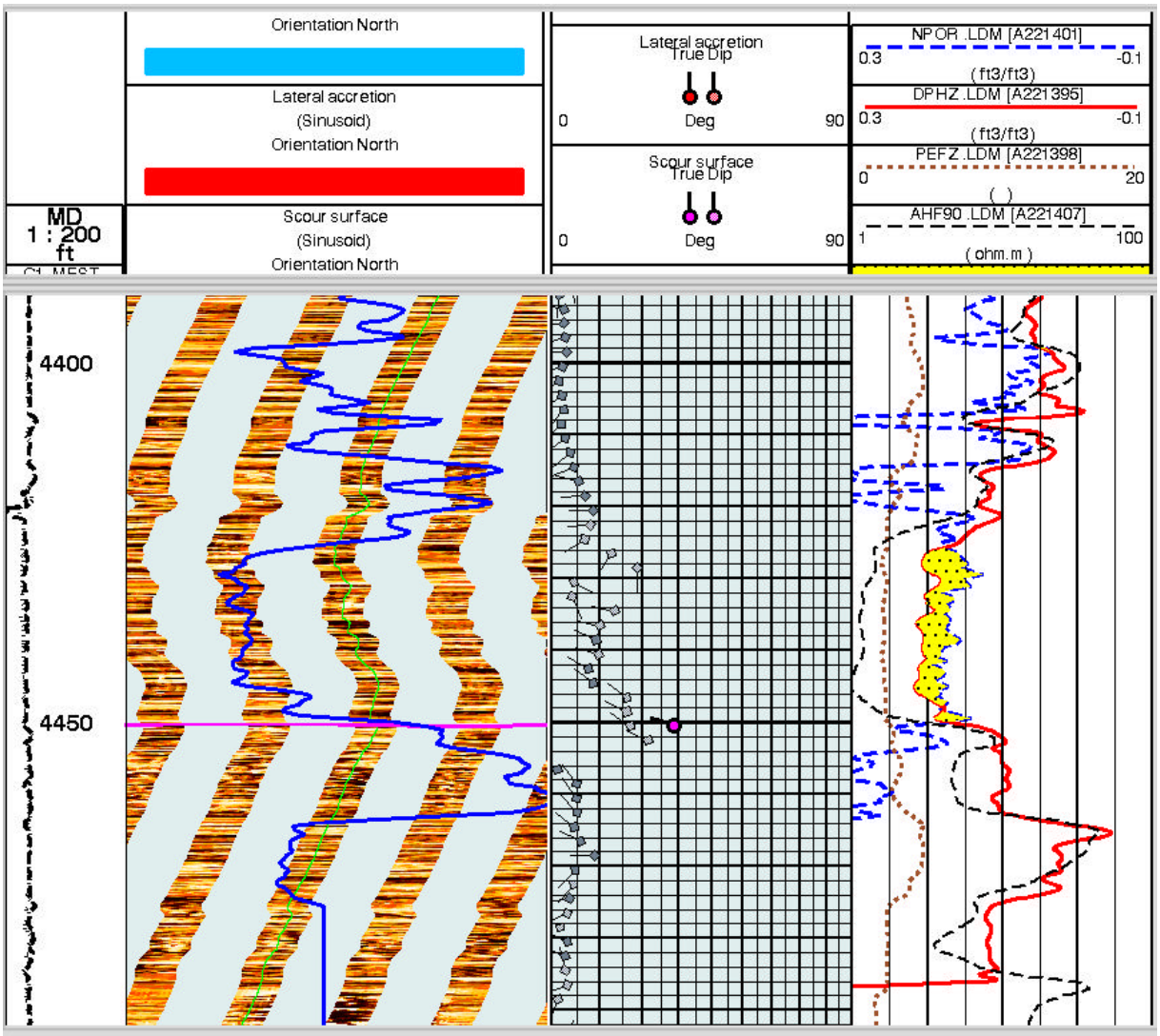

Relationship of Paleocurrent and Thalweg Indicators

Vertical Relation

Current bedding is the result of migrating sand waves. These usually occur near the channel thalweg. Lateral accretion is a process which occurs on the inner bank of the point bar. In a normal process, the current bedding deposition occurs first and then the point bar lateral accretion occurs over the current bedding.

In single channel deposition, the vertical relationship of the sedimentary structure is the lower section contains primarily current bedding while lateral accretion occurs in the upper section.

Azimuthal Relation

Paleocurrent flow is aligned with the channel axis and thalweg indicators are perpendicular to the channel axis; therefore, a right angle relation normally exists between the paleocurrent and the thalweg indicators in fluvial channel systems. The meander and braided channel models shown on page 4 indicate this right angle relationship.

The paleocurrent and the thalweg indicators are normally at right angles in a fluvial channel. If the azimuths of the paleocurrent and the thalweg directions are not at right angles, this indicates a sinuous channel model.

The relative position where the borehole has penetrated the point bar can determined from the angle relation between the paleocurrent azimuth and the lateral accretion azimuth:

- the upstream end of the point bar exhibits a greater than 90 degree relation.
- the middle of the point bar is at right angles.
- the downstream end of the point bar is less than 90 degrees.

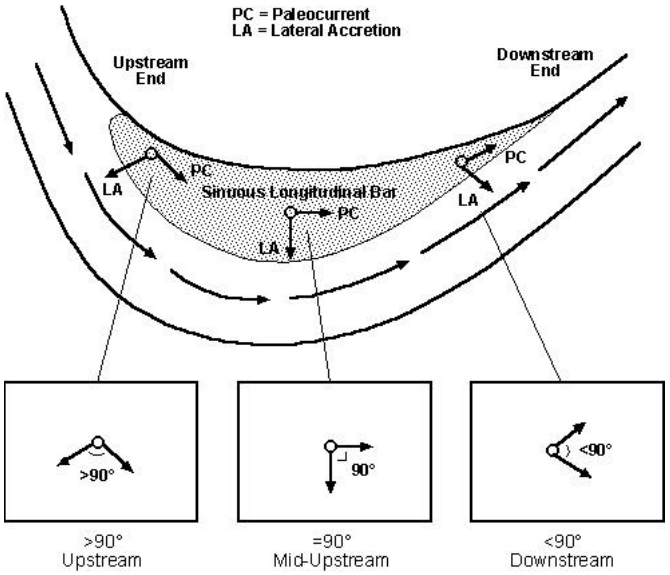

Fluvial Channel Exercise 6

Objective of this exercise: Interpretation of point bar position.

Geological Background: Pennsylvanian Sand.

Available Data: Electrical Images with arrow plot and azimuth histogram.

Questions:

1. Which part of the point bar has this well penetrated?_____
2. Where does the sand develop?_____

Driggers 1-165

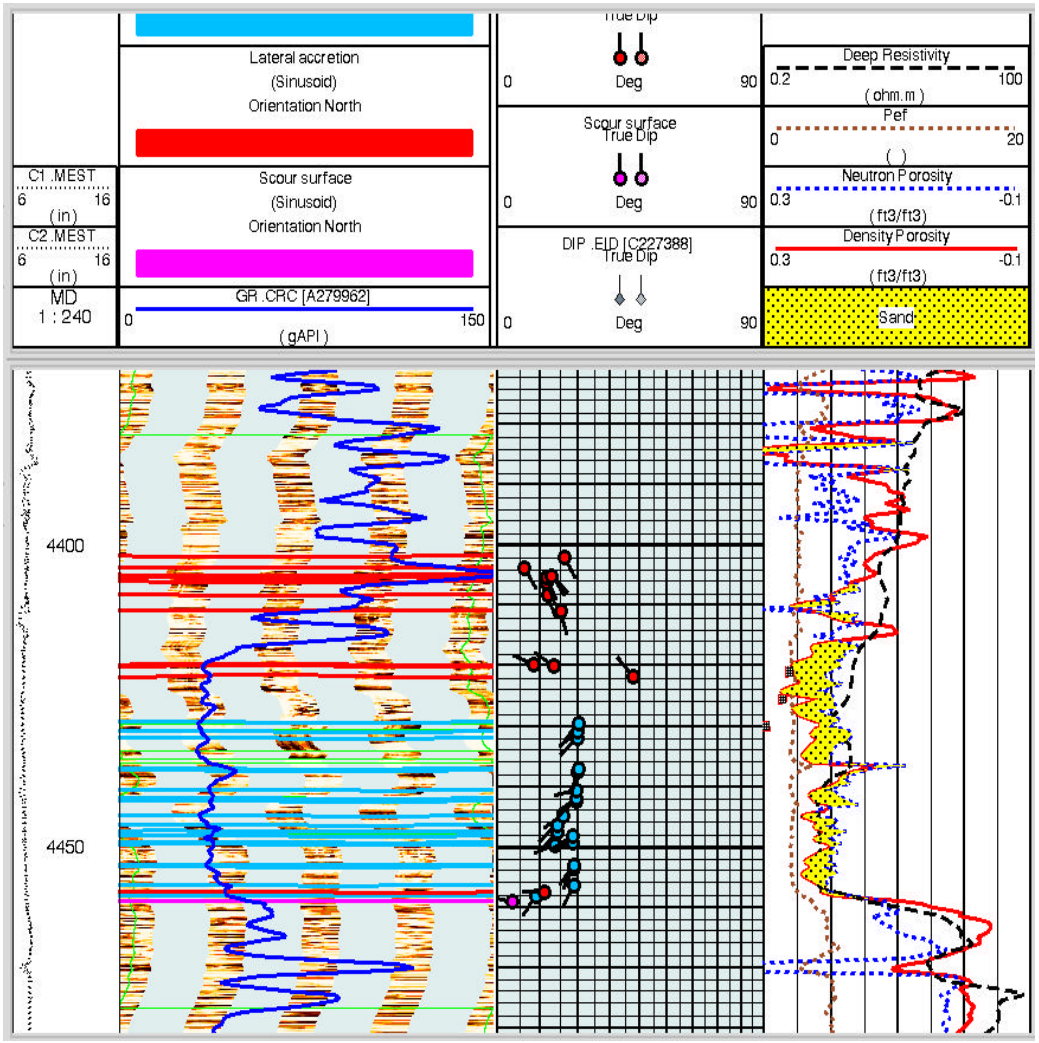

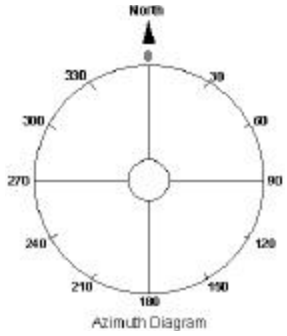

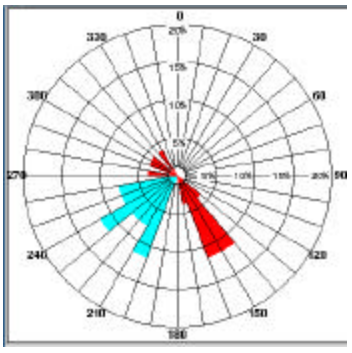

Fluvial Channel Exercise 8

Objective of this exercise: Interpretation of point bar position.

Geological Background: Pennsylvanian Sand.

Available Data: Electrical Images with arrow plot.

1. Which end of the point bar has this well penetrated?_____
2. Where does the sand develop?_____

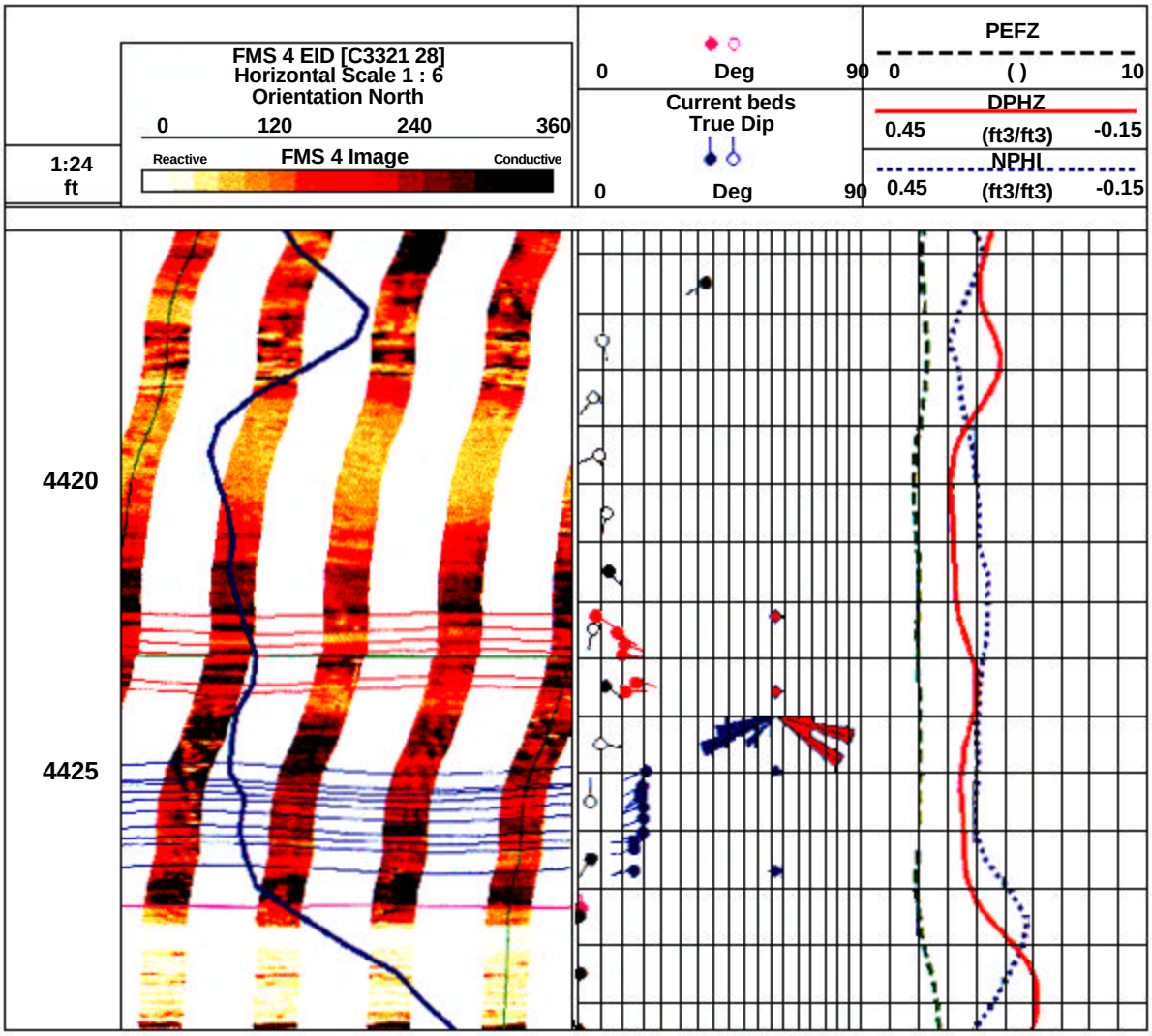

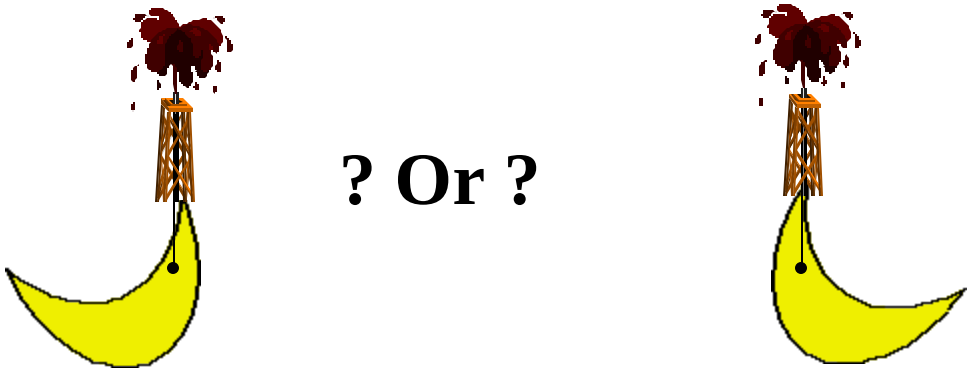

Fluvial Channel Exercise 9

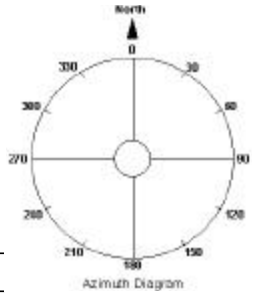

Objective of this exercise: Point bar interpretation
Geological Background. Fluvial channel
Available Data: Electrical Images
Questions: 1. What part of the point bar? _____
2. Where does the sand develop? _____

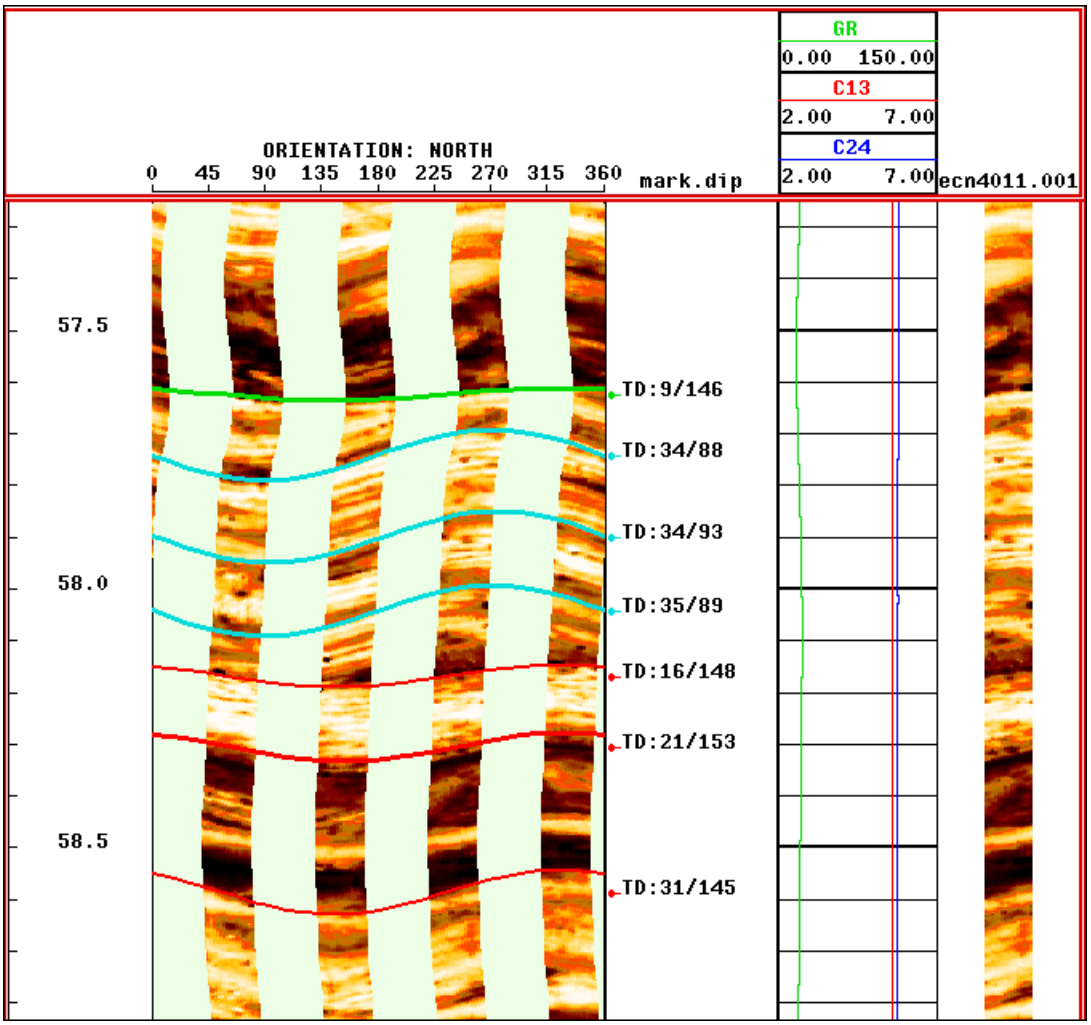

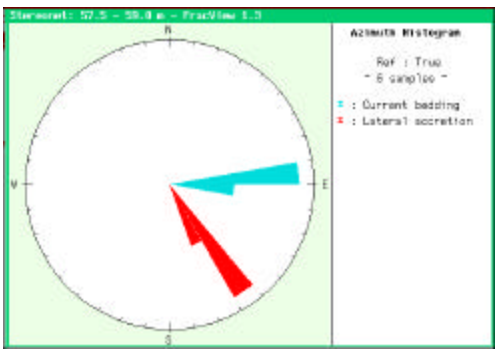

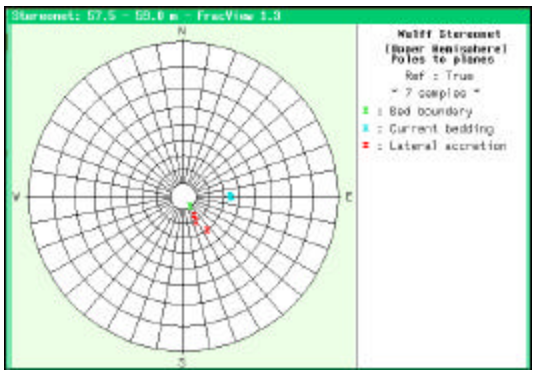

Fluvial Channel Exercise 10

Objective of this exercise: Interpretation of a fluvial channel.

Geological Background: Pennsylvanian Sand.

Available Data: Electrical images and arrow plots.

1. What is the interpretation?

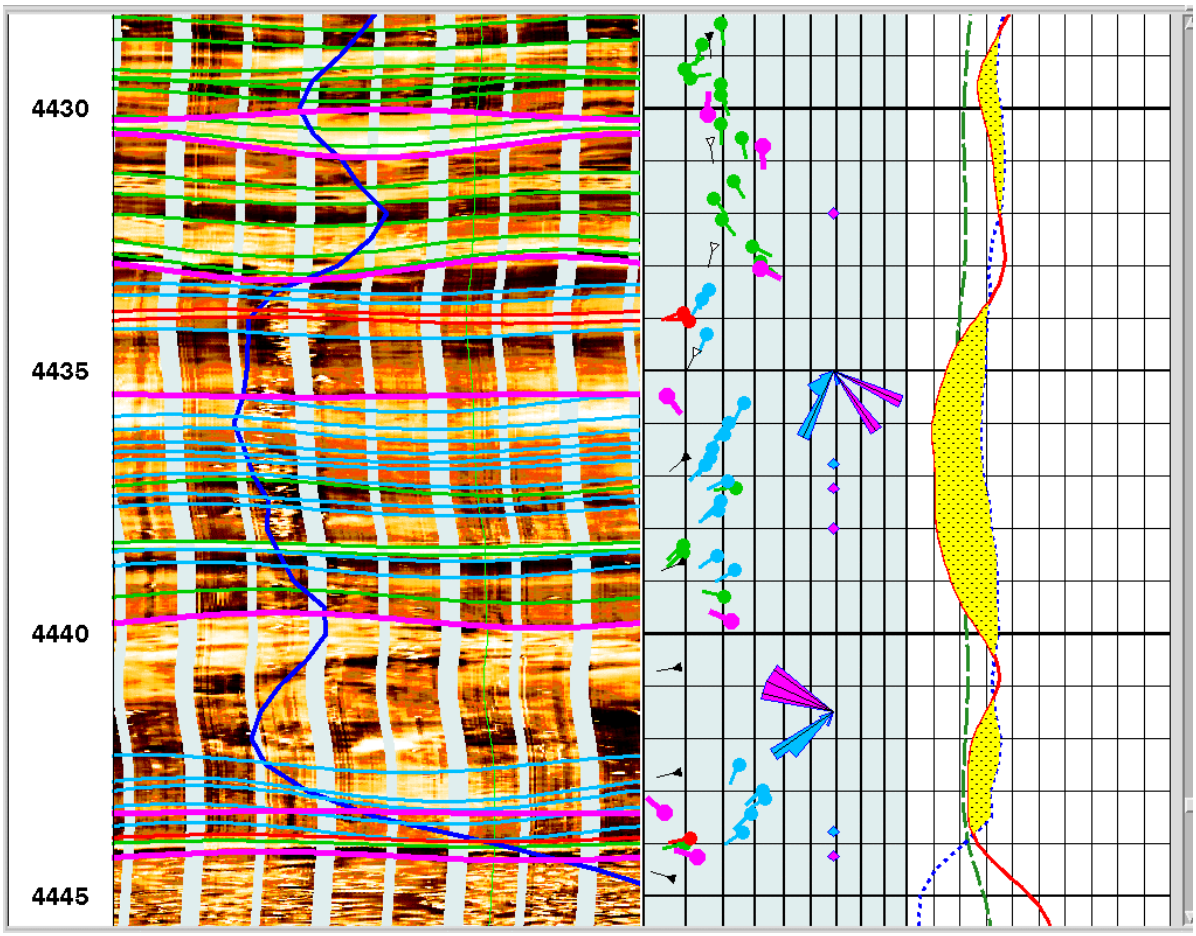

Fluvial Channel Exercise 11

Objective of this exercise: Interpretation of braided channel.

Geological Background: Pennsylvanian Sand.

Available Data: Dipmeter arrow plot, induction, density.

1. What is the channel orientation?_____
2. Where does the sand develop?_____

Big "RRR" Field

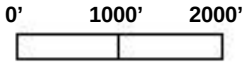

Dual Induction - Well RRR-4

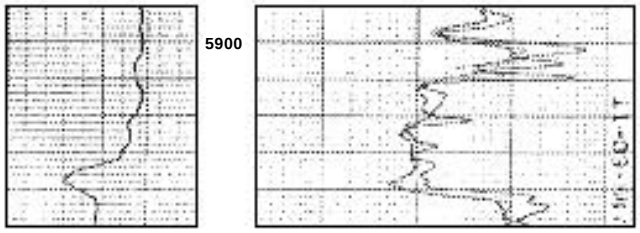

● **RRR-4**

Litho-Density/Gamma Ray
RRR-4

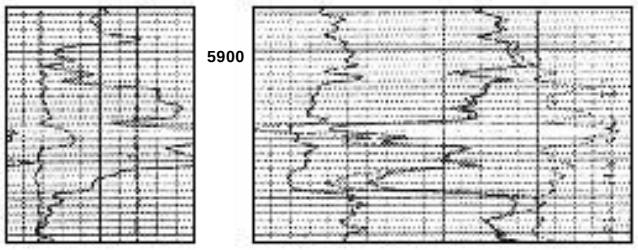

Dipmeter 6 in. x 2 in. x 40° CSB

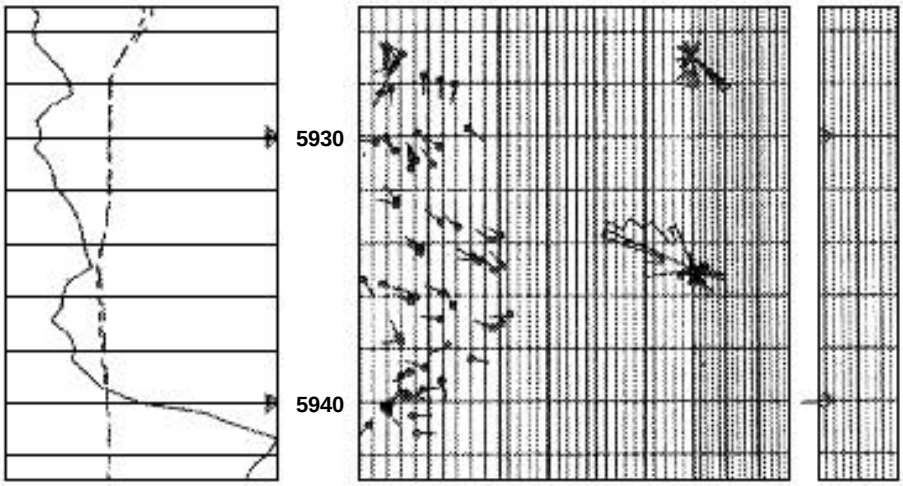

Fluvial Channel Exercise 12

Objective of this exercise: Interpretation of braided channel.

Geological Background: Pennsylvanian Sand.

Available Data: Dipmeter arrow plot, induction, density.

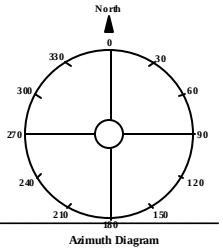

1. What is the channel orientation?_____
2. Where does the sand develop?_____

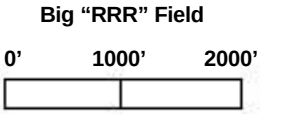

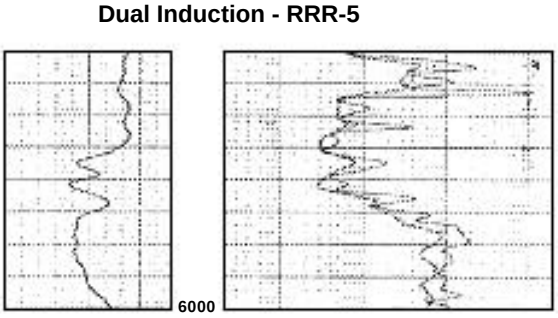

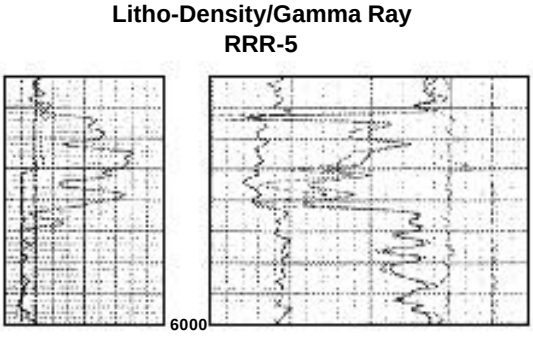

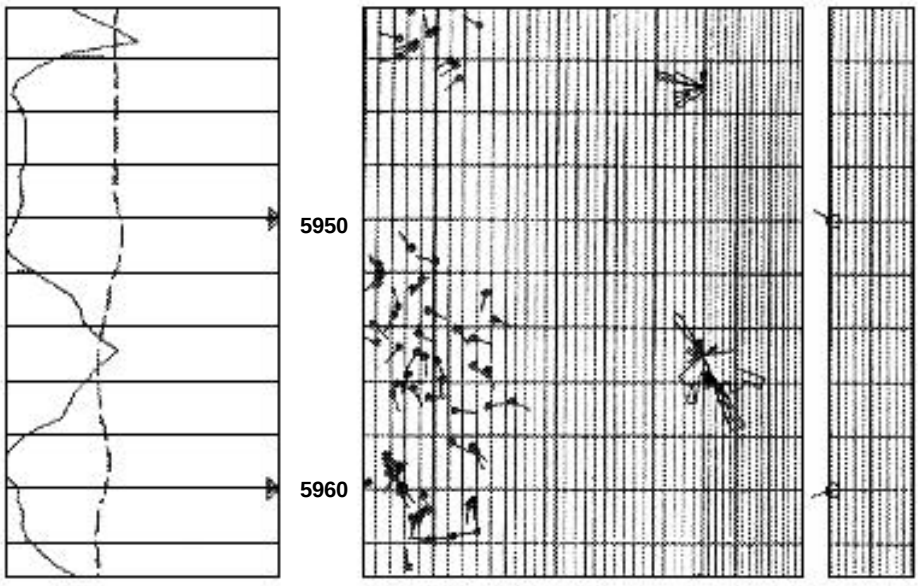

Fluvial Channel Exercise 12 Continued

Plat of RRR Field

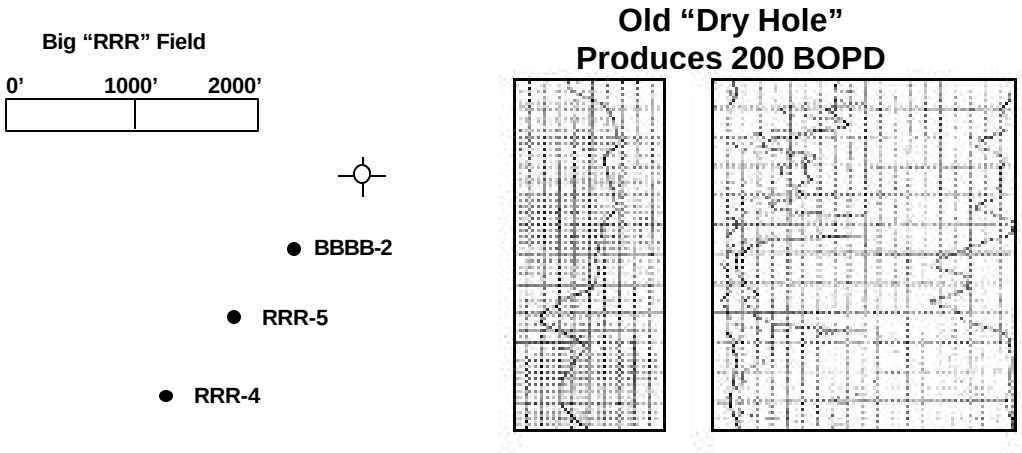

References

Cannon, R.E.:*Navigator Field: A Case for Integration,*San Antonio:AAPG, 1999.
Friedman, G.M., and Sanders, J.E.: *Principles of Sedimentology*, New York: John Wiley & Sons.
Galloway, W.E., and Hobday, D.K.: *Terrigenous Clastic Depositional Systems,* New York: Springer-Verlag.
Gilreath, J.A.: "Strategies for Dipmeter Interpretation,": *The Technical Review*, v. 35, no. 3 (July, 1987), pp. 28-39.
Gilreath, J.A., Cox, J.A., Fett, T.H., and Grace, L.M.: *Practical Dipmeter Interpretation,* Houston: Schlumberger Educational Services, 1985.
Leeder, M.R.,: *Sedimentology*, London: George Allen & Unwin, 1982.
Pettijohn, F.J., Potter, P.E., and Siever, R.: *Sand and Sandstone,* New York: Springer-Verlag, 1986.
Potter, P.E., and Pettijohn, F.J.: *Paleocurrents and Basin Analysis,* Berlin-Gottingen-Heidelberg: Springer-Verlag, 1963.
Reading, H.G.: *Sedimentary Environments and Facies,* Oxford: Blackwell Scientific Publications, 1986.
Reineck, H.E., and Singh, I.B.: *Depositional Sedimentary Environments,* Berlin-Heidelberg-New York: Springer-Verlag, 1980.

Fluvial Channel Exercises - Answers

1. Current flow is to the East; Concave; there is a “blue pattern” is to the East.

2. A. Current flow is to the SW; Angular; NE-SW orientation

   B.Current flow is to the SSW; Tangential: N9E-S9W orientation

   C.Current flow is to the SSE; Concave; NNW-SSE orientation

3. Lateral accretion is to the NE; NW-SE orientation;

4. Lateral accretion is to the ESE; the orientation is perpendicular to the lateral accretion direction: NNE-SSW

5. Scour surface dips are to the West and East; note the most meaningful dips are when the dip magnitude is greater than 15 degrees.

6. The scour azimuth is WNW; the channel orientation is perpendicular to this azimuth or NNE-SSW; there is a “red dip pattern” immediately above the scour surface, this is a basal conform sedimentary structure which is discussed in the Deltas Chapter.

7. Dips in the lower part of the sand are to the South while dips in the upper section are to the West. The images show the current beds have a Southerly azimuth while the lateral accretion is to the West. This is the right angle azimuthal relation observed in the middle of a point bar.

8. Current flow is WSW & lateral accretion is ESE: the azimuths are greater than 90 thus the borehole has penetrated the upstream end of the point bar. The sand develops to the SW.

9. Current flow is to the East and lateral accretion is to the SE; the azimuths are less than 90 thus the borehole has penetrated the downstream end of the point bar. The sand develops to the West.

10. Multiple scour surfaces with opposing azimuths indicates a braided or anastomosed system; the orientation is perpendicular to these scour surfaces or NE-SW.

11. Multiple lateral accretions to the NW indicates a NE-SW channel orientation; the sand develops along this trend.

12. Multiple lateral accretions to the SE indicates a NE-SW channel orientation; the sand develops along this trend.

Thin Beds

The objectives of this chapter are:

The identification and quantitative characterization of thinly bedded sands in order to determine net sand fraction and provide better information for petrophysical analysis. This includes:

Thin Bed Determination
Sand Count
Sharpened Porosity
Sharpened Resistivity

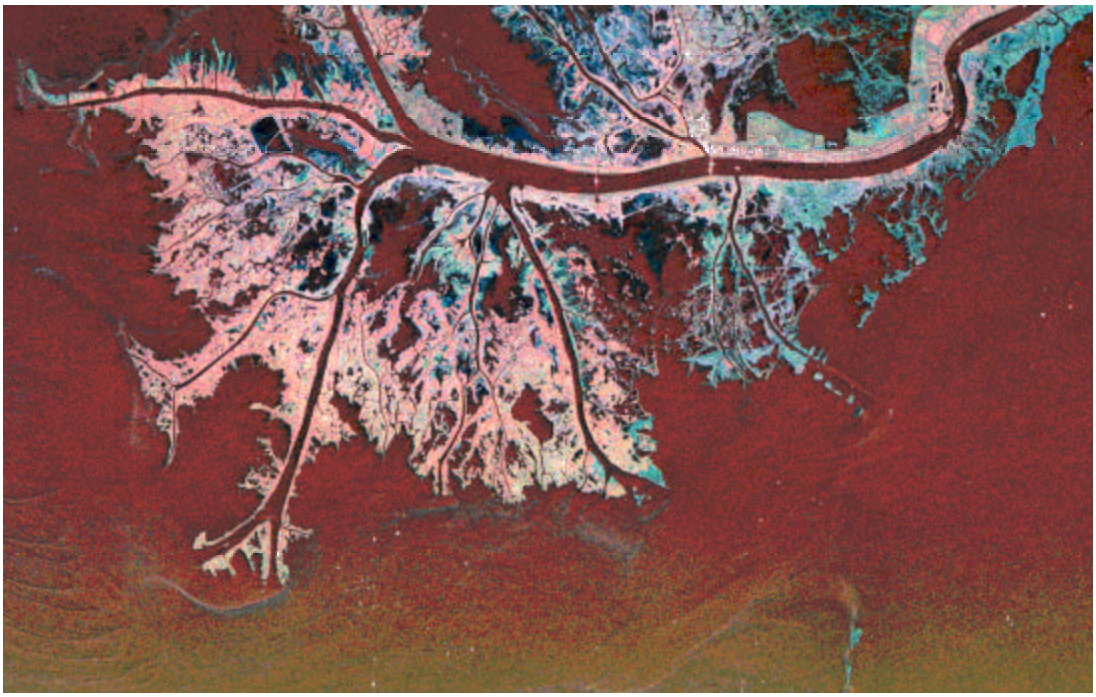

Turbidite Reservoir Classification

Generalized end-member, turbidite reservoir types, from outcrop and subsurface studies by Shell. Different reservoir types may be juxtaposed within a field, or even within a seismic mapping horizon, but reservoir zones or subzones are generally of one type only.

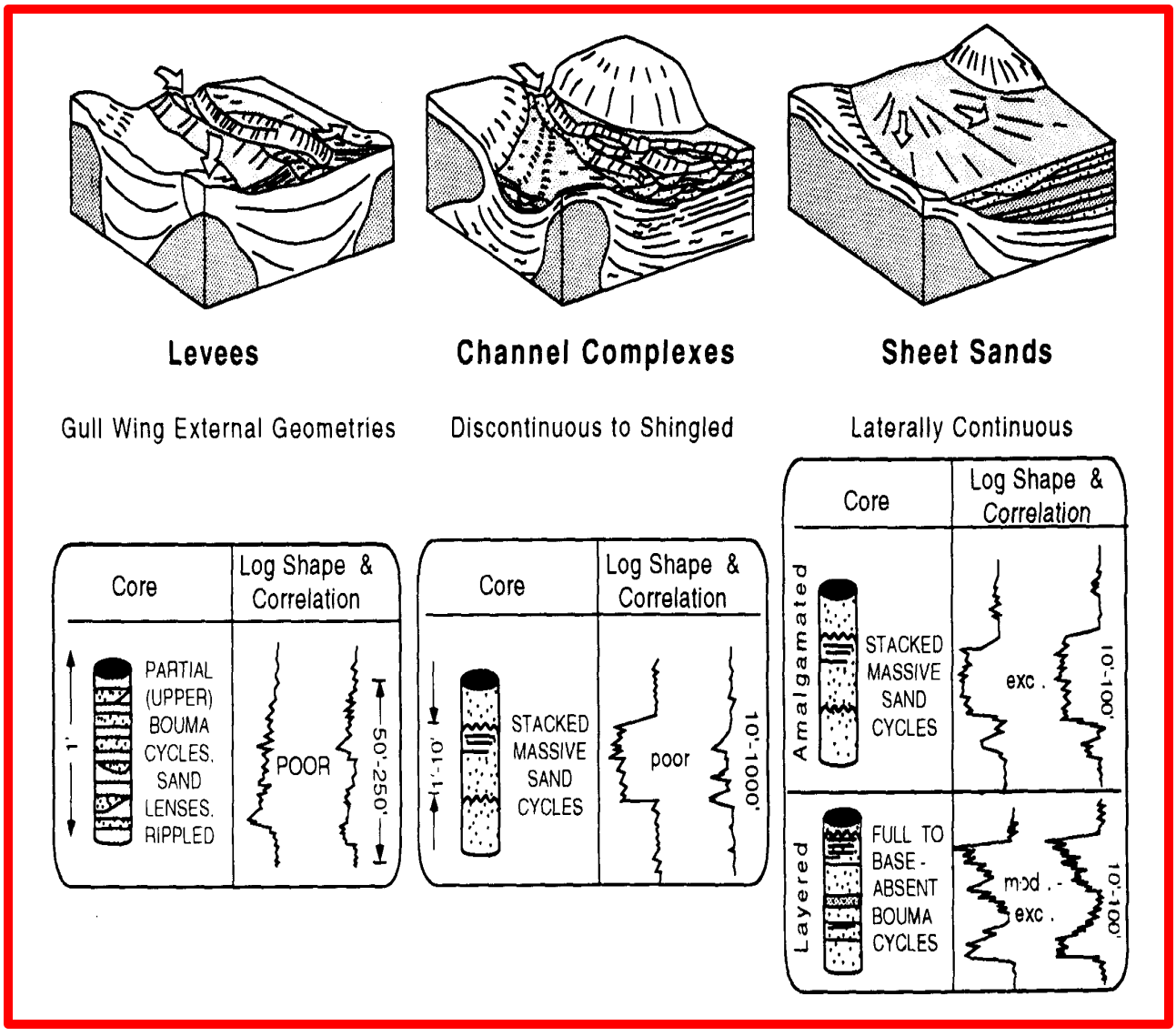

Mahaffies 1995

Building Blocks of Deepwater Cycles

	Depositional Environment	*Log Facies / Response*	*Dipmeter Pattern*
ed Strata	Across slope during periods of very little to no clastic input, sedimentation dominated by hemipelagic sedimentation	Clean shales, Marls	Dips very poorly preserved to no t present, Probably due to extensive bioturbation
Muds	Hemipelagic fallout, toesets to shelf margin deltas/muddy turbidities Small scale debris flows	Silty shales	Dips poorly organized, poor quality, high scatter To dips. Some bedded deposits
ked Sands	Throughout slope during slowdown in sedimentation	Sands may be associated with marls/carbonate-rich muds	Dips fairly well organized, below angle of repose
umps	Occurs throughout the slope, very common in shelf margin/ Upper slope and along active tectonic features. May be triggered by high sedimentation rate/oversteepening or tectonic movement (salt withdrawl, faulting, seismicity)	Highly Variable, depending upon what type material has been slumped	Dips may show folded strata, slumped Strata or have low quality, high anble dips, Contorted strat/folded strata may be Recognizedon FMI
is Flow	Occurs anywhere in the slope, common in the middle and lower slope, common in areas of high sedimentation rate.	Depending on lithology of debris, GR can look dirty, resistivity seperatation common	Dips are low quality and scattered with high spread where measurable dips can be obtained, contorted beds and clasts may be observed in FMI
channels	Observed in all parts of the slope, better developed, lower anble, downdip in middle/loer slope, upper slope channel lovees tend to be smaller, muddier more complex, system may have erosional base	Often thinning/fining upward, Interbedded sands and shales, often stacked thinning upward packages	Low angle, consistent good quality dips in levee/overbank, more disorganized scattered dip response in channel or base of sand. Interbeds / lamination seen on FMI
d Channels	Observed in all parts of the slope, more common in upper/middle slope, probably better developed in higher angle slopes. Channel Fill highly variable: amalgamated channel sands, debris flows, mud turbidites or suspension muds	Varied log response for channel fill, may contain blocky sands to muds. Base and sides of channel may contain mud clasts or debris flows which supress GR response	Wide range of dip responses, disorganized scattered low quality dips in massive sands
obes	More common in middle and lower slope environments, probably more unconfined flow, blocky sands often associated with debris flow	Often a blocky, good quality sand with sharp base and top, sometimes cleaning upward, sands appear to be composites of multiple flows.	Dips often good quality and below angle of repose, poorer quality in very clean sands, dipmeter sometimes show 10-60 degree azimuth spread

Deep Water Clastic Features:

Deep water deposition occurs in cycles, defined by Bouma which can be identified on FMI images.

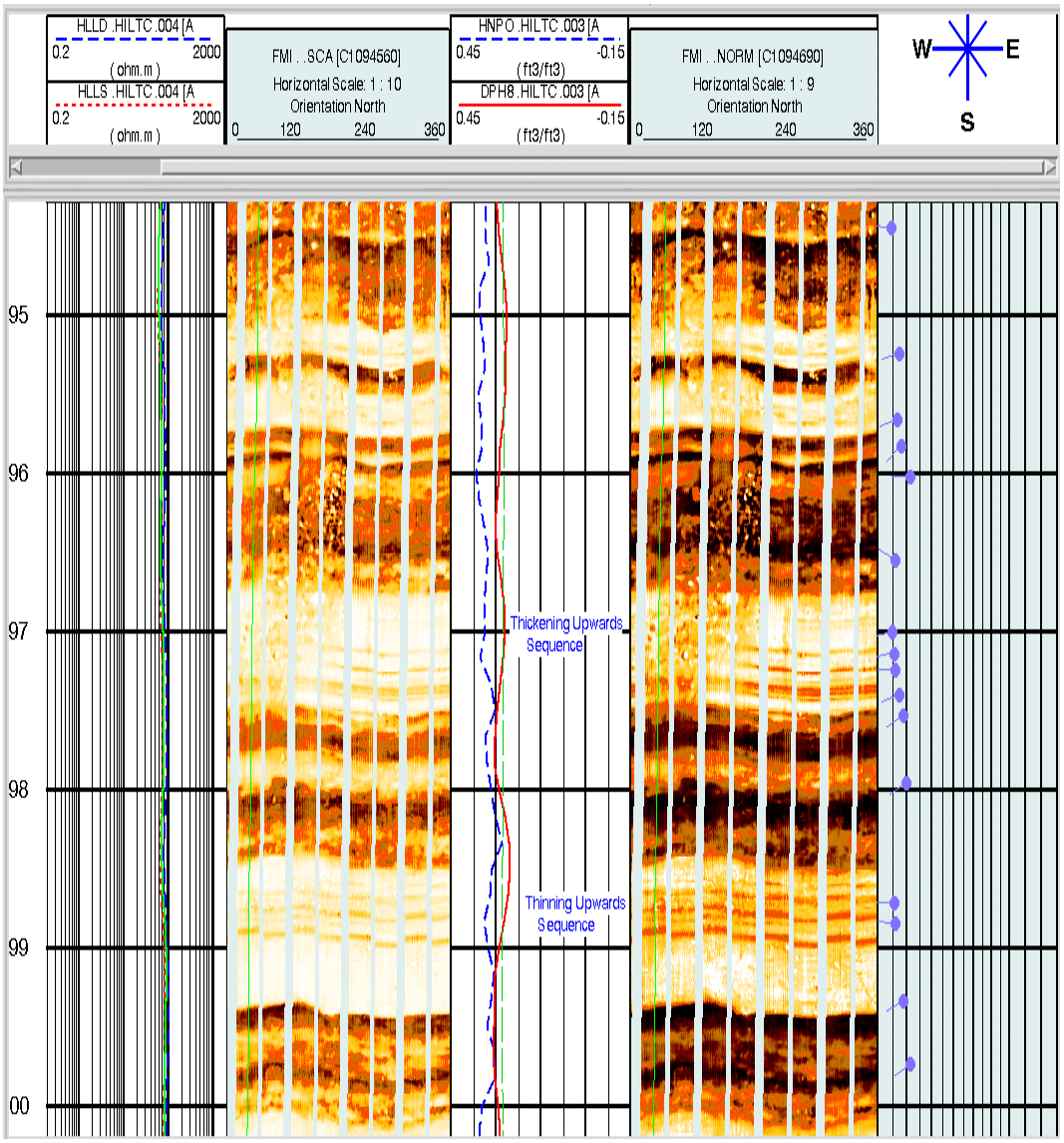

Deep Water Clastic Features:

Channels base typically exhibits an erosional surface, with rip-up clasts in the base. The actual channel base surface is commonly clay lined.

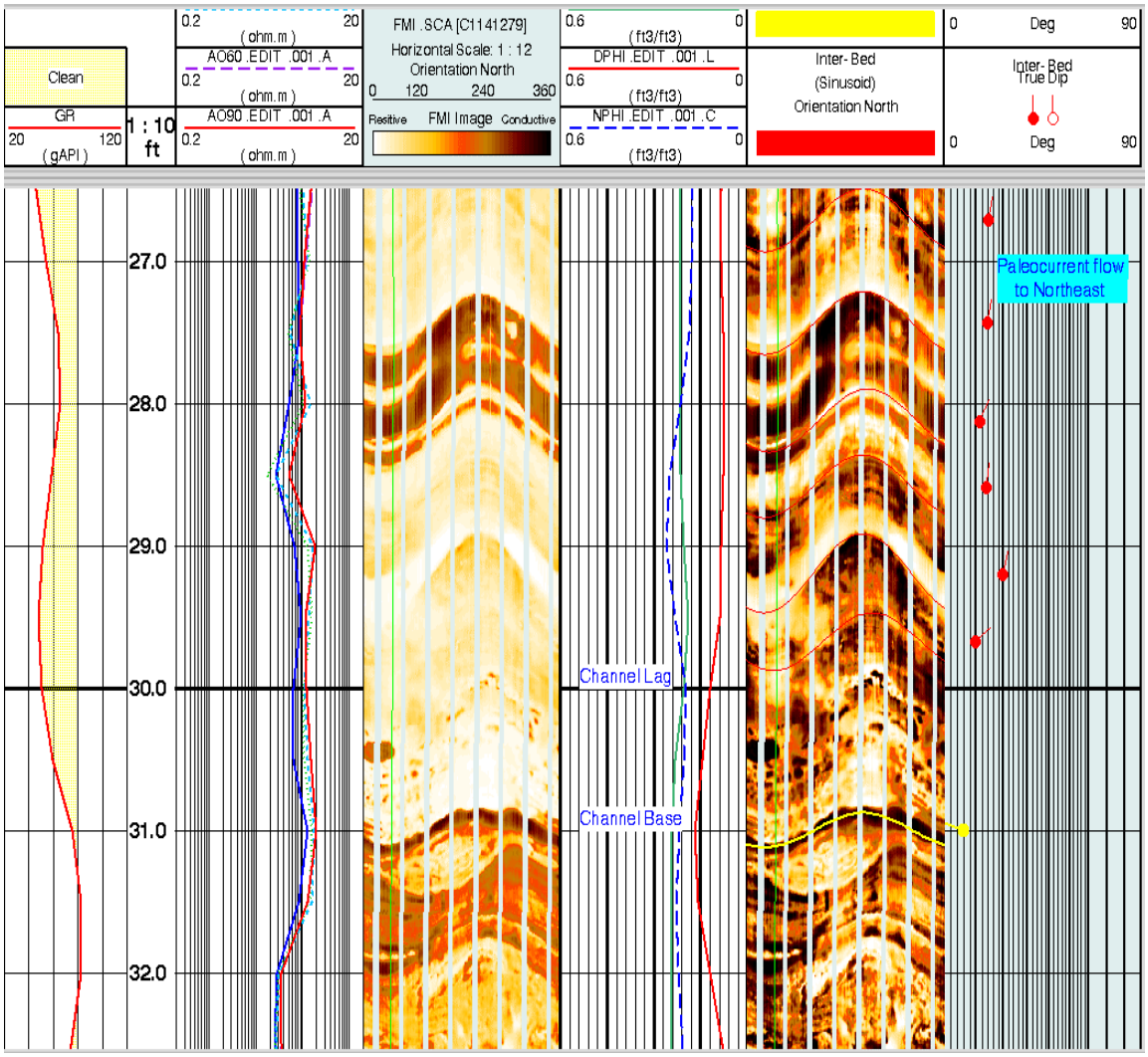

Deep Water Clastic Features:

Distortion of the sand layers greatly reduces the continuity and thus producability of the zone.

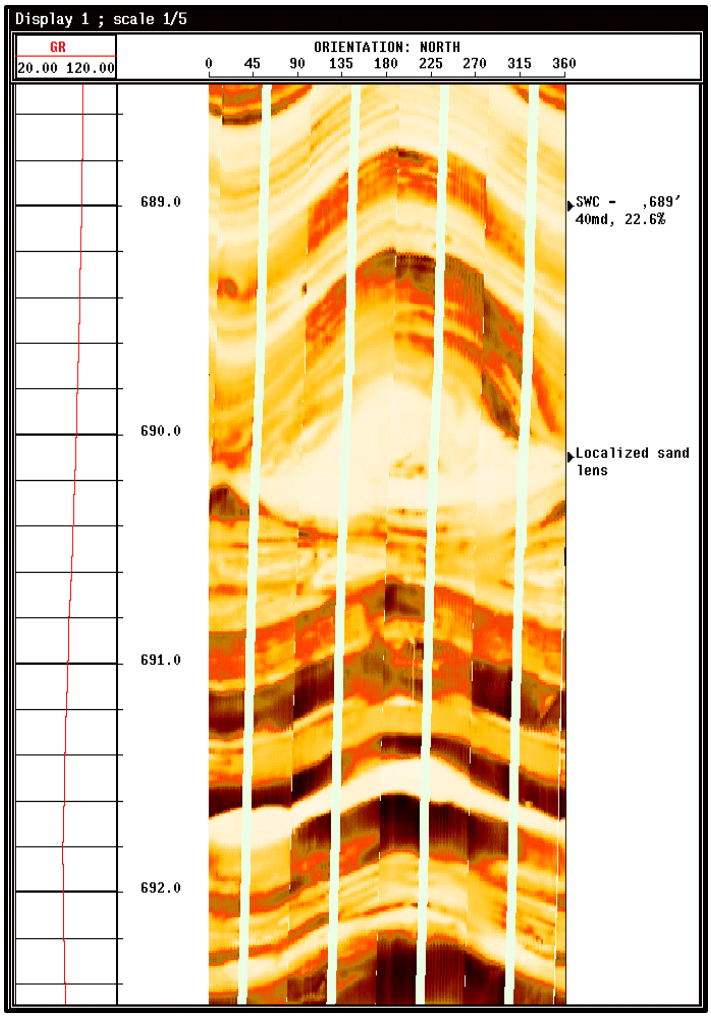

Deep Water Clastic Features:

Shales can be well laminated as seen in the top of this example or not bedded at all as seen in the middle of the example. Without images it would be impossible to determine the reasons for the lack of tadpoles in such an interval.

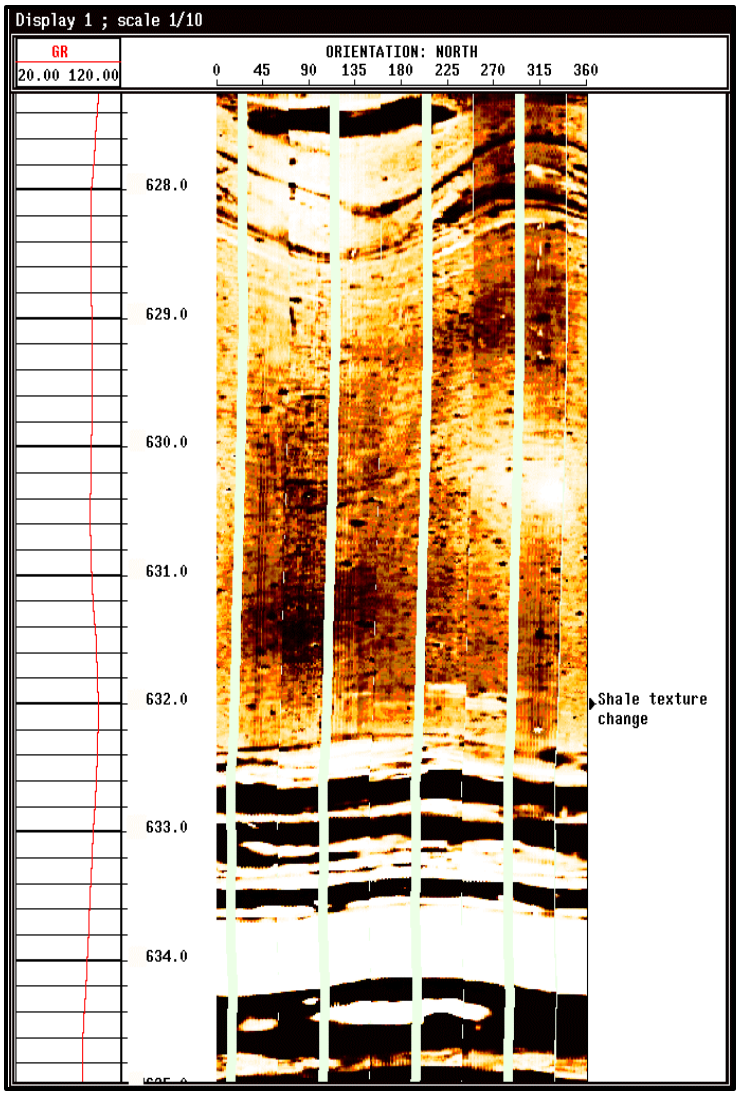

Deep Water Clastic Features:

Sands deposited as pods have no continuity away from the wellbore. Sidewall cores in these intervals may be very misleading as the small sand pockets can have excellent perm and hydrocarbon indications.

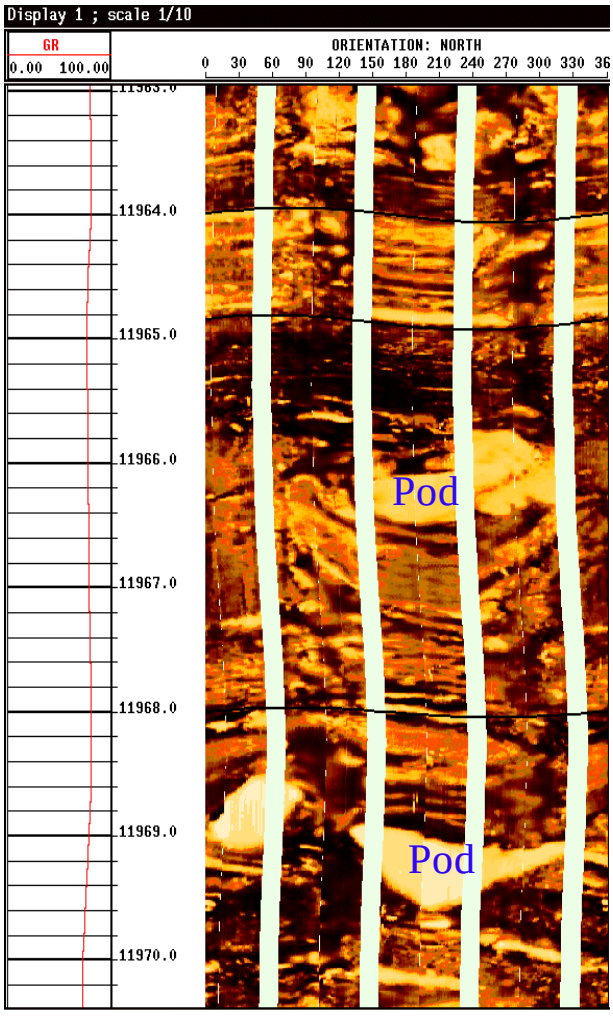

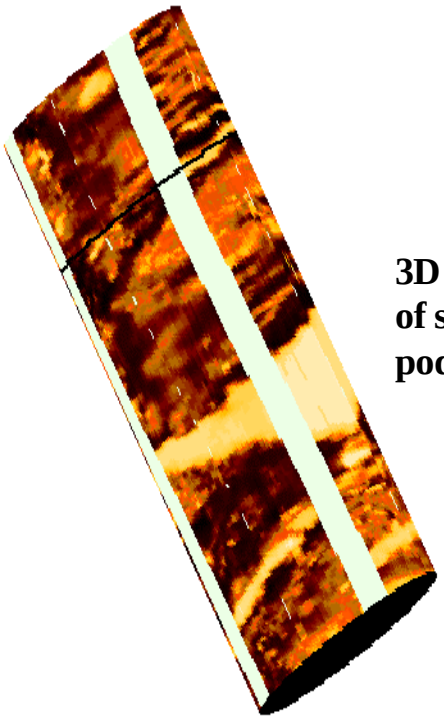

3D view of sand pods

Deep Water Clastic Features:

Marl on open hole logs (x40’ - x80’) shows a clean Gamma-Ray, with an increase in resistivity along with a change in N-D response which can be misinterpreted as a thin bedded interval. The images with a CMR show the zone to have no continuous layers and low permeability.

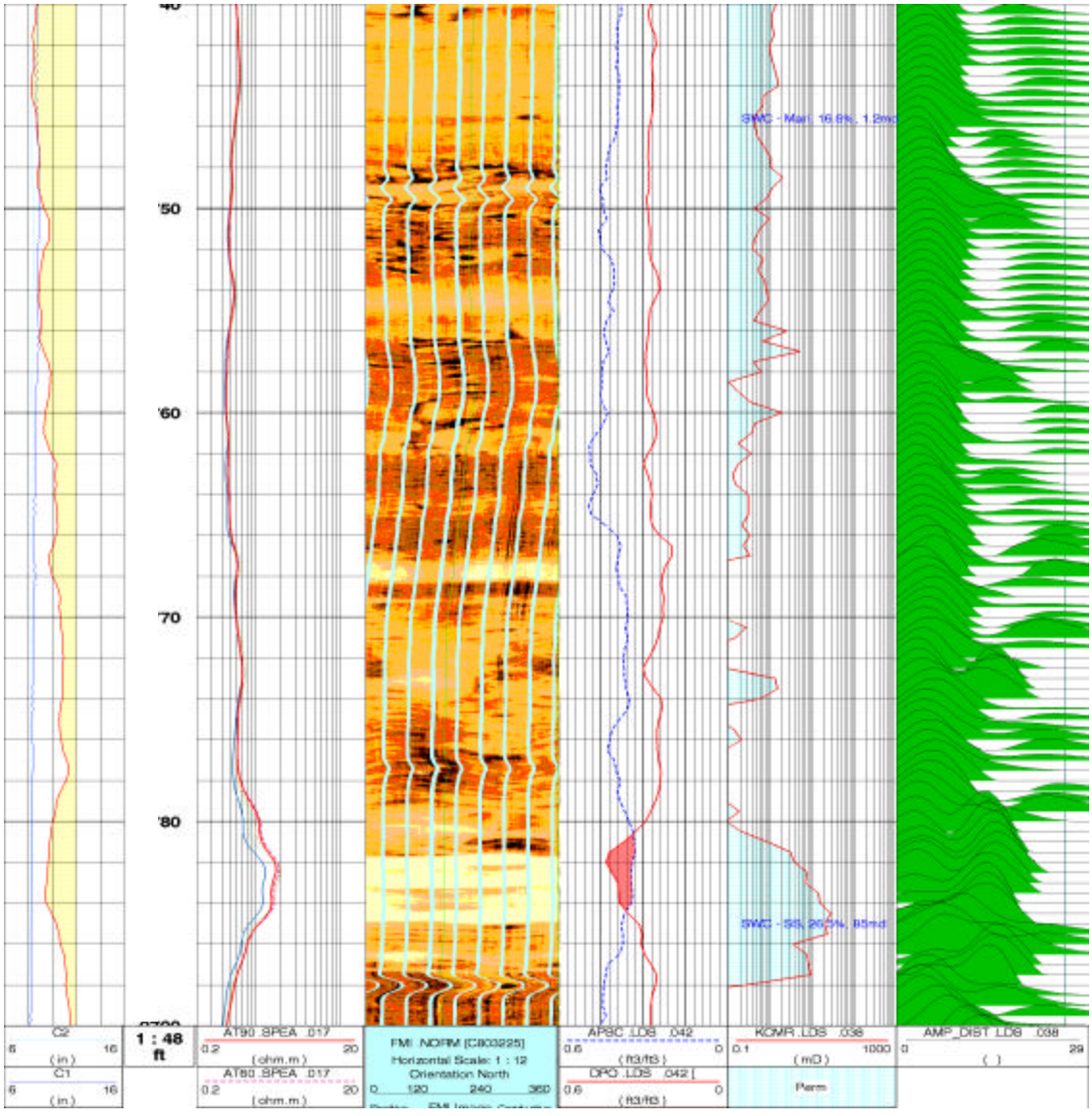

Deep Water Clastic Features:

Debis flow show clasts supported in this case a mud matrix.

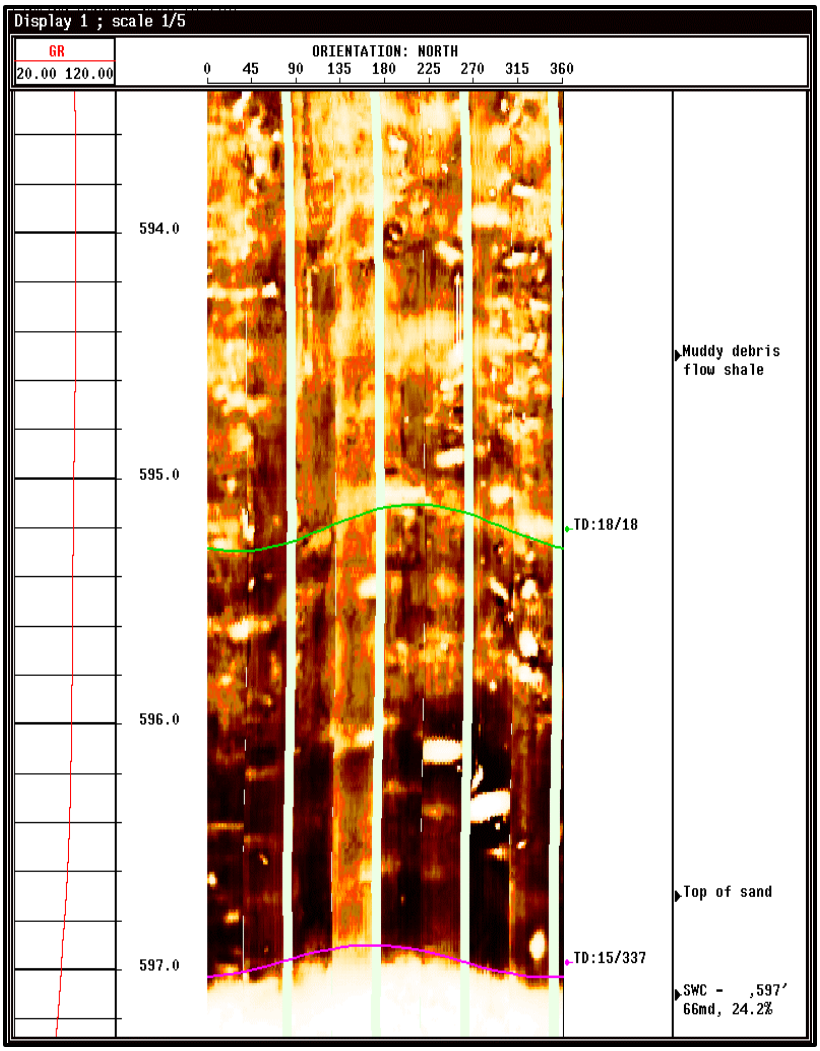

Deep Water Clastic Features:

Debis flow show clasts supported in a mud matrix. Dips from a computer program would be impossible to calculate. Dips in theses environments have to be hand picked.

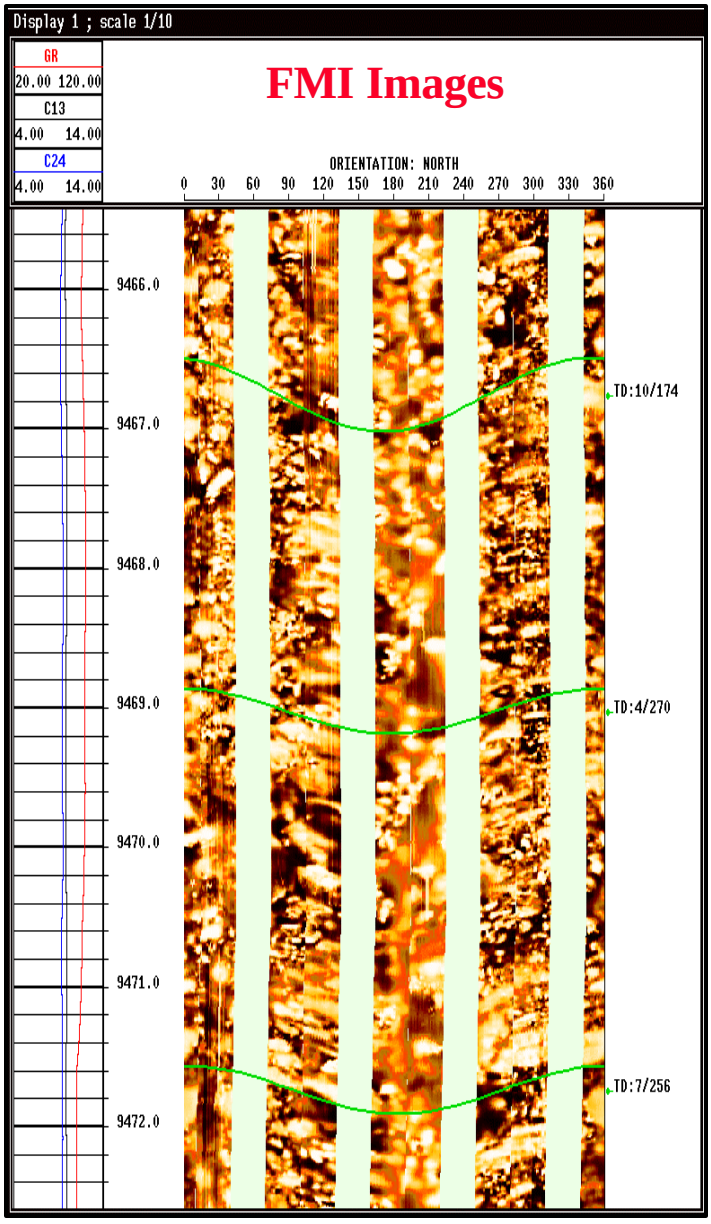

Deep Water Clastic Features:

Contorted bedding destroys an otherwise producable sand. The soft sediment deformation changes the connectivity of the reservoir to virtually zero. Although a good sand with shows is present here the interval tested tight.

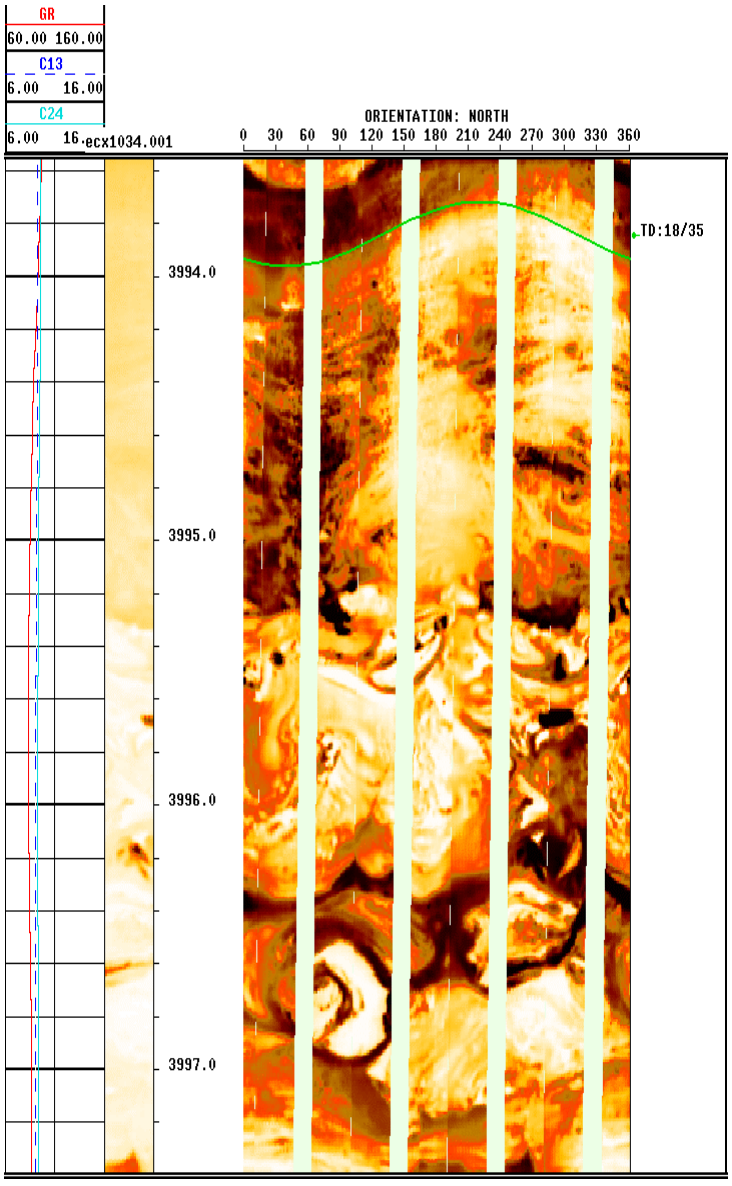

Deep Water Clastic Features:

Secondary cementation is local in nature as it does not extend across the wellbore. The amount and location of cementation can effect other log readings.

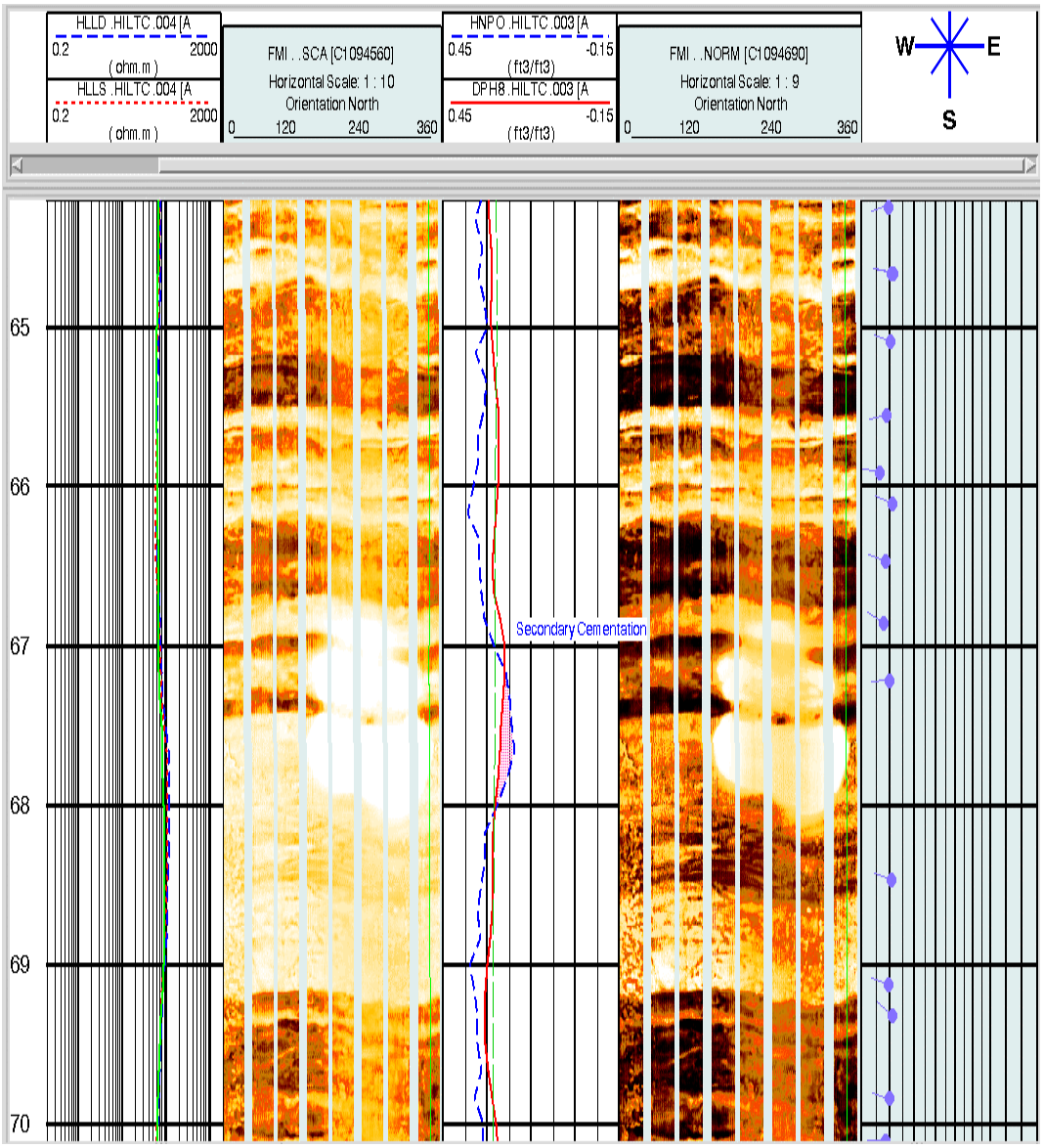

Thin Bed Analysis Exercise ?

Objective of this Exercise: Determine structure and deformation feature

Geological Background: Deep water marine sand

Available Data: Static Images (3D and unrolled), Dynamic Images, Gamma-Ray, Caliper, Resistivity, Neutron-Density and Dips

Question: **What feature is shown here and what is its orientation**

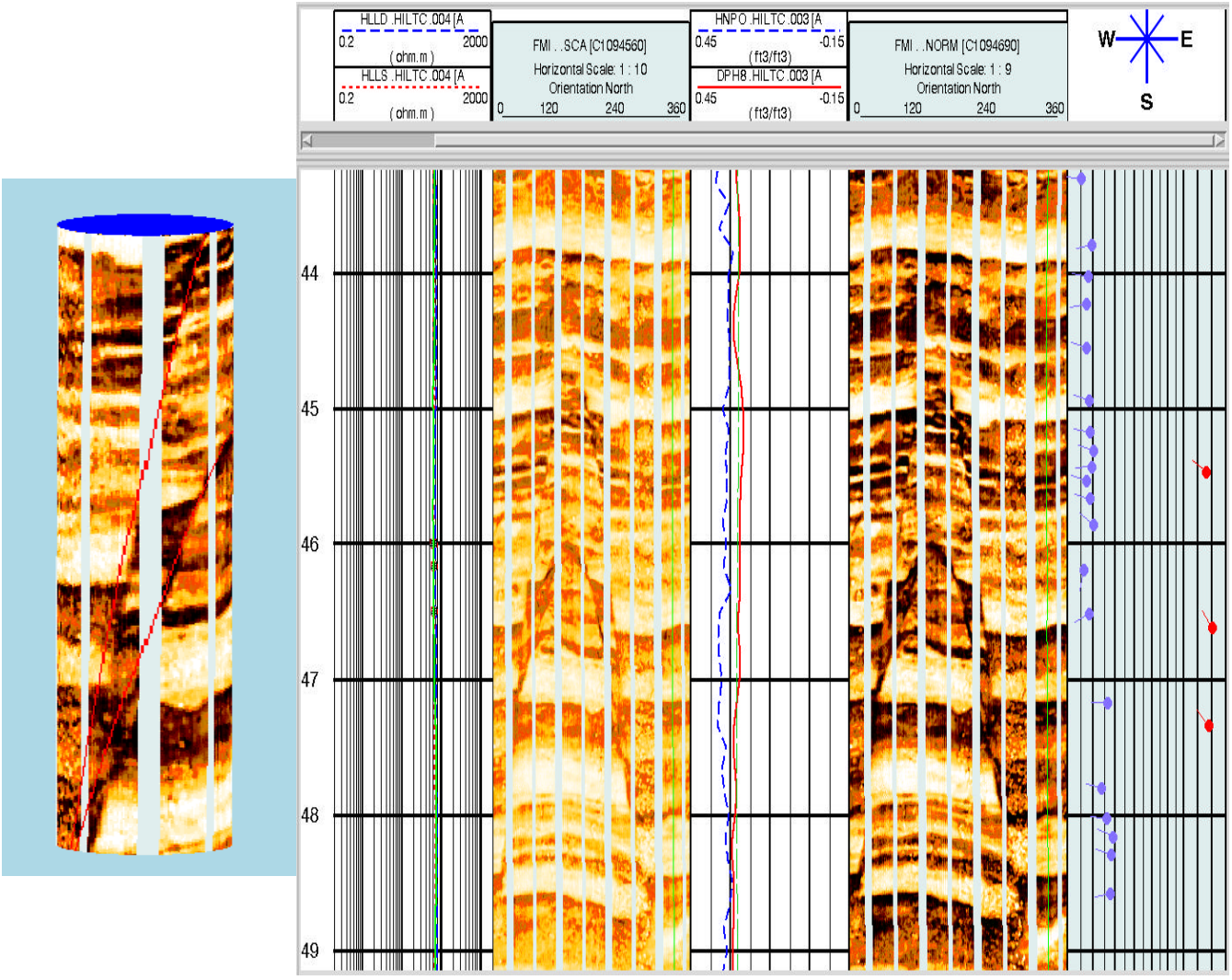

Thin Bed Analysis Exercise ?

Objective of this Exercise: Determine feature and slope orientation

Geological Background: Deep water marine sand

Available Data: Static Images (3D and unrolled), Gamma-Ray and Caliper

Question: **What is the feature at 3951.5?, Determine paleo slope**

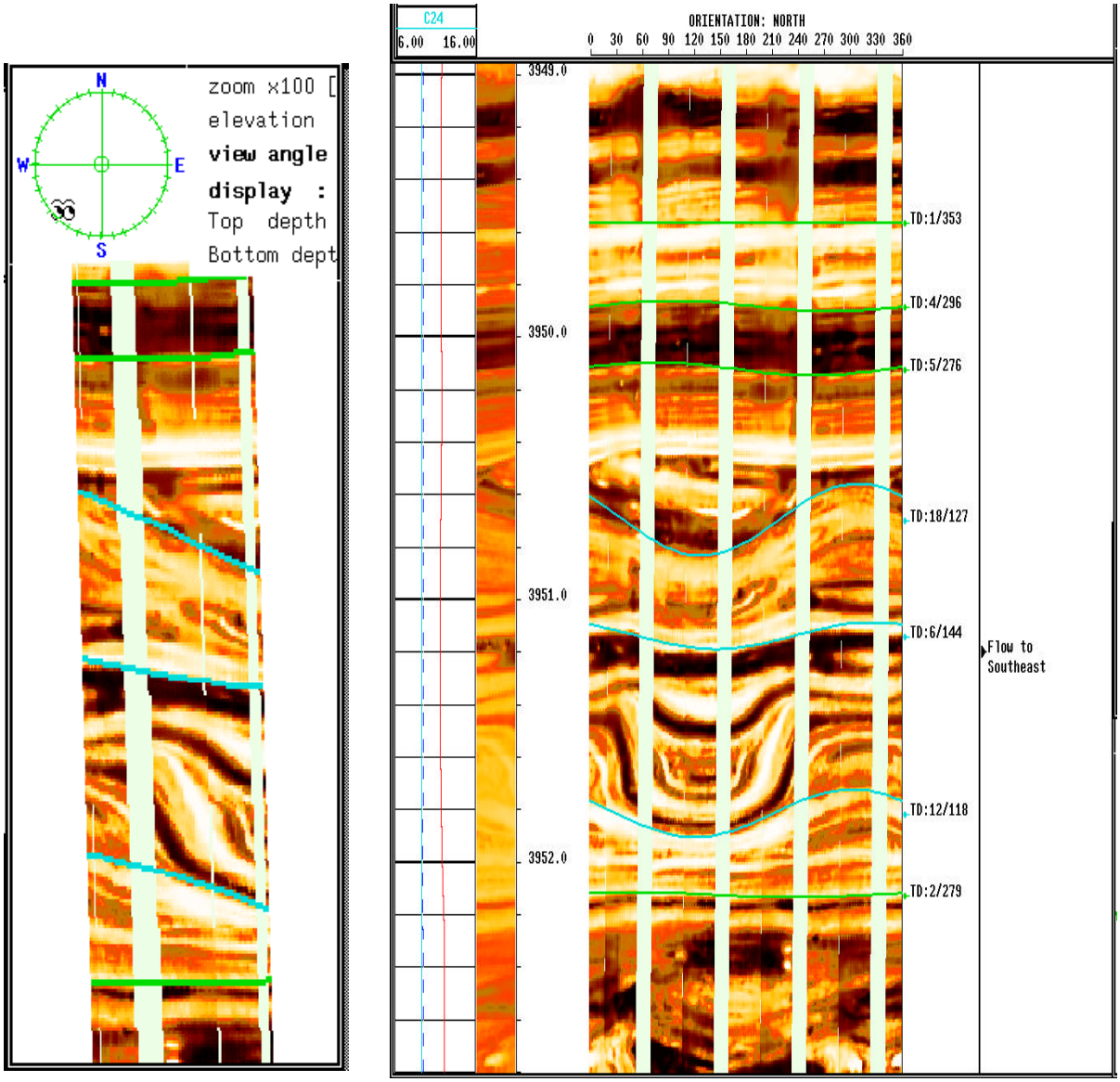

Thin Bed Analysis Exercise ?

Objective of this Exercise: Determine feature

Geological Background: Deep water marine sand

Available Data: Static Images, Gamma-Ray and Caliper

Question: **What is the feature at x451'?**

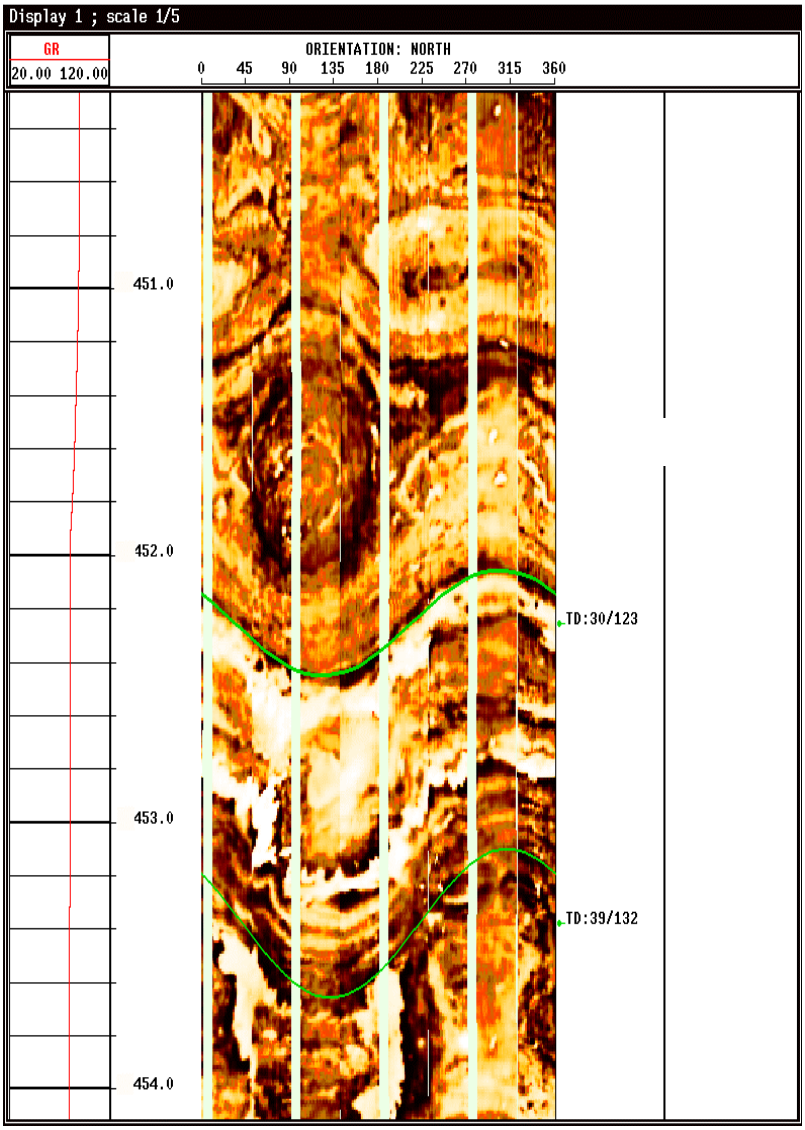

Thin Bed Analysis Exercise ?

Objective of this Exercise: Determine type of channel and channel orientation

Geological Background: Deep water marine sand

Available Data: Static and Dynamic Images, Gamma-Ray, Caliper, Resistivity and Neutron-Density

Question: **What is the channel orientation?**

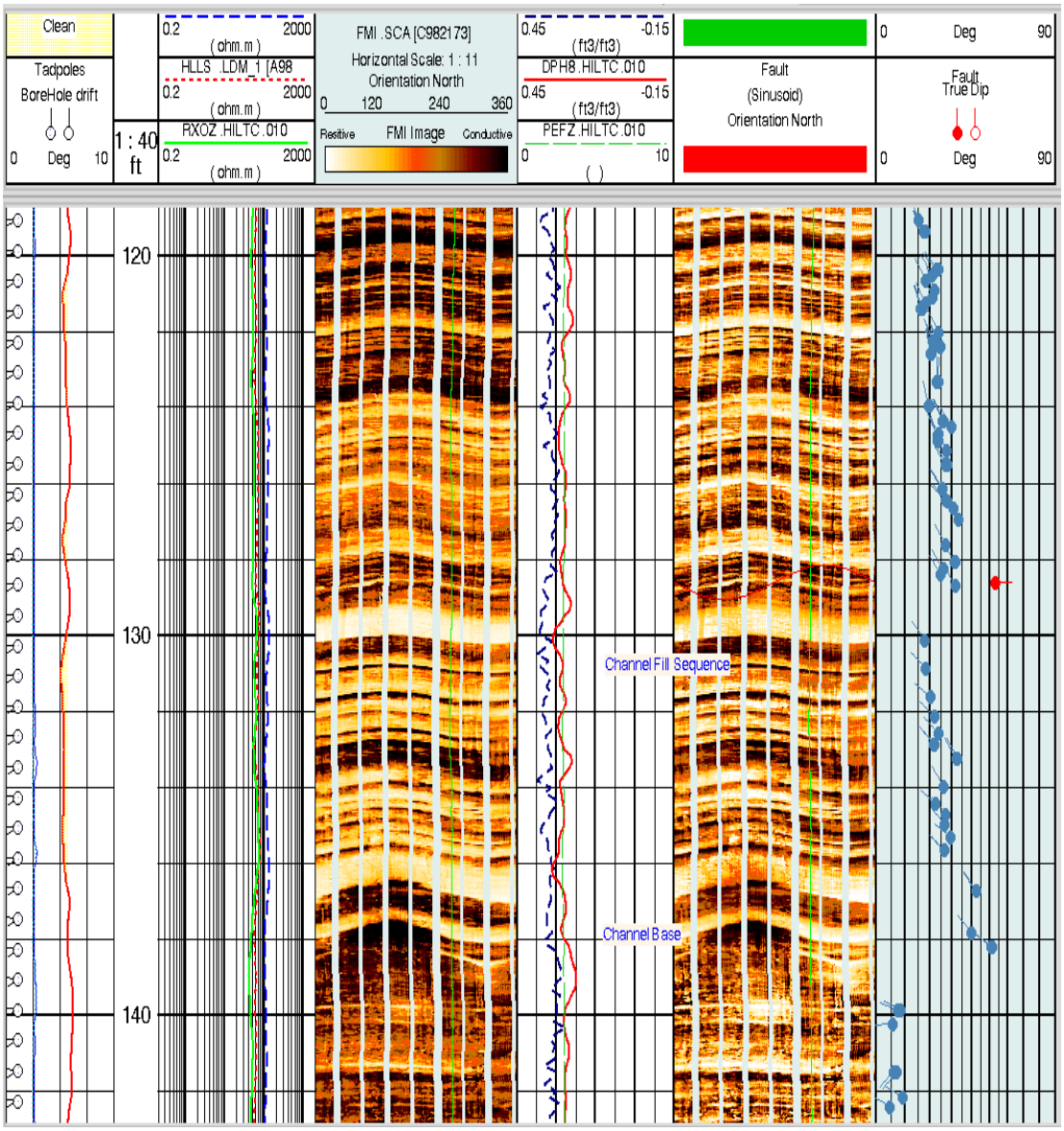

Thin Bed Analysis Exercise ?

Objective of this Exercise: Flow unit determination

Geological Background: Deep water marine sand

Available Data: Calibrated Images, Resistivity, Neutron-Density Log and Dips

Question: **Determine flow units, Depths and Orientation**

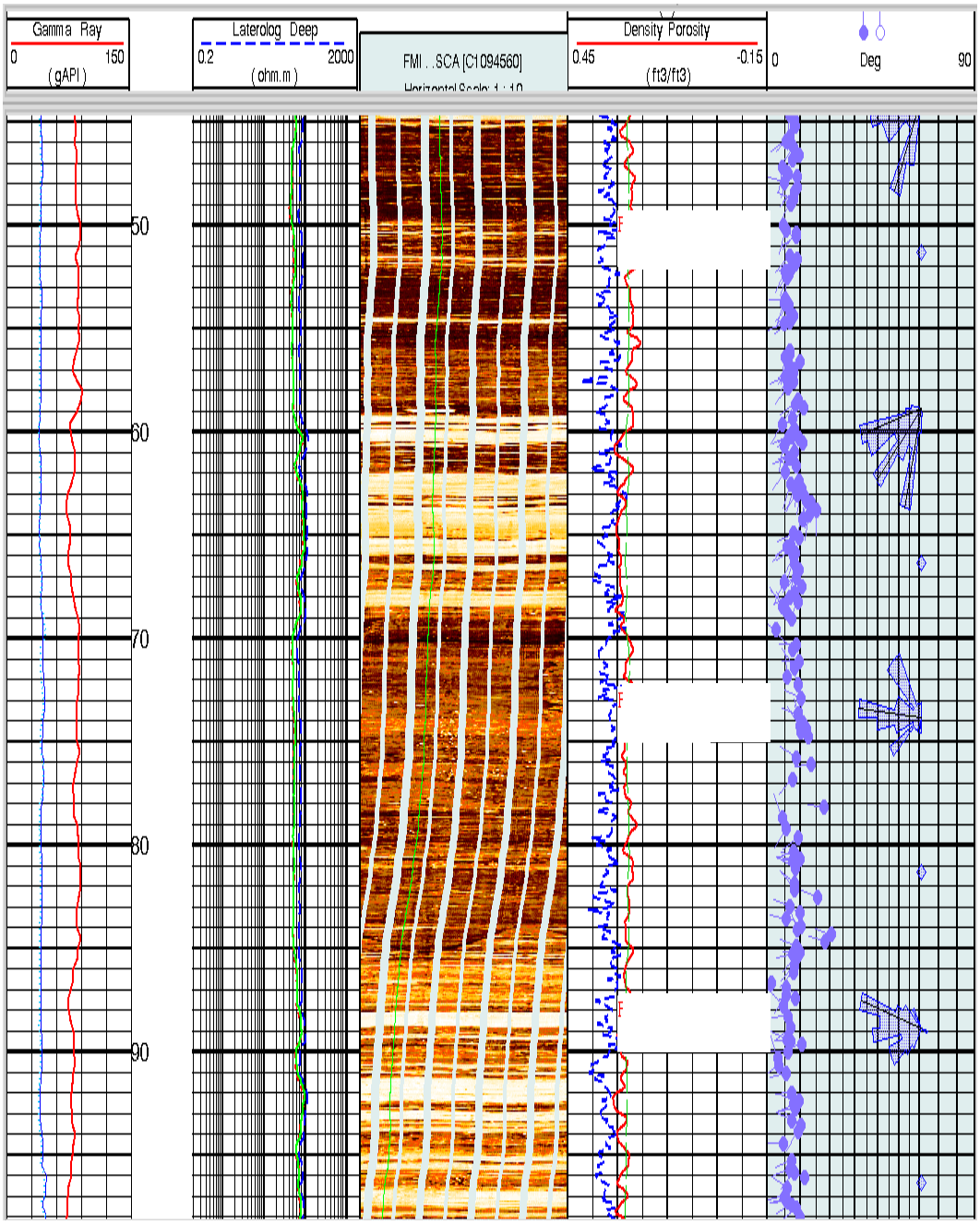

Thin Bed Analysis Exercise ?

Objective of this Exercise: Flow unit determination

Geological Background: Deep water marine sand

Available Data: Rose plots of True Structural and Stratigraphic dip

Question: **Determine flow orientation after Structural dip removal**

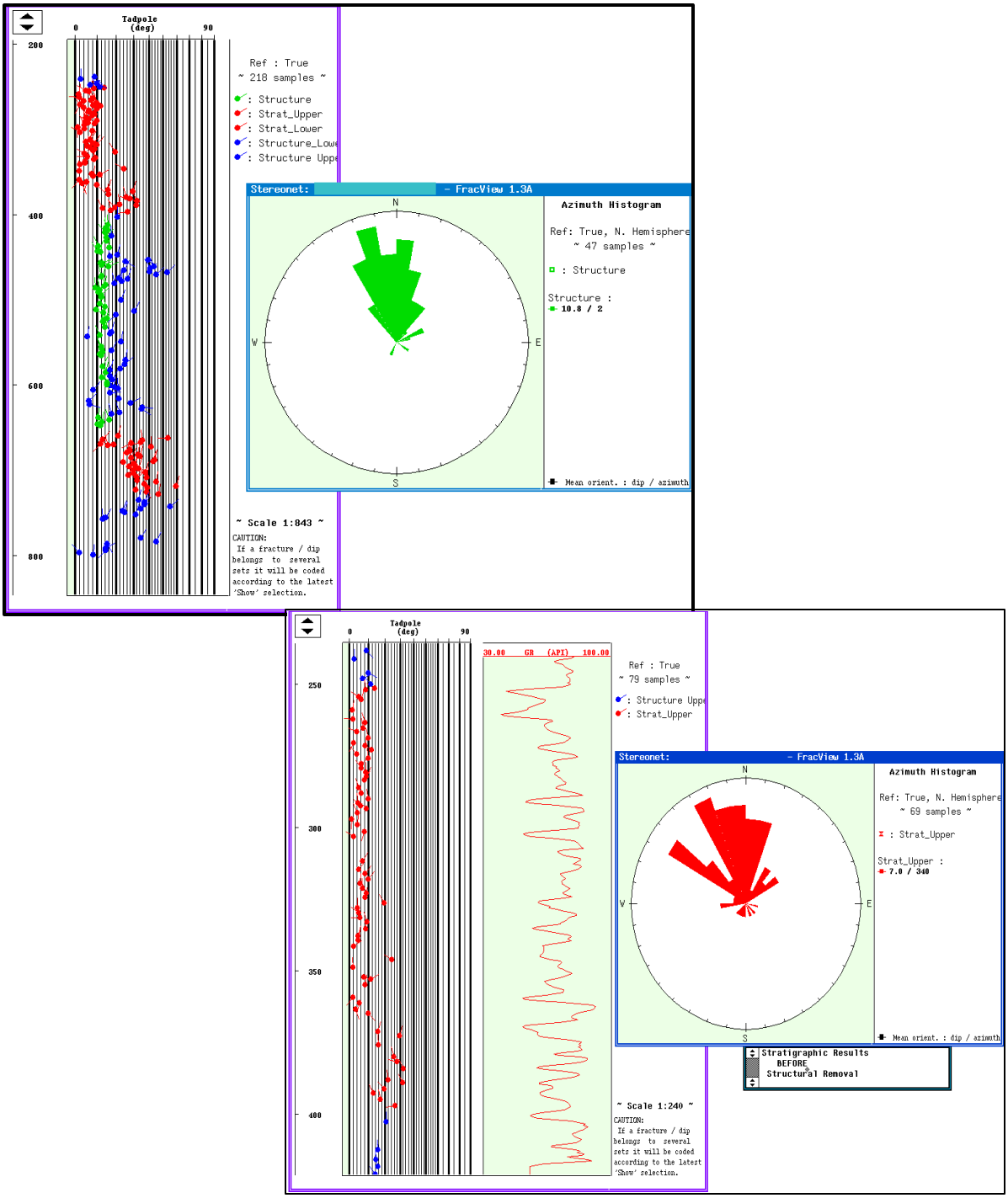

Thin Bed Analysis Answer

Objective of this Exercise: Flow unit determination

Geological Background: Deep water marine sand

Available Data: Rose plots of Stratigraphic dip after structural dip removal

Question: **Determine flow orientation after Structural dip removal**

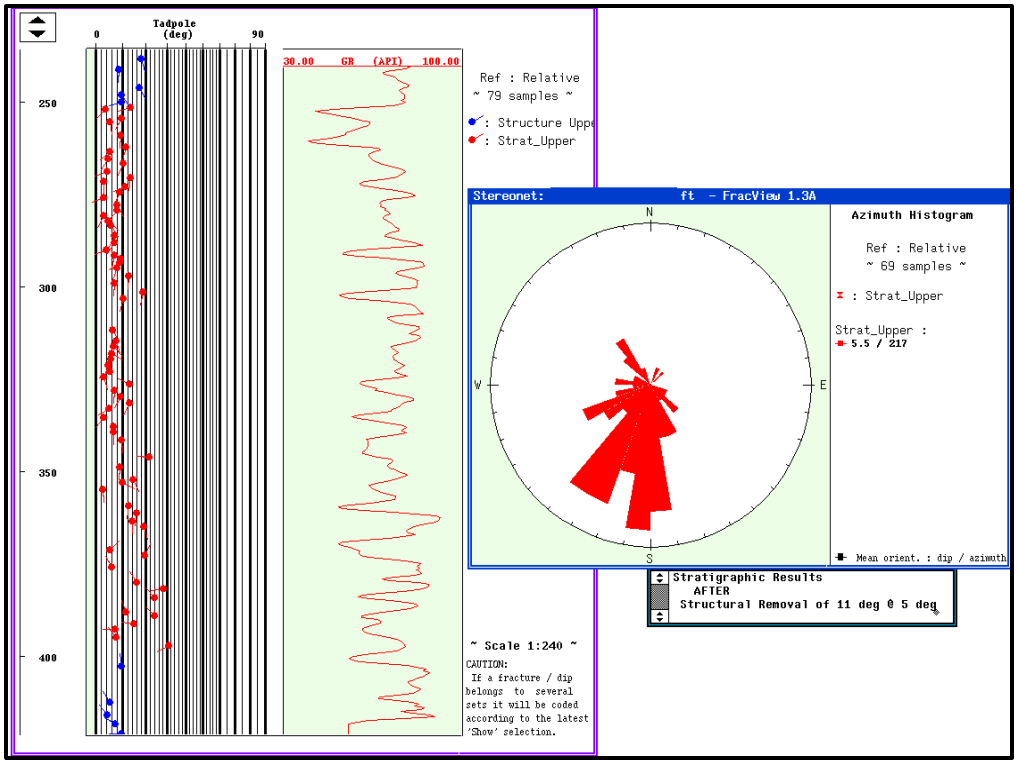

Histograms

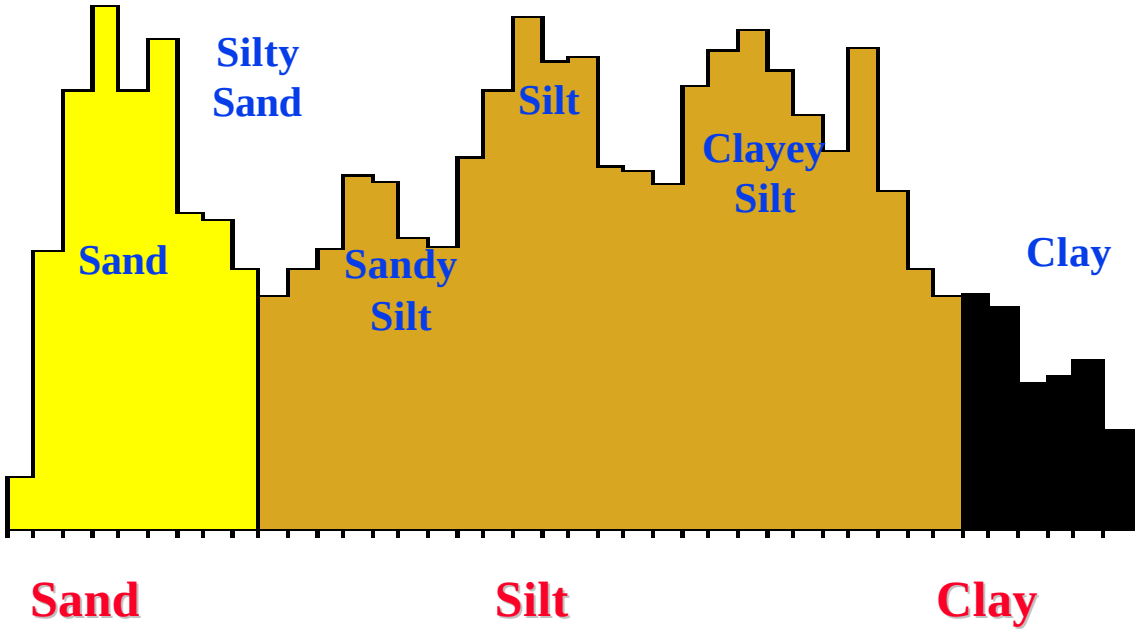

Perm

Very Good	Good	Fair	Some	Low	Very Low
1000	100	10		1	.1

Resistivity

Example of Threshold Imaging for Sand Count

Images can converted into 3 color clasess and histograms computed over the zone of interest inorder to determine portions of each subfacies.

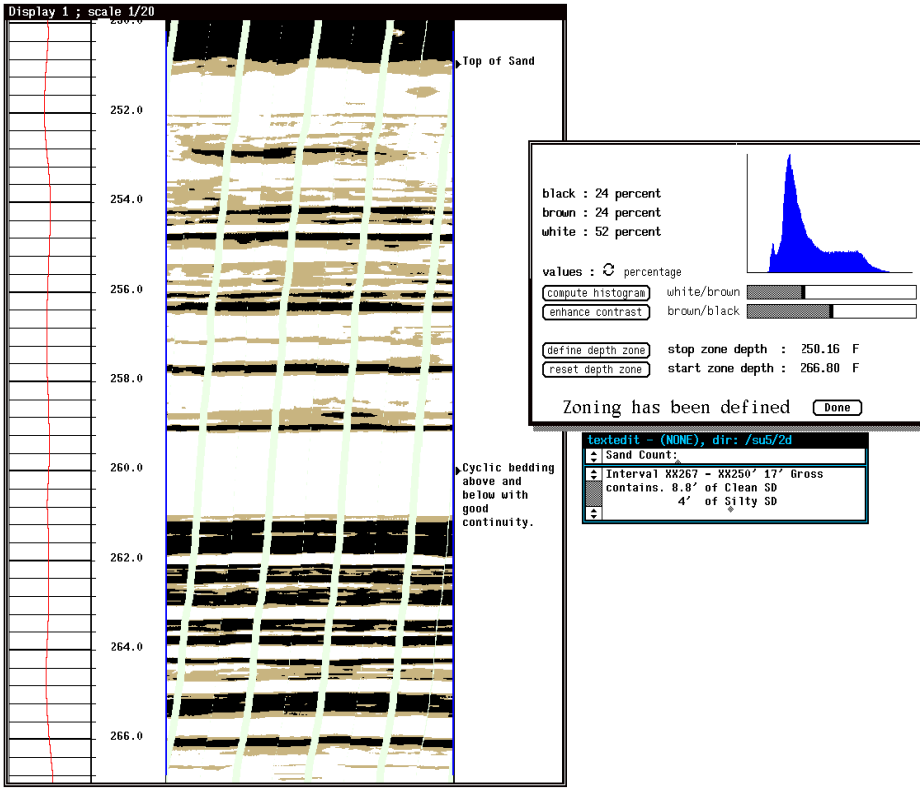

Thin Bed Analysis Example

Objective of this Exercise: Sand determination in a deep marine environment

Geological Background: Deep marine sand with very little response on Resistivity or Neutron-Density

Available Data: Calibrated Images, Gamma-Ray, Caliper, Resistivity, Neutron-Density Logs and Core Permeability

The core perm data in conjunction with the resistivity of the images is used to determine the cut-offs for sand and silt computations. The columns on the right are cumulative integrations of the sand and silt cut-offs.

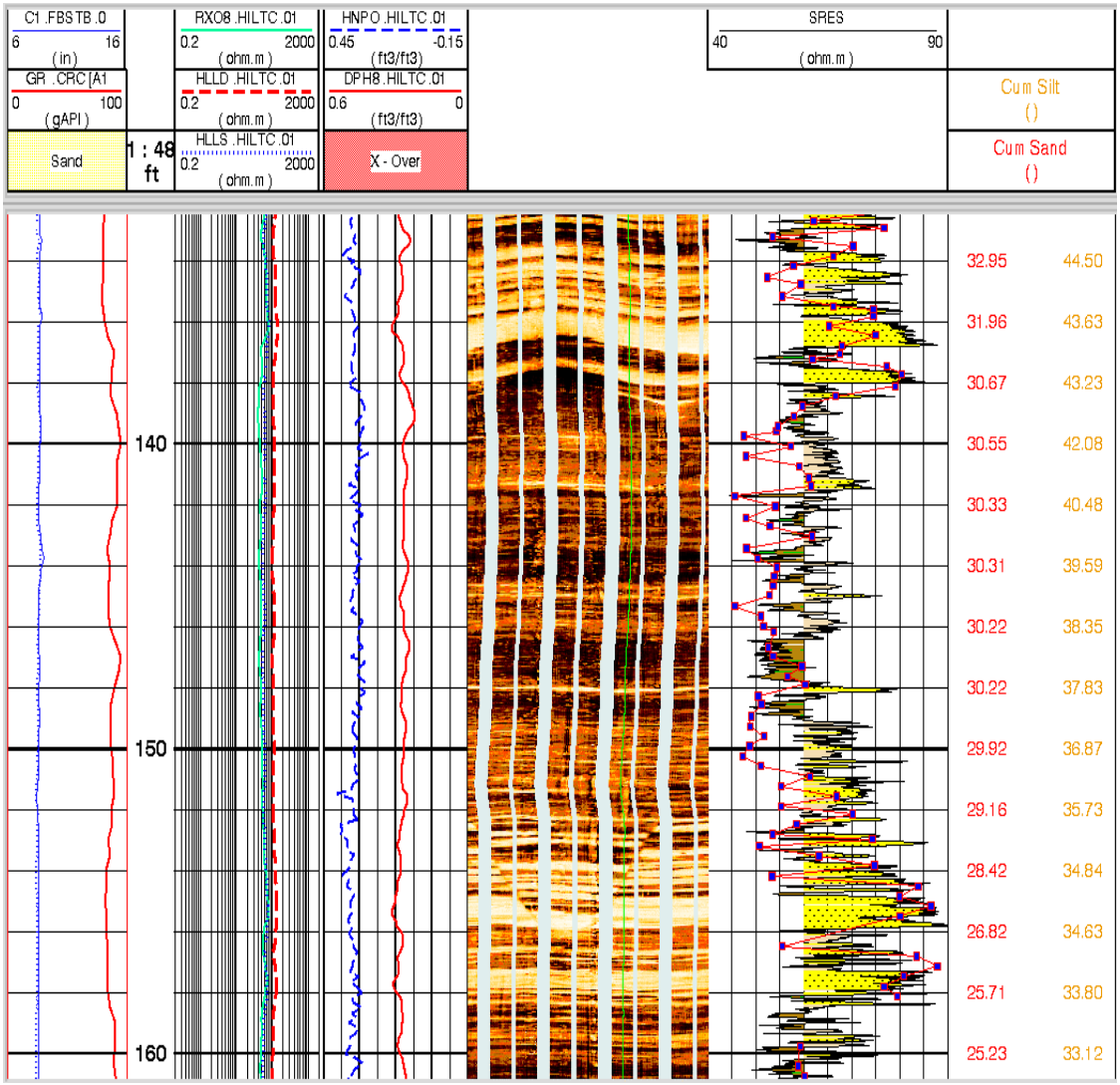

Thin Bed Analysis Exercise ?

Objective of this Exercise: Sand determination in a deep marine environment

Geological Background: Deep marine sand with no response on Resistivity or Neutron-Density

Available Data: Calibrated Images, Gamma-Ray, Caliper, Resistivity and Neutron-Density Log.

Question: **Should this well be perforated?**

Where should this well be perforated?

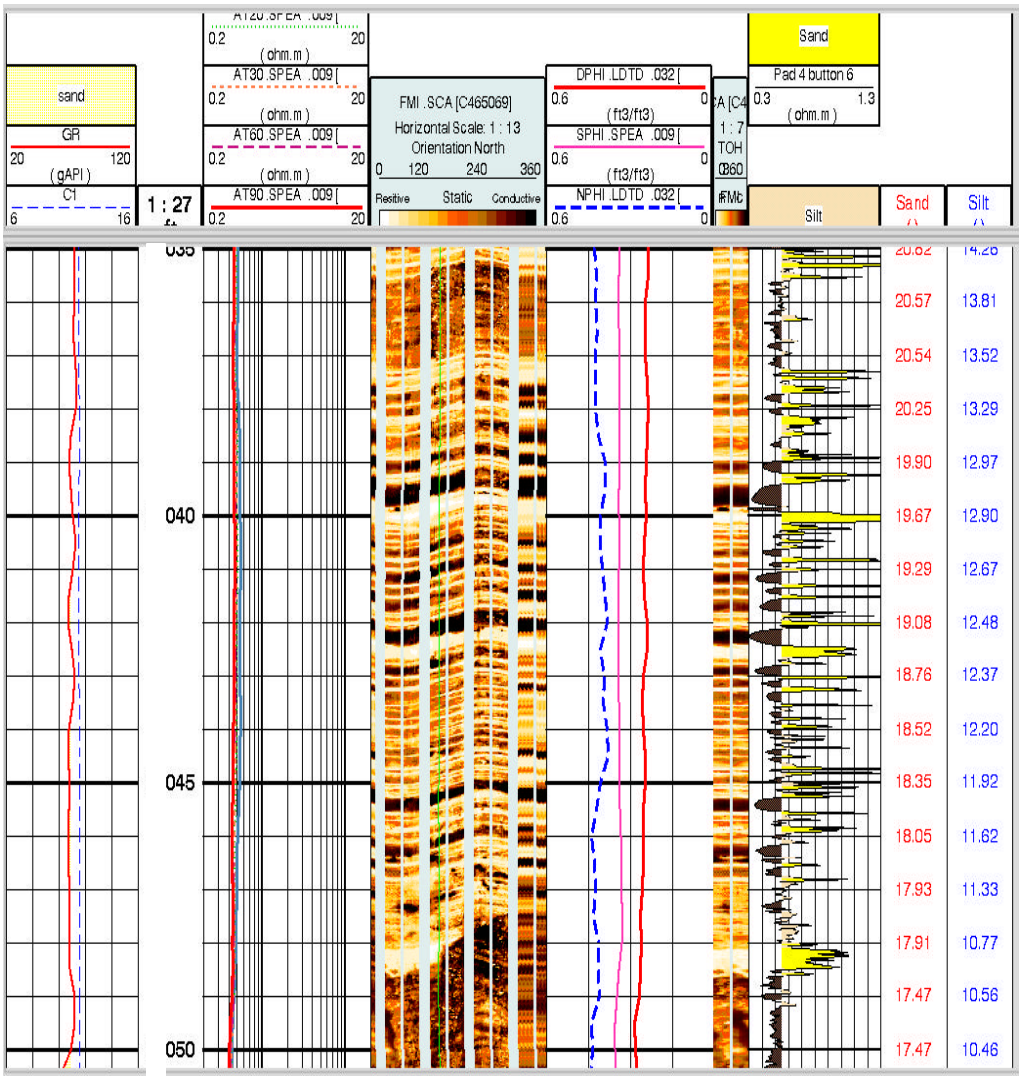

Thin Bed Analysis Example

Objective of this Exercise: Sand determination in a deep marine environment

Geological Background: Deep marine sand with no response on Resistivity or Neutron-Density

Available Data: Calibrated and Dynamic Images, Gamma-Ray, Caliper, Resistivity and Neutron-Density Logs

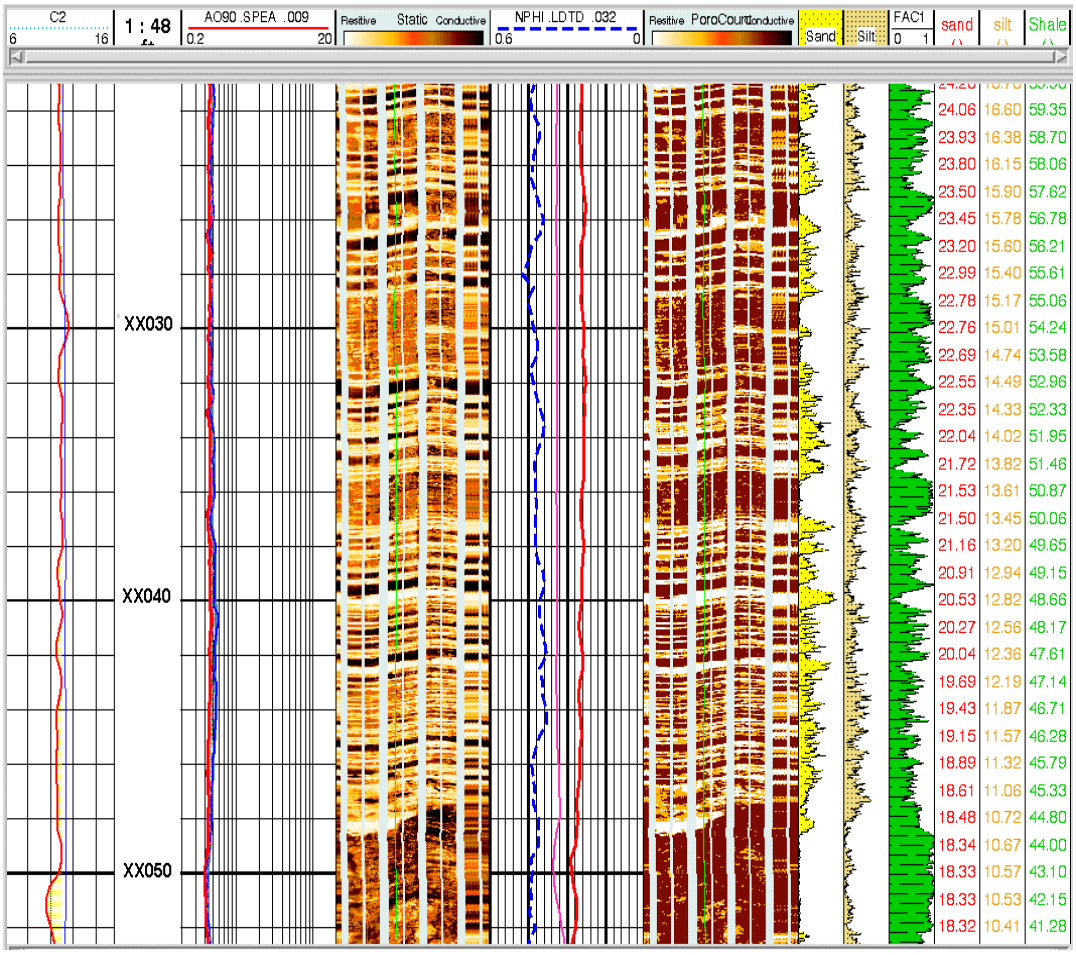

Thin Bed Analysis Exercise ?

Objective of this Exercise: Sand determination in a deep marine environment

Geological Background: Deep marine sand with no response on Resistivity or Neutron-Density

Available Data: Calibrated Images, Gamma-Ray, Caliper, Core Perm and Porosity data, Resistivity and Neutron-Density Log.

Question: **Should this well be perforated?**

Where should this well be perforated?

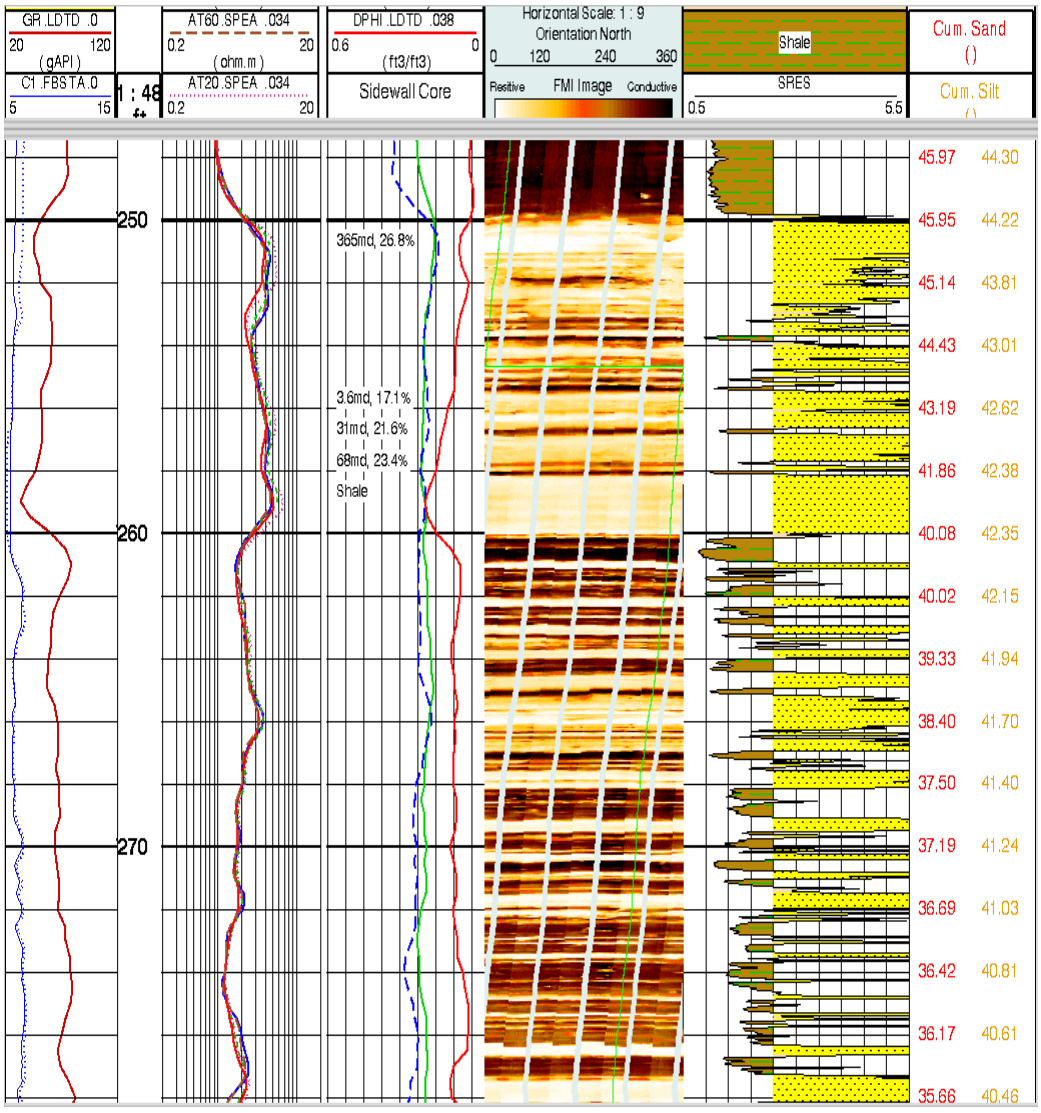

Thin Bed Analysis Answer

Objective of this Exercise: Sand determination in a deep marine environment

Geological Background: Deep marine sand

Available Data: Calibrated Images, Gamma-Ray, Caliper, Core Perm and Porosity Data, Resistivity and Neutron-Density Log.

Answer: **Tested interval xx250' - xx440' 16MMCF**

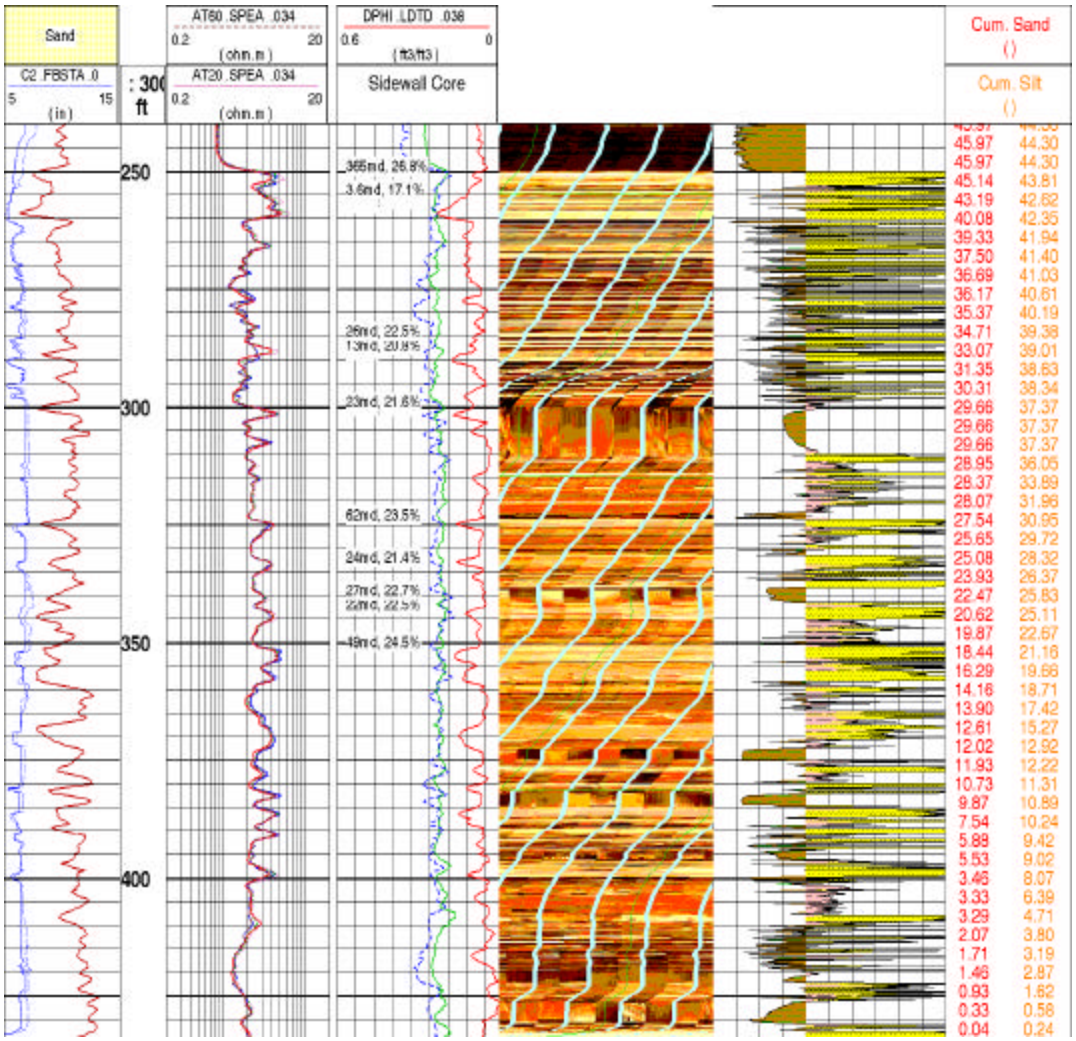

Thin Bed Analysis Exercise ?

Objective of this Exercise: Sand determination in a deep marine environment

Geological Background: Deep marine sand with no response on Resistivity or Neutron-Density

Available Data: Calibrated Images, Gamma-Ray, Caliper, Resistivity and Neutron-Density Log.

Question: **Should this well be perforated?**

Where should this well be perforated?

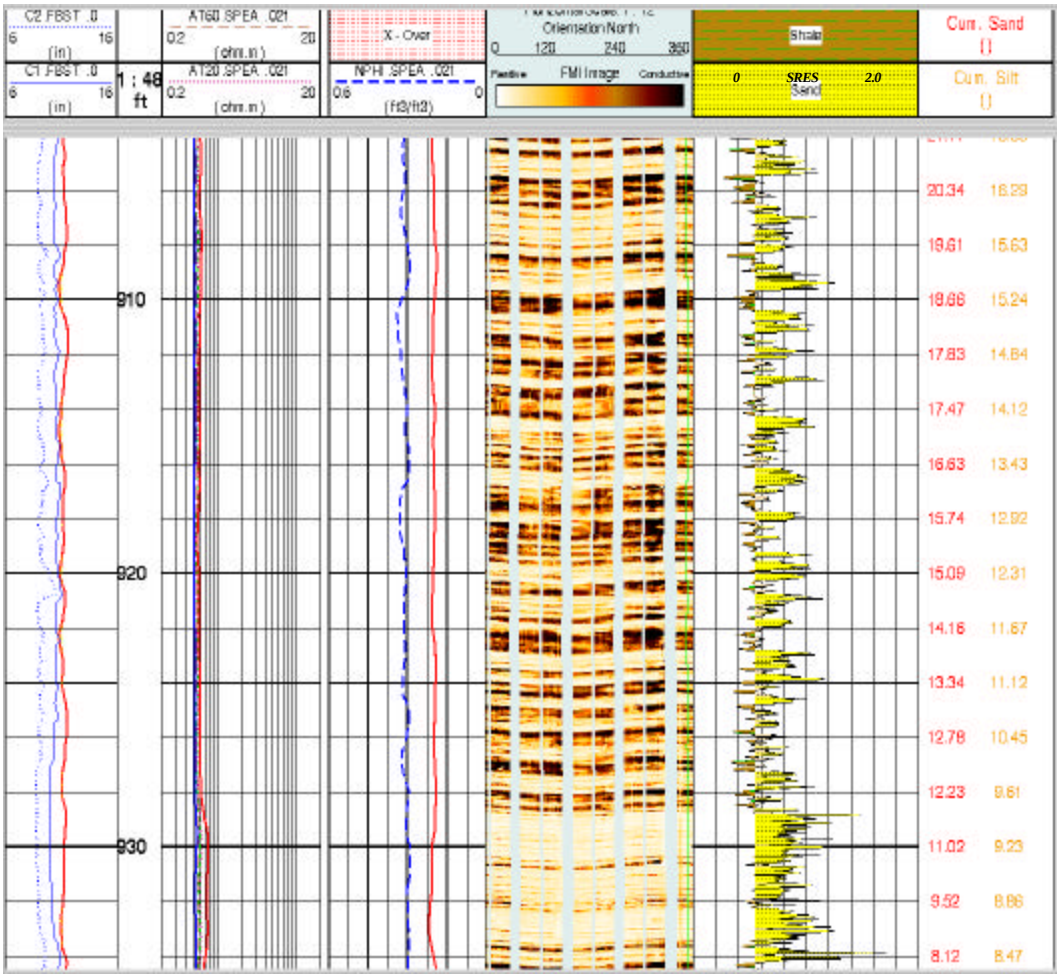

Thin Bed Analysis Answer

Objective of this Exercise: Sand determination in a deep marine environment

Geological Background: Deep marine sand with no response on Resistivity or Neutron-Density

Available Data: Calibrated Images, Gamma-Ray, Caliper, Resistivity and Neutron-Density Log.

Answer: **Tested interval xx875' - xx960' 3742 BOPD**

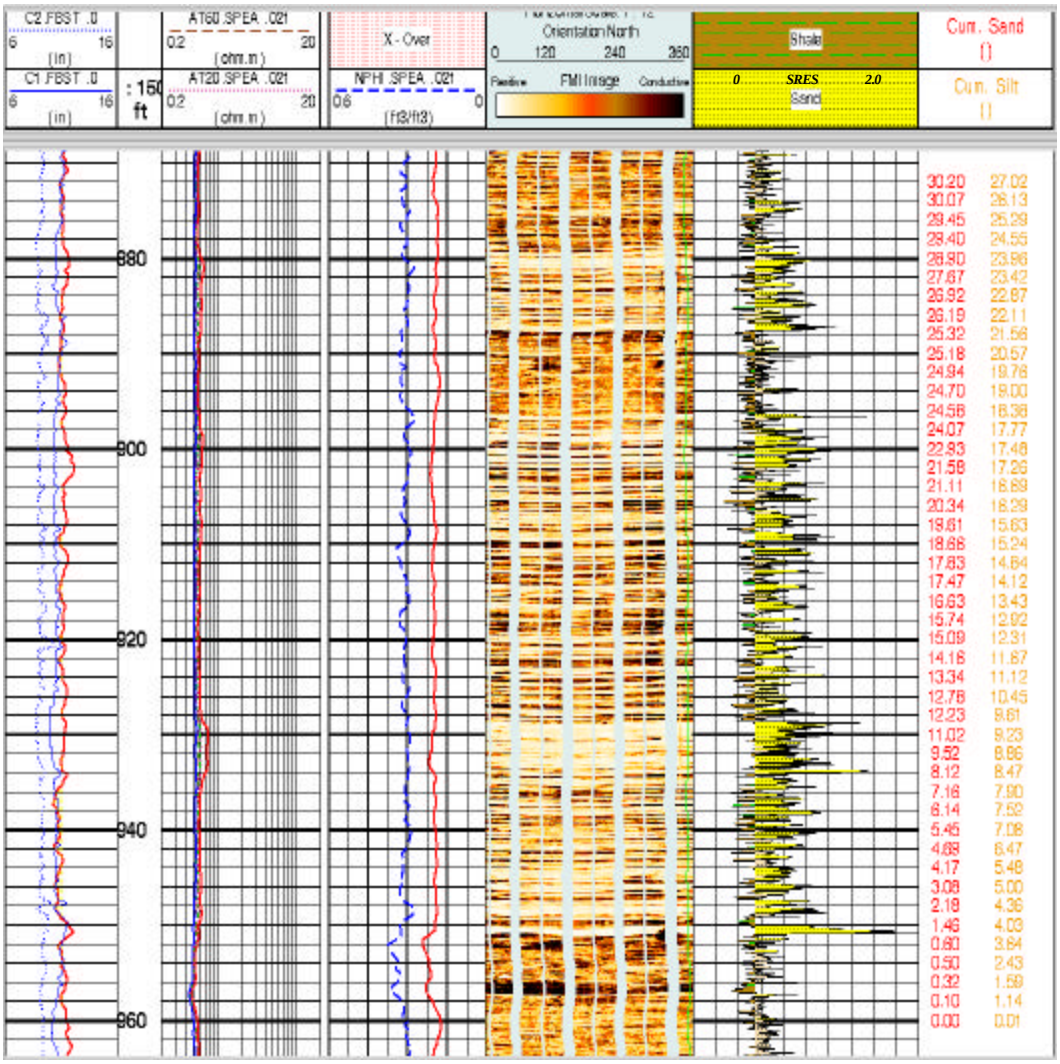

Thin Bed Analysis Exercise ?

Objective of this Exercise: Sand determination in a deep marine environment

Geological Background: Deep marine sand with some response on Resistivity or Neutron/Density

Available Data: Calibrated Images, Gamma-Ray, Caliper, Core Perm and Porosity Data, Resistivity and Neutron-Density Log.

Question: **Should this well be perforated?**

Where should this well be perforated?

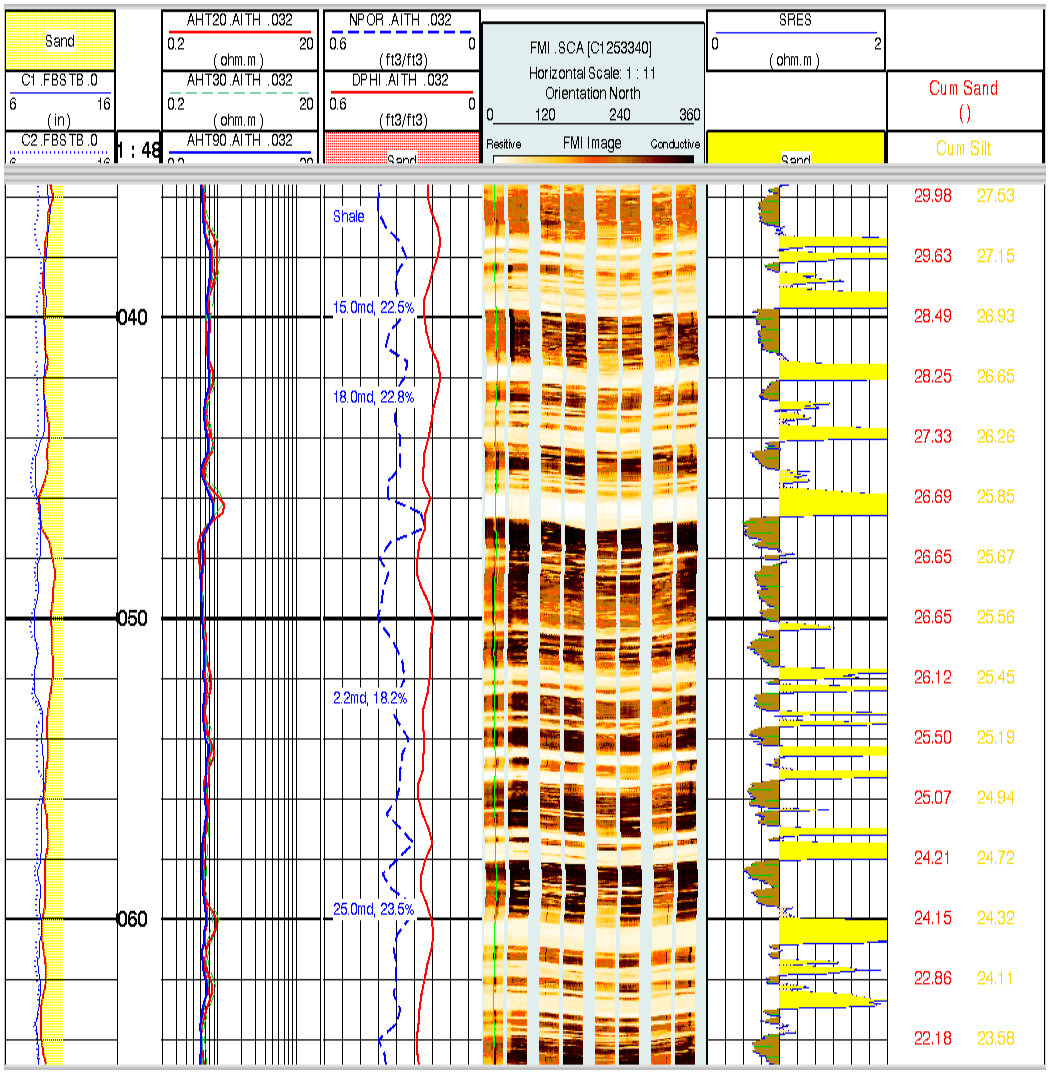

Thin Bed Analysis Answer

Objective of this Exercise: Sand determination in a deep marine environment

Geological Background: Deep marine sand with some response on Resistivity or Neutron-Density

Available Data: Calibrated Images, Gamma-Ray, Caliper, Core Perm and Porosity Data, Resistivity and Neutron-Density Log.

Answer: **Tested interval xx038' - xx098' 182 mcf and 213 BWPD**

The core data shown calcareous to slight calcareous which reduced the perms and porosity in this well.

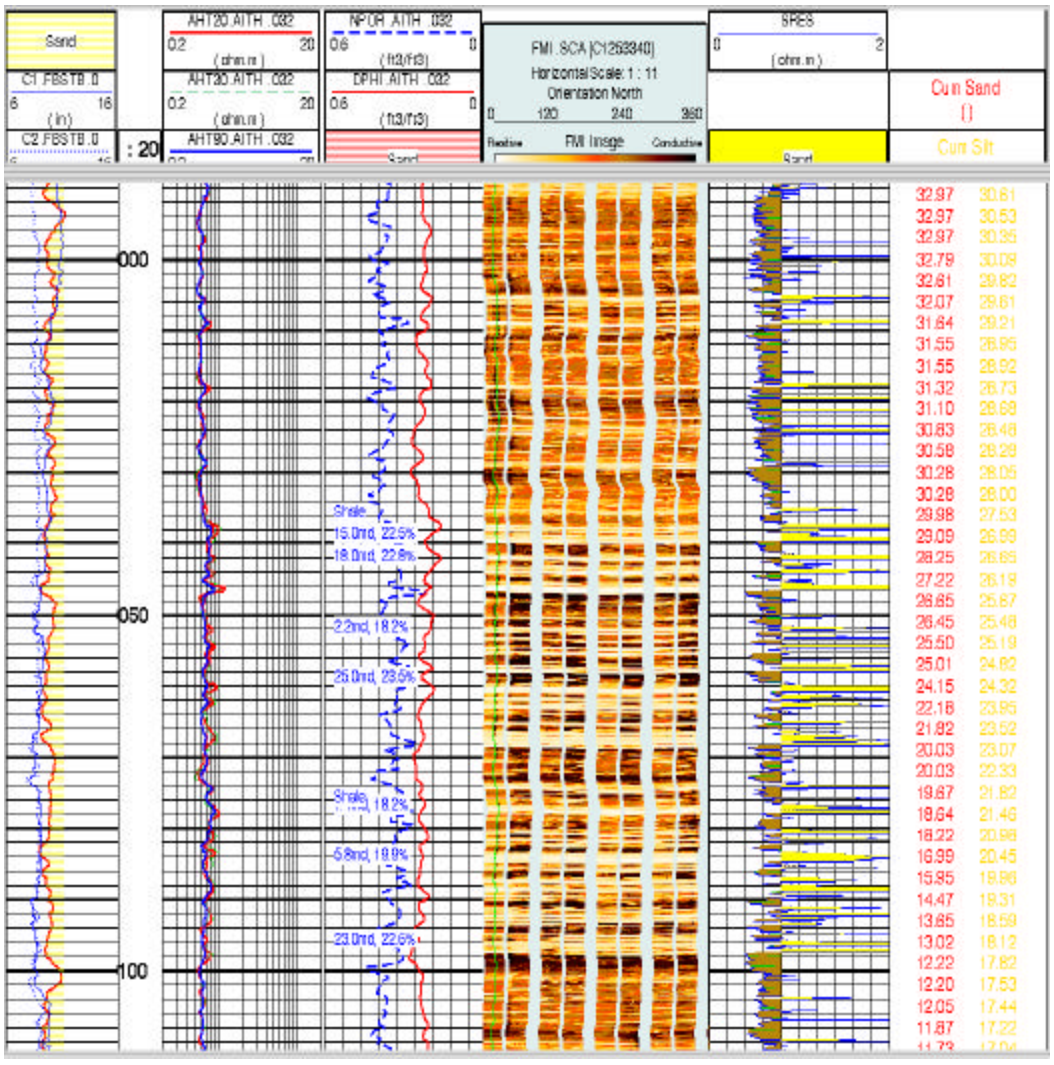

SHARP Processing

The idea is to deconvolve all petrophysical logs with constraints on the bedding as determined from a high-resolution log, such as FMS resistivity or EPT. A simplification of the deconvolution involves the assumption that the sequence of beds is made up of a finite number of facies with fixed (finite) number of log values. The problem is thus reduced to finding the optimum set of these finite number of values that win best reconstruct the observed logs after convolution with each tool's response function.

The procedure has been implemented on the Sun Workstation with emphasis on maximum interactivity. The methodology is to step the data through the five SHARP modules with the resulting SHARPened log used as inputs into standard interpretation procedures. such as ELAN.

Our original objective for using the SHARP chain was to ascertain if an accurate, high resolution Rt could be determined in Gulf Coast laminated sands. These laminated sands have very low adjacent shale resistivities of about 0.5 ohms and adjacent thick pay sands of 10 plus ohms. Often because of this situation we are operating outside of the design limits of LSAREC and were looking for an alternative approach.

Methodology

First a geological model is defined. This process starts with Squarelog. The inputs to Squarelog can be FMI, FMS, SHDT, OBDT, EPT or high resolution LDT. Squarelog produces a squared high resolution log in order to define bedding. This is done by doubly differentiating the filtered high-resolution log with the resulting zero crossings defining bed boundaries. The derivative length and derivative threshold are set to control sensitivity to bed boundaries.

The next step is to define a finite number of "electrofacies". This is done by constructing a histogram from the high resolution log . The analyst interactively picks "facies" boundaries on the histogram display. Local maxima are isolated by placing the cutoffs at local minima, thereby picking the "facies". Each individual bed from Squarelog is then automatically assigned to one of three "facies".

When the analyst is satisfied with his cutoffs ("facies") the Mode Inversion (MODINV) process is started. Once inside this module the "facies" are imported from Histogram.

Sharp Example

Example of AO90 (Deep Resistivity) and Gamma-ray after the sharpening process.

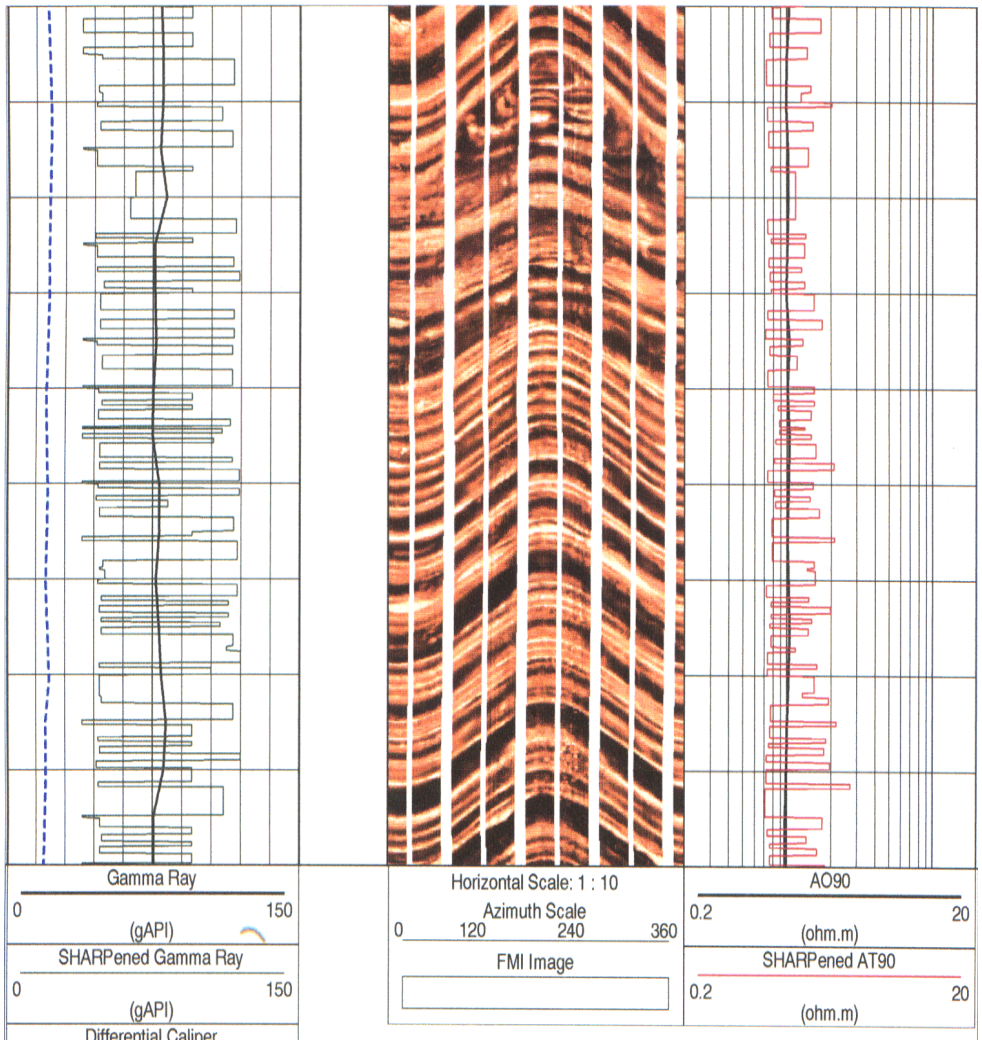

Enhancement of Low Resolution Logs

Knowing the response function for each standard resolution measurement. Mode Inversion performs an amplitude modal inversion where now the number of unknowns is limited to the number of "facies". The results of this mode inversion is an estimate of the high resolution rectangular profile for the input standard resolution measurement.

Next, the result of MODINV is displayed in Logplot. The analyst can now interactively modify the computed square value for each bed. As the high resolution rectangular profile is interactively modified it is convolved with the associated tool response to output the modified result. The log analyst can observe the comparison of the convolved reconstruction with the original log and continue to make adjustments to the high resolution rectangular profile to achieve a match with the original log. This confirms the geological model.

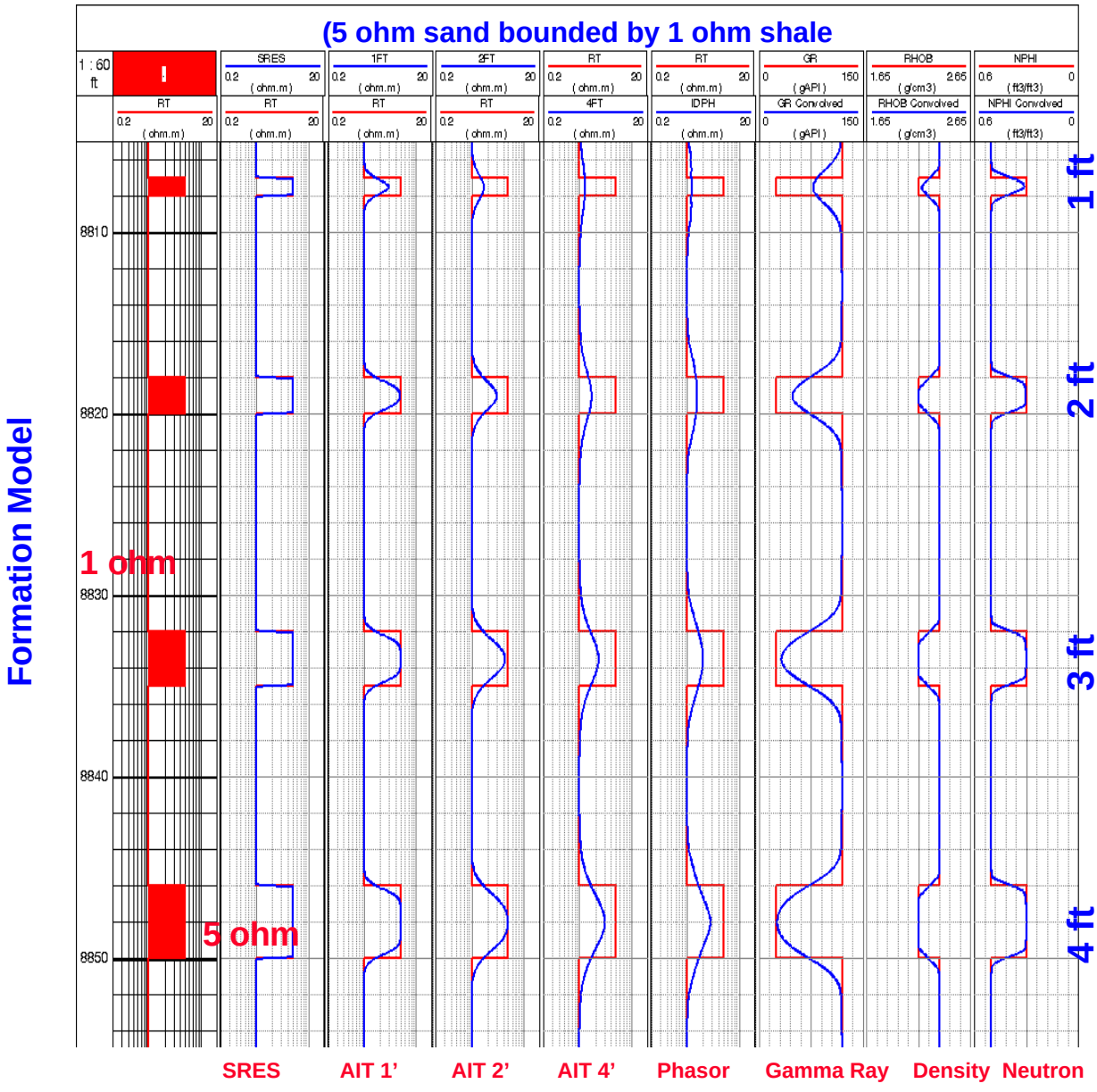

Sharpened Elan Example

Elan (Elemental Analysis) using sharpened data, plotted with FMI.